Thèse de Doctorat de Sorbonne Université

présentée et soutenue publiquement le 9 décembre 2019
au Laboratoire Jacques-Louis Lions

pour l'obtention du grade de
Docteure en Mathématiques Appliquées

par
Anouk Nicolopoulos-Salle

Formulations variationnelles d'équations de Maxwell résonantes et problèmes aux coins en propagation d'ondes

après avis des rapporteurs

Anne-Sophie Bonnet-Ben Dhia	*Directrice de Recherche à l'ENSTA Paris*
Ralf Hiptmair	*Professeur à l'ETH Zürich*

devant le jury composé de

François Alouges	*École Polytechnique*	examinateur
Anne-Sophie Bonnet-Ben Dhia	*ENSTA Paris*	rapporteure
Martin Campos Pinto	*Sorbonne Université*	directeur de thèse
Anne-Laure Dalibard	*Sorbonne Université*	examinatrice
Bruno Després	*Sorbonne Université*	directeur de thèse
Ralf Hiptmair	*ETH Zürich*	rapporteur
Francesca Rapetti	*Université Côte d'Azur*	examinatrice

École Doctorale de Sciences Mathématiques Paris Centre
ED 386

Faculté de Mathématiques
UFR 929

Remerciements

Bruno et Martin, merci de m'avoir proposé de participer à ce projet il y a quatre ans. Vous m'avez beaucoup appris et j'ai eu plaisir à travailler avec vous. Je vous remercie aussi d'avoir été si attentifs tout au long de la thèse. Je retiendrai votre bonne humeur, votre curiosité et votre détermination !

Patrick, je te remercie pour l'intérêt que tu portes à mon travail depuis le début de ma thèse, pour les discussions mathématiques et pour les discussions plus pratiques que nous avons eues. Bertrand, merci pour tous tes tips ! Je suis contente d'avoir eu l'occasion de travailler avec vous deux.

Je remercie vivement les membres du jury. Je suis très honorée qu'Anne-Sophie Bonnet-Ben Dhia et Ralf Hiptmair aient pris le temps de lire ce manuscrit. Merci beaucoup pour vos commentaires, j'espère que la présentation viendra compléter votre lecture du document. François Alouges, Anne-Laure Dalibard et Francesca Rapetti, je suis tout aussi honorée que vous ayez accepté de faire partie de ce jury, et vous remercie pour les discussions que nous avons eues autour de ce travail.

Je suis très heureuse d'avoir passé ces dernières années à Jussieu. Après avoir eu un certain nombre de membres du labo comme profs au cours de mes études, c'était amusant de les retrouver en salle café ou en salle de séminaire et d'apprendre à les connaître différemment. Laurent, c'est en partie grâce aux conseils que tu m'as donnés depuis que je suis arrivée à Jussieu que j'en suis là, et je te remercie pour ton soutien. Xavier, merci de m'avoir fait suivre toutes ces annonces de postdoc ! Merci à Catherine, Malika, Nathalie, Salima et aux membres du support informatique pour l'aide apportée au quotidien. Enfin, j'espère que les réflexions du nouveau comité parité vont continuer à mûrir et à être encouragées par les autres membres du labo !

Merci à Emmanuel, Lise-Marie et Mehdi, qui avez été à ma place il y a sept, six et trois ans, pour vos invitations à Strasbourg, Washington et Nantes, et pour les anectodes racontées dans une taverne à Gärching, autour d'une torta à Columbia Heights ou de pimientos de padrón à Valence.

Celles et ceux que je tiens le plus à remercier ici, ce sont tou·te·s les thésard·e·s croisé·e·s ces dernières années. Alexandre, Clément, Louis, Marc et Nicolas, du stress pour la bourse de thèse au stress pour la soutenance, finalement c'est allé vite ! Je suis vraiment contente d'être passée par toutes les étapes avec vous, avec détours au bord des gorges d'Opedettes, en haut de la Sainte-Victoire ou du Monte Cinto, à Guérande, Pantin ou Strasbourg, autour d'une potée à Gentos, d'un barbecue rue d'Olomouc ou de farcis à Tourette, en sirotant un Spritz au bord du canal ou en descendant une pinte autour de Ju. Carlo, t'es le premier doctorant du labo que j'ai rencontré, et je me réjouis toujours de te croiser à Nancy, Londres, Paris ou Zürich. Antonin, Cécile T., Geneviève, Guillaume, Léo, Lilian, Lucile, Olivier et le reste de la bande de ma première année, merci pour tous ces vendredi soirs ! ! Lucile, Étienne, Geneviève, Helin, Lilian et Anne-Françoise, puis Valentin, Virgile, Jules, Houssam, Cristina et Gong, vous aurez été des cobureaux bavards mais studieux, pile ce qu'il faut. Une pensée spéciale pour Christophe, Jean, Louis, Lydie, Marc, Nicolas, Pierre et Yangyang, avec qui on est passés à peu près en même temps par l'étape de rédaction. Alexandre R. et Valentin, qui prenez la relève dans l'équipe plasma, bonne continuation ! Et biensûr mille mercis aux chéri·e·s du libanais, Allen, Amaury, Ana, Antoine, Camille, Gabriela, Julia, Katia, Lydie, Michael et Ziad, et aussi à l'équipe du râ quand même, David, Élise, Eugenio, Fatima, Gontran, Idriss, Jean-François, Lise, Ludovic et Nicolas la star de cinéma. Merci à Cécile D.V. pour mon recrutement au mercato. Ao Federi, t'es mon troll favori. Merci pour le risotto sino-milanais. Allen, Marc et Po-Yi, merci

pour les astuces, les cadeaux, les échanges et les victoires ! Salut aussi à Anthony, Aurélien, Fabian, Juliette et aux autres que j'ai rencontré en conférence. Même s'ils ne sont plus en thèse, j'en profite pour dire merci aux postdocs passés par le labo, Benjamin, Camilla, Cécile C., Grigorio, James, Teddy et Xavier, pour leur support en connaissance de cause. Ariles, Élodie et Gabriel, de la piscine de Cachan au foyer vietnamien, c'est toujours sympa de partager nos expériences. Emanuela et Giulio, grazie pour vos photos du bout du monde, et aussi de toujours nous préparer un festin à Lydie et à moi entre deux de vos destinations exotiques. Et Lydie, avec tous tes projets menés de front, merci d'être toujours ludisponible pour écouter, relativiser et donner des conseils !

Je veux aussi dire merci à Aisa, Alice, Chelsea, Delia, Laurent, Nathan et Sophia qui sont là depuis longtemps. C'était important de pouvoir sortir du monde universitaire pour un petit séjour à Wivenhoe, jamais eu aussi froid de ma vie, une matinée de sculpture avant d'aller engloutir des 餃子, une baignade avec des ours noirs dans le lac Surprise sous le Grand Teton ou juste manger comme au resto au bout de la 7bis.

Olivier, merci de compter sur moi et de me laisser compter sur toi, de me donner envie de faire mieux à chaque fois, et d'avoir été là quand c'était dur. Merci pour tout quoi, sans toi ç'aurait pas été pareil.

Enfin, pour leur soutien depuis toujours, merci aux membres de ma famille ! Et plus particulièrement à ma soeur, mes parents et ma grand-mère pour leur implication durant toutes ces années, et pour leur passion nouvelle pour l'organisation de pots de thèse. Merci !

à Z A D
et B

Contents

Introduction générale

Les questions à l'origine de cette thèse sont celles du comportement et de l'approximation de solutions singulières aux équations de Maxwell résonantes dans un plasma hétérogène et anisotrope. Ce sont des équations aux dérivées partielles linéaires et dégénérées à l'intérieur du domaine sur lequel elles sont posées.

Ces équations font partie des différents modèles utilisés pour étudier la fusion nucléaire [106, 17, 110]. Ce sont des modèles complexes et variés, et il est important d'en avoir des approximations numériques précises et robustes. Les conditions de température et de densité à l'intérieur d'un tokamak sont telles qu'on ne peut pas tout mesurer. Les équations qui décrivent le comportement d'un plasma, comme les équations cinétiques, sont connues et ont été étudiées en détail. Mais la variété des échelles caractéristiques et la non-linéarité de ces modèles font qu'il est difficile de les discrétiser, et on travaille alors sur des modèles réduits. Il y a de nombreux régimes différents, ceux qui correspondent à la réflexion et l'absorption d'ondes au coeur du plasma [107], aux intéractions du plasma avec la paroi où il n'y a plus d'équilibre des charges [4, 116], ou encore aux turbulences dues aux forts gradients de température et qui affectent le confinement du plasma [58]. D'autre part, certains phénomènes correspondent à des fréquences précises et sont étudiés en régime harmonique en temps, alors que d'autres requièrent une étude en temps long. Enfin, certains modèles sont posés sur une géométrie réaliste, et exploitent par exemple la structure hamiltonienne en régime non-dissipatif, tirent profit du fait que la dynamique des particules suit les lignes de champ [18, 21], tandis que d'autres sont posés sur une géométrie simplifiée. Une source de questions originales consiste alors à trouver comment aborder chacun de ces problèmes de manière à pouvoir le discrétiser avec précision. Un autre intérêt de ce sujet est l'actualité de l'enjeu énergétique industriel, qui permet notamment des collaborations transdisciplinaires sur des projets de recherche comme ITER et l'élaboration de codes numériques associés.

Un plasma est un état de la matière où les particules chargées, ici les ions et les électrons, sont libres. Les particules peuvent se déplacer sous l'effet d'un champ électromagnétique, et les noyaux d'atomes peuvent éventuellement fusionner. Générer ces phénomènes de fusion nucléaire et récupérer l'énergie ainsi créée est l'objectif des tokamaks. Dans ces machines, un fort champ magnétique est imposé par des bobines externes et crée une asymétrie dans la réponse des particules. On considère dans ce travail un champ imposé simplifié $\mathbf{B}_0$, constant et de direction colinéaire à l'axe toroïdal z. Chacun des modèles évoqués plus haut comporte une description de l'évolution du champ électromagnétique et une description de la dynamique des particules, couplées par le courant généré par les particules et source des équations sur le champ. La description du champ électromagnétique est faite par les équations de Maxwell. Dans le régime qui nous intéresse, celui des résonances hybrides, nous utiliserons un modèle fluide pour les particules. On appelle ce couplage entre des champs électromagnétiques et un fluide conducteur la magnétohydrodynamique. Nous nous intéressons plus précisément au système d'Euler-Maxwell. On travaille en régime harmonique autour de la fréquence $\omega > 0$ d'une onde plane incidente, dont on note $\mathbf{k} \in \mathbb{C}^3$ le vecteur d'onde associé. Les deux systèmes d'équations se combinent alors pour former ce qu'on appelle ici le

système d'équations de Maxwell résonantes qui porte uniquement sur le champ électrique

$$\nabla \wedge \nabla \wedge \mathbf{E} - \underline{\underline{\varepsilon}}\mathbf{E} = 0 \quad \text{dans} \quad \Omega \subset \mathbb{R}^3,$$

où le tenseur de permittivité $\underline{\underline{\varepsilon}}$, hétérogène et anisotrope, varie en espace via la pulsation plasma ω_p dont l'intensité est proportionnelle à la racine carrée de la densité électronique, et dépend du champ magnétique imposé via la pulsation cyclotron ω_c dont l'intensité est proportionnelle à celle du champ. Ce tenseur dégénère à l'intérieur du domaine le long de la courbe de résonance hybride $\Sigma = \{\mathbf{x} \in \Omega, \omega^2 = \omega_p^2(\mathbf{x}) + \omega_c^2\}$ dans le sens où son coefficient diagonal α se comporte comme une distance signée à cette courbe : positif d'un côté, négatif de l'autre, et nul sur la courbe. Certaines composantes du champ électrique vont être régulières, mais d'autres seront singulières et non intégrables. On réintroduit un champ qu'on appelle magnétique et défini par $\mathbf{B} = \nabla \wedge \mathbf{E}$, au lieu de $(i\omega)^{-1}\nabla \wedge \mathbf{E}$, pour des raisons pratiques.

Avant le début de cette thèse, l'étude du problème a été menée en dimension un, c'est à dire sous l'hypothèse d'un plasma ne variant que dans une direction $\underline{\underline{\varepsilon}} = \underline{\underline{\varepsilon}}(x)$ avec x dans $I \subset \mathbb{R}$, et sous l'hypothèse d'une onde incidente avec une direction de propagation normale au fort champ magnétique sous-jacent, $\mathbf{k} = (k_x, 0, 0)$. L'hypothèse d'incidence normale permet de découpler les équations de Maxwell en un système sur (E_x, E_y) dit extraordinaire (X-mode) et une équation sur E_z dite ordinaire (O-mode). Une solution analytique a été décrite, mais l'approximation numérique posait problème pour deux raisons. D'abord, parce que le problème est dégénéré et qu'il n'y a pas unicité de la solution. Ensuite, parce que la solution analytique que nous cherchons à capturer est singulière : la composante E_x est la somme d'une valeur principale en $1/x$ et d'une masse de Dirac, non intégrables localement, et d'un reste de carré intégrable. Une méthode courante utilisée pour résoudre numériquement ce problème est de désingulariser les équations, en ajoutant de la friction entre les particules. Cela correspond à prendre en diagonale de $\underline{\underline{\varepsilon}}$ le coefficient $\alpha + i\nu$, avec un $\nu > 0$. C'est d'ailleurs via un principe d'absorption limite, en faisant tendre ce paramètre de régularisation vers zéro, que la solution analytique a été obtenue. Mais ce petit paramètre impose au niveau discret une contrainte non triviale sur les paramètres de discrétisation. Il est souhaitable de ne pas imposer de contrainte sur le maillage pour pouvoir obtenir des résultats sans avoir à régler le pas de discrétisation par rapport à ν. Le réglage simultané de plusieurs petits paramètres est souvent source de difficultés numériques. De plus, un maillage fin est coûteux, et on veut pouvoir prendre un pas de discrétisation raisonnable indépendamment du paramètre ν qu'on fait tendre vers 0. Le premier objectif de cette thèse était donc de développer une méthode numérique pour l'approximation des équations de Maxwell résonantes qui soit indépendante d'un paramètre de régularisation et capture la solution analytique voulue. Pour en revenir au phénomène physique associé, le transfert d'énergie de l'onde aux ions par résonance hybride, le problème de la discrétisation par éléments finis des équations régularisées avec une petite friction est illustré par l'observation de résonances proches de l'antenne émettrice : il n'est pas clair que ces résonances soient justifiées ou qu'elles correspondent à un artéfact lié au manque de précision de la méthode numérique.

À cause du changement de signe de la permittivité, notre problème est proche de l'étude des interfaces entre un métamatériau et un diélectrique. Dans ce cas, la permittivité, homogène par morceaux, ne dégénère pas. Elle est négative d'un côté de l'interface, positive de l'autre avec une discontinuité. Le problème est alors bien posé sous des conditions de compatibilité qui dépendent des valeurs de ces permittivités et de la géométrie de l'interface. Mais lorsque le coefficient dégénère sur la frontière, et que la solution explose, on perd des informations nécessaires à la dérivation de ces conditions. Il n'est plus possible d'utiliser les traces de Dirichlet ou les estimations elliptiques de type Agmon-Douglis-Nirenberg utilisées par Bonnet-Ben Dhia, Chesnel, Ciarlet Jr. et Claeys [34, 33, 36, 35] et Nguyen [91, 92].

Notre problème est aussi à rapprocher de la théorie des équations elliptiques dégénérées avec un opérateur différentiel qui à u associe $-\nabla \cdot (\alpha \nabla u)$ et un coefficient α qui s'annule sur une partie du bord. En séparant notre problème de chaque côté de la courbe de résonance Σ, on obtient deux équations signées qui dégénèrent sur une partie du bord, le coefficient de permittivité étant proportionnel à la distance au bord. Lorsqu'on travaille dans l'espace de Sobolev à poids associé à ce coefficient, le théorème de Lax-Milgram et les résultats classiques de régularité elliptiques se transposent dans ce cadre, voir l'étude de Baouendi et Goulaouic [7]. Dans notre cas, on a un couplage de deux problèmes dégénérés par la partie du bord qui correspond à la singularité, la courbe de résonance. Et les solutions qui nous intéressent sont plus singulières que les fonctions de ces espaces de Sobolev à poids : ce sont celles dont la singularité est critique par rapport à ce poids précis. On relève aussi l'étude de la régularité Hölderienne locale des solutions d'EDP dégénérées par Fabes, Kenig et Serapioni dans [49], mais dans un cas où le poids est dans l'espace de Muckenhoupt A_2, c'est à dire localement intégrable et d'inverse localement intégrable et qui n'est pas notre cas ici. Il s'agit pour nous de trouver une condition de transmission à travers la singularité. Cela est rendu possible par un théorème d'injection compacte et par une décomposition de la solution u en parties régulières solutions des équations elliptiques signées de chaque côté de la courbe, et en une partie singulière caractérisée par le flux $\alpha \partial_n u$ à travers la courbe via une fonction auxiliaire.

C'est par ce biais, et par la proximité avec la communauté travaillant sur l'élaboration de méthodes numériques pour des problèmes d'ondes électromagnétiques, que la décomposition de domaine a été abordée dans cette thèse. La question principale qui est posée, de manière indépendante au problème de résonance hybride, est celle du traitement des coins sur la frontière d'un domaine dans les méthodes de Schwarz sans recouvrement, avec comme objectif à terme de traiter les coins sur les frontières de sous-domaines et les points de croisement. Pour pouvoir traiter numériquement des problèmes de propagation d'ondes acoustiques dans l'espace total $\mathbb{R}^2$ ou $\mathbb{R}^3$, avec des termes source et éventuellement des obstacles localisés, il est nécessaire de se ramener à un domaine borné Ω. À la frontière de celui-ci, des conditions doivent alors être imposées pour modéliser le comportement dans l'espace total, régi par une condition de radiation à l'infini. Nous nous intéressons ici à l'utilisation d'une approximation de cette condition de radiation par une condition aux bords absorbante d'ordre 2. À cet ordre, il devient nécessaire de définir un traitement spécifique aux coins présents sur $\partial\Omega$ pour une solution que l'on cherche dans $H^1(\Omega)$. Les coins sont source d'erreurs s'ils ne sont pas étudiés spécifiquement, et des phénomènes de réflexion numérique ont lieu. Pour les méthodes de décomposition de domaine, lorsque $\overline{\Omega} = \overline{\cup \Omega_i}$ avec $\Omega_i \cap \Omega_j = \emptyset$ pour tous $i \neq j$, en plus d'une condition d'absorption sur le bord $\partial\Omega$, des conditions de transmission sur chaque frontière entre deux sous-domaines adjacents doivent être prescrites pour faire communiquer entre eux les sous-domaines. Idéalement, on souhaite que ces conditions assurent la continuité de la solution ainsi que celle de sa dérivée normale à travers chaque frontière de sous-domaine $u_i = u_j$ et $\partial_{\mathbf{n}^i} u_i = -\partial_{\mathbf{n}^j} u_j$ sur $\partial\Omega_i \cap \partial\Omega_j$. De même, lorsque les sous-domaines ont des frontières en lignes brisées, ou de manière plus cruciale, aux points de croisement entre trois sous-domaines ou plus, sans traitement particulier des coins les résultats numériques sont très imprécis. Il est alors possible de considérer une subdivision en couches de Ω. Mais si l'on veut considérer des géométries obtenues avec des générateurs automatiques de maillages, par exemple, il est nécessaire pour augmenter la précision de répondre à la question du traitement des coins. L'objectif de notre travail est alors de définir une condition absorbante d'ordre 2 aux coins qui puisse être adaptée en une condition de transmission.

Avant de préciser la structure de ce document, on note qu'il existe une autre grande famille de modèles pour les particules qui ne sera pas abordée dans ces travaux : celle des modèles cinétiques

et des équations de Vlasov-Maxwell. Ce sont alors les fonctions de distribution des particules, qui décrivent leur répartition dans l'espace des phases, qui sont étudiées. Cela permet de décrire les comportements d'une manière plus fine, au prix d'une augmentation significative de la taille des problèmes : ce sont des modèles en dimension 7, en temps, en espace et en vitesse. Les modèles fluides sont eux en dimension 4, en temps et en espace, et ils sont suffisants pour décrire le comportement du plasma sous l'hypothèse dite de plasma froid, ou à température finie et à pression donnée, voir l'article de Bernstein et Trehan de 1960 [11], ou le cours plus récent de Dumont [41].

Structure du document et résultats principaux

Ce document est composé de deux parties indépendantes, dont les premiers chapitres sont des introductions. Les notations de chaque partie diffèrent sur quelques points. Certaines de ces notations sont précisées dans un préambule page 17.

Une **Première Partie** regroupe les travaux effectués autour des équations de Maxwell résonantes.

Le **Chapitre 1** commence par un exposé des principes de la fusion nucléaire par confinement magnétique, et détaille ensuite les étapes de modélisation pour arriver au système d'équations qui nous intéresse. Un lien est fait avec d'autres études mathématiques analysant ces phénomèmes, et on présente le cas de l'étude des équations en dimension un et en incidence normale. Pour finir, on décrit les méthodes et les outils utilisés dans la suite.

Les **Chapitres 2 et 3** sont des articles présentant respectivement l'étude des équations en dimension un et en incidence oblique $\mathbf{k} = (k_x, 0, k_z)$, et l'étude des équations en dimension deux, avec un tenseur homogène dans la direction z, et en incidence normale $\mathbf{k} = (k_x, 0, 0)$.

Dans le cas unidimensionnel, la résolution des équations de Maxwell passe par celle dans H^1 du système

$$-\mathbf{u}''(x) + \frac{1}{\alpha(x)}\mathsf{N}(x)\mathbf{u}(x) = 0 \quad \text{dans} \quad (-1,1) - \{0\} \tag{1}$$

avec un coefficient réel $\alpha(x) = rx + O(x^2)$, pour un r non nul, et avec une matrice complexe N régulière et bornée, à valeurs dans $\mathbb{C}^{2\times 2}$, dépendant elle-même de α, telle que $\mathsf{N}(0)$ est de rang 1. L'inconnue $\mathbf{u}$, à valeurs dans $\mathbb{C}^2$, correspond aux composantes régulières E_y et B_y, et les autres composantes E_x, E_z, B_x et B_z sont définies à partir de celles-ci de de leurs dérivées. La composante la plus singulière est E_x, définie à partir de E_y/α et de B_y/α. Associé à des conditions aux bords mixtes en $x = \pm 1$, ce problème, qui consiste en deux EDO (équations différentielles ordinaires) d'ordre deux associées à deux conditions aux bords et à une relation de continuité en $x = 0$, est donc mal posé : il reste un degré de liberté à déterminer. On le régularise en prenant $\alpha + i\nu$ et la matrice associée N^ν à la place de α et de N, et en gardant les mêmes conditions aux bords. Sous quelques hypothèses sur les conditons aux bords et la régularité des coefficients, les deux résultats principaux sont les suivants.

Théorème 1 (Corollaire 2.2.5)**.** *L'unique solution $\mathbf{u}^\nu$ du système régularisé converge faiblement dans H^1 vers une fonction $\mathbf{u}^+$. Cette fonction est une solution forte du système* (1) *en dehors de $x = 0$ et vérifie les conditions aux bords associées. On l'appelle solution de viscosité limite.*

Théorème 2 (Théorème 2.3.3)**.** *La solution de viscosité limite $\mathbf{u}^+$ est l'unique solution d'une*

formulation variationnelle mixte de la forme

$$\begin{array}{l}\textit{Trouver } ((\mathbf{u},s),\boldsymbol{\lambda}) \in V \times Q \textit{ tel que}\\ \left\{\begin{array}{lcll} a^+((\mathbf{u},s),(\mathbf{v},t)) - \overline{b(\mathbf{v},\boldsymbol{\lambda})} & = & 0, & \forall (\mathbf{v},t) \in V,\\ b(\mathbf{u},\boldsymbol{\mu}) & = & \ell(\boldsymbol{\mu}), & \forall \boldsymbol{\mu} \in Q^0. \end{array}\right.\end{array}$$

La forme sesquilinéaire a^+ est indexée ainsi pour insister sur le fait que c'est là qu'est comprise l'information qui manquait dans le système initial et qui a été obtenue par absorption limite $\nu \to 0^+$. La seconde ligne de la formulation, qui implique la forme sesquilinéaire b et la forme antilinéaire ℓ, correspond au système initial (1) dont on impose la vérification sous forme de contrainte. Un troisième résultat important de cette étude est la stabilité de la formulation mixte, schématisée en Figure 1. Le paramètre ν correspond à la modélisation de la friction entre les ions et les electrons, que l'on prend en compte dans la dynamique des particules, et dans un autre régime que celui qui nous intéresse ici, il peut ne pas être négligeable. Il est pratique d'avoir une implémentation similaire pour ces différents régimes. Pour $\nu > 0$, une formulation mixte similaire avec des formes a^ν, b^ν et un espace Q^ν correspondants est alors décrite. Elle correspond alors d'une certaine manière à une formulation *asymptotic preserving* [73] du problème régularisé avec un petit $\nu > 0$. Pour les

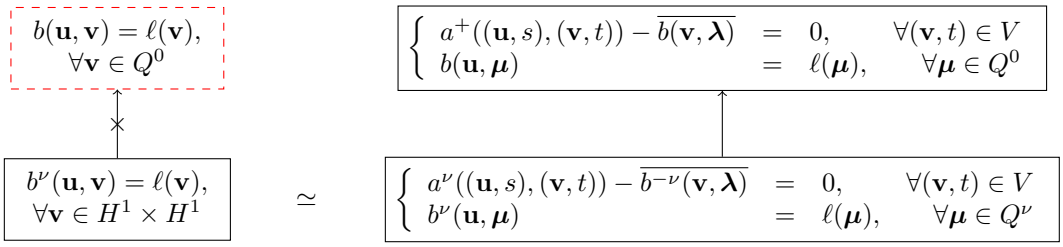

FIGURE 1 – Schéma des liens entre les différentes formulations variationnelles associées à (1) et à sa régularisation. L'inconnue principale $\mathbf{u}$ est toujours cherchée dans $H^1 \times H^1$. Le cadre autour de la formulation en haut à gauche est en pointillés rouges pour signifier qu'elle est mal posée contrairement aux trois autres.

deux formulations avec régularisation, non mixte et mixte en bas en Figure 1, l'inconnue principale $\mathbf{u}$ de l'unique solution prend la même valeur $\mathbf{u}^\nu$. La formulation non mixte dans $H^1 \times H^1$ n'a pas de limite quand $\nu \to 0$ à cause du coefficient $1/\alpha$. Dans la formulation mixte, l'espace test $H^1 \times H^1$ est réduit à Q^ν, qui converge vers Q^0 et pour lequel $b(\mathbf{u},\mathbf{v})$ a un sens pour $\mathbf{u} \in H^1 \times H^1$ et $\mathbf{v} \in Q^0$. On souligne que le choix de l'espace test $Q^\nu \subset H^1 \times H^1$ requiert un soin particulier : le choix simple de prendre $Q^\nu = Q^0$ ne convient pas par exemple. D'un point de vue physique, ces formulations, et plus précisément les formes a^+ et a^ν, sont en fait liées à la dissipation d'énergie associée à l'onde électromagnétique qui a lieu à la résonnance.
Ce chapitre est un article soumis en avril 2018 et accepté en mai 2019 par le *Journal of Computational and Applied Mathematics* [93] complémenté d'une annexe sur le modèle mathématique correspondant au second cas test numérique.

En dimension deux, quelques simplifications amènent à l'étude de l'équation aux dérivées partielles suivante

$$-\nabla \cdot (\alpha(\mathbf{x}) \nabla u(\mathbf{x})) - u(\mathbf{x}) = 0 \quad \text{dans} \quad \Omega \subset \mathbb{R}^2. \tag{2}$$

Ici le coefficient réel α est proportionnel à la distance signée à une courbe Σ régulière, simple et fermée, à l'intérieur de Ω. La dégénérescence a lieu sur cette courbe, et le domaine Ω est

séparé par Σ en deux sous-domaines, Ω_1 où α est positif et Ω_2 où α est négatif. L'équation est elliptique dégénérée sur Ω_2 et elle l'est aussi à un terme compact près sur Ω_1. A priori, il n'est plus possible d'identifier de composantes du champ EM régulières en fonction desquelles exprimer les composantes singulières comme en dimension une : la dépendance en une seconde variable d'espace couple fortement les équations sur les différentes composantes du champ E_x, E_y et B_z. Chaque champ aura une composante régulière et une composante singulière. C'est l'étude de l'équation (2) en 1D qui va nous indiquer le type de singularité attendu, à savoir un logarithme en la distance à Σ, et surtout indiquer l'ansatz pour la décomposition en parties régulière et singulière. On utilise ensuite le fait que bien que les traces de Dirichlet et de Neumann sur Σ du logarithme de la distance n'existent pas, la trace de Neumann à poids $\alpha\partial_n$ existe, et on introduit une variable auxiliaire g définie sur la courbe Σ et qui prend la valeur $\alpha\partial_n u$. La partie régulière de la solution est dans le Sobolev à poids des fonctions de carré intégrable v telles que $|\alpha||\nabla v|^2$ soit intégrable, et la partie singulière est caractérisée par cette variable auxiliaire définie sur Σ facteur d'un logarithme. Comme en dimension un, c'est par un principe d'absorption limite via la régularisation $\alpha + i\nu$ qu'on obtient la formulation à $\nu = 0^+$. On a le résultat d'existence et d'unicité suivant.

Théorème 3 (Théorème 3.4.3)**.** *La limite formelle $\nu = 0^+$ de la solution de l'équation* (2) *régularisée est l'unique solution d'une formulation variationnelle mixte de la forme*

$$\begin{array}{l} \textit{Trouver } (((\mathbf{u},g),h),\boldsymbol{\lambda}) \in V \times Q^0 \textit{ tel que} \\ \left\{ \begin{array}{lcll} a_r^+(((\mathbf{u},g),h),((\mathbf{v},k),l)) - \overline{b((\mathbf{v},k),\boldsymbol{\lambda})} & = & 0, & \forall((\mathbf{v},k),l) \in V, \\ b((\mathbf{u},g),\boldsymbol{\mu}) & = & \ell(\boldsymbol{\mu}), & \forall \boldsymbol{\mu} \in Q^0. \end{array} \right. \end{array}$$

Par rapport à la formulation du Théorème 2 du chapitre précédent, l'inconnue principale $\mathbf{u}$, régulière, est remplacée par $(\mathbf{u}, g)$ qui comprend les composantes régulières sur Ω_1 et sur Ω_2 dans $\mathbf{u}$ et la caractérisation de la singularité le long de Σ dans g, et les scalaires s et t sont remplacés par h et l des fonctions à valeur sur Σ. La forme sesquilinéaire b correspond aux équations elliptiques dégénérées sur chaque sous-domaine, et la forme a_r^+ correspond encore une fois à une information recouverte par absorption limite. Le sous-indice r indique une régularisation le long de la courbe de singularité. Elle est à relativiser par rapport à la régularisation de la singularité via le paramètre ν. Bien que cette régularisation ait été utilisée pour obtenir de la coercivité, il semble qu'elle n'a pas d'incidence sur les résultats numériques.
Ce chapitre est un article soumis [94].

En **Chapitre 4**, on présente ensuite quelques résultats d'analyse numérique associés aux études en dimension un et deux. Un premier résultat issu de la littérature est cité concernant l'estimation d'erreur pour la discrétisation du problème par éléments finis dans le cas où le problème est bien posé. Les éléments et les maillages choisis pour la discrétisation de chaque problème sont présentés. Une table de convergence à double entrée concernant les trois formulations bien posées en dimension un, voir la Figure 1, est aussi donnée. On aborde ensuite la relaxation de la régularisation dans le cas 2D, et un second résultat issu de la littérature est présenté concernant l'estimation d'erreur dans le cas où le problème n'est pas coercif dans la même norme qu'il n'est continu.

Cette partie se termine sur une question de modélisation en **Chapitre 5**. On montre que la méthode des fonctions manufacturées peut être adaptée à un modèle prenant en compte plus de physique, avec l'ajout d'effets de température finie : c'est le modèle de plasma tiède. Dans ce modèle, sous certaines hypothèses reliant le paramètre de viscosité et le paramètre de température, les termes de viscosité ne sont plus linéaires d'ordre 0 comme pour le plasma froid mais différentiels.

Une **Seconde Partie** est dédiée au traitement des coins dans les méthodes de décomposition de

domaine pour la propagation d'ondes.

Le **Chapitre 6** est une introduction aux méthodes de décomposition de domaine. Après un bref retour sur l'historique de ces méthodes, imaginées pour résoudre l'équation de la chaleur sur des géométries complexes par Schwarz à la fin du dix-neuvième siècle et utilisées depuis les années 90 pour faire du calcul parallèle et du préconditionnement de système linéaire, on présente ensuite plus en détail l'usage qui en est fait aujourd'hui et les difficultés rencontrées dans le cadre de l'approximation de solutions de l'équation de Helmholtz.

Dans le **Chapitre 7**, une méthode est proposée qui prend en compte les coins sur le bord du domaine en dimension deux. On commence par définir une condition aux bords absorbante globale pour un domaine polygonal, puis celle-ci est adaptée pour une résolution du problème en utilisant une méthode de décomposition de domaine. Les conditions présentées sont basées sur des relations algébriques et font intervenir des variables auxiliaires.
Ce chapitre fait l'objet d'un article en préparation.

General introduction

The questions at the origin of this thesis are the behavior and the approximation of singular solutions to resonant Maxwell's equations in a heterogeneous and anisotropic plasma. They are linear partial differential equations that degenerate inside the domain of interest.

This system of equations is one of the various models used to study nuclear fusion [106, 17, 110]. It is important to be able to have accurate and robust numerical approximations of their solutions because the temperature and density conditions inside a tokamak are such that it is unconcievable to measure everything. Equations describing the behaviour of a plasma, such as kinetic equations, are known and have been studied thoroughly. But the variety of characteristic scales and the non-linearity of these models make it difficult to discretize them, we thus use reduced models. There are many different regimes, those for the reflection and absorption of waves in the core of the plasma [107], those for the interactions of the plasma with the walls where there is no charge equilibrium any longer [4, 116], or those for the turbulences due to high temperature gradients and which affect the confinement of the plasma [58]. Moreover, some phenomena correspond to specific frequencies and are studied in a harmonic regime in time, while others require a study in long time. Finally, some models are based on realistic geometries, and exploit, for example, the Hamiltonian structure in non-dissipative regimes, take advantage of the fact that the particle dynamics follow the field lines [18, 21], while others are based on simplified geometries. A source for original questions consists in finding ways to adress each of these problems in such a way that they can be accurately discretized. Another interest of this subject is the relevance of the industrial energy issue, which allows for transdisciplinary collaborations on research projects such as ITER and the development of associated numerical codes.

The advantage of a plasma is that it is a state of matter where charged particles, here ions and electrons, are free. Particles can move under the effect of an electromagnetic field, and atomic nuclei can eventually fuse. Generating these nuclear fusion phenomena and recovering the energy created is the objective of tokamaks. In these machines, a strong magnetic field is imposed by external coils and creates an asymmetry in the particle response. In this work, we prescribe a simplified magnetic field $\mathbf{B}_0$, constant and of colinear direction to the toroidal axis z. Each of the models mentioned above includes a description of the evolution of the electromagnetic field and a description of the dynamics of the particles, coupled by the current which is generated by the particles and is a source for the equations on the field. Maxwell's equations describe the electromagnetic field. In the regime of hybrid resonances, which is the one we are interested in, we choose to use a fluid model for the particles. This coupling between an electromagnetic field and a conductive fluid is called magneto-hydrodynamics. We are more specifically interested in the Euler-Maxwell system. We work in the harmonic in time regime around the frequency $\omega > 0$ of an incident plane wave, for which we note $\mathbf{k} \in \mathbb{C}^3$ the associated wave vector. The two systems of equations are then combined to form what is called in this thesis the system of resonant Maxwell equations, which only acts on the electric field unknown

$$\nabla \wedge \nabla \wedge \mathbf{E} - \underline{\underline{\varepsilon}}\mathbf{E} = 0 \quad \text{in} \quad \Omega \subset \mathbb{R}^3,$$

where the heterogeneous and anisotropic permittivity tensor $\underline{\underline{\varepsilon}}$ depends on space via the plasma

frequency ω_p whose intensity is proportional to the square root of the electronic density, and also depends on the magnetic field $\mathbf{B}_0$ via the cyclotron frequency ω_c whose intensity is proportional to the fields intensity. This tensor degenerates inside the domain, along the hybrid resonance curve $\Sigma = \left\{\mathbf{x} \in \Omega,\, \omega^2 = \omega_p^2(\mathbf{x}) + \omega_c^2\right\}$, in the sense that its diagonal coefficient α behaves as a signed distance to this curve: positive on one side, negative on the other side, and zero on the curve. Some components of the electric field will be regular, but some will be singular and non integrable. For practical reasons, we reintroduce a field that we call magnetic field, defined as $\mathbf{B} = \nabla \wedge \mathbf{E}$ instead of $(i\omega)^{-1}\nabla \wedge \mathbf{E}$.

Prior to this work, the study of the problem was carried out in dimension one, i.e. under the hypothesis of a plasma varying only in one direction $\underline{\underline{\varepsilon}} = \underline{\underline{\varepsilon}}(x)$ with x in $I \subset \mathbb{R}$, and under the hypothesis of an incident wave with a propagation direction $\mathbf{k} = (k_x, 0, 0)$, normal to the bulk magnetic field. The normal incidence hypothesis allows to decouple Maxwell's equations into a system on (E_x, E_y) called extraordinary mode (X-mode) and an equation on E_z called ordinary mode (O-mode). An analytical solution was described, but the numerical approximation remained problematic for two reasons. First, because of the degeneracy of the problem and the non uniqueness of the solution. Second, because the analytical solution we are trying to capture is singular: the E_x component is the sum of a principal value in $1/x$ and of a Dirac mass, not integrable locally, and of an square integrable remainder. A common method for the numerical resolution of this problem is to desingularize the equations, by adding friction between ions and electrons. This corresponds to taking as diagonal coefficient of $\underline{\underline{\varepsilon}}$ the term $\alpha + i\nu$, for $\nu > 0$. Incidentally, it is also by using this regularization that the analytical solution was obtained, making the parameter ν go to zero via a limit absorption principle. But this small parameter imposes a non-trivial constraint on the discretization parameters at the discrete level. In general terms, we do not want any constraint on the mesh size, to be able to obtain results without having to adjust the discretization step compared to ν. The simultaneous adjustment of several small parameters often causes numerical difficulties. Moreover, a fine mesh is costly, and we want to be able to take a reasonable discretization step independently of the parameter ν which is intended to go to 0. The first objective of this thesis was therefore to develop a numerical method for the approximation of resonant Maxwell equations that is independent of this regularization parameter, and which captures the desired analytical solution. In regard of the associated physical phenomenon, which is the transfer of energy from the wave to the ions by hybrid resonance, the problem of the finite element discretization of the regularized equations with small friction is illustrated by the observation of resonances close to the transmitting antenna: it is not clear whether these resonances are justified or whether they correspond to an artifact related to the lack of precision of the numerical method.

Because of this sign changing permittivity, our problem is related to the study of interfaces between a metamaterial and a dielectric. In this case, the permittivity, homogeneous by parts, does not degenerate. It is negative on one side of the interface, positive on the other, with a discontinuity in between. The problem is then well posed under some compatibility conditions that depend on the values of these permittivities and on the geometry of the interface. But when the coefficient degenerates on the border as in our model, and that the solution blows up, we lose information required to derive these conditions. It is no longer possible to use Dirichlet's traces or Agmon-Douglis-Nirenberg's elliptic estimates used by Bonnet-Ben Dhia, Chesnel, Ciarlet Jr. and Claeys [34, 33, 36, 35] and Nguyen [91, 92].

Our problem is also connected to the theory of degenerate elliptic equations with a differential operator $-\nabla \cdot (\alpha \nabla u)$ and a coefficient α which vanishes on a subset of the boundary. By splitting our problem on each side of the resonance curve, we obtain two signed equations that degenerate

on a subset of the boundary, the diagonal coefficient of the permittivity being proportional to the distance to the boundary. Working in the weighted Sobolev's space associated to this coefficient, the Lax-Milgram theorem and classical elliptic regularity results can be adapted to this framework, see the study by Baouendi and Goulaouic [7]. In our case, however, we consider a coupling of two degenerate problems through the part of the boundary that corresponds to the singularity, the resonance curve. The solutions we are interested in are more singular than the functions in these weighted Sobolev spaces: their singularity is critical with respect to the weight. We also note the study of the local Hölderian regularity of solutions to degenerate PDEs by Fabes, Kenig and Serapioni in [49], but in a case where the weight is in the space of Muckenhoupt A_2, i.e. locally integrable and of locally integrable inverse, which is not our case here. In our case, it is a question of finding a transmission condition through the singularity. This question is solved by using a compact injection theorem and by decomposing the solution u into a regular part that is a solution of the signed equations on each side of the curve, and into a singular part characterized via an auxiliary function by the flow $\alpha\partial_n u$ through the resonant curve.

It is through this bias, and by the proximity to the community working on the development of numerical methods for electromagnetic wave problems, that domain decomposition has been addressed in this thesis. The main question here, which arises independently of the hybrid resonance problem, is the one of corner treatment in Schwarz's methods without overlap. The issue of corners on the boundary of the domain is tackled in this work, with in perspective the extension of the results to corners on subdomain boundaries, and ideally to cross-points between more than three subdomains. In order to be able to address numerically problems of acoustic wave propagation in the total space $\mathbb{R}^2$ or $\mathbb{R}^3$ with localized source terms and obstacles, it is necessary to start by truncating the free space into a bounded computational domain Ω. On the boundary of this domain, conditions must therefore be prescribed to model the behaviour in the free space, which is governed by a radiation condition at infinity. We are interested here in the approximation of this radiation condition by a boundary condition, thus called absorbing, of second order. At this order, for an $H^1(\Omega)$ solution, it becomes necessary to define a specific treatment at the corners of $\partial\Omega$. Without any treatment, corners are a source of error, and a phenomenon of numerical reflection occurs. For domain decomposition methods, when $\overline{\Omega} = \overline{\cup\Omega_i}$ with $\Omega_i \cap \Omega_j = \emptyset$ for all $i \neq j$, in addition to an absorbing boundary condition on the boundary $\partial\Omega$, transmission conditions on each interface between two adjacent subdomains must also be prescribed for the subsolutions to communicate. Ideally, these conditions should ensure the continuity of the solution as well as the continuity of its normal derivative across each subdomain interface $u_i = u_j$ and $\partial_{\mathbf{n}^i} u_i = -\partial_{\mathbf{n}^j} u_j$ on $\partial\Omega_i \cap \partial\Omega_j$. Once again, when the interfaces between subdomains are broken lines, or more crucially, at cross points where three or more subdomains meet, without any special corner treatment the numerical results are not accurate. A possibility is to consider layered decompositions of the domain Ω. But if we want to consider geometries obtained with automatic mesh generators, for example, it is necessary to tackle the question of corners in order to increase the accuracy. The idea of our work is thus to define a second order absorbing boundary condition for corners that can be adapted into transmission conditions.

Before describing more precisely the structure of this document, we point out that there is another large family of particle models that will not be addressed in this work: kinetic models and Vlasov-Maxwell equations. In these models, it is the particle distribution functions, which describe their distribution in the phase space, that are studied. This makes it possible to describe behaviours more accurately, at the cost of a significant increase of the size of the problems: they are models in 7 dimension, in time, space and speed. The fluid models are in 4 dimension, time and space, and are sufficient to describe the behaviour under the cold plasma hypothesis, or at finite temperature

and given pressure, see Bernstein and Trehan's 1960 paper [11], or Dumont's more recent lecture notes [41].

Structure of the document and main results

This document is composed of two independent parts, the first chapters of which are introductory. The notations of each part differ on a few points. Some of these notations are defined in the preamble page 17.

A **First Part** gathers the work on Maxwell's resonant equations.

Chapter 1 begins with a presentation of the principles of nuclear fusion by magnetic confinement, and then details the modelling steps to arrive to the system of equations of our interest. A link is made with prior mathematical studies analyzing this phenomenon. The methods and tools used in the sequel are described, and each idea is illustrated on the equations in dimension one and in normal incidence to facilitate understanding.

Chapters 2 and 3 are research papers presenting respectively the study of equations in dimension one and oblique incidence $\mathbf{k} = (k_x, 0, k_z)$, and the study of equations in dimension two, with a homogeneous tensor in the z direction, and in normal incidence $\mathbf{k} = (k_x, 0, 0)$.

In the unidimensional case, the resolution of Maxwell's equations comes down to the resolution in H^1 of

$$-\mathbf{u}''(x) + \frac{1}{\alpha(x)}\mathsf{N}(x)\mathbf{u}(x) = 0 \quad \text{in} \quad (-1,1) - \{0\} \tag{1}$$

with a real coefficient $\alpha(x) = rx + O(x^2)$, for a non zero coefficient r, and with a regular and bounded complex matrix N with values in $\mathbb{C}^{2\times 2}$, itself depending on α, and such that $\mathsf{N}(0)$ is of rank 1. The unknown $\mathbf{u}$ with values in $\mathbb{C}^2$ corresponds to the regular components E_y and B_y, and the other components E_x, E_z, B_x and B_z are recovered from these two and from their derivatives. The most singular component is E_x, defined as a combination of E_y/α and of B_y/α. Coupled to mixed boundary conditions at $x = \pm 1$, this problem, which consists of two second order ODEs (ordinary differential equations), two boundary conditions, and a continuity relation at $x = 0$, is therefore ill-posed: a degree of freedom remains to be determined. The problem is regularized by taking $\alpha + i\nu$ and the associated matrix N^ν instead of α and N, and keeping the same boundary conditions. Under some hypotheses on the boundary conditions and on the regularity of the matrix' coefficients, the two main results are the following.

Theorem 1 (Corollary 2.2.5)**.** *The unique solution $\mathbf{u}^\nu$ of the regularized system of equations converges weakly in H^1 towards a function $\mathbf{u}^+$. This function is a strong solution to system* (1) *away from $x = 0$ and verifies the associated boundary conditions. It is called the limit viscosity solution.*

Theorem 2 (Theorem 2.3.3)**.** *The limit viscosity solution $\mathbf{u}^+$ is the unique solution of a mixed variational formulation of type*

$$\begin{array}{l} \textit{Find } ((\mathbf{u},s),\boldsymbol{\lambda}) \in V \times Q \textit{ such that} \\ \left\{ \begin{array}{lcll} a^+((\mathbf{u},s),(\mathbf{v},t)) - \overline{b(\mathbf{v},\boldsymbol{\lambda})} & = & 0, & \forall (\mathbf{v},t) \in V, \\ b(\mathbf{u},\boldsymbol{\mu}) & = & \ell(\boldsymbol{\mu}), & \forall \boldsymbol{\mu} \in Q^0. \end{array} \right. \end{array}$$

The sesquilinear form a^+ is indexed with a plus sign to emphasize that it is there that lies the information that was missing in the initial system, and that was obtained by limit absorption $\nu \to 0^+$. The second line of the formulation, which involves the sesquilinear form b and the antilinear form l, corresponds to the initial system (1). The fact we seek solutions of this system is thus imposed as a constraint in the mixed variational form. A third important result of this study is the stability of the mixed formulation, sketched in Figure 2. The parameter ν corresponds to the friction between ions and electrons, which is taken into account in the particle dynamics. In another regime than the one of interest here, it may not be small. It is convenient to have a similar implementation for the problem with viscosity and for the problem at the limit. For $\nu > 0$, a similar mixed formulation with corresponding forms a^ν and b^ν and a space Q^ν is described. It can be thought of as an asymptotic preserving formulation [73] of the regularized equation for small $\nu > 0$. For both formulations with regularization, the mixed one and the classical one at the bottom of

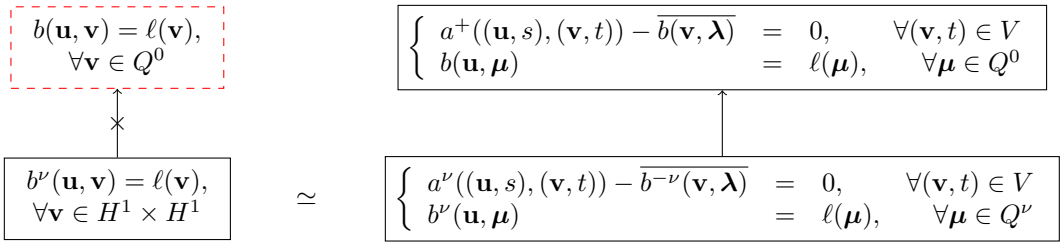

Figure 2 – Scheme of the relations between the different variational formulations associated to (1) and its regularization. The main unknown $\mathbf{u}$ is always seeked in $H^1 \times H^1$. The frame around the formulation up left is dashed to signify it is ill-posed, unlike the three other formulations.

Figure 2, the main parts $\mathbf{u}$ of the unique solutions to these problems take the same value $\mathbf{u}^\nu$. The classical non mixed formulation in $H^1 \times H^1$ has no limit when $\nu \to 0$ due to the singular coefficient $1/\alpha$. In the mixed formulation, the test space is reduced from $H^1 \times H^1$ to Q^ν, that converges towards Q^0 for which $b(\mathbf{u},\mathbf{v})$ is well defined for $\mathbf{u} \in H^1 \times H^1$ and $\mathbf{v} \in Q^0$. We point out that the choice of the test space $Q^\nu \in H^1 \times H^1$ requires particular attention: the simple choice of taking $Q^\nu = Q^0$ is not appropriate for example. From a physical point of view, these formulations, and more precisely the forms a^+ and a^ν, are in fact related to the energy dissipation associated with the electromagnetic wave that takes place at resonance.
This chapter is an article submitted in April 2018 and accepted in May 2019 in the *Journal of Computational and Applied Mathematics* [93] to which is appended a section detailing the changes made in the model for the second numerical test case.

In dimension two, a few simplifications of the model lead to the study of the following partial differential equation

$$-\nabla \cdot (\alpha(\mathbf{x}) \nabla u(\mathbf{x})) - u(\mathbf{x}) = 0 \quad \text{in} \quad \Omega \subset \mathbb{R}^2. \tag{2}$$

Here the real coefficient α is proportional to the signed distance to a regular, simple and closed curve Σ located inside Ω. This curve is the support of the degeneracy, and the domain Ω is separated by Σ into two subdomains, Ω_1 where α is positive and Ω_2 where α is negative. The equation is degenerate elliptic on Ω_2 and it is elliptic up to a compact term on Ω_1. A priori, it is no longer possible to identify regular EM field components according to which the singular components can be expressed as in one dimension: the dependence in a second space variable strongly couples the equations on the different components E_x, E_y and B_z. Each component will have a regular part and a singular part. The study of equation (2) in 1D indicates the type of the expected singularity, namely a logarithm of the distance to Σ. In particular, it gives a necessary insight to be able to

define an ansatz for the decomposition into regular and singular parts. Although the Dirichlet and Neumann traces of this distance to Σ logarithm do not exist, the weighted Neumann trace $\alpha\partial_n$ does. Therefore, we introduce an auxiliary variable g supported on the curve Σ which takes the value $\alpha\partial_n u$. The regular part of the solution is in the weighted Sobolev space of square integrable functions v such that $|\alpha||\nabla v|^2$ is integrable, and the singular part is characterized by this auxiliary variable defined on Σ with a logarithm in factor. As in dimension one, it is by a limiting absorption principle via the regularization $\alpha + i\nu$ that we obtain the formulation at $\nu = 0^+$. We have the following result of existence and uniqueness.

Theorem 3 (Theorem 3.4.3)**.** *The formal limit $\nu = 0^+$ of the solution to the regularization of equation* (2) *is the unique solution to a mixed variational formulation of type*

$$\begin{array}{l} \textit{Find } (((\mathbf{u},g),h),\boldsymbol{\lambda}) \in V \times Q^0 \textit{ such that} \\ \left\{ \begin{array}{lcll} a_r^+(((\mathbf{u},g),h),((\mathbf{v},k),l)) - \overline{b((\mathbf{v},k),\boldsymbol{\lambda})} & = & 0, & \forall((\mathbf{v},k),l) \in V, \\ b((\mathbf{u},g),\boldsymbol{\mu}) & = & \ell(\boldsymbol{\mu}), & \forall \boldsymbol{\mu} \in Q^0. \end{array} \right. \end{array}$$

Compared to the formulation of Theorem 2 of the previous chapter, the main unknown $\mathbf{u}$, regular, is replaced by $(\mathbf{u}, g)$ which includes the regular components of u on Ω_1 and on Ω_2 and g, the characterization of the singularity along Σ. The scalars s and t are replaced by h and l, functions supported on Σ. The sesquilinear form b corresponds to the degenerate elliptic equations on each subdomain, and the form a_r^+ corresponds once again to the information recovered by using the limit absorption principle. The lower index r indicates a regularization along the singularity curve. Unlike in the case of the desingularization via the parameter ν, this regularization along Σ does not impact the singularity of the solution. Furthermore, although this regularization was used to obtain coercivity, it does not appear to have an impact on the numerical results.
This chapter is a submitted article [94].

In **Chapter 4**, some numerical analysis results from the literature associated with the one and two dimensional studies are presented. The first result concerns the error estimate of the discretization of a mixed variational formulation by finite elements in the case the problem is well posed. The elements and meshes chosen for the discretization of our formulations derived in 1D and in 2D are presented. A double entry convergence table for the three well posed formulations in dimension one, see Figure 2, is then given. Finally, we discuss the relaxation of the regularization in the 2D case, and cite a second result from the literature that concerns error estimates in the case where the problem is not coercive in the same norm as it is continuous.

This section ends with a modelling issue in **Chapter 5**. The first step towards an adaptation of the manufactured functions method to a model that takes into account more physics are given. We consider the addition of finite temperature effects: this is the warm plasma model. In this model, under some assumptions binding the viscosity and the temperature parameters, the viscosity terms are no longer linear and of respect to the electric field $\mathbf{E}$ as in the cold plasma model: they involve the differential term $\nabla \otimes \nabla \mathbf{E}$.

The **Second Part** of this thesis is devoted to corner treatment in domain decomposition methods for the study of acoustic wave propagation.

Chapter 6 is an introduction to domain decomposition methods. After a brief historical review of these methods, designed originally to solve the heat equation on complex geometries by Schwarz at the end of the nineteenth century and used since the 1990s for parallel computing and linear system preconditioning, we then present the difficulties encountered in approximating solutions to the Helmholtz equation with these methods.

In **Chapter 7**, a method is proposed taking into account corners on the boundary of the domain in 2D. First, a global absorbing boundary condition is defined for a polygonal domain. It is then adapted in a domain decomposition framework. The conditions presented are based on algebraic relations and involve auxiliary variables. This chapter is the subject of an article under preparation.

Notations

Part I

$\omega, \mathbf{k}$	frequency and wave vector of the wave sent by the antenna, fixed
$\mathbf{E}, \mathbf{B}$	harmonic in time electromagnetic field, depends on space
$\mathbf{B}_0$	imposed static magnetic field, constant
$\mathbf{u}_e$	harmonic in time speed of electrons, depends on space
m_e	electron mass
N_e	density of electrons, depends on space
q_e	electron charge
$\mathbf{J}$	harmonic in time current, depends on space
ε_0, μ_0	vacuum permittivity and permeability
c	speed of light in vacuum
$\underline{\underline{\varepsilon}}$	permittivity tensor, space dependent
$\omega_c = \frac{\lvert q_e \rvert \lVert \mathbf{B}_0 \rVert}{m_e}$	electronic cyclotron frequency, constant
$\omega_p = \sqrt{\frac{N_e q_e^2}{m_e \varepsilon_0}}$	electronic plasma frequency, space dependent
$\underline{\underline{p}}$	pressure tensor
k_B	Boltzmann constant
$T_{\mathrm{ref}}, v_{\mathrm{th}}$	temperature of the electrons and thermal speed of the electrons

$$\mathbf{u}^{\perp} = \begin{pmatrix} 0 & -1 \\ 1 & 0 \end{pmatrix} \mathbf{u}$$

$$\mathbf{curl}\, u = \begin{pmatrix} \partial_y \\ -\partial_x \end{pmatrix} u \quad \text{and} \quad \operatorname{curl} \mathbf{u} = \begin{pmatrix} -\partial_y \\ \partial_x \end{pmatrix} \cdot \mathbf{u}$$

Part II

$\mathbf{i}$	$\mathbf{i}^2 = -1$
$\omega, \eta, \mathbf{d}_\eta$	frequency, angle and wave vector of the incident plane wave
i, j, N_{dom}	subdomain indexes and number of subdomains
k, ℓ, K	exterior boundary edges indexes and number of edges
p	algorithm iteration index
Ω, Ω_i	polygonal domain and subdomains
$\Gamma, \Gamma_k, \Gamma_k^i$	boundary of Ω, edges of the boundary and intersections with $\partial\Omega_i$
$\mathbf{n}, \mathbf{t}$	normal and tangential unit vectors on the boundary Γ
$\mathbf{n}_k, \mathbf{t}_k$	normal and tangential unit vectors on the k^{th} edge of the exterior boundary
$\mathbf{n}^i, \mathbf{t}^i$	normal and tangential unit vectors on the boundary $\partial\Omega_i$
$\boldsymbol{\tau}_k$	outgoing unit tangential vector at the extremities of the k^{th} edge
$\mathbf{A}_{k\ell}$	corner at the intersection of edges Γ_k and Γ_ℓ
$\theta_{k\ell}$	interior angle at corner $\mathbf{A}_{k\ell}$, in $(-2\pi, 0)$
$\mathbf{A}_{k\ell}^{ij}, \mathcal{C}_k^i$	an endpoint and the set of endpoints of Γ_k^i that are corners of Γ, i.e. non flat corners
$\mathbf{B}_k^{ij}, \mathcal{F}_k^i$	an endpoint and the set of endpoints of Γ_k^i that are interior points of Γ_k, i.e. flat corners

I Resonant Maxwell's equations

1 Introduction to resonant Maxwell's equations

This chapter is an overview of the physics at stake and of prior mathematical results and tools. We start by giving a broad description of the mechanisms involved in a tokamak. We then focus on the study of waves in plasmas, in particular on the reflection and absorption phenomena, and derive the system of Maxwell's equations in the hybrid resonance regime, that we call resonant Maxwell's equations. A synthesis of previous and related mathematical work is then presented, pointing out the difficulties of this system. Finally, the method of manufactured solutions is introduced, and developed on the simplest configuration of resonant Maxwell's equations: transverse electric (TE) waves in a 1D plasma.

1.1 Nuclear fusion and tokamaks

Nuclear fusion is a reaction that binds two light atoms together, releasing energy. To fuse Deuterium and Tritium nucleides, which is the fuel tested in current projects, extreme conditions of temperature and pressure are needed. For the ITER [71] project: the temperature must be of the order of 10^8 degrees Celsius, ten times the temperature in the core of the sun; the density must be greater than 10^{20} particles per cubic meter. This implies in particular that it is complicated to insert probes inside the tokamak to make measurements, and that numerical models describing the plasma inside the machine are needed.

The machine is a toroidal chamber subject to strong magnetic fields[1] to confine the matter inside. To do so, as pictured in Figure 1.1, different types of magnetic fields are generated by coils and are combined to form a helicoidal field that confines the plasma [69]:

- the toroidal coils create a toroidal magnetic field of the order of 10^5 times the terrestrial magnetic field,
- the interior poloidal coils create a toroidal current of the order of 10^6 Ampères which induces a poloidal magnetic field,
- the exterior poloidal coils keep the plasma away from the wall to limit the deterioriation of the materials.

[1] which is what tokamak stands for in russian: **то**роидалнаиа **ка**мера с **ма**гнитными **к**атушками

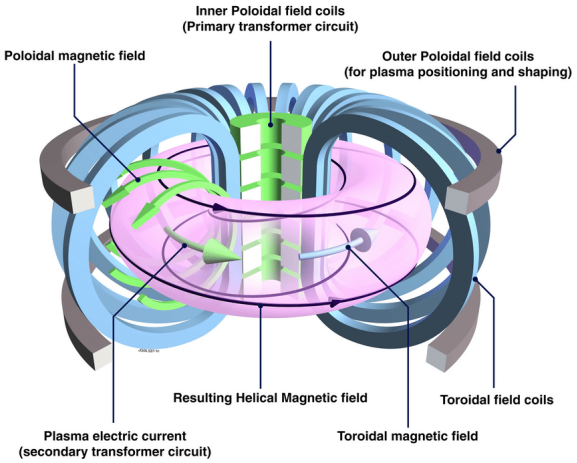

Figure 1.1 – The confinement of plasma in a tokamak [47].

To ensure the fusion reaction can take place, a certain amount of energy must be supplied, and in particular in order to heat the plasma to the required temperature. We focus here on the modelization of ion cyclotron resonance heating (ICRH), where waves of different frequencies are sent in the plasma by radio frequency antennas in the range of $40 - 55$MHz, see Figure 1.2. This is one of the three different external heat sources in the ITER tokamak, among with electron cyclotron resonant heating (ECRH), that sends waves of about 170GHz, and neutral beam injection, that sends a beam of deuterium atoms.

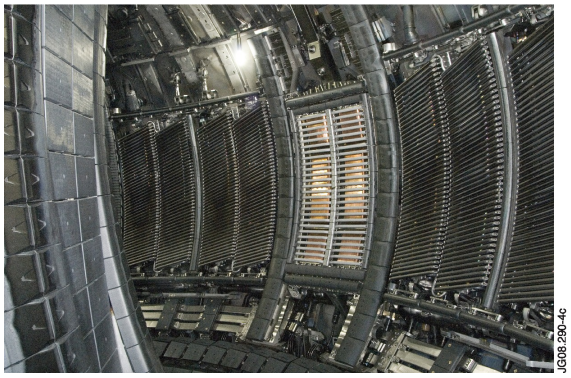

Figure 1.2 – A radio frequency antenna in a tokamak [47].

Until now, the total output-input energy ratio has never exceeded 1. The objective of the ITER international collaboration, involving 35 different nations, is to obtain a ratio of order 10. The tokamak is currently under construction in Cadarache, in south of France.

These information and more can be found on the websites of the ITER project and of the IRFM institute [71, 69].

1.2 Waves in plasmas

The propagation of electromagnetic waves of given frequency $\omega > 0$ in a media characterized by a **permittivity tensor** $\underline{\underline{\varepsilon}} : \Omega \to \mathbb{C}^{3\times 3}$, which varies in space and depends on ω, is described by a **wave equation**

$$\nabla \wedge \nabla \wedge \mathbf{E} - \underline{\underline{\varepsilon}}\mathbf{E} = 0 \quad \Omega \subset \mathbb{R}^3, \tag{1.2.1}$$

where the unknown $\mathbf{E} : \mathbb{R}^3 \to \mathbb{C}^3$ is the amplitude of the harmonic in time electric field $\mathbf{E}(\mathbf{x})\exp(-i\omega t)$. This equation, with a permittivity tensor $\underline{\underline{\varepsilon}}$ corresponding to the hybrid resonance regime, is the object of our study.

The permittivity details how the medium responds to electromagnetic perturbations: if the medium were isotropic, $\underline{\underline{\varepsilon}} = \varepsilon I$ and the permittivity would be characterized by a scalar function ε; if the medium were homogeneous, $\underline{\underline{\varepsilon}}$ would have constant coefficients. Under one or both of these hypotheses, there is now an extensive mathematical theory [90, 65, 14, 2]. In this work, we are interested by a plasma subject to a constant bulk background magnetic field $\mathbf{B}_0$. The direction of $\mathbf{B}_0$ will have an impact on the structure of the tensor $\underline{\underline{\varepsilon}}$, providing anisotropy. We fix the direction $\mathbf{e}_z = \mathbf{B}_0/|\mathbf{B}_0|$ of the spatial basis. In addition, we also assume inhomogeneity in the x, y-plane.

The wave equation (1.2.1) is obtained by combining Maxwell's equations with the particles' dynamics, which are described by the plasma model. The interdependency between the electromagnetic fields and the plasma particles is schematized in Figure 1.3. We make the hypothesis that the ions, which have a mass $m_i \gg m_e$, are static. We thus consider the motion of electrons only, and use a fluid model to describe this motion. We denote $\mathbf{u}_e$ the speed of electrons. The full system of equations describing the interaction between the wave and the particles is composed of harmonic in time Maxwell's equations

$$\begin{cases} \nabla \wedge \mathbf{B} + \dfrac{i\omega}{c^2}\mathbf{E} = \mu_0 \mathbf{J}, \\ i\omega\mathbf{B} - \nabla \wedge \mathbf{E} = 0, \end{cases} \tag{1.2.2}$$

coupled with a harmonic in time Euler equation with Lorentz force, friction and pressure effects

$$m_e N_e \left(-i\omega\mathbf{u}_e + (\mathbf{u}_e \cdot \nabla)\mathbf{u}_e\right) = -q_e N_e(\mathbf{E} + \mathbf{u}_e \wedge \mathbf{B}) - m_e N_e \nu \mathbf{u}_e - \nabla \underline{\underline{p}}, \tag{1.2.3}$$

through a linear current

$$\mathbf{J} = -q_e N_e \mathbf{u}_e. \tag{1.2.4}$$

Here, N_e is the density of electrons, q_e the charge of an electron, ν is a term of friction between ions and electrons, and $\underline{\underline{p}}$ is the pressure tensor. This system of equations is nonlinear, but as it is known since the classical work of Stix [106] the study of its linearization up to the 1st order is already rich, and we will focus on the associated linear system.

The wave equation (1.2.1) is then obtained by linearizing the system of equations and expressing $\mathbf{u}_e$ in terms of the electric field $\mathbf{E}$ using (1.2.3), and by substituting $\mathbf{u}_e$ by this expression in the current (1.2.4).

1.2.1 Cold plasma model

The cold plasma model is obtained when temperature and pressure effects are neglected as well as the friction between the particles, which is to say $\underline{\underline{p}} = 0$ and $\nu = 0$. Linearizing equation (1.2.3)

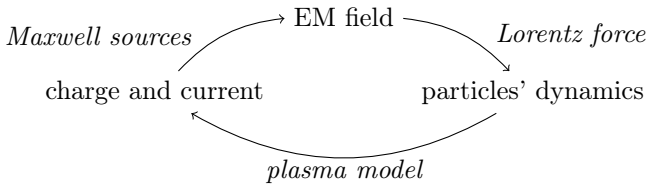

Figure 1.3 – Self-consistent description of a plasma, to which corresponds the system of equations (1.2.2)-(1.2.3)-(1.2.4).

around the steady state $(\widetilde{\mathbf{E}}, \widetilde{\mathbf{B}}, \widetilde{\mathbf{u}_e}) = (0, \mathbf{B}_0, 0)$, it reduces at first order to

$$-i\omega m_e N_e \mathbf{u}_e = -q_e N_e \left(\mathbf{E} + \mathbf{u}_e \wedge \mathbf{B}_0\right). \tag{1.2.5}$$

It is now possible to express the velocity in function of the electric field, and since $\mathbf{B}_0 = B_0 \mathbf{e}_z$,

$$\mathbf{u}_e = \frac{q_e}{m_e} \begin{pmatrix} \frac{-i\omega}{\omega^2-\omega_c^2} & \frac{\omega_c}{\omega^2-\omega_c^2} & 0 \\ \frac{-\omega_c}{\omega^2-\omega_c^2} & \frac{-i\omega}{\omega^2-\omega_c^2} & 0 \\ 0 & 0 & \frac{1}{i\omega} \end{pmatrix} \mathbf{E},$$

for $\omega_c = \frac{|q_e|B_0}{m_e}$. This constant frequency is called the cyclotron frequency, and corresponds to the frequency of the gyration of the electrons around the magnetic field lines.
Combined to (1.2.2) and (1.2.4), it yields

$$\nabla \wedge \nabla \wedge \mathbf{E} - \underline{\underline{\varepsilon}} \mathbf{E} = 0 \tag{1.2.6}$$

with tensor

$$\underline{\underline{\varepsilon}} = \left(\frac{\omega}{c}\right)^2 \begin{pmatrix} 1 - \frac{\omega_p^2}{\omega^2-\omega_c^2} & \frac{i\omega_p^2\omega_c}{\omega(\omega^2-\omega_c^2)} & 0 \\ \frac{-i\omega_p^2\omega_c}{\omega(\omega^2-\omega_c^2)} & 1 - \frac{\omega_p^2}{\omega^2-\omega_c^2} & 0 \\ 0 & 0 & 1 - \frac{\omega_p^2}{\omega^2} \end{pmatrix} \tag{1.2.7}$$

and $\omega_p = \sqrt{\frac{N_e q_e^2}{m_e \varepsilon_0}}$. This frequency is called the plasma frequency, and corresponds to the frequency of oscillations of a slightly perturbed electron. Notice that ω_p is not a constant frequency, since it depends on the density of electrons in the plasma N_e. We make the assumption that N_e is linear in a privileged direction. Because of the structure

$$\underline{\underline{\varepsilon}} = \left(\frac{\omega}{c}\right)^2 \begin{pmatrix} S & -iD & 0 \\ iD & S & 0 \\ 0 & 0 & P \end{pmatrix}, \tag{1.2.8}$$

the permittivity tensor is also referred to as a Stix tensor [106]. In this model, ω_c, ω are considered as fixed parameters, and ω_p varies in space.

1.2.2 Dispersion relation

The tool widely used in the plasma community is the derivation of dispersion relations. It consists of the study of so-called propagation modes, which are non trivial plane waves $\mathbf{E}(\mathbf{x}) = \hat{\mathbf{E}} \exp(i\mathbf{k} \cdot \mathbf{x})$ solution to (1.2.6). Necessarily, this study is valid for freezed plasma coefficients. Although it does

not allow for a global analysis of the problem, the insight it gives at least locally is known to be valuable [106, 41]. It leads to relations between the wave vector $\mathbf{k}$, the wave frequency ω, and fixed plasma parameters ω_c and ω_p. These hypotheses come down to study wave propagation in homogeneous plasma. Indeed, for the operator $\mathbb{M} := -\mathbf{k} \wedge \mathbf{k} \wedge -\underline{\underline{\varepsilon}}$, the amplitude vector $\hat{\mathbf{E}}$ verifies $\mathbb{M}\hat{\mathbf{E}} = 0$ and $\hat{\mathbf{E}} \neq 0$, so that necessarily

$$\det \mathbb{M} = 0. \tag{1.2.9}$$

Up to a change of variable, since only $\mathbf{e}_z$ has been fixed, aligned to $\mathbf{B}_0$, we can consider that the wave vector $\mathbf{k}$ has a component along z and a component along x, but no component along y. For $\mathbf{k} = (k_x, 0, k_z)$, that we write as $\mathbf{k} = (k \sin\theta, 0, k\cos\theta) = k\mathbf{n}$, see Figure 1.4. For the cold plasma

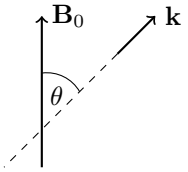

Figure 1.4 – Wave vector $\mathbf{k} \in \mathbb{R}^3$ of an incident plane wave in the x-z plane.

tensor (1.2.8), and writing $\lambda = (\frac{\omega}{ck})^2$, the relation (1.2.9) multiplicated by k^{-2} reads

$$\begin{vmatrix} \cos^2\theta - \lambda S & \lambda i D & -\sin\theta\cos\theta \\ -\lambda i D & 1-\lambda S & 0 \\ -\sin\theta\cos\theta & 0 & \sin^2\theta - \lambda P \end{vmatrix} = 0,$$

or equivalently

$$-\lambda^2 P(S^2 - D^2) + \lambda\left((S^2 - D^2)\sin^2\theta + SP(1+\cos^2\theta)\right) - (S\sin^2\theta + P\cos^2\theta) = 0. \tag{1.2.10}$$

Equation 1.2.10 is called the **dispersion relation** (Section 1.3 in Stix [106]). The discriminant of this second order polynomial in λ is

$$(S^2 - D^2 - SP)^2 \sin^4\theta + 4D^2P^2\cos^2\theta > 0,$$

so that λ is either positive, and $k \in \mathbb{R}$, or negative, and $k \in \mathbb{C}\backslash\mathbb{R}$. The wave $\mathbf{E}$ is thus propagative, if $\mathbf{k} \in \mathbb{R}^3$, or evanescent, if not. Indeed, if $\mathbf{k} \in \mathbb{C}^3\backslash\mathbb{R}^3$, the field has a real exponent in the exponential part. It can be either exponentially increasing and lead to growing waves, or exponentially decreasing and lead to evanescent waves, according to the sign of the real part. The first are discarded by energy considerations when considering a cold homogeneous unbounded plasma. There are two types of transition between propagative and evanescent waves: **cut-offs**, where $k = 0$; **resonances**, where $k \to \infty$.

1.2.3 Hybrid resonance

A necessary condition for resonance to occur is that the 0^{th} order term in (1.2.10) vanishes. For a perpendicular propagation to the background magnetic field $\mathbf{B}_0$, which is expressed by $\theta = \pi/2$, this condition comes down to $S = 0$, which referring to (1.2.7) means that

$$\omega^2 = \omega_p^2 + \omega_c^2. \tag{1.2.11}$$

This relation is verified at what we call the upper hybrid frequency, denoted $\omega = \omega_{\mathrm{UH}}$. Hybrid because it mixes the plasma and cyclotron frequencies, and upper because there exists another hybrid frequency called lower ω_{LH}, such that $\omega_{\mathrm{LH}} < \omega_c < \omega_{\mathrm{UH}}$.

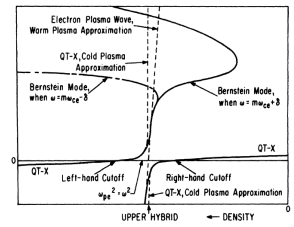

FIG. 1. The square of the index of refraction (n_x^2) is plotted against density. The frequency, which is fixed, is equal to the hybrid frequency at the value of density indicated. For an inhomogeneous plasma with linearly increasing density, the abscissa is proportional to distance (x). Dotted lines represent extrapolations of approximate dispersion relations beyond their regions of validity. Thus the extrapolated cold-plasma hybrid resonance ($n_x^2 \to \infty$) point is seen to coincide with the cut-off ($n_x^2 \to 0$) point for the warm-plasma-approximation plasma wave. QT-X designates the quasitransverse extraordinary (electromagnetic) mode. The parallel wave number, k_z, is assumed small or zero. At the top of the figure the bulge out to the right corresponds to the maximum of the right-hand side in Eq. (11) which occurs under the conditions of Eq. (12).

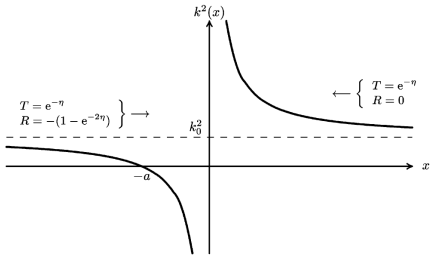

Figure 6.5. Spatial variation of $k^2(x)$ for a tunneling problem with a resonance at $x = 0$ and a cutoff at $x = -a$.

Figure 1.5 – Diagrams representing the dispersion relations around resonances from Stix [107] (left) and Swanson [110] (right) for space varying coefficients.

In Figure 1.5, dispersion relations around the upper hybrid resonance are illustrated by the spatial behavior of $k^2(x)$, when the density $N_e(\mathbf{x})$ is linear and proportionnal to x. The illustration on the right, from Swanson (Subsection 6.2.4 in[110]), corresponds to the Budden simplification around the upper hybrid resonance, where essentially a cut-off and a resonance are present, and $k^2(x)$ behaves as $1 + 1/x$. The coefficients T and R on Figure 1.5 are the transmission and reflection coefficients, and it appears there is a loss of energy from the wave, illustrated here by the fact $R^2 + T^2 < 1$. This problem is usually tackled by adding friction again, as a small regularizing term parametered by $\nu > 0$.

Our objective in this work is to understand the behavior of model (1.2.6) with a coefficient ω_p that varies in a given direction, and is such that the upper hybrid relation (1.2.11) is satisfied at a given location, in the limit regime $\nu = 0^+$.

1.3 Mathematical tools

In this section, we present the different systems of equations studied in this thesis and corresponding to different hypotheses on the model. A few properties verified by these equations are then illustrated

in a simple case in subsection 1.3.2, and one of the main tools that will be used in our approach, the **manufactured solutions method**, is introduced in subsection 1.3.3.

1.3.1 The different systems of equations

The system of equations we consider is thus

$$\begin{cases} \nabla \wedge \mathbf{B} - \underline{\underline{\varepsilon}}\mathbf{E} &= 0 & \text{in } \Omega, \\ \mathbf{B} - \nabla \wedge \mathbf{E} &= 0 & \text{in } \Omega, \\ -(\mathbf{B} \wedge \mathbf{n}) \wedge \mathbf{n} + i\lambda \mathbf{E} \wedge \mathbf{n} &= \mathbf{f} \wedge \mathbf{n} & \text{on } \partial\Omega, \end{cases} \tag{1.3.1}$$

on a bounded domain $\Omega \subset \mathbb{R}^3$, with a permittivity tensor of the form

$$\underline{\underline{\varepsilon}}(\mathbf{x}) = \begin{pmatrix} \alpha(\mathbf{x}) & i\delta(\mathbf{x}) & 0 \\ -i\delta(\mathbf{x}) & \alpha(\mathbf{x}) & 0 \\ 0 & 0 & \gamma(\mathbf{x}) \end{pmatrix}, \tag{1.3.2}$$

and Robin boundary conditions with a $\lambda > 0$, $\mathbf{f} : \partial\Omega \to \mathbb{C}^3$, and $\mathbf{n}$ the outgoing normal to Ω.

Here α, δ and γ are real valued functions. The following assumption is made to model the hybrid resonance regime.

Assumption 1.3.1. The extra diagonal coefficients $\delta, \gamma \in W^{1,\infty}(\Omega)$ are smooth, bounded and positive $\delta, \gamma > 0$. The diagonal coefficient $\alpha \in W^{2,\infty}(\Omega)$ is smooth, bounded, and changes sign continuously over a surface $\Sigma = \{\alpha = 0\}$ inside the domain Ω.

We will consider the following configurations.

- The tensor is **1D or 2D**, $\underline{\underline{\varepsilon}}(\mathbf{x}) = \underline{\underline{\varepsilon}}(x)$ or $\underline{\underline{\varepsilon}}(x, y)$, corresponding to homogeneity in the directions y and z or simply in direction z. A Fourier transform in z is undertaken hence the ansatz of solutions considered

$$\mathbf{E}(\mathbf{x}) = \mathbf{E}(x, y)\exp(ik_z z) \quad \text{and} \quad \mathbf{B}(\mathbf{x}) = \mathbf{B}(x, y)\exp(ik_z z), \tag{1.3.3}$$

  for $\mathbf{E}, \mathbf{B} : \Omega \to \mathbb{C}^3$. For convenience, the domain Ω will either denote a subset of $\mathbb{R}$ in 1D or a subset of $\mathbb{R}^2$ in 2D.

- The incident plane wave $\mathbf{E}_{\text{inc}}(\mathbf{x}) = \hat{\mathbf{E}}_{\text{inc}} \exp(i\mathbf{k} \cdot \mathbf{x})$ is called of **oblique incidence** $\mathbf{k} = (k_x, 0, k_z)$ in the general case, or of **normal incidence** $\mathbf{k} = (k_x, 0, 0)$ with respect to the bulk magnetic field $\mathbf{B}_0 = B_0 \mathbf{e}_z$. The Fourier mode (1.3.3) considered is the one corresponding to the value of k_z.

For a Fourier mode k_z, the curl operator reads

$$\nabla\wedge = \begin{pmatrix} 0 & -ik_z & \partial_y \\ ik_z & 0 & -\partial_x \\ -\partial_y & \partial_x & 0 \end{pmatrix},$$

and the complete system (1.3.1) is a priori a linear system of 6 coupled equations with boundary conditions.

Chapter 2 corresponds to the study of the 1D system in oblique incidence, and Chapter 3 deals with the 2D in normal incidence.

Oblique incidence in 1D

In the case of oblique incidence, in 1D, the system of equations is

$$\left\{\begin{array}{ccccccccc} & - & ik_zB_y & - & \alpha E_x & - & i\delta E_y & = & 0, \\ ik_zB_x & - & B_z' & + & i\delta E_x & - & \alpha E_y & = & 0, \\ B_y' & & & - & \gamma E_z & & & = & 0, \\ & & B_x & & & + & ik_zE_y & = & 0, \\ & & B_y & - & ik_zE_x & + & E_z' & = & 0, \\ & & B_z & - & E_y' & & & = & 0, \end{array}\right. \tag{1.3.4}$$

in Ω, with boundary conditions

$$\left\{\begin{array}{rcl} B_y + i\lambda E_z n & = & f_z n, \\ B_z - i\lambda E_y n & = & -f_y n, \end{array}\right. \tag{1.3.5}$$

on $\partial\Omega$, where n is the outgoing normal.

Normal incidence in 2D

When $k_z = 0$, the system decouples into two independent systems of size 3. Denoting in this case $\mathbf{E} = (E_x, E_y)$, $\mathbf{B} = (B_x, B_y)$ and $\mathbf{f} = (f_x, f_y)$, these systems write

$$\left\{\begin{array}{rcll} \mathbf{curl}\, B_z - \begin{pmatrix} \alpha & i\delta \\ -i\delta & \alpha \end{pmatrix}\mathbf{E} & = & 0 & \text{in } \Omega, \\ B_z - \operatorname{curl}\mathbf{E} & = & 0 & \text{in } \Omega, \\ B_z + i\lambda\mathbf{E}\cdot\mathbf{n}^\perp & = & \mathbf{f}\cdot\mathbf{n}^\perp & \text{on } \partial\Omega, \end{array}\right. \tag{X-mode}$$

$$\left\{\begin{array}{rcll} \operatorname{curl}\mathbf{B} - \gamma E_z & = & 0 & \text{in } \Omega, \\ \mathbf{B} - \mathbf{curl}\, E_z & = & 0 & \text{in } \Omega, \\ -\mathbf{B}\cdot\mathbf{n}^\perp + i\lambda E_z & = & f_z & \text{on } \partial\Omega, \end{array}\right. \tag{O-mode}$$

for $\mathbf{n}$ the outgoing normal to $\partial\Omega$, and $\mathbf{n}^\perp$ its rotation of angle $\pi/2$. The definitions of the two dimensional curl operators are stated in the Symbols appendice. The first system is called the **X-mode**, for extraordinary, and contains the resonance phenomenon. The second system is called the **O-mode**, for ordinary, and consists in a Helmholtz equation on E_z

$$-\Delta E_z - \gamma E_z = 0.$$

Therefore, when studying hybrid resonances in the normal incidence case, we will always refer to the X-mode equations.

In the 1D X-mode case, which corresponds to taking $\partial_y = 0$, a singular analytic solution was described by Després, Imbert-Gérard and Weder in 2014 [32], as a limit of the solution to regularized equations. A method to characterize this limit solution in order to do numerical approximations has later been proposed by Campos Pinto and Després in 2017 [99]. These results are summarized in the next section.

1.3.2 Singular analytical solutions

The two important information of this section are that for the resonant Maxwell's equations (1.3.1)

- there is no unicity of the solution,
- there exist singular solutions in the sense that the components of $\mathbf{E}$ are not necessarily in L^2, nor in L^1.

We illustrate these properties in the simplest case, the 1D X-mode.

Example 1 (Singular solutions: illustration in the 1D-Xmode)**.** The X-mode equations with Robin boundary conditions in 1D for $\Omega = (-1, 1)$ are

$$\left\{\begin{array}{rcll} -\alpha E_x - i\delta E_y &=& 0 & \text{in } \Omega = (-1,1), \\ -B_z' + i\delta E_x - \alpha E_y &=& 0 & \text{in } \Omega, \\ B_z - E_y' &=& 0 & \text{in } \Omega, \end{array}\right. \tag{1.3.6}$$

associated to

$$B_z(\pm 1) \mp i\lambda E_y(\pm 1) = f_z(\pm 1), \tag{1.3.7}$$

for $\lambda > 0$ and $f : \{-1, 1\} \to \mathbb{C}$. One has the two relations

$$E_x = \frac{-i\delta}{\alpha} E_y \quad \text{and} \quad B_z = E_y',$$

and the main unknown is E_y, which we want to search for in $H^1(\Omega)$. Solving the system of equations comes down to solving the second order ODE

$$-E_y'' + \left(\frac{\delta^2}{\alpha} - \alpha\right) E_y = 0, \tag{1.3.8}$$

with mixed boundary conditions at $x = \pm 1$. For the particular values $\alpha(x) = -x$ and $\delta(x) = \sqrt{1 - x/4 + x^2}$, equation (1.3.8) corresponds to the Whittaker equation (Section 13.14 in Olver-Lozier-Boisvert-Clark with $\kappa = 1$ and $\mu = 1/2$ [95])

$$-E_y'' + \left(\frac{1}{x} - \frac{1}{4}\right) E_y = 0.$$

The solutions outside of $x = 0$ are linear combinations of the continuous functions on $(-1, 0)$ and $(0, 1)$

$$u : x \mapsto x e^{-x/2} \quad \text{and} \quad v : x \mapsto -e^{x/2} + \left(\ln|x| + \int_1^x \frac{e^y - 1}{y} \mathrm{d}y\right) x e^{-x/2}.$$

In addition to the two boundary conditions, the continuity of E_y can be imposed at $x = 0$. However:

- the logarithmic singularity of v' near $x = 0$ does not allow to determine the fourth degree of freedom of the system, and results in lack of unicity,
- a priori, $E_y(0) \neq 0$, and the component E_x is non integrable and behaves as $1/x$.

To deal with these flaws, the system (1.3.1) is regularized using a small parameter $\nu \in \mathbb{R}$

$$\left\{\begin{array}{rcll} \nabla \wedge \mathbf{B}^\nu - \underline{\underline{\varepsilon}}^\nu \mathbf{E}^\nu &=& 0 & \text{in } \Omega, \\ \mathbf{B}^\nu - \nabla \wedge \mathbf{E}^\nu &=& 0 & \text{in } \Omega, \\ -(\mathbf{B}^\nu \wedge \mathbf{n}) \wedge \mathbf{n} + i\lambda \mathbf{E}^\nu \wedge \mathbf{n} &=& \mathbf{f} \wedge \mathbf{n} & \text{on } \partial\Omega, \end{array}\right. \tag{1.3.9}$$

where the tensor is defined in Ω by

$$\underline{\underline{\varepsilon}}^{\nu}(\mathbf{x}) = \begin{pmatrix} \alpha(\mathbf{x}) + i\nu & i\delta(\mathbf{x}) & 0 \\ -i\delta(\mathbf{x}) & \alpha(\mathbf{x}) + i\nu & 0 \\ 0 & 0 & \gamma(\mathbf{x}) + i\nu \end{pmatrix}. \tag{1.3.10}$$

Remark 1.3.2. A physical remark is that, for $\nu > 0$, this regularized system is a simplification of the case where friction between ions and electrons is considered in equation (1.2.3) describing the electrons dynamics [32, 31].

Remark 1.3.3. A qualitative remark is that, as γ is positive and bounded below, it is the regularization of α, in the two first diagonal coefficients, that is crucial.

The following theorem was proved in 1D in normal incidence, where the system (X-mode) reduces to (1.3.6), associated to the boundary conditions (1.3.7).

Assumption 1.3.4. Let $\alpha \in W^{2,\infty}(\Omega)$ be such that $\alpha(x) = rx + O(x^2)$ for $r \in \mathbb{R}_*$, and $\delta \in W^{1,\infty}(\Omega)$ be positive.

Proposition 1.3.5 (Theorem 1.1., Proposition 5.16. [32])**.** *For any $\lambda > 0$ and complex-valued function f_z and under Assumptions 1.3.4, the solution $(E_x^\nu, E_y^\nu, B_z^\nu)$ to the regularized problem converges toward a solution (E_x^+, E_y^+, B_z^+) to* (1.3.6)-(1.3.7) *in the sense of distributions when $\nu \to 0^+$. This limit solution has a singular component E_x^+ that contains a singular term proportional to $1/\alpha$ plus a Dirac mass, that do not lie in $L^1(\Omega)$, and an $L^2(\Omega)$ remainder. The components E_y^+ and B_y^+ lie in $L^2(\Omega)$.*
Moreover, when $\nu \to 0^-$, $(E_x^\nu, E_y^\nu, B_z^\nu)$ converges toward a solution $(E_x^-, E_y^-, B_z^-) \neq (E_x^+, E_y^+, B_z^+)$ to (1.3.6)-(1.3.7) *in the sense of distributions, with the same type of singular behaviour.*

This singular behaviour is not an artefact of the model and corresponds to the hybrid resonance, enabling an energy transfer from the wave to the ions. Indeed, one can compute the energy dissipation

$$\mathrm{Im} \int_\Omega \nabla \cdot \left(\mathbf{E}^\nu \wedge \overline{\mathbf{B}^\nu} \right) \mathrm{d}\mathbf{x} = \nu \|\mathbf{E}^\nu\|^2_{L^2(\Omega)} \underset{\nu \to 0^+}{\nrightarrow} 0. \tag{1.3.11}$$

The limit solution $\nu \to 0^+$ is the physical solution, corresponding to vanishing friction, to (1.3.1). However, since the resonant Maxwell's equations are ill-posed and admit multiple solutions, their numerical approximation is classicaly carried on by discretizing for a small regularizing parameter $\nu > 0$ a variational formulation of the well-posed system (1.3.9). The space discretization is then constrained by the small parameter ν in a non trivial way. This is why our objective is to characterize explicitely the solution at the limit, to let go of the regularization parameter ν.

The energy relation (1.3.11) can not be used directly at $\nu = 0^+$ to obtain information about the singularity, mainly because some terms in the quadratic form on the left hand side do not converge in $L^1(\Omega)$. This is the initial motivation for defining quasi-solutions $\mathbf{F}^\nu$ and $\mathbf{C}^\nu$ associated to $\mathbf{E}^\nu$ and $\mathbf{B}^\nu$, and such that this time, the quadratic form related to the heating

$$\begin{aligned} \mathcal{J}^\nu(\mathbf{E}^\nu, \mathbf{B}^\nu) \quad = \quad & \mathrm{Im} \int_\Omega \left((\mathbf{E}^\nu - \mathbf{F}^\nu) \wedge \overline{(\mathbf{B}^\nu - \mathbf{C}^\nu)} \right) \cdot \nabla \varphi \mathrm{d}\mathbf{x} \\ & + \mathrm{Im} \int_\Omega \left(\overline{(\mathbf{E}^\nu - \mathbf{F}^\nu)} \cdot \mathbf{g}^\nu - \overline{(\mathbf{B}^\nu - \mathbf{C}^\nu)} \cdot \mathbf{q}^\nu \right) \varphi \mathrm{d}\mathbf{x}, \end{aligned}$$

where $\mathbf{g}^\nu$ and $\mathbf{q}^\nu$ are the sources of the quasi-solutions, is composed of terms converging in $L^1(\Omega)$, for any cutoff φ around the singularity.

1.3.3 The manufactured solutions method

We define here a tool for the general system of resonant Maxwell's equations, illustrated at the end of this Subsection in the simplest case, the 1D X-mode.

What we call manufactured solutions for (1.3.1)-(1.3.9) are fields $\mathbf{F}^\nu$ and $\mathbf{C}^\nu$ and sources $\mathbf{g}^\nu$ and $\mathbf{q}^\nu$, defined in Ω, verifying the relations

$$\left\{\begin{array}{rcl} \nabla\wedge\mathbf{C}^\nu-\underline{\underline{\varepsilon}}^\nu\mathbf{F}^\nu &=& \mathbf{g}^\nu,\\ \mathbf{C}^\nu-\nabla\wedge\mathbf{F}^\nu &=& \mathbf{q}^\nu,\end{array}\right. \tag{1.3.12}$$

and such that:

- they are known analytically and have limits as $\nu\to 0^+$ trivial to determine, hence the name *manufactured* solutions, (H1)
- some products of these functions against the exact solution fields $\mathbf{E}^\nu$ and $\mathbf{B}^\nu$ admit limits in $L^1(\Omega)$ as $\nu\to 0^+$. (H2)

The first hypothesis is crucial to be able to use these quasi-solutions in a numerical discretization. The second one permits to write an integral relation at $\nu=0^+$ expressing the energy transfer at the resonance.

The divergence of the Poynting vector associated to the difference fields

$$\nabla\cdot\Pi\left(\mathbf{E}^\nu-\mathbf{F}^\nu,\mathbf{B}^\nu-\mathbf{C}^\nu\right)=\operatorname{Im}\nabla\cdot\left(\left(\mathbf{E}^\nu-\mathbf{F}^\nu\right)\wedge\overline{\left(\mathbf{B}^\nu-\mathbf{C}^\nu\right)}\right)$$

is expanded using equations (1.3.9) and (1.3.12). One has indeed

$$\left\{\begin{array}{rcl} \nabla\wedge\left(\mathbf{B}^\nu-\mathbf{C}^\nu\right)-\underline{\underline{\varepsilon}}^\nu\left(\mathbf{E}^\nu-\mathbf{F}^\nu\right) &=& -\mathbf{g}^\nu,\\ \left(\mathbf{B}^\nu-\mathbf{C}^\nu\right)-\nabla\wedge\left(\mathbf{E}^\nu-\mathbf{F}^\nu\right) &=& -\mathbf{q}^\nu,\end{array}\right. \tag{1.3.13}$$

so that

$$\begin{aligned}&\nabla\cdot\left(\left(\mathbf{E}^\nu-\mathbf{F}^\nu\right)\wedge\overline{\left(\mathbf{B}^\nu-\mathbf{C}^\nu\right)}\right)\\ &=\nabla\wedge\left(\mathbf{E}^\nu-\mathbf{F}^\nu\right)\cdot\overline{\left(\mathbf{B}^\nu-\mathbf{C}^\nu\right)}-\left(\mathbf{E}^\nu-\mathbf{F}^\nu\right)\cdot\nabla\wedge\overline{\left(\mathbf{B}^\nu-\mathbf{C}^\nu\right)}\\ &=\left|\mathbf{B}^\nu-\mathbf{C}^\nu\right|^2+\mathbf{q}^\nu\cdot\overline{\left(\mathbf{B}^\nu-\mathbf{C}^\nu\right)}-\left(\mathbf{E}^\nu-\mathbf{F}^\nu\right)\cdot\overline{\underline{\underline{\varepsilon}}^\nu\left(\mathbf{E}^\nu-\mathbf{F}^\nu\right)}+\left(\mathbf{E}^\nu-\mathbf{F}^\nu\right)\cdot\overline{\mathbf{g}^\nu}.\end{aligned}$$

Since $\underline{\underline{\varepsilon}}^\nu=\underline{\underline{\varepsilon}}+i\nu I$ with $\underline{\underline{\varepsilon}}$ a Hermitian matrix, see (1.3.10), it results

$$\nabla\cdot\Pi=\operatorname{Im}\left(\mathbf{q}^\nu\cdot\overline{\left(\mathbf{B}^\nu-\mathbf{C}^\nu\right)}+\left(\mathbf{E}^\nu-\mathbf{F}^\nu\right)\cdot\overline{\mathbf{g}^\nu}\right)+\nu\left|\mathbf{E}^\nu-\mathbf{F}^\nu\right|^2. \tag{1.3.14}$$

In particular, for any cutoff φ around the resonance defined as a non-negative function of $\mathcal{C}_0^1(\Omega)$ that is equal to 1 on Σ, one has the signed integral relation

$$\operatorname{Im}\int_\Omega\left(\overline{\left(\mathbf{E}^\nu-\mathbf{F}^\nu\right)}\wedge\left(\mathbf{B}^\nu-\mathbf{C}^\nu\right)\cdot\nabla\varphi+\left(\overline{\left(\mathbf{E}^\nu-\mathbf{F}^\nu\right)}\cdot\mathbf{g}^\nu-\mathbf{q}^\nu\cdot\overline{\left(\mathbf{B}^\nu-\mathbf{C}^\nu\right)}\right)\varphi\right)\mathrm{d}\mathbf{x}\geq 0. \tag{1.3.15}$$

To precise (H2), what is required is that in $L^1(\Omega)$, the following convergences hold when $\nu\to 0^+$

$$\left\{\begin{array}{rcl} \mathbb{P}_\Sigma\operatorname{Im}\left(\overline{\left(\mathbf{E}^\nu-\mathbf{F}^\nu\right)}\wedge\left(\mathbf{B}^\nu-\mathbf{C}^\nu\right)\right) &\to& \mathbb{P}_\Sigma\operatorname{Im}\left(\overline{\left(\mathbf{E}^+-\mathbf{F}^+\right)}\wedge\left(\mathbf{B}^+-\mathbf{C}^+\right)\right),\\ \operatorname{Im}\left(\overline{\left(\mathbf{E}^\nu-\mathbf{F}^\nu\right)}\cdot\mathbf{g}^\nu\right) &\to& \operatorname{Im}\left(\overline{\left(\mathbf{E}^+-\mathbf{F}^+\right)}\cdot\mathbf{g}^+\right),\\ \operatorname{Im}\left(\mathbf{q}^\nu\cdot\overline{\left(\mathbf{B}^\nu-\mathbf{C}^\nu\right)}\right) &\to& \operatorname{Im}\left(\mathbf{q}^+\cdot\overline{\left(\mathbf{B}^+-\mathbf{C}^+\right)}\right),\end{array}\right. \tag{H2'}$$

where $\mathbb{P}_\Sigma$ is a projector along the direction normal to Σ. In this case, the integral relation (1.3.15) passes to the limit.

In addition to (H1)-(H2), a key idea for the definition of manufactured solutions is to introduce information about the singularity. We define $\mathbf{F}^\nu$ and $\mathbf{C}^\nu$ to be proportional to the type of singularity expected for the solution. This introduces an unknown k defined on Σ, corresponding to the proportionnality coefficient, that characterizes the singularity. For $\nu > 0$ and φ a cutoff around the resonance, according to (1.3.14), one has

$$\begin{aligned}&\mathrm{Im}\int_\Omega \left(\overline{(\mathbf{E}^\nu - k\mathbf{F}^\nu)} \wedge (\mathbf{B}^\nu - k\mathbf{C}^\nu)\cdot\nabla\varphi + \left(\overline{(\mathbf{E}^\nu - k\mathbf{F}^\nu)}\cdot k\mathbf{g}^\nu - k\mathbf{q}^\nu\cdot\overline{(\mathbf{B}^\nu - k\mathbf{C}^\nu)}\right)\varphi\right)\mathrm{d}\mathbf{x}\\ &= \nu\|(\mathbf{E}^\nu - k\mathbf{F}^\nu)\sqrt{\varphi}\|^2_{L^2(\Omega)}.\end{aligned}$$

Gathering all these information, we then search to minimize the distance between the solution $(\mathbf{E}^\nu, \mathbf{B}^\nu)$ and the manufactured solution $(\mathbf{F}^\nu, \mathbf{C}^\nu)$ using the above relation, looking for solutions to Euler-Lagrange equations associated to the limit of the quadratic form

$$\begin{aligned}\mathcal{J}^+(\mathbf{E},\mathbf{B},k) = \mathrm{Im}\int_\Omega &\left(\overline{(\mathbf{E} - k\mathbf{F}^+)} \wedge (\mathbf{B} - k\mathbf{C}+)\cdot\nabla\varphi\right.\\ &\left. + \left(\overline{(\mathbf{E} - k\mathbf{F}^+)}\cdot k\mathbf{g}^+ - k\mathbf{q}^+\cdot\overline{(\mathbf{B} - k\mathbf{C}^+)}\right)\varphi\right)\mathrm{d}\mathbf{x},\end{aligned}$$

under the constraint of $(\mathbf{E}, \mathbf{B})$ being one of the solutions to the resonant Maxwell's equations for $\nu = 0$.

To conclude this introduction to resonant Maxwell's equations we develop this method on the 1D X-mode case.

Example 2 (Manufactured solutions: illustration in the 1D-Xmode)**.** For the system (1.3.6) and under Assumptions 1.3.4, formally, the singular component of the field is

$$E_x = \frac{-i\delta}{\alpha}E_y.$$

A priori, $E_y \in H^1(\Omega)$ and $B_z \in L^2(\Omega)$ verify

$$\left\{\begin{array}{rcccl} -B_z' & + & \left(\dfrac{\delta^2}{\alpha} - \alpha\right)E_y & = & 0 \quad \text{in } \Omega,\\ B_z & - & E_y' & = & 0 \quad \text{in } \Omega,\end{array}\right. \tag{1.3.16}$$

with boundary conditions (1.3.7). However, this system of ODEs is ill-posed. It consists of two first order equations, and corresponds to 4 degrees of freedom. Yet only two boundary conditions and one continuity relation at $x = 0$ are prescribed. As explained in Subsection 1.3.2, we define the physical solution using a limiting absorption principle as $\nu \to 0^+$.

Regularization using viscosity. The regularization of (1.3.16) is

$$\left\{\begin{array}{rcccl} -B_z^{\nu\prime} & + & \left(\dfrac{\delta^2}{\alpha + i\nu} - (\alpha + i\nu)\right)E_y^\nu & = & 0 \quad \text{in } \Omega,\\ B_z^\nu & - & E_y^{\nu\prime} & = & 0 \quad \text{in } \Omega.\end{array}\right. \tag{1.3.17}$$

We state the limiting absorption result more precisely.

Proposition 1.3.6 (Proposition 4 in [99]). *Let $\nu > 0$, $\lambda > 0$ and f_z be a complex-valued function. There exists a unique solution $(E_y^\nu, B_z^\nu) \in L^2(\Omega)^3$ to* (1.3.17)-(1.3.7). *Moreover, it verifies for a constant $C > 0$ independent of ν*

$$\|E_y^\nu\|_{L^2(\Omega)} + \|B_z^\nu\|_{L^2(\Omega)} \leq C.$$

Corollary 1.3.7 (Corollary 1 in [99]). *Consider the same assumptions as in Proposition 1.3.6. Up to a subsequence, E_y^ν and B_z^ν admit strong limits in $L^2(\Omega)$ as $\nu \to 0^+$ that we denote E_y^+ and B_z^+. They are solution of the following variational formulation of* (1.3.16)-(1.3.7)

$$\left\{ \begin{array}{rcl} \displaystyle\int_\Omega \left(B_z^+ \psi' + \left(\frac{\delta^2}{\alpha} - \alpha \right) E_y^+ \psi \right) \mathrm{d}x &=& 0, \quad \forall \psi \in H^1_{0,0}(\Omega), \\ \displaystyle\int_\Omega \left(E_y^+ \phi' + B_z^+ \phi \right) \mathrm{d}x &=& 0, \quad \forall \phi \in H^1_0(\Omega), \end{array} \right. \tag{1.3.18}$$

where $H^1_{0,0}(\Omega) := \{v \in H^1_0(\Omega),\, v(0) = 0\}$.

At this point, it is known that the viscosity solution (E_y^ν, B_z^ν) converges in $L^2(\Omega)$ (up to a subsequence) towards a solution to the limit problem (1.3.16)-(1.3.7), but unicity of the solution still has not been obtained. We also note that the singularity will be of type $1/x$.

Construction of manufactured solutions. For a family of manufactured solutions, the relation (1.3.15) holds, and rewrites in 1D X-mode

$$\begin{aligned} \mathrm{Im} \int_\Omega \Big(& \overline{(E_y^\nu - F_y^\nu)} (B_z^\nu - C_z^\nu) \varphi' \\ & + \left(\overline{(E_x^\nu - F_x^\nu)} g_x^\nu + \overline{(E_y^\nu - F_y^\nu)} g_y^\nu - q_z^\nu \overline{(B_z^\nu - C_z^\nu)} \right) \varphi \Big) \mathrm{d}x \geq 0. \end{aligned} \tag{1.3.19}$$

We now define a manufactured solution. A solution is composed of (F_x^ν, F_y^ν) and C_z^ν, and source terms (g_x^ν, g_y^ν) and q_z^ν such that

$$\left\{ \begin{array}{rcrcrcl} & - & (\alpha + i\nu) F_x^\nu & - & i\delta F_y^\nu & = & g_x^\nu, \\ -C_z^{\nu\prime} & + & i\delta F_x^\nu & - & (\alpha + i\nu) F_y^\nu & = & g_y^\nu, \\ C_z^\nu & & & - & F_y^{\nu\prime} & = & q_z^\nu, \end{array} \right. \tag{1.3.20}$$

and such that (H1)-(H2) are verified. We recall that the hypotheses amount to explicit manufactured solutions for $\nu > 0$ and at the limit $\nu = 0^+$ and being able to determine the limit of the integral in relation (1.3.19). Since E_y^ν and B_z^ν converge in $L^2(\Omega)$ up to a subsequence, the singular term is

$$\mathrm{Im} \int_\Omega \overline{(E_x^\nu - F_x^\nu)} g_x^\nu \varphi \mathrm{d}x. \tag{1.3.21}$$

It is cancelled by setting

$$g_x^\nu = 0.$$

We also chose F_x^ν that mimics the expected singularity

$$F_x^\nu(x) = \frac{-1}{\alpha(x) + i\nu} \quad \text{in } \Omega.$$

Hence, the first equation from (1.3.20) imposes $F_y^\nu(x) = (i\delta(x))^{-1}$ in Ω. For g_y^ν to be in $L^2(\Omega)$, we set

$$C_z^\nu(x) = -i\delta(0)\frac{1}{r}\left(\frac{1}{2}\log(r^2x^2+\nu^2) - i\arctan\left(\frac{rx}{\nu}\right)\right) \quad \text{in } \Omega.$$

Indeed, one can check that $C_z^{\nu\prime}(x) = -i\delta(0)/(rx+i\nu)$, and

$$\begin{aligned} -C_z^{\nu\prime}(x) + i\delta F_x^\nu(x) &= \frac{i\delta(0)}{rx+i\nu} - \frac{i\delta(x)}{\alpha(x)+i\nu} \\ &= \frac{i(\delta(0)-\delta(x))}{rx+i\nu} + i\delta(x)\left(\frac{1}{rx+i\nu} - \frac{1}{\alpha(x)+i\nu}\right). \end{aligned}$$

Assumption 1.3.4 ensures this term is in $L^\infty(\Omega)$ since

$$\left|\frac{1}{rx+i\nu} - \frac{1}{\alpha(x)+i\nu}\right| = \frac{|\alpha-rx|}{|\alpha(x)+i\nu||rx+i\nu|} \le \frac{|\alpha-rx|}{|\alpha(x)rx|} = O(1),$$

and that

$$\left|\frac{\delta(0)-\delta(x)}{rx+i\nu}\right| \le \frac{|\delta(0)-\delta(x)|}{|rx|} = O(1),$$

for small x. Therefore $g_y^\nu = -C_z^{\nu\prime} + i\delta F_x^\nu - (\alpha+i\nu)F_y^\nu \in L^2(\Omega)$, independently of ν. Lastly, $q_z^\nu = C_z^\nu - F_y^{\nu\prime}$ is also in $L^2(\Omega)$.

We have defined an explicit manufactured solution

$$\left\{\begin{array}{rcl} F_x^\nu(x) &=& \dfrac{-1}{\alpha(x)+i\nu}, \\ F_y^\nu(x) &=& \dfrac{1}{i\delta(x)}, \\ C_z^\nu(x) &=& -i\delta(0)\dfrac{1}{r}\left(\dfrac{1}{2}\log(r^2x^2+\nu^2) - i\arctan\left(\dfrac{rx}{\nu}\right)\right), \\ g_x^\nu(x) &=& 0, \\ g_y^\nu(x) &=& \dfrac{i\delta(0)}{rx+i\nu} - \dfrac{i\delta(x)}{\alpha(x)+i\nu} - \dfrac{\alpha(x)+i\nu}{i\delta(x)}, \\ q_z^\nu(x) &=& -i\delta(0)\dfrac{1}{r}\left(\dfrac{1}{2}\log(r^2x^2+\nu^2) - i\arctan\left(\dfrac{rx}{\nu}\right)\right) + \dfrac{\delta'(x)}{i\delta(x)^2}. \end{array}\right. \tag{1.3.22}$$

with corresponding limits as $\nu \to 0^+$

$$\left\{\begin{array}{rcl} F_x^+(x) &=& \dfrac{-1}{\alpha(x)}, \\ F_y^+(x) &=& \dfrac{1}{i\delta(x)}, \\ C_z^+(x) &=& -i\delta(0)\dfrac{1}{r}\left(\log|rx| - i\dfrac{\pi}{2}\operatorname{sign}(rx)\right), \\ g_x^+(x) &=& 0, \\ g_y^+(x) &=& \dfrac{i(\delta(0)-\delta(x))}{rx} + i\delta(x)\left(\dfrac{1}{rx} - \dfrac{1}{\alpha(x)}\right) - \dfrac{\alpha(x)}{i\delta(x)}, \\ q_z^+(x) &=& -i\delta(0)\dfrac{1}{r}\left(\log|rx| - i\dfrac{\pi}{2}\operatorname{sign}(rx)\right) + \dfrac{\delta'(x)}{i\delta(x)^2}. \end{array}\right. \tag{1.3.23}$$

Exept from F_x^ν, all of these functions are in $L^2(\Omega)$ uniformly with respect to ν. The limit (1.3.23) of system (1.3.22) holds in $L^2(\Omega)$ as $\nu \to 0^+$ for all components but F_x^ν. They verify the relations (1.3.20) as well as (H1) and (H2), and thus form a manufactured solution associated to the resonant Maxwell's equations.

Energy of the scaled difference. Now that such a manufactured solution has been constructed, with a singularity expected to be proportional to the one of E_x^ν at $x = 0$, we introduce a new unknown $k \in \mathbb{C}$ to characterize the singularity. For all $k \in \mathbb{C}$, one has the dissipation relation on the scaled difference between the solution and the manufactured solution

$$\mathrm{Im} \int_\Omega \left(\overline{(E_y^+ - kF_y^+)}(B_z^+ - kC_z^+)\varphi' + \left(\overline{(E_y^+ - kF_y^+)} k g_y^+ - k q_z^+ \overline{(B_z^+ - kC_z^+)} \right) \varphi \right) \mathrm{d}x \geq 0. \quad (1.3.24)$$

We seek to minimize the energy of (1.3.24), in order for kF_x^ν to be as close as possible to the singular part of E_x^ν. To do so, we minimize the quadratic form defined on $V := L^2(\Omega) \times L^2(\Omega) \times \mathbb{C}$ by

$$\mathcal{J}^+(E, B, k) = \mathrm{Im} \int_\Omega \left(\overline{(E - kF_y^+)}(B - kC_z^+)\varphi' + \left(\overline{(E - kF_y^+)} k g_y^+ - k q_z^+ \overline{(B - kC_z^+)} \right) \varphi \right) \mathrm{d}x$$

under the constraint of verifying weakly the resonant Maxwell's equations

$$b\left((E, B), \boldsymbol{\lambda}\right) = \ell(\boldsymbol{\lambda}) \quad \forall \boldsymbol{\lambda} \in Q^0,$$

where b is defined according to (1.3.18) on $L^2(\Omega)^2 \times Q^0$ for

$$Q^0 := \{(v, w) \in H^1(\Omega)^2, v(0) = 0\},$$

by

$$b\left((E, B), \boldsymbol{\lambda}\right) = \int_\Omega \left(B\lambda_1' + \left(\frac{\delta^2}{\alpha} - \alpha \right) E\lambda_1 \right) \mathrm{d}x + \int_\Omega \left(E\lambda_2' + B\lambda_2 \right) \mathrm{d}x,$$

and ℓ is defined according to the boundary conditions (1.3.7). The associated Lagrangian is defined on $V \times Q^0$ by

$$\mathcal{L}^+\left((E, B, k), \boldsymbol{\lambda}\right) = \mathcal{J}^+(E, B, k) + \mathrm{Im}\left(b\left((E, B), \boldsymbol{\lambda}\right) - \ell(\boldsymbol{\lambda}) \right).$$

The Euler-Lagrange equations, corresponding to $d\mathcal{L}^+_{((E,B,k),\boldsymbol{\lambda})} = 0$, consist in a closed system and the solution is such that (E, B) verify the resonant Maxwell's equations.

In the context of this work, the remaining questions are: is this system well-posed, in the sense of existence and uniqueness of the solution? If so, are the components (E, B) of this solution limits as $\nu \to 0^+$ of (E_y^ν, B_y^ν), the solutions of the regularized Maxwell's equations? If so, the second question concerns the meaning behind this minimization principle: it is not straightforward that the solution is the physical solution we seek for.

The first question will be answered positively for both the 1D problem in mode coupling and the 2D X-mode. The structure of the Euler-Lagrange equations in each of these cases is the one of mixed variational fomulations, for which necessary and sufficient conditions are well known [13]. Operator theory tools such as coercive and compact decompositions and the Fredholm alternative then lead to well-posedness. A positive answer to the second question was also provided in 1D mode coupling, by deriving a priori estimates on the solution and a variational formulation for $\nu > 0$ that converges towards the Euler-Lagrange equations, as sketched in the General Introduction in Figure 1. In 2D, numerical simulations with a straight interface validate this 1D answer.

2 A stable formulation for 1D oblique incidence

This work with Martin Campos Pinto and Bruno Després is the subject of an article accepted in the Journal of Computational and Applied Mathematics, entitled *A Stable Formulation of Resonant Maxwell's Equations in Cold Plasma*.
In the Appendix 2.5, additional computations concerning the second test case that are not in the published version are added.

We consider a boundary value problem (BVP) for a reduced system of time harmonic Maxwell equations in magnetized plasma. The dielectric tensor is strongly anisotropic and the system admits resonant solutions in the context of the limit absorption principle. In particular, in the vanishing viscosity limit the normal component of the electric field becomes infinite and non integrable at the resonant point, and the system becomes ill-posed. In this article we recast the problem in the framework of mixed variational problems and we propose a well-posed formulation that characterizes the singular limit solutions. A key tool is the method of manufactured solutions [99] to construct an integral variational characterization of the jump conditions at the resonance. The well posedness is demonstrated and basic numerical results illustrate the robustness of our approach.

2.1 Introduction

Linear cold plasma models are routinely used to compute the propagation of radio-frequency electromagnetic (EM) waves in magnetized plasmas, with applications in the ionosphere and in tokamaks [20, 106, 110, 3]. However, to our knowledge, a sound analysis of the well-posedness of these models has never been proposed in the context of variational formulations which are the basis of computational tools in the plasma physics community [87, 85]. The reason is that the mathematical or physical solutions present White-Chen strong vectorial singularities [114] which make questionable the accuracy of finite element solvers in this context. In this work we contribute to establish the first rigorous mathematical and computational treatment for such problems by constructing an original and stable mixed variational formulation of the equations.

In the cold plasma model problem, the time harmonic Maxwell's equations are coupled with a Newton law for the linearized response of the non-homogeneous electron plasma. After elementary manipulations the electron current density can be eliminated from the equations, and the time-

harmonic EM field ($\mathbf{E}^\nu$, $\mathbf{B}^\nu$) satisfies a system of the form

$$\left\{ \begin{array}{rcrcl} \mathbf{B}^\nu & - & \nabla \times \mathbf{E}^\nu & = & 0 \\ \nabla \times \mathbf{B}^\nu & - & \underline{\underline{\varepsilon}}^\nu \mathbf{E}^\nu & = & 0 \end{array} \right. . \tag{2.1.1}$$

Here $\mathbf{E}^\nu$ is the unknown electric field. The physical magnetic field is actually $\frac{1}{i\omega}\mathbf{B}^\nu$ with ω the frequency of the wave sent into the plasma, but for convenience we call $\mathbf{B}^\nu := \nabla \wedge \mathbf{E}^\nu$ the magnetic field. The presence of a bulk magnetic field results in a planar structure for the dielectric tensor. If the plasma density varies only in the x direction and the bulk magnetic field is aligned with the z direction, we may consider a simplified tensor of the form

$$\underline{\underline{\varepsilon}}^\nu(\mathbf{x}) = \begin{pmatrix} \alpha(x) + i\nu & i\delta(x) & 0 \\ -i\delta(x) & \alpha(x) + i\nu & 0 \\ 0 & 0 & 1 \end{pmatrix}, \qquad \mathbf{x} = (x, y, z) \tag{2.1.2}$$

with α a smooth function vanishing at $x = 0$ and $\delta > 0$. The planar configuration is obtained by considering fields of the form $(\mathbf{E}^\nu, \mathbf{B}^\nu)(\mathbf{x}) = e^{ik_z z}(\hat{\mathbf{E}}^\nu, \hat{\mathbf{B}}^\nu)(x)$ which corresponds to waves being sent into the plasma with a wave vector $\mathbf{k} = (k_x, 0, k_z)$, see [114]. Writing $\hat{\mathbf{E}}^\nu = (e_x^\nu, e_y^\nu, e_z^\nu)^t$ and $\hat{\mathbf{B}}^\nu = (b_x^\nu, b_y^\nu, b_z^\nu)^t$, we rewrite system (2.1.1) as

$$\left\{ \begin{array}{rcrcl} b_x^\nu & + ik_z e_y^\nu & = & 0 \\ b_y^\nu & - ik_z e_x^\nu + e_z^{\nu\prime} & = & 0 \\ b_z^\nu & - e_y^{\nu\prime} & = & 0 \end{array} \right. , \quad \left\{ \begin{array}{rcrcl} - ik_z b_y^\nu & -(\alpha + i\nu) e_x^\nu - i\delta e_y^\nu & = & 0 \\ ik_z b_x^\nu - b_z^{\nu\prime} & + i\delta e_x^\nu - (\alpha + i\nu) e_y^\nu & = & 0 \\ b_y^{\nu\prime} & - e_z^\nu & = & 0 \end{array} \right. \tag{2.1.3}$$

and we observe that all the components of the fields can be expressed in terms of e_y^ν and b_y^ν. As ν goes to 0 which is a physical regime encountered in fusion plasma physics, the main singularity concerns

$$e_x^\nu = -\frac{i\delta}{\alpha + i\nu} e_y^\nu - \frac{ik_z}{\alpha + i\nu} b_y^\nu. \tag{2.1.4}$$

The problem is that the field $\mathbf{E}^\nu$ becomes non integrable for $\nu = 0$. This non integrability phenomenon is not compatible with the standard finite element treatment of Maxwell's equations [90]. Related problems have been studied in the framework of metamaterials [34, 91] where the permittivity changes sign. Here an additional difficulty comes from the fact that α also vanishes at $x = 0$.

A convenient approach to have a better understanding of the problem and to propose a solution is to consider a White-Chen reformulation in planar geometry. We write it as

$$-\frac{d^2}{dx^2}\mathbf{u}^\nu(x) + \frac{1}{\alpha(x) + i\nu}\mathsf{N}^\nu(x)\mathbf{u}^\nu(x) = 0 \qquad \text{in } \Omega = (-1, 1), \tag{2.1.5}$$

where the unknown $\mathbf{u}^\nu = (e_y^\nu, b_y^\nu)^t$ is made of the second components of the electromagnetic field. It is completed with natural dissipative boundary conditions

$$\frac{d}{dx}\mathbf{u}^\nu(\pm 1) \mp \begin{pmatrix} i\sigma & 0 \\ 0 & i/\sigma \end{pmatrix} \mathbf{u}^\nu(\pm 1) = \mathbf{f}(\pm 1), \tag{2.1.6}$$

for $\sigma > 0$ and $\mathbf{f}$ a $\mathbb{C}^2$-valued field defined on $\partial\Omega = \{-1, 1\}$.

Here the matrix $\mathsf{N}^\nu(x) \in \mathcal{M}_2(\mathbb{C})$ is also a smooth function of x as

$$\mathsf{N}^\nu(x) = \begin{pmatrix} k_z^2(\alpha(x) + i\nu) + \delta(x)^2 - (\alpha(x) + i\nu)^2 & \delta(x)k_z \\ \delta(x)k_z & k_z^2 - (\alpha(x) + i\nu) \end{pmatrix} \qquad \text{for } x \in \Omega, \tag{2.1.7}$$

which does not vanish at $x = 0$. Therefore for $\nu = 0$ the coefficients of (2.1.5) blow up at this resonant point and the boundary value problem (BVP) is ill-posed. The limit equation can only be formulated outside 0

$$-\frac{d^2}{dx^2}\mathbf{u}(x) + \frac{1}{\alpha(x)}\mathsf{N}(x)\mathbf{u}(x) = 0 \qquad \text{in } \Omega - \{0\}. \tag{2.1.8}$$

However, a preliminary mathematical remark is that the matrix $\mathsf{N} = \mathsf{N}^0$ satisfies at the resonance the important condition $\operatorname{rank}(\mathsf{N}(0)) = 1$, so that there exist functions $\mathbf{v} \in H^1(\Omega)^2$ such that $\frac{1}{\alpha}\mathsf{N}\mathbf{v}$ is square integrable on Ω although $\mathbf{v}(0) \neq 0$.

The case $k_z = 0$ corresponds to a wave being sent with a *normal incidence* with respect to the bulk magnetic field [114]. In this case the equations on e_y^ν and b_y^ν decouple. The wave corresponding to the latter field is called an ordinary mode (O-mode) and in the limit $\nu \to 0$ it satisfies a standard Helmholtz equation. The wave corresponding to the former one is called an extraordinary mode (X-mode) and is the singular one. In the generic situation considered here of a function α that vanishes locally at $x = 0$ the component $e_x^\nu = -i\frac{\delta}{\alpha + i\nu}e_y^\nu$ may become non-integrable, and the problem needs be addressed using a limit absorption principle with vanishing positive viscosity $\nu \to 0^+$. It has been mathematically analyzed in [32]. However it must be noticed that classical literature [90] does not say anything about this problem, because of the strongly anisotropic nature of the dielectric tensor which generates these strong singular vectorial solutions.

In this article we develop a mathematical theory that covers the case $k_z \neq 0$ corresponding to a wave being sent in the plasma with an *oblique incidence* with respect to the bulk magnetic field [114]. We still have the same type of potentially non-integrable field e_x^ν, see (2.1.4), but this case is notoriously more complicated to analyze since it brings what is called a mode coupling: as the extra-diagonal coefficients are non zero in the matrix (2.1.7), it is no longer possible to decouple the equations on e_y^ν and b_y^ν. Our goal is thus to characterize and analyze the reduced model (2.1.5) in the limit $\nu \to 0^+$. For that purpose we will use the classical framework [13] for mixed variational formulations. The most original tool in our approach will be the method of manufactured solutions recently introduced in [99] which is used to characterize the singular solutions within the mixed variational framework.

The very singular behavior of the solutions corresponds to an interesting and fundamental resonance phenomenon that takes place at $x = 0$. In the context of controlled nuclear fusion this is one of the methods used to heat the plasma in a tokamak. The resonant heating is tied to the amplitude of the singularity. Letting $\Pi^\nu = \operatorname{Im}(\mathbf{E}^\nu \times \overline{\mathbf{B}^\nu})$ denote an ad-hoc Poynting vector, it can be written as

$$\lim_{\nu \to 0^+} \int_\Omega \nabla \cdot \Pi^\nu \mathrm{d}x = \lim_{\nu \to 0^+} \nu \int_\Omega |\mathbf{E}^\nu(x)|^2 \, \mathrm{d}x > 0 \tag{2.1.9}$$

where the positivity of the limit is already an indication of its singular nature. We refer to [31, 99] for additional mathematical results on the X-mode resonance, and to [23] for a numerical study.

Assumptions and notations. Before stating the main results we need to particularize the class of matrices which is encompassed by our theory. As written above, for $\nu \in \mathbb{R}$ the matrix-valued functions considered here are of the form (2.1.7).

Assumption 2.1.1. We suppose that $\alpha \in W^{3,\infty}(\Omega)$ is real-valued and such that 0 is its only root, with $r = \alpha'(0) \neq 0$. In addition we assume that $\delta \in W^{3,\infty}(\Omega)$ is real and positive. Finally the Fourier variable $k_z \in \mathbb{R}$ is arbitrary, to handle the mode coupling phenomenon described in [114].

Notation 2.1.2. As N^ν depends continuously on ν, for $\nu = 0$ we denote the limit matrix by $\mathsf{N} := \mathsf{N}^0$.

The symmetry properties of (2.1.2) can be characterized as follows.

Proposition 2.1.3. *For $\nu \in \mathbb{R}$, N^ν is such that*

$$\mathsf{N}^\nu = (\mathsf{N}^\nu)^t, \quad \overline{\mathsf{N}^\nu} = \mathsf{N}^{-\nu}, \quad \textit{and} \quad \ker \mathsf{N}(0) = \mathrm{Span}_{\mathbb{C}}\big\{\big(k_z, -\delta(0)\big)^t\big\}.$$

For $\nu \geq 0$, it also verifies the dissipation property

$$\frac{1}{2i}\Big(\frac{1}{\alpha + i\nu}\mathsf{N}^\nu - \frac{1}{\alpha - i\nu}\mathsf{N}^{-\nu}\Big) = \mathrm{Im}\,\Big(\frac{1}{\alpha + i\nu}\mathsf{N}^\nu\Big) \leq 0, \tag{2.1.10}$$

in the sense that it is negative semi-definite.

Proof. Given (2.1.7), the three first properties are immediate as α, δ, k_z and ν are real-valued and as $\alpha(0) = 0$. For the last one we use

$$\mathrm{Im}\,\Big(\frac{1}{\alpha + i\nu}\mathsf{N}^\nu\Big) = \mathrm{Im}\,\Big(\frac{\alpha - i\nu}{\alpha^2 + \nu^2}\mathsf{N}^\nu\Big) = \frac{-\nu}{\alpha^2 + \nu^2}\begin{pmatrix} \delta^2 + \alpha^2 + \nu^2 & \delta k_z \\ \delta k_z & k_z^2 \end{pmatrix}.$$

Because $\delta^2|c_1|^2 + 2\delta k_z c_1\overline{c_2} + k_z^2|c_2|^2 = |\delta c_1 + k_z c_2|^2$ for $c_1, c_2 \in \mathbb{C}$, it establishes $\mathrm{Im}(\mathsf{N}^\nu/(\alpha + i\nu)) \leq 0$. Finally as $\overline{\mathsf{N}^\nu/(\alpha + i\nu)} = \mathsf{N}^{-\nu}/(\alpha - i\nu)$, the announced property is verified. □

New results. Our main mathematical results can now be formulated as follows.

Theorem 2.1.4. *Under the above assumptions, the unique solution $\mathbf{u}^\nu$ of system* (2.1.5)-(2.1.6) *converges for $\nu \to 0^+$ weakly in $H^1(\Omega)^2$ towards a function $\mathbf{u}^+$. This function is a strong solution to the limit equation* (2.1.8) *except at the resonance and satisfies strongly the boundary conditions* (2.1.6).

This first result establishes the existence of a limit for vanishing viscosity parameter ν, but the limit equation (2.1.8) does not allow to completely characterize $\mathbf{u}^+$ since the equation is not valid at $x = 0$ due to the singularity. The next result establishes that $\mathbf{u}^+$ is the solution of a well posed mixed variational formulation in the spaces

$$V = H^1(\Omega)^2 \times \mathbb{C} \quad \text{and} \quad Q = \big\{\mathbf{v} \in H^1(\Omega)^2,\ \mathsf{N}(0)\mathbf{v}(0) = 0\big\}.$$

Theorem 2.1.5. *The viscosity limit $\mathbf{u}^+$ is the unique solution of a mixed variational formulation*

$$\begin{array}{l} \textit{Find } ((\mathbf{u}, s), \boldsymbol{\lambda}) \in V \times Q \textit{ such that} \\ \left\{ \begin{array}{lcll} a^+\big((\mathbf{u}, s), (\mathbf{v}, t)\big) - \overline{b\big((\mathbf{v}, t), \boldsymbol{\lambda}\big)} & = & 0, & \forall (\mathbf{v}, t) \in V, \\ b\big((\mathbf{u}, s), \boldsymbol{\mu}\big) & = & \ell(\boldsymbol{\mu}), & \forall \boldsymbol{\mu} \in Q, \end{array} \right. \end{array} \tag{2.1.11}$$

where the sesquilinear form b is defined in (2.2.4), the antilinear form ℓ is defined in (2.2.6) and the sesquilinear form a^+ is defined in (2.3.5).

The proof heavily relies on the theory of mixed variational formulation [13] applied to a convenient characterization of the limit solution $\mathbf{u}^+$, where the sesquilinear form a^+ appears to be exactly

what is needed to complement the missing information stressed in Theorem 2.1.4. We will also propose in the core of this work another mixed variational formulation which is valid for $\nu > 0$ and has the limit (2.1.11) for $\nu = 0^+$.

We will show at the end of this work how to reconstruct all components of the electromagnetic field from the numerical computation of $\mathbf{u}$. It will illustrate the highly singular nature of the electromagnetic field and the computational efficiency of this new method. The gain of numerical accuracy, with respect to a classical finite element formulation, will be illustrated on the numerical computation of the resonant heating.

Outline of the paper. Preliminary material, such as the sesquilinear form b and simple a priori bounds, are introduced in Section 2.2. The mixed variational formulation is constructed and studied in Section 2.3. Since the theory of mixed variational formulation is completed with a well established theory of numerical discretization, we take this opportunity to illustrate our main results with simple and reliable numerical results in Section 2.4. It also helps to better understand the physics which is behind the model problem (2.1.5). An application to an accurate calculation of the resonant heating is finally shown.

Additional conventions. Vectors will be written in bold lower-case letters as $\mathbf{u}$ or $\boldsymbol{\lambda}$, matrices will be written in bold upper-case letters as N. The dependency on ν will be upper-indexed, as for N^ν. When the limit as ν goes to 0 depends on the sign of ν, it will be upper-indexed with a plus or a minus sign, as for $\mathbf{u}^+$ or a^+. And when the limit does not depend on the way ν goes to 0, it will not be indexed, as for N, to simplify the notations. We will use the notations $\big\{f\big\}_{-1}^{1} = f(1) + f(-1)$ and $\big[f\big]_{-1}^{1} = f(1) - f(-1)$ for a scalar function f defined in -1 and 1. When the context makes it non ambiguous, the norm $\|.\|_{H^1(\Omega)^2}$ will often be denoted by $\|.\|_{H^1(\Omega)}$ or even simpler by $\|.\|_{H^1}$. The dual spaces will be noted with a prime, for example Q' is the space of all continuous linear maps from Q to $\mathbb{C}$.

2.2 Preliminary material

Let us start the construction with two natural variational formulations associated to (2.1.5)-(2.1.6) and (2.1.6)-(2.1.8). For $\nu > 0$, the viscosity problem can be written in $H^1(\Omega)^2$ as a first variational formulation:

$$\begin{array}{l} \text{Find } \mathbf{u} \in H^1(\Omega)^2 \text{ such that} \\ b^\nu\big(\mathbf{u}, \mathbf{v}\big) = \ell^\nu(\mathbf{v}) \quad \text{for all test functions } \mathbf{v} \in H^1(\Omega)^2. \end{array} \tag{2.2.1}$$

Here the sesquilinear form is

$$b^\nu\big(\mathbf{u}, \mathbf{v}\big) = \int_\Omega \left(\mathbf{u}' \cdot \overline{\mathbf{v}}' + \mathbf{u} \cdot \frac{\mathsf{N}^\nu}{\alpha + i\nu} \overline{\mathbf{v}} \right) \mathrm{d}x - \left\{ \begin{pmatrix} i\sigma & 0 \\ 0 & i/\sigma \end{pmatrix} \mathbf{u} \cdot \overline{\mathbf{v}} \right\}_{-1}^{1}, \tag{2.2.2}$$

for $(\mathbf{u}, \mathbf{v}) \in H^1(\Omega)^2 \times H^1(\Omega)^2$, and the antilinear form is

$$\ell^\nu(\mathbf{v}) = \big[\mathbf{f} \cdot \overline{\mathbf{v}}\big]_{-1}^{1}, \quad \text{for } \mathbf{v} \in H^1(\Omega)^2. \tag{2.2.3}$$

In order to pass to the limit $\nu = 0^+$, in a way or another we must handle the fact that $\mathsf{N}(0)$ does not vanish so that the integral may be ill defined. In this work, we decide to impose a constraint on the test functions.

Definition 2.2.1. For $\nu = 0^+$, we introduce a space of test functions

$$Q = \big\{\mathbf{v} \in H^1(\Omega)^2,\, \mathsf{N}(0)\mathbf{v}(0) = 0\big\}.$$

The limit of (2.2.2) for $\nu = 0^+$ is naturally written for $\mathbf{u} \in H^1(\Omega)^2$ and $\mathbf{v} \in Q \subset H^1(\Omega)^2$:

$$\begin{array}{l}\text{Find } \mathbf{u} \in H^1(\Omega)^2 \text{ such that}\\ b\big(\mathbf{u},\mathbf{v}\big) = \ell(\mathbf{v}) \quad \text{for all test functions } \mathbf{v} \in Q.\end{array} \tag{2.2.4}$$

where the sesquilinear form is

$$b\big(\mathbf{u},\mathbf{v}\big) = \int_\Omega \left(\mathbf{u}'\cdot\overline{\mathbf{v}}' + \mathbf{u}\cdot\frac{\mathsf{N}}{\alpha}\overline{\mathbf{v}}\right)\mathrm{d}x - \left\{\begin{pmatrix} i\sigma & 0\\ 0 & i/\sigma\end{pmatrix}\mathbf{u}\cdot\overline{\mathbf{v}}\right\}_{-1}^{1}, \tag{2.2.5}$$

for $\mathbf{u} \in H^1(\Omega)^2$, $\mathbf{v} \in Q$, and the antilinear form is the same as (2.2.3)

$$\ell = \ell^\nu \quad \text{on } Q. \tag{2.2.6}$$

Remark 2.2.2. The fact that (2.2.5) is well defined for $\mathbf{u} \in H^1(\Omega)^2$ and $\mathbf{v} \in Q$ is a consequence of Hardy's inequality [19]

$$\int_\Omega \frac{f^2(x)}{x^2}\mathrm{d}x \le 4\int_\Omega f'^2(x)\mathrm{d}x$$

for f a real-valued function of $H^1(\Omega)$ vanishing at 0.

It is sufficient to apply this inequality separately to the first and second components of the vector $\mathsf{N}\mathbf{v}$ to show that $\frac{\mathsf{N}}{\alpha}\mathbf{v} \in L^2(\Omega)^2$.

It is easy to show that solutions $\mathbf{u} = (e,b)^t \in H^1(\Omega)^2$ to (2.2.4) are in fact strong solutions except at $x = 0$ of a system of second-order ODEs. They verify on $(-1,0)$ and on $(0,1)$

$$\left\{\begin{array}{rcrcrcl} -e'' & + & \Big(k_z^2 + \dfrac{\delta^2}{\alpha} - \alpha\Big)e & + & \dfrac{\delta k_z}{\alpha}b & = & 0,\\ -b'' & + & \dfrac{\delta k_z}{\alpha}e & + & \Big(\dfrac{k_z^2}{\alpha} - 1\Big)b & = & 0,\end{array}\right. \tag{2.2.7}$$

as well as two boundary conditions on the left at $x = -1$ and two on the right at $x = 1$. Now, because of the constraint imposed on the test function space Q it is only possible to show that three linear combinations of the solutions, namely e, b and $k_z e' - \delta(0)b'$, are in $H^1(\Omega)$, which yields three continuity relations at 0. Thus we see that one constraint is missing to define uniquely a solution on Ω. The problem here is similar to what is known for the X-mode equation corresponding to $k_z = 0$, as described in the introduction: for $\nu = 0$ the system (2.2.7) completed with boundary conditions admits multiple solutions, see e.g. [32] or Proposition 2.4.1. In order to obtain the missing information (if there is one), we begin by gathering simple a priori bounds before passing to the limit.

2.2.1 A priori bounds

A priori bounds are derived in this section for the solution of problem (2.1.5)-(2.1.6) with positive viscosity $\nu > 0$. We remind that here $\mathbf{u}^\nu = (e_y^\nu, b_y^\nu)^t$ consists of the second components of the electric and magnetic fields in the cold plasma model (2.1.3). As observed before the other components are easily recovered from these two ones, and we may point out that $e_x^\nu = -i\frac{\delta}{\alpha+i\nu}e_y^\nu - i\frac{k_z}{\alpha+i\nu}b_y^\nu$, so that a singularity of order $1/\alpha$ is expected at the limit.

Proposition 2.2.3. *For $\nu \in (0,1]$, $\sigma > 0$ and $\mathbf{f}$ defined on $\partial\Omega$ with values in $\mathbb{C}^2$, the weak formulation (2.2.1) of (2.1.5)-(2.1.6) has a unique solution in $H^1(\Omega)^2$. This solution is denoted $\mathbf{u}^\nu$.*

Proof. The right-hand side ℓ^ν is antilinear and continuous. Let us focus on the sesquilinear and continuous form b^ν. From Proposition 2.1.3 we see that the real and imaginary parts of $\frac{\mathsf{N}^\nu}{\alpha+i\nu}$ are Hermitian. It follows that for $\mathbf{v} = (v_1, v_2) \in H^1(\Omega)^2$, the decomposition into real and imaginary parts of $b^\nu(\mathbf{v},\mathbf{v})$ writes

$$\begin{aligned} b^\nu(\mathbf{v},\mathbf{v}) &= \int_\Omega \big(\mathbf{v}'\cdot\overline{\mathbf{v}}' + \mathbf{v}\cdot\frac{\mathsf{N}^\nu\overline{\mathbf{v}}}{\alpha+i\nu}\big)\mathrm{d}x - \Big\{\begin{pmatrix} i\sigma & 0\\ 0 & i/\sigma\end{pmatrix}\mathbf{v}\cdot\overline{\mathbf{v}}\Big\}_{-1}^{1} \\ &= \|\mathbf{v}'\|_{L^2}^2 + \int_\Omega \mathbf{v}\cdot\mathrm{Re}\,\big(\frac{\mathsf{N}^\nu}{\alpha+i\nu}\big)\overline{\mathbf{v}}\mathrm{d}x \\ &\quad + i\left(\int_\Omega \mathbf{v}\cdot\mathrm{Im}\,\big(\frac{\mathsf{N}^\nu}{\alpha+i\nu}\big)\overline{\mathbf{v}}\mathrm{d}x - \Big\{\sigma|v_1|^2 + \frac{|v_2|^2}{\sigma}\Big\}_{-1}^{1}\right). \end{aligned}$$

Since $\alpha, \delta \in L^\infty(\Omega)$ and $\nu > 0$, it results that for a non-negative constant $C_1 \geq 0$,

$$\begin{aligned} \mathrm{Re}\, b^\nu(\mathbf{v},\mathbf{v}) &= \|\mathbf{v}'\|_{L^2}^2 + \int_\Omega \mathbf{v}\cdot\mathrm{Re}\,\big(\frac{\mathsf{N}^\nu}{\alpha+i\nu}\big)\overline{\mathbf{v}}\mathrm{d}x \\ &\geq \|\mathbf{v}'\|_{L^2}^2 - C_1\|\mathbf{v}\|_{L^2}^2. \end{aligned} \tag{2.2.8}$$

One has

$$\begin{aligned} \mathrm{Im}\, b^\nu(\mathbf{v},\mathbf{v}) &= \int_\Omega \mathbf{v}\cdot\mathrm{Im}\,\big(\frac{\mathsf{N}^\nu}{\alpha+i\nu}\big)\overline{\mathbf{v}}\mathrm{d}x - \Big\{\sigma|v_1|^2 + \frac{|v_2|^2}{\sigma}\Big\}_{-1}^{1} \\ &= \int_\Omega \frac{-\nu}{\alpha^2+\nu^2}\big|(\delta,k_z)^t\cdot\mathbf{v}\big|^2\mathrm{d}x - \nu\|v_1\|_{L^2}^2 - \Big\{\sigma|v_1|^2 + \frac{|v_2|^2}{\sigma}\Big\}_{-1}^{1}. \end{aligned} \tag{2.2.9}$$

Consider $k_z \neq 0$. In this case, one has the inequality

$$\mathrm{Im}\, b^\nu(\mathbf{v},\mathbf{v}) \leq -C_2\|\mathbf{v}\|_{L^2}^2$$

with a positive constant $C_2 > 0$. This way,

$$\begin{aligned} \mathrm{Re}\Big(\big(C_2 + i(1+C_1)\big)b^\nu(\mathbf{v},\mathbf{v})\Big) &= C_2\,\mathrm{Re}\, b^\nu(\mathbf{v},\mathbf{v}) - (1+C_1)\,\mathrm{Im}\, b^\nu\big(\mathbf{v},\mathbf{v}\big) \\ &\geq C_2(\|\mathbf{v}'\|_{L^2}^2 - C_1\|\mathbf{v}\|_{L^2}^2) + (1+C_1)C_2\|\mathbf{v}\|_{L^2} \\ &\geq C_2\|\mathbf{v}\|_{H^1}^2. \end{aligned}$$

So the formulation (2.2.1) is coercive and the Lax-Milgram theorem [Corollary 5.8 in Brezis [19]] ensures that there exists a unique solution in $H^1(\Omega)^2$, denoted $\mathbf{u}^\nu$.

The second case is $k_z = 0$. The coercivity of $\mathrm{Im}\, b^\nu$ with respect to the second component u_2^ν is lost. But it is not a problem because the system is decoupled in two scalar equations, as the matrix (2.1.7) is diagonal. The equation for u_1^ν is still coercive, see computations above (2.2.8)-(2.2.9). The equation for u_2^ν is the classical Helmholtz equation

$$-u_2^{\nu\prime\prime} - u_2^\nu = 0 \quad \text{on } \Omega,$$

with dissipative boundary conditions, that admits a unique solution. □

Lemma 2.2.4. *There exists $C > 0$ such that for all $\nu \in (0,1]$, $\|\mathbf{u}^\nu\|_{H^1(\Omega)} \leq C$.*

Proof. The proof is performed in two steps. Firstly we show that the boundary values $\mathbf{u}^\nu(\pm 1)$ and $\mathbf{u}^{\nu\prime}(\pm 1)$ are bounded uniformly with respect to ν. This is the easy step. Secondly we show that these uniform bounds propagate inside Ω.
First step. Taking the imaginary part of (2.2.1) with $\mathbf{u} = \mathbf{v} = \mathbf{u}^\nu$, it yields

$$\int_\Omega \mathbf{u}^\nu \cdot \mathrm{Im}(\frac{1}{\alpha + i\nu}\mathsf{N}^\nu)\overline{\mathbf{u}^\nu}\mathrm{d}x - \left\{\sigma|u_1^\nu|^2 + \frac{1}{\sigma}|u_2^\nu|^2\right\}_{-1}^{1} = \mathrm{Im}\left[\mathbf{f}\cdot\overline{\mathbf{u}^\nu}\right]_{-1}^{1},$$

so that thanks to the dissipation property (2.1.10) and using $\mathrm{Im}\left[\mathbf{f}\cdot\overline{\mathbf{u}^\nu}\right]_{-1}^{1} \geq -2\left[|\mathbf{f}||\mathbf{u}^\nu|\right]_{-1}^{1}$,

$$\left\{\sigma|u_1^\nu|^2 + \frac{1}{\sigma}|u_2^\nu|^2\right\}_{-1}^{1} - 2\left[|\mathbf{f}||\mathbf{u}^\nu|\right]_{-1}^{1} \leq 0.$$

This second-order polynomial on the four variables $|u_1^\nu(-1)|$, $|u_1^\nu(1)|$, $|u_2^\nu(-1)|$ and $|u_2^\nu(1)|$ has positive leading coefficients thus it can only be non-positive on a given compact set. And this compact set depends on the coefficients of the polynomial, which are σ and $\mathbf{f}$, but not on ν.
Second step. One has

$$\left|\mathbf{u}^{\nu\prime\prime}(x)\right| = \left|\frac{\mathsf{N}^\nu(x)}{\alpha(x) + i\nu}\mathbf{u}^\nu(x)\right| \leq \frac{C}{|x|}\left|\mathbf{u}^\nu(x)\right|, \quad x \neq 0, \tag{2.2.10}$$

with $C > 0$ a positive constant depending only on α, δ and k_z, so independent of ν and x. Introduce the auxiliary function g

$$\left\{\begin{array}{lcl} g''(x) & = & \dfrac{C}{|x|}\left|\mathbf{u}^\nu(x)\right| \geq \left|\mathbf{u}^{\nu\prime\prime}(x)\right| \quad \text{in (-1,0)}, \\ g'(-1) & = & \left|\mathbf{u}^{\nu\prime}(-1)\right|, \\ g(-1) & = & \left|\mathbf{u}^\nu(-1)\right|. \end{array}\right. \tag{2.2.11}$$

We notice that $g'(-1)$ and $g(-1)$ are bounded uniformly with respect to ν. The functions g, g' and g'' are non-negative for $-1 \leq x < 0$. One has $g'(x) = g'(-1) + \int_{-1}^{x} g''(y)dy$ so relation (2.2.10) ensures

$$g'(x) \geq \left|\mathbf{u}^{\nu\prime}(-1)\right| + \int_{-1}^{x}\left|\mathbf{u}^{\nu\prime\prime}(y)\right|dy \geq \left|\mathbf{u}^{\nu\prime}(x)\right| \quad \text{in } (-1,0). \tag{2.2.12}$$

Integrating a second time yields

$$\begin{array}{rcl} g(x) = g(-1) + \displaystyle\int_{-1}^{x} g'(y)dy & = & |\mathbf{u}^\nu(-1)| + \displaystyle\int_{-1}^{x} g'(y)dy \\ & \geq & |\mathbf{u}^\nu(-1)| + \displaystyle\int_{-1}^{x}\left|\mathbf{u}^{\nu\prime}(y)\right|dy \quad \geq \quad |\mathbf{u}^\nu(x)|, \end{array} \tag{2.2.13}$$

for x in $(-1,0)$. Use again (2.2.11) to get

$$g(x) \geq \frac{|x|}{C}g''(x) \quad \text{in } (-1,0).$$

This last inequality is used to obtain a bound on g. Indeed $(\ln g)'' = g''/g - (g'/g)^2 \leq g''/g \leq C/|x|$ for x in $(-1,0)$. Since the primitive of $1/x$ is the logarithm, which is an integrable function, a double integration on $(-1,x)$ gives a $L^\infty(-1,0)$ bound on g. Therefore relation (2.2.13) guarantees

$$|\mathbf{u}^\nu(x)| \leq C \quad \text{in } (-1,0), \quad \text{for } 0 < \nu \leq 1,$$

for a positive constant $C > 0$ independent of ν. And it follows

$$\left|\mathbf{u}^{\nu\prime}(x)\right| \leq \tilde{C}(1 + |\ln|x||) \quad \text{in } (-1,0), \quad \text{for } 0 < \nu \leq 1,$$

for another positive constant $\tilde{C} > 0$ independent of ν. Therefore $\mathbf{u}^\nu$ is in fact bounded in $H^1(-1,0)^2$ independently of ν. A similar bound uniform with respect to ν holds in $H^1(0,1)^2$. Finally since $\mathbf{u}^\nu \in H^1(\Omega)$ is continuous at $x = 0$, it establishes

$$\|\mathbf{u}^\nu\|_{H^1(\Omega)} = \|\mathbf{u}^\nu\|_{H^1(-1,0)} + \|\mathbf{u}^\nu\|_{H^1(0,1)} \leq C$$

for a positive constant independent of ν. The proof is ended. □

Corollary 2.2.5. *As $\nu \to 0^+$ and up to a subsequence, $\mathbf{u}^\nu$ admits a weak limit in $H^1(\Omega)^2$, that we denote $\mathbf{u}^+$. This limit is a solution of (2.2.4) for all $\mathbf{v} \in Q$.*

Throughout the paper, $\mathbf{u}^+$ will denote the weak limit of one subsequence of $\mathbf{u}^\nu$. The goal is now to derive a variational formulation satisfied by $\mathbf{u}^+$. We will see that $\mathbf{u}^+$ is actually the solution of a well-posed formulation, in the sense that it has a unique solution. Therefore $\mathbf{u}^+$ will be the weak limit in $H^1(\Omega)^2$ of the whole sequence $\mathbf{u}^\nu$ as $\nu \to 0^+$, and not only of a subsequence.

Remark 2.2.6. Choosing $\nu < 0$ and $\nu \to 0^-$ leads to another limit denoted $\mathbf{u}^-$. A priori $\mathbf{u}^+ \neq \mathbf{u}^-$. The analytical solution (2.4.8) at the end of this paper is an example where indeed $\mathbf{u}^+ \neq \mathbf{u}^-$.

2.2.2 Manufactured solutions

In this Section we consider the diagonal coefficient of the dielectric tensor has a vanishing second order derivative at the resonance, that is $\alpha''(0) = 0$ and $\alpha(x) = rx + O(x^3)$. This is only for the simplicity of notations, the general situation $\alpha''(0) \neq 0$ is treated in Remark 2.2.9.

For $\nu > 0$ define

$$\mathbf{w}_1^\nu = \begin{pmatrix} \dfrac{i}{\delta}\left(1 - \dfrac{k_z^2}{\alpha + i\nu} + \dfrac{k_z^2}{rx + i\nu}\right) \\ \\ \dfrac{ik_z}{\alpha + i\nu} - \dfrac{ik_z}{rx + i\nu} \end{pmatrix}, \tag{2.2.14}$$

$$\mathbf{w}_2^\nu = \begin{pmatrix} \delta(0) \\ k_z \end{pmatrix} \frac{i}{r}\left(\frac{\log(r^2x^2 + \nu^2)}{2} - i\,\mathrm{atan}(\frac{rx}{\nu})\right). \tag{2.2.15}$$

These functions intend to approximate the electromagnetic field $\mathbf{w}_1^\nu \approx (e_y^\nu, b_y^\nu)^t$ and $\mathbf{w}_2^\nu \approx (b_z^\nu, e_z^\nu)^t = (e_y^{\nu\prime}, b_y^{\nu\prime})^t$ at the singularity. They are solutions of the non-homogeneous system

$$\left\{ \begin{array}{rcl} -\mathbf{w}_2^{\nu\prime} + \dfrac{1}{\alpha + i\nu}\mathsf{N}^\nu \mathbf{w}_1^\nu & = & \mathbf{z}_1^\nu, \\ \mathbf{w}_2^\nu - \mathbf{w}_1^{\nu\prime} & = & \mathbf{z}_2^\nu, \end{array} \right. \quad \text{in } \Omega, \tag{2.2.16}$$

with right hand sides

$$\mathbf{z}_1^\nu = \begin{pmatrix} \dfrac{i\delta}{\alpha+i\nu} - \dfrac{i\delta(0)}{rx+i\nu} + i\dfrac{k_z^2-(\alpha+i\nu)}{\delta}\left(1-\dfrac{k_z^2}{\alpha+i\nu}+\dfrac{k_z^2}{rx+i\nu}\right) \\ 0 \end{pmatrix}, \tag{2.2.17}$$

$$\mathbf{z}_2^\nu = \begin{pmatrix} \left(\dfrac{i\delta(0)}{r}\left(\dfrac{\log(r^2x^2+\nu^2)}{2} - i\,\mathrm{atan}(\dfrac{rx}{\nu})\right) \right. \\ \qquad +\dfrac{i\delta'}{\delta^2}\left(1-\dfrac{k_z^2}{\alpha+i\nu}+\dfrac{k_z^2}{rx+i\nu}\right) \\ \left. \qquad -\dfrac{ik_z^2}{\delta}\left(\dfrac{\alpha'}{(\alpha+i\nu)^2}-\dfrac{r}{(rx+i\nu)^2}\right)\right) \\ \dfrac{ik_z\alpha'}{(\alpha+i\nu)^2} - \dfrac{ik_zr}{(rx+i\nu)^2} + \dfrac{ik_z}{r}(\dfrac{\log(r^2x^2+\nu^2)}{2} - i\,\mathrm{atan}(\dfrac{rx}{\nu})) \end{pmatrix}. \tag{2.2.18}$$

Proposition 2.2.7. *For $\nu \in (0,1]$, the manufactured solution $(\mathbf{w}_1^\nu, \mathbf{w}_2^\nu)$ and the right hand side $(\mathbf{z}_1^\nu, \mathbf{z}_2^\nu)$ are bounded in $L^2(\Omega)^2$ uniformly with respect to ν.*

Proof. The non trivial part concerns $1/(\alpha+i\nu) - 1/(rx+i\nu)$ and $\alpha'/(\alpha+i\nu)^2 - r/(rx+i\nu)^2$. First,

$$\left|\frac{1}{\alpha+i\nu} - \frac{1}{rx+i\nu}\right| \le \frac{|rx-\alpha|}{\sqrt{(\alpha rx-\nu^2)^2+\nu^2(\alpha+rx)^2}}.$$

The denominator is equal to $\sqrt{\alpha^2r^2x^2+\nu^4+\nu^2\alpha^2+\nu^2r^2x^2}$ so that independently of ν,

$$\left|\frac{1}{\alpha+i\nu} - \frac{1}{rx+i\nu}\right| \le \left|\frac{rx-\alpha}{\alpha rx}\right| = O(1) \quad \text{for small } x, \tag{2.2.19}$$

because $\alpha = rx + O(x^2)$ thanks to Assumption 2.1.1. So $\frac{1}{\alpha+i\nu} - \frac{1}{rx+i\nu} \in L^\infty(\Omega)$ with a bound uniform with respect to ν. For the second estimation,

$$\frac{\alpha'}{(\alpha+i\nu)^2} - \frac{r}{(rx+i\nu)^2} = \frac{\alpha'r^2x^2-\alpha^2r+2i\nu(\alpha'rx-\alpha r)-\nu^2(\alpha'-r)}{(\alpha+i\nu)^2(rx+i\nu)^2}.$$

Assuming $\alpha = rx + O(x^3)$ and keeping track of ν,

$$\left|\frac{\alpha'r^2x^2-\alpha^2r}{(\alpha+i\nu)^2(rx+i\nu)^2}\right| \le \frac{|\alpha'r^2x^2-\alpha^2r|}{(\alpha rx)^2} + \frac{O(\nu x^3)}{\nu\alpha(rx)^2} + \frac{O(\nu^2x^2)}{\nu^2(rx)^2} = O(1) \text{ for small } x \text{ and } \nu.$$

Each term is again in $L^\infty(\Omega)$, and the dependency on ν is cancelled as it is of the same order at the numerator and denominator of each fraction. □

Remark 2.2.8. According to (2.2.16), we have the sharper bound $\|\mathbf{w}_1^\nu\|_{H^1} \le C$ for a positive constant $C > 0$ independent of ν.

Remark 2.2.9. General coefficients are $\alpha = rx + px^2 + O(x^3)$ with p non necessarily zero. A solution is to replace occurrences of $r/(rx+i\nu)^2$ by $(r+2px)/(rx+px^2+\frac{p^2}{r}x^3+i\nu)^2$ in (2.2.18). Indeed one can check that

$$\left|\frac{\alpha'}{(\alpha+i\nu)^2} - \frac{r+2px}{(rx+px^2+\frac{p^2}{r}x^3+i\nu)^2}\right| = O(1) \text{ for small } x \text{ and } \nu.$$

The p^2x^3/r term is here to filter out the non zero root of $rx+px^2$.

Lemma 2.2.10. *As $\nu \to 0^+$, the manufactured functions defined above admit the following limits in $L^2(\Omega)^2$*

$$\mathbf{w}_1^+ = \begin{pmatrix} \frac{i}{\delta}\left(1 - \frac{k_z^2}{\alpha} + \frac{k_z^2}{rx}\right) \\ \\ \frac{ik_z}{\alpha} - \frac{ik_z}{rx} \end{pmatrix}, \tag{2.2.20}$$

$$\mathbf{w}_2^+ = \begin{pmatrix} \delta(0) \\ k_z \end{pmatrix} \frac{i}{r}\left(\log|rx| - i\,\mathrm{sign}(rx)\frac{\pi}{2}\right), \tag{2.2.21}$$

$$\mathbf{z}_1^+ = \begin{pmatrix} \frac{i\delta}{\alpha} - \frac{i\delta(0)}{rx} + i\frac{k_z^2-\alpha}{\delta}\left(1 - \frac{k_z^2}{\alpha} + \frac{k_z^2}{rx}\right) \\ \\ 0 \end{pmatrix}, \tag{2.2.22}$$

$$\mathbf{z}_2^+ = \begin{pmatrix} \left(\frac{i\delta(0)}{r}\left(\log|rx| - i\,\mathrm{sign}(rx)\frac{\pi}{2}\right) + \frac{i\delta'}{\delta^2}\left(1 - \frac{k_z^2}{\alpha} + \frac{k_z^2}{rx}\right) - \frac{ik_z^2}{\delta}\left(\frac{\alpha'}{\alpha^2} - \frac{r}{(rx)^2}\right)\right) \\ \\ \frac{ik_z\alpha'}{\alpha^2} - \frac{ik_z r}{(rx)^2} + \frac{ik_z}{r}\left(\log|rx| - i\,\mathrm{sign}(rx)\frac{\pi}{2}\right) \end{pmatrix}. \tag{2.2.23}$$

Proof. This is immediate using Proposition 2.2.7. □

Remark 2.2.11. To characterize $\mathbf{u}^-$, we could define a family of manufactured functions for a negative viscosity by the same formula and have similar ν-independent bounds. The limits as $\nu \to 0^-$ of $\mathbf{w}_2^\nu$ and $\mathbf{z}_2^\nu$ would then be different as $\mathrm{atan}(rx/\nu) \underset{\nu\to 0^-}{\to} \mathrm{sign}(-rx)\frac{\pi}{2}$.

2.2.3 An energy relation

As introduced at the beginning of the paper, a key observation is the energy identity (2.1.9). We make this remark instrumental in our context by considering specific quadratic forms associated to the Poynting vector of the scaled difference between the electromagnetic field and the corresponding manufactured solutions. This is performed introducing the set of non negative test-functions that do not vanish at the singularity location

$$\mathcal{C}^1_{0,+}(\Omega) = \left\{\psi \in \mathcal{C}^1_0(\Omega),\ \psi \geq 0,\ \psi(0) > 0\right\}. \tag{2.2.24}$$

This technical tool is essential in our method.

Definition 2.2.12. For $\nu > 0$, $\varphi \in \mathcal{C}^1_{0,+}(\Omega)$ and $(\mathbf{u}, s) \in H^1(\Omega)^2 \times \mathbb{C}$, set the quadratic form $\mathcal{J}^\nu$

$$\begin{aligned} \mathcal{J}^\nu(\mathbf{u}, s) \quad = \quad & -\mathrm{Im}\int_\Omega (\mathbf{u} - s\mathbf{w}_1^\nu)\cdot\overline{(\mathbf{u}' - s\mathbf{w}_2^\nu)}\varphi'\mathrm{d}x \\ & +\mathrm{Im}\int_\Omega \left(s\mathbf{z}_1^\nu\cdot\overline{(\mathbf{u} - s\mathbf{w}_1^\nu)} - s\mathbf{z}_2^\nu\cdot\overline{(\mathbf{u}' - s\mathbf{w}_2^\nu)}\right)\varphi\,\mathrm{d}x. \end{aligned} \tag{2.2.25}$$

Define the limit quadratic form $\mathcal{J}^+$ on $H^1(\Omega)^2 \times \mathbb{C}$ such that $\mathcal{J}^+(\mathbf{u}, s) = \lim_{\nu\to 0^+} \mathcal{J}^\nu(\mathbf{u}, s)$ for all $(\mathbf{u}, s) \in H^1(\Omega)^2 \times \mathbb{C}$.

We will pass to the limit in $\mathcal{J}^\nu(\mathbf{u}^\nu, s)$ as $\nu \to 0^+$. In this direction it will be imperative in our analysis to establish that the quantities arising from (2.2.25)

$$\mathbf{u}^\nu \cdot \overline{\mathbf{u}^{\nu\prime}}\varphi', \quad \mathbf{w}_1^\nu \cdot \overline{\mathbf{u}^{\nu\prime}}\varphi', \quad \mathbf{u}^\nu \cdot \overline{\mathbf{w}_2^\nu}\varphi', \quad \mathbf{u}^\nu \cdot \overline{\mathbf{z}_1^\nu}\varphi, \quad \mathbf{w}_1^\nu \cdot \overline{\mathbf{z}_1^\nu}\varphi, \quad \mathbf{u}^{\nu\prime} \cdot \overline{\mathbf{z}_2^\nu}\varphi, \quad \mathbf{w}_2^\nu \cdot \overline{\mathbf{z}_2^\nu}\varphi,$$

are bounded in $L^1(\Omega)$ independently of ν.

Proposition 2.2.13. *For $\nu > 0$, $s \in \mathbb{C}$ and $\mathbf{u}^\nu$ the solution considered in Proposition 2.2.3, the following identity is verified*

$$\mathcal{J}^\nu(\mathbf{u}^\nu, s) = \nu \int_\Omega \Big(\frac{1}{\alpha^2+\nu^2} \big|(\delta, k_z)^t \cdot (\mathbf{u}^\nu - s\mathbf{w}_1^\nu)\big|^2 + \big|(1,0)^t \cdot (\mathbf{u}^\nu - s\mathbf{w}_1^\nu)\big|^2 \Big) \varphi \, \mathrm{d}x \geq 0. \tag{2.2.26}$$

Moreover, up to a subsequence,

$$\begin{aligned} \lim_{\nu\to 0^+} \mathcal{J}^\nu(\mathbf{u}^\nu, s) &= \mathcal{J}^+(\mathbf{u}^+, s) \\ &= \frac{\pi}{|r|} \big|(\delta(0), k_z)^t \cdot \big(\mathbf{u}^+(0) - s\mathbf{w}_1^+(0)\big)\big|^2 \varphi(0). \end{aligned} \tag{2.2.27}$$

Proof. As $\mathbf{u}^\nu$ verifies (2.1.5), $(\mathbf{w}_1^\nu, \mathbf{w}_2^\nu)$ verifies (2.2.16), it follows

$$\left\{ \begin{array}{rcl} -(\mathbf{u}^{\nu\prime} - s\mathbf{w}_2^\nu)' + \dfrac{\mathsf{N}^\nu}{\alpha + i\nu}(\mathbf{u}^\nu - s\mathbf{w}_1^\nu) &=& -s\mathbf{z}_1^\nu, \\ (\mathbf{u}^{\nu\prime} - s\mathbf{w}_2^\nu) - (\mathbf{u}^\nu - s\mathbf{w}_1^\nu)' &=& -s\mathbf{z}_2^\nu. \end{array} \right.$$

Since φ is compactly supported in Ω, integrating by parts and elementary manipulations give that

$$\begin{aligned} &- \operatorname{Im} \int_\Omega (\mathbf{u}^\nu - s\mathbf{w}_1^\nu) \cdot \overline{(\mathbf{u}^{\nu\prime} - s\mathbf{w}_2^\nu)} \varphi' \mathrm{d}x \\ &= \operatorname{Im} \int_\Omega (\mathbf{u}^\nu - s\mathbf{w}_1^\nu) \varphi \cdot \overline{(\mathbf{u}^{\nu\prime} - s\mathbf{w}_2^\nu)'} \mathrm{d}x + \operatorname{Im} \int_\Omega (\mathbf{u}^\nu - s\mathbf{w}_1^\nu)' \varphi \cdot \overline{(\mathbf{u}^{\nu\prime} - s\mathbf{w}_2^\nu)} \mathrm{d}x \\ &= \operatorname{Im} \int_\Omega (\mathbf{u}^\nu - s\mathbf{w}_1^\nu) \varphi \cdot \overline{\frac{\mathsf{N}^\nu}{\alpha + i\nu}(\mathbf{u}^\nu - s\mathbf{w}_1^\nu)} \mathrm{d}x \\ &\quad + \operatorname{Im} \int_\Omega (\mathbf{u}^\nu - s\mathbf{w}_1^\nu) \varphi \cdot \overline{s\mathbf{z}_1^\nu} \mathrm{d}x - \operatorname{Im} \int_\Omega (\mathbf{u}^\nu - s\mathbf{w}_1^\nu)' \varphi \cdot \overline{s\mathbf{z}_2^\nu} \, \mathrm{d}x \\ &= \operatorname{Im} \int_\Omega (\mathbf{u}^\nu - s\mathbf{w}_1^\nu) \varphi \cdot \overline{\frac{\mathsf{N}^\nu}{\alpha + i\nu}(\mathbf{u}^\nu - s\mathbf{w}_1^\nu)} \mathrm{d}x \\ &\quad - \operatorname{Im} \int_\Omega \Big(\overline{(\mathbf{u}^\nu - s\mathbf{w}_1^\nu)} \cdot s\mathbf{z}_1^\nu - \overline{(\mathbf{u}^{\nu\prime} - s\mathbf{w}_2^\nu)} \cdot s\mathbf{z}_2^\nu \Big) \varphi \, \mathrm{d}x. \end{aligned}$$

Therefore

$$\begin{aligned} \mathcal{J}^\nu(\mathbf{u}^\nu, s) &= \operatorname{Im} \int_\Omega (\mathbf{u}^\nu - s\mathbf{w}_1^\nu) \cdot \overline{\frac{\mathsf{N}^\nu}{\alpha + i\nu}(\mathbf{u}^\nu - s\mathbf{w}_1^\nu)} \varphi \, \mathrm{d}x \\ &= -\int_\Omega (\mathbf{u}^\nu - s\mathbf{w}_1^\nu) \cdot \operatorname{Im}\Big(\frac{\mathsf{N}^\nu}{\alpha + i\nu}\Big) \overline{(\mathbf{u}^\nu - s\mathbf{w}_1^\nu)} \varphi \, \mathrm{d}x \\ &= \nu \int_\Omega \Big(\frac{1}{\alpha^2+\nu^2} \big|(\delta, k_z)^t \cdot (\mathbf{u}^\nu - s\mathbf{w}_1^\nu)\big|^2 + \big|(1,0)^t \cdot (\mathbf{u}^\nu - s\mathbf{w}_1^\nu)\big|^2 \Big) \varphi \, \mathrm{d}x. \end{aligned} \tag{2.2.28}$$

The second part of the integral is controlled by ν, and therefore converges towards 0. To tackle the first part with coefficient $\nu/(\alpha^2+\nu^2)$, observe that there exists a continuous function ϵ defined on $\mathbb{R}_+$ and vanishing at 0, such that

$$\nu \int_\Omega \frac{\mathrm{d}x}{\alpha^2+\nu^2} = \frac{1}{|r|} \int_{-|r|/\nu}^{|r|/\nu} \frac{\mathrm{d}x}{x^2+1} + \epsilon(\nu) \underset{\nu\to 0^+}{\to} \frac{\pi}{|r|}.$$

Since $\mathbf{u}^\nu$ is bounded in $H^1(\Omega)^2$ uniformly with respect to ν, there exists $C>0$ independent of ν such that

$$\begin{aligned}\big|\mathbf{u}^\nu(0)-\mathbf{u}^+(0)\big|^2 &= \int_0^1 \big((1-x)|\mathbf{u}^\nu-\mathbf{u}^+|^2\big)'\,\mathrm{d}x\\ &\le 3\|\mathbf{u}^\nu-\mathbf{u}^+\|_{L^2}\|\mathbf{u}^\nu-\mathbf{u}^+\|_{H^1} \le C\|\mathbf{u}^\nu-\mathbf{u}^+\|_{L^2}.\end{aligned}$$

Up to a subsequence the right hand side tends to 0, therefore $\mathbf{u}^\nu(0)\to\mathbf{u}^+(0)$ as $\nu\to 0^+$. The same reasons imply $\mathbf{w}_1^\nu(0)\to\mathbf{w}_1^+(0)$ as $\nu\to 0^+$.

Consequently $\mathcal{J}^\nu(\mathbf{u}^\nu,s)$ converges towards $\frac{\pi}{|r|}\big|(\delta(0),k_z)^t\cdot\big(\mathbf{u}^+(0)-s\mathbf{w}_1^+(0)\big)\big|^2\varphi(0)$, and the result is proven. □

Lemma 2.2.14. *For $\mathbf{u}\in H^1(\Omega)^2$, the quadratic forms can be expanded as second order polynomials with respect to $s\in\mathbb{C}$. One has*

$$\begin{aligned}\mathcal{J}^\nu(\mathbf{u},s) &= -\operatorname{Im}\int_\Omega \mathbf{u}\cdot\overline{\mathbf{u}'}\varphi\,\mathrm{d}x\\ &\quad+\operatorname{Im}\big(s\textstyle\int_\Omega\big((\overline{\mathbf{u}'}\cdot\mathbf{w}_1^\nu-\overline{\mathbf{u}}\cdot\mathbf{w}_2^\nu)\varphi'+(\overline{\mathbf{u}}\cdot\mathbf{z}_1^\nu-\overline{\mathbf{u}'}\cdot\mathbf{z}_2^\nu)\varphi\big)\mathrm{d}x\big)\\ &\quad-|s|^2\int_\Omega \mathbf{w}_1^\nu\cdot\operatorname{Im}\big(\frac{1}{\alpha+i\nu}\mathsf{N}^\nu\big)\overline{\mathbf{w}_1^\nu}\varphi\,\mathrm{d}x,\end{aligned}\tag{2.2.29}$$

and

$$\begin{aligned}\mathcal{J}^+(\mathbf{u},s) &= -\operatorname{Im}\int_\Omega \mathbf{u}\cdot\overline{\mathbf{u}'}\varphi\,\mathrm{d}x\\ &\quad+\operatorname{Im}\big(s\textstyle\int_\Omega\big((\overline{\mathbf{u}'}\cdot\mathbf{w}_1^+-\overline{\mathbf{u}}\cdot\mathbf{w}_2^+)\varphi'+(\overline{\mathbf{u}}\cdot\mathbf{z}_1^+-\overline{\mathbf{u}'}\cdot\mathbf{z}_2^+)\varphi\big)\mathrm{d}x\big)\\ &\quad+|s|^2\frac{\pi\varphi(0)}{|r|}.\end{aligned}\tag{2.2.30}$$

Proof. Expand expression (2.2.25) with respect to s

$$\begin{aligned}\mathcal{J}^\nu(\mathbf{u},s) &= -\operatorname{Im}\int_\Omega \mathbf{u}\cdot\overline{\mathbf{u}'}\varphi\,\mathrm{d}x\\ &\quad+\operatorname{Im}s\textstyle\int_\Omega\big((\overline{\mathbf{u}'}\cdot\mathbf{w}_1^\nu-\overline{\mathbf{u}}\cdot\mathbf{w}_2^\nu)\varphi'+(\overline{\mathbf{u}}\cdot\mathbf{z}_1^\nu-\overline{\mathbf{u}'}\cdot\mathbf{z}_2^\nu)\varphi\big)\mathrm{d}x\\ &\quad-|s|^2\operatorname{Im}\int_\Omega\big(\mathbf{w}_1^\nu\cdot\overline{\mathbf{w}_2^\nu}\varphi'+(\mathbf{z}_1^\nu\cdot\overline{\mathbf{w}_1^\nu}-\mathbf{z}_2^\nu\cdot\overline{\mathbf{w}_2^\nu})\varphi\big)\mathrm{d}x.\end{aligned}$$

As in the proof of Proposition 2.2.13, it follows by an integration by parts that

$$\operatorname{Im}\int_\Omega\big(\mathbf{w}_1^\nu\cdot\overline{\mathbf{w}_2^\nu}\varphi'+(\mathbf{z}_1^\nu\cdot\overline{\mathbf{w}_1^\nu}-\mathbf{z}_2^\nu\cdot\overline{\mathbf{w}_2^\nu})\varphi\big)\mathrm{d}x=\int_\Omega\mathbf{w}_1^\nu\cdot\operatorname{Im}\big(\frac{\mathsf{N}^\nu}{\alpha+i\nu}\big)\overline{\mathbf{w}_1^\nu}\varphi\,\mathrm{d}x,\tag{2.2.31}$$

which yields relation (2.2.29). Again, according to the definition of $\mathbf{w}_1^+$ and $\mathbf{w}_2^+$, when ν goes to 0^+

$$\begin{aligned}\int_\Omega\mathbf{w}_1^\nu\cdot\operatorname{Im}\big(\frac{\mathsf{N}^\nu}{\alpha+i\nu}\big)\overline{\mathbf{w}_1^\nu}\varphi\,\mathrm{d}x &= -\nu\int_\Omega\big(\frac{1}{\alpha^2+\nu^2}\big|(\delta,k_z)^t\cdot\mathbf{w}_1^\nu\big|^2+\big|(1,0)^t\cdot\mathbf{w}_1^\nu\big|^2\big)\varphi\,\mathrm{d}x\\ &\to \frac{\pi}{|r|}\big|(\delta(0),k_z)^t\cdot\mathbf{w}_1^+(0)\big|^2\varphi(0)\end{aligned}\tag{2.2.32}$$

as detailed at the end of the proof of Proposition 2.2.13. Finally, see (2.2.20), $\mathbf{w}_1^+(0)=(\frac{i}{\delta(0)},0)^t$ so (2.2.30) is established. □

Another integral relation, which will be used in the numerical section, is the following.

Proposition 2.2.15. *The limit solution satisfies a second integral relation: for any $\varphi \in \mathcal{C}_0^1(\Omega)$, it holds*

$$\int_\Omega (\mathbf{u}^+ \cdot \mathbf{w}_2^+ - \mathbf{u}^{+\prime} \cdot \mathbf{w}_1^+)\varphi' \mathrm{d}x = \int_\Omega (\mathbf{u}^+ \cdot \mathbf{z}_1^+ - \mathbf{u}^{+\prime} \cdot \mathbf{z}_2^+)\varphi \,\mathrm{d}x. \tag{2.2.33}$$

Proof. For $\nu > 0$, using again (2.2.1) and (2.2.16)

$$\begin{aligned}
\int_\Omega (\mathbf{u}^\nu \cdot \mathbf{w}_2^\nu - \mathbf{u}^{\nu\prime} \cdot \mathbf{w}_1^\nu)\varphi' \mathrm{d}x &= \int_\Omega ((\mathbf{u}^\nu\varphi)' \cdot \mathbf{w}_2^\nu - \mathbf{u}^{\nu\prime}\varphi \cdot \mathbf{w}_2^\nu)\mathrm{d}x \\
&\quad - \int_\Omega (\mathbf{u}^{\nu\prime} \cdot (\mathbf{w}_1^\nu\varphi)' - \mathbf{u}^{\nu\prime} \cdot \mathbf{w}_1^{\nu\prime}\varphi)\mathrm{d}x \\
&= \int_\Omega (\mathbf{u}^\nu\varphi \cdot (-\frac{\mathsf{N}^\nu}{\alpha + i\nu}\mathbf{w}_1^\nu + \mathbf{z}_1^\nu) - \mathbf{u}^{\nu\prime}\varphi \cdot \mathbf{w}_2^\nu)\mathrm{d}x \\
&\quad - \int_\Omega (-\frac{\mathsf{N}^\nu}{\alpha + i\nu}\mathbf{u}^\nu \cdot (\mathbf{w}_1^\nu\varphi) - \mathbf{u}^{\nu\prime} \cdot \mathbf{w}_1^{\nu\prime}\varphi)\mathrm{d}x \\
&= \int_\Omega (\mathbf{u}^\nu\varphi \cdot \mathbf{z}_1^\nu - \mathbf{u}^{\nu\prime}\varphi \cdot \mathbf{z}_2^\nu)\mathrm{d}x.
\end{aligned}$$

Now, up to a subsequence, as $\mathbf{u}^\nu$ converges towards $\mathbf{u}^+$ weakly in $H^1(\Omega)^2$ and the manufactured functions converge in $L^2(\Omega)^2$, (2.2.33) is obtained passing to the limit $\nu \to 0^+$. □

2.3 A mixed variational formulation for the limit problem

The minimization of the quantity $\mathcal{J}^+$ on the product space of weak solutions of (2.1.6)-(2.1.8) and of complex scalars yields a mixed variational formulation in the Hilbert spaces equipped with natural norms

$$\begin{array}{cc}
V = H^1(\Omega)^2 \times \mathbb{C}, & Q = \big\{\mathbf{v} \in H^1(\Omega)^2,\, \mathsf{N}(0)\mathbf{v}(0) = 0\big\}, \\
\|(\mathbf{u}, s)\|_V = \|\mathbf{u}\|_{H^1(\Omega)^2} + |s|. & \|\mathbf{v}\|_Q = \|\mathbf{v}\|_{H^1(\Omega)^2}.
\end{array} \tag{2.3.1}$$

We extend the form b defined in (2.2.5) from $H^1(\Omega)^2 \times Q$ to $V \times Q$ by

$$b\big((\mathbf{u}, s), \boldsymbol{\lambda}\big) = \int_\Omega \big(\mathbf{u}' \cdot \overline{\boldsymbol{\lambda}}' + \mathbf{u} \cdot \frac{\mathsf{N}\overline{\boldsymbol{\lambda}}}{\alpha}\big)\mathrm{d}x - \Big\{ \begin{pmatrix} i\sigma & 0 \\ 0 & i/\sigma \end{pmatrix} \mathbf{u} \cdot \overline{\boldsymbol{\lambda}} \Big\}_{-1}^{1}, \tag{2.3.2}$$

for $(\mathbf{u}, s) \in V$ and $\boldsymbol{\lambda} \in Q$, and recall that ℓ is the antilinear form such that for all $\boldsymbol{\lambda} \in Q$, $\ell(\boldsymbol{\lambda}) = \big[\mathbf{f} \cdot \overline{\boldsymbol{\lambda}}\big]_{-1}^{1}$.

We are able to write the Lagrangian associated to the minimization of $\mathcal{J}^+$ on the space of weak solutions of (2.1.6)-(2.1.8).

Definition 2.3.1. For $(\mathbf{u}, s) \in V$ and $\boldsymbol{\lambda} \in Q$, let $\mathcal{L}^+$ be defined as

$$\mathcal{L}^+\big((\mathbf{u}, s), \boldsymbol{\lambda}\big) = \mathcal{J}^+(\mathbf{u}, s) + \mathrm{Im}\,\big(b\big((\mathbf{u}, s), \boldsymbol{\lambda}\big) - \ell(\boldsymbol{\lambda})\big). \tag{2.3.3}$$

2.3.1 Euler-Lagrange equations and main Theorem

The Euler-Lagrange equations associated to the extremalization of $\mathcal{L}^+$ are

$$\left\{ \begin{array}{lcll}
d\mathcal{J}^+_{(\mathbf{u},s)}(\mathbf{v}, t) + \mathrm{Im}\, b\big((\mathbf{v}, t), \boldsymbol{\lambda}\big) &=& 0, & \forall (\mathbf{v}, t) \in V, \\
\mathrm{Im}\, b\big((\mathbf{u}, s), \boldsymbol{\mu}\big) &=& \mathrm{Im}\,\ell(\boldsymbol{\mu}), & \forall \boldsymbol{\mu} \in Q.
\end{array} \right. \tag{2.3.4}$$

Let a^+ be the sesquilinear form defined by $\operatorname{Im} a^+\big((\mathbf{u},s),(\mathbf{v},t)\big) = d\mathcal{J}^+_{(\mathbf{u},s)}(\mathbf{v},t)$ for all $(\mathbf{u},s),(\mathbf{v},t) \in H$.

Lemma 2.3.2. *One has for* $(\mathbf{u},s),(\mathbf{v},t) \in H$

$$\begin{aligned} a^+\big((\mathbf{u},s),(\mathbf{v},t)\big) \;=\; & \int_\Omega (\overline{\mathbf{v}}\cdot\mathbf{u}' - \mathbf{u}\cdot\overline{\mathbf{v}}')\varphi' \mathrm{d}x \\ & -s\int_\Omega \big((\mathbf{w}_2^+\cdot\overline{\mathbf{v}} - \mathbf{w}_1^+\cdot\overline{\mathbf{v}}')\varphi' + (\mathbf{z}_2^+\cdot\overline{\mathbf{v}}' - \mathbf{z}_1^+\cdot\overline{\mathbf{v}})\varphi\big)\mathrm{d}x \\ & +\bar{t}\int_\Omega \big((\overline{\mathbf{w}_2^+}\cdot\mathbf{u} - \overline{\mathbf{w}_1^+}\cdot\mathbf{u}')\varphi' + (\overline{\mathbf{z}_2^+}\cdot\mathbf{u}' - \overline{\mathbf{z}_1^+}\cdot\mathbf{u})\varphi\big)\mathrm{d}x \\ & +2\frac{\pi\varphi(0)}{|r|} i s\bar{t}. \end{aligned} \tag{2.3.5}$$

Proof. Differentiate (2.2.30) to get

$$\begin{aligned} d\mathcal{J}^+_{(\mathbf{u},s)}(\mathbf{v},t) \;=\; & -\operatorname{Im}\int_\Omega (\mathbf{u}\cdot\overline{\mathbf{v}'} + \mathbf{v}\cdot\overline{\mathbf{u}'})\varphi\,\mathrm{d}x \\ & +\operatorname{Im}\left(s\int_\Omega \big((\overline{\mathbf{v}'}\cdot\mathbf{w}_1^+ - \overline{\mathbf{v}}\cdot\mathbf{w}_2^+)\varphi' + (\overline{\mathbf{v}}\cdot\mathbf{z}_1^+ - \overline{\mathbf{v}'}\cdot\mathbf{z}_2^+)\varphi\big)\,\mathrm{d}x\right) \\ & +\operatorname{Im}\left(t\int_\Omega \big((\overline{\mathbf{u}'}\cdot\mathbf{w}_1^+ - \overline{\mathbf{u}}\cdot\mathbf{w}_2^+)\varphi' + (\overline{\mathbf{u}}\cdot\mathbf{z}_1^+ - \overline{\mathbf{u}'}\cdot\mathbf{z}_2^+)\varphi\big)\,\mathrm{d}x\right) \\ & +2\operatorname{Re}(s\bar{t})\frac{\pi\varphi(0)}{|r|}. \end{aligned}$$

Defining a^+ the sesquilinear form such that $\operatorname{Im} a^+\big((\mathbf{u},s),(\mathbf{v},t)\big) = d\mathcal{J}^+_{(\mathbf{u},s)}(\mathbf{v},t)$, it yields (2.3.5). □

Our problem (2.3.4) can be recast as

$$\begin{array}{l} \text{Find } ((\mathbf{u},s),\boldsymbol{\lambda}) \in V\times Q \text{ such that} \\ \left\{\begin{array}{lcll} \operatorname{Im} a^+((\mathbf{u},s),(\mathbf{v},t)) + \operatorname{Im} b((\mathbf{v},t),\boldsymbol{\lambda}) & = & 0, & \forall(\mathbf{v},t)\in V, \\ \operatorname{Im} b((\mathbf{u},s),\boldsymbol{\mu}) & = & \operatorname{Im}\ell(\boldsymbol{\mu}), & \forall\boldsymbol{\mu}\in Q. \end{array}\right. \end{array} \tag{2.3.6}$$

The interest of this formulation is that it fits into the frame of classical mixed variational formulations, see [13]. We are now able to state the main result of this paper.

Theorem 2.3.3 (Well-posedness of the limit problem)**.** *The variational formulation (2.3.6) is equivalent to*

$$\begin{array}{l} \textit{Find } \big((\mathbf{u},s),\boldsymbol{\lambda}\big) \in V\times Q \textit{ such that} \\ \left\{\begin{array}{lcll} a^+\big((\mathbf{u},s),(\mathbf{v},t)\big) - \overline{b\big((\mathbf{v},t),\boldsymbol{\lambda}\big)} & = & 0, & \forall(\mathbf{v},t)\in V, \\ b\big((\mathbf{u},s),\boldsymbol{\mu}\big) & = & \ell(\boldsymbol{\mu}), & \forall\boldsymbol{\mu}\in Q. \end{array}\right. \end{array} \tag{2.3.7}$$

This problem has a unique solution in the space $V\times Q$. In addition, the first component of the solution coincides with the function $\mathbf{u}^+$ introduced in Corollary 2.2.5. This function is the weak limit of the whole sequence $\mathbf{u}^\nu$ in $H^1(\Omega)^2$.

Proof. The equivalence between (2.3.7) and (2.3.6) is immediate since $\operatorname{Im} b = -\operatorname{Im}\bar{b}$ and that V and Q are both complex-valued. The second part, namely the well-posedness, is proven in Subsection 2.3.2. The last part is proven in Subsection 2.3.3, where the expressions of s^+ and $\boldsymbol{\lambda}^+$ are also precised. □

Remark 2.3.4. One could think of using another sequence of manufactured solutions leading to another well-posed variational formulation of the same form. Our result shows that the first component $\mathbf{u}$ of the solution will be the same. In particular $\mathbf{u}$ does not depend on the choice of manufactured solution.

2.3.2 Proof of the second part of the Well-posedness Theorem 2.3.3

First of all, note that problem (2.3.7) can be reformulated using the operators $A^+ : V \to V'$, $B : V \to Q'$ and $h \in Q'$ such that for all $(\mathbf{u}, s), (\mathbf{v}, t) \in V$ and $\boldsymbol{\lambda} \in Q$,

$$\begin{gathered}\big(A^+(\mathbf{u}, s), (\mathbf{v}, t)\big)_{V',V} = a^+\big((\mathbf{u}, s), (\mathbf{v}, t)\big), \quad \big(B(\mathbf{u}, s), \boldsymbol{\lambda}\big)_{Q',Q} = b\big((\mathbf{u}, s), \boldsymbol{\lambda}\big), \\ (h, \boldsymbol{\lambda})_{Q',Q} = \ell(\boldsymbol{\lambda}).\end{gathered} \tag{2.3.8}$$

The variational problem (2.3.7) then writes

$$\begin{array}{l}\text{Find } \big((\mathbf{u}, s), \boldsymbol{\lambda}\big) \in V \times Q \text{ such that} \\ \left\{\begin{array}{lcll} A^+(\mathbf{u}, s) - \overline{B^t \boldsymbol{\lambda}} & = & 0, & \text{in } V', \\ B(\mathbf{u}, s) & = & h, & \text{in } Q'. \end{array}\right.\end{array} \tag{2.3.9}$$

Set $K = \ker B$. Define $A^+_{KK'} : K \to K'$ as the *restriction* of A^+ on $K \subset V$ with values in $K' \supset V'$, such that for all $(\mathbf{u}, s)$, $(\mathbf{v}, t) \in K$,

$$\big(A^+_{KK'}(\mathbf{u}, s), (\mathbf{v}, t)\big)_{K',K} = \big(A^+(\mathbf{u}, s), (\mathbf{v}, t)\big)_{V',V}. \tag{2.3.10}$$

An important well-posedness result for complex valued mixed systems we will use is the following, for which we recall the assumptions:

Assumption 2.3.5. Let V and Q be two Hilbert spaces, and $a^+(.,.)$ on $V \times V$, $b(.,.)$ on $V \times Q$ be two continuous sesquilinear forms. We denote by A^+ and B the linear continuous operators associated with them. And we set $K = \ker B$.

Theorem 2.3.6 (Theorem 4.2.2 in Boffi-Brezzi-Fortin [13])**.** *Assume that Assumption 2.3.5 holds, and let $A^+_{KK'}$ be defined as in* (2.3.10)*. Then, problem*

$$\begin{array}{l}\textit{Find } \big((\mathbf{u}, s), \boldsymbol{\lambda}\big) \in V \times Q \textit{ such that} \\ \left\{\begin{array}{lcll} A^+(\mathbf{u}, s) - \overline{B^t \boldsymbol{\lambda}} & = & \kappa, & \textit{in } V', \\ B(\mathbf{u}, s) & = & h, & \textit{in } Q'. \end{array}\right.\end{array} \tag{2.3.11}$$

has a unique solution for every $(\kappa, h) \in V' \times Q'$ if and only if the two following conditions are satisfied: $A^+_{KK'}$ is an isomorphism from K to K' and $\operatorname{Im} B = Q'$.

The verification of these conditions for our problem is given in three steps. Firstly we characterize K, then we prove that $A^+_{KK'}$ is bijective and finally we prove that B is onto. Therefore it proves the second part of Theorem 2.3.3.

Proposition 2.3.7. *There exists $\mathbf{v}$, $\mathbf{w} \in H^1(\Omega)^2$ such that a basis of K is $\mathcal{B}_K = \big\{(\mathbf{v}, 0), (\mathbf{w}, 0), (0, 1)\big\}$ with $\mathbf{v}(\pm 1) \neq 0$ and $\mathbf{w}(\pm 1) \neq 0$. In particular $dim(K) = 3$.*

Proof. Since the bilinear form b defined in (2.3.2) has no dependance with respect to the scalar s, the space spanned by $(0, 1)$ is in K. Let us now consider $(\mathbf{u}, 0)$ belonging to $K \subset H^1(\Omega)^2 \times \mathbb{C}$. The function $\mathbf{u}$ is a continuous function, and the continuity in 0 will have its importance in the sequel.

The claim will be proved if and only if we can show that such functions span a vectorial space of dimension 2. This part of the proof is as follows. For any $\varepsilon \in (0,1)$, one has that $\mathbf{u} \in H^2(-1,-\varepsilon)^2 \cup H^2(\varepsilon,1)^2$ and that outside of 0, $-\mathbf{u}'' + \frac{\mathsf{N}}{\alpha}\mathbf{u} = 0$. Also, it verifies the boundary conditions

$$\mathbf{u}'(\pm 1) \mp \begin{pmatrix} i\sigma & 0 \\ 0 & i/\sigma \end{pmatrix} \mathbf{u}(\pm 1) = 0.$$

Define $\mathbf{v}_L$ and $\mathbf{w}_L$ the solutions to the Cauchy problems associated to that ODE on $(-1,0)$ for the boundary conditions

$$\begin{cases} \mathbf{v}_L(-1) = (1,0)^t, \\ \mathbf{v}_L'(-1) = (-i\sigma,0)^t, \end{cases} \quad \text{and} \quad \begin{cases} \mathbf{w}_L(-1) = (0,1)^t, \\ \mathbf{w}_L'(-1) = (0,-i/\sigma)^t. \end{cases}$$

Similarly, define $\mathbf{v}_R$ and $\mathbf{w}_R$ the solutions to the Cauchy problems associated to that ODE on $(0,1)$ for the boundary conditions

$$\begin{cases} \mathbf{v}_R(1) = (1,0)^t, \\ \mathbf{v}_R'(1) = (i\sigma,0)^t, \end{cases} \quad \text{and} \quad \begin{cases} \mathbf{w}_R(1) = (0,1)^t, \\ \mathbf{w}_R'(1) = (0,i/\sigma)^t. \end{cases}$$

Then $\mathbf{u}$ is a complex linear combination of $\mathbf{v}_L$ and $\mathbf{w}_L$ on $(-1,0)$, and of $\mathbf{v}_R$ and $\mathbf{w}_R$ on $(0,1)$.

These solutions to Cauchy problems on the left and right hand sides can all be extended continuously in 0, reasoning as in the proof of Lemma 2.2.4 for the $H^1(-1,0)^2$ and $H^1(0,1)^2$ bounds for $\mathbf{u}^\nu$, using the ODE on $(-1,0)$ and on $(0,1)$ respectively.

On the left, it defines an operator $\phi_L : \mathbf{c} \in \mathbb{C}^2 \mapsto \mathbf{u}(0^-) \in \mathbb{C}^2$ by solving the Cauchy problem

$$\begin{cases} -\mathbf{u}'' + \dfrac{\mathsf{N}}{\alpha}\mathbf{u} = 0, & \text{in } (-1,0), \\ \mathbf{u}(-1) = \mathbf{c}, \\ \mathbf{u}'(-1) = -\begin{pmatrix} i\sigma & 0 \\ 0 & i/\sigma \end{pmatrix} \mathbf{c}. \end{cases}$$

On the right, it defines an operator $\phi_R : \mathbf{d} \in \mathbb{C}^2 \mapsto \mathbf{u}(0^+) \in \mathbb{C}^2$ by solving the Cauchy problem

$$\begin{cases} -\mathbf{u}'' + \dfrac{\mathsf{N}}{\alpha}\mathbf{u} = 0, & \text{in } (0,1), \\ \mathbf{u}(1) = \mathbf{d}, \\ \mathbf{u}'(1) = \begin{pmatrix} i\sigma & 0 \\ 0 & i/\sigma \end{pmatrix} \mathbf{d}. \end{cases} \tag{2.3.12}$$

The condition that $\mathbf{u} \in H^1(\Omega)^2$ is now equivalent to the continuity condition $\mathbf{u}(0^-) = \mathbf{u}(0^+)$, that is $T(\mathbf{u}(-1), \mathbf{u}(1)) = 0$ where the linear mapping $T : \mathbb{C}^4 \to \mathbb{C}^2$ is defined by $T(\mathbf{c},\mathbf{d}) = \phi_L(\mathbf{c}) - \phi_R(\mathbf{d})$.

It is in fact easy to show that the dimension of the range of T is equal to 2: a sufficient and simpler condition is to show that the dimension of the range of ϕ_R is also equal to 2, and this is equivalent to saying that ϕ_R is one-to-one. The condition $\phi_R(\mathbf{d}) = 0$ is equivalent to say that $\mathbf{u}$ in (2.3.12) is such that $\mathbf{u}(0^+) = 0$. For $\varepsilon \in (0,1)$, integrating the equation against $\overline{\mathbf{u}}$ on $(\varepsilon,1)$ yields

$$\int_\varepsilon^1 \left(|\mathbf{u}'|^2 + \mathbf{u} \cdot \frac{\mathsf{N}}{\alpha}\overline{\mathbf{u}}\right) \mathrm{d}x - \begin{pmatrix} i\sigma & 0 \\ 0 & i/\sigma \end{pmatrix} \mathbf{d} \cdot \overline{\mathbf{d}} + \mathbf{u}'(\varepsilon) \cdot \overline{\mathbf{u}(\varepsilon)} = 0.$$

Refer again to the proof of Lemma 2.2.4 to get $|\mathbf{u}'(\varepsilon)| \leq C(1 + |\ln \varepsilon|) = C(1 - \ln \varepsilon)$. One has

$$|\mathbf{u}(\varepsilon)| \leq \int_0^\varepsilon |\mathbf{u}'(y)| dy \leq C \int_0^\varepsilon (1 - \ln y) dy = C\varepsilon(2 - \ln \varepsilon).$$

So one can pass to the limit $\mathbf{u}'(\varepsilon)\cdot\overline{\mathbf{u}(\varepsilon)}\to 0$ as $\varepsilon\to 0$. It yields

$$\int_0^1 \big(|\mathbf{u}'|^2+\mathbf{u}\cdot\frac{\mathsf{N}}{\alpha}\overline{\mathbf{u}}\big)\mathrm{d}x-\begin{pmatrix} i\sigma & 0\\ 0 & i/\sigma\end{pmatrix}\mathbf{d}\cdot\overline{\mathbf{d}}=0,$$

which is well-defined thanks to Hardy's inequality. Taking the imaginary part, it yields $\mathbf{d}=0$. So ϕ_R is one-to-one, and bijective. A similar computation establishes ϕ_L is bijective. So the dimension of the range of ϕ_R is equal to 2, and the dimensions of the range and kernel of T are also equal to 2.

Take $(\mathbf{v},0)$ and $(\mathbf{w},0)\in K$ defined such that $\mathbf{v}(-1)=(1,0)^t$ and $\mathbf{w}(-1)=(0,1)^t$. These functions coincide with $\mathbf{v}_L$ and $\mathbf{w}_L$ respectively on the interval $(-1,0)$, and they span a 2 dimensional subspace of K. Necessarily $\phi_R(\mathbf{v}(1))=\phi_L(\mathbf{v}(-1))\neq 0$ so $\mathbf{v}(1)\neq 0$. For the same reason $\mathbf{w}(1)\neq 0$. The claim is proved. □

Proposition 2.3.8. *$A^+_{KK'}$ is a bijection between K and K'.*

Proof. The space K being of finite dimension, it is sufficient to prove $A^+_{KK'}$ is one-to-one. Consider the basis $\mathcal{B}_K$ of K defined in Proposition 3.4.7. The operator $A^+_{KK'}$ is associated to a matrix M

$$M=\begin{pmatrix} \int(\mathbf{v}'\cdot\overline{\mathbf{v}}-\mathbf{v}\cdot\overline{\mathbf{v}}')\varphi' & \int(\mathbf{w}'\cdot\overline{\mathbf{v}}-\mathbf{w}\cdot\overline{\mathbf{v}}')\varphi' & a_1\\ \int(\mathbf{v}'\cdot\overline{\mathbf{w}}-\mathbf{v}\cdot\overline{\mathbf{w}}')\varphi' & \int(\mathbf{w}'\cdot\overline{\mathbf{w}}-\mathbf{w}\cdot\overline{\mathbf{w}}')\varphi' & a_2\\ -\overline{a_1} & -\overline{a_2} & 2i\pi\frac{\varphi(0)}{|r|}\end{pmatrix}$$

for a_1, $a_2\in\mathbb{C}$ two given scalars, see (2.3.5). Let $(c_1,c_2,c_3)\in\mathbb{C}^3$ be in the kernel of this matrix. In particular

$$\overline{(c_1,c_2,-c_3)}M(c_1,c_2,c_3)^t=0.$$

That is

$$|c_1|^2\,\mathrm{Im}\int_\Omega \mathbf{v}'\cdot\overline{\mathbf{v}}\varphi'\mathrm{d}x+|c_2|^2\,\mathrm{Im}\int_\Omega \mathbf{w}'\cdot\overline{\mathbf{w}}\varphi'\mathrm{d}x-|c_3|^2\frac{\pi\varphi(0)}{|r|}=0.$$

Remark that for $\mathbf{u}\in K$,

$$\begin{aligned}\mathrm{Im}\int_\Omega \mathbf{u}'\cdot\overline{\mathbf{u}}\varphi'\mathrm{d}x &= -\,\mathrm{Im}\int_\Omega \mathbf{u}\cdot\frac{\mathsf{N}}{\alpha}\overline{\mathbf{u}}(\varphi-\varphi(0))\mathrm{d}x\\ &\quad+\mathrm{Im}\Big\{\begin{pmatrix} i\sigma & 0\\ 0 & i/\sigma\end{pmatrix}\mathbf{u}\cdot\overline{\mathbf{u}}(\varphi-\varphi(0))\Big\}_{-1}^{1}\\ &= -\big(\sigma\{|u_1|^2\}_{-1}^{1}+\frac{1}{\sigma}\{|u_2|^2\}_{-1}^{1}\big)\varphi(0)\le 0.\end{aligned}$$

For $\mathbf{u}=\mathbf{v}$ or $\mathbf{u}=\mathbf{w}$, this quantity does not vanish as $\mathbf{v}(\pm1)\neq 0$ and $\mathbf{w}(\pm1)\neq 0$. Moreover $\varphi(0)>0$. Necessarily, $(c_1,c_2,c_3)=0$, and $A^+_{KK'}$ is one-to-one. □

Proposition 2.3.9. *B is onto from V to Q'.*

Proof. Proving B is onto from $Q\times\{0\}\subset V$ to Q' is sufficient. In the sequel of the proof there will be the abuse of notation that B is defined from Q to Q'.

For all $\mathbf{u}$, $\boldsymbol{\lambda}\in Q$, decompose $b\big((\mathbf{u},0),\boldsymbol{\lambda}\big)$ as the sum of two sesquilinear forms $b_0(\mathbf{u},\boldsymbol{\lambda})+b_1(\mathbf{u},\boldsymbol{\lambda})$ with

$$b_0(\mathbf{u},\boldsymbol{\lambda})=\int_\Omega(\mathbf{u}'\cdot\overline{\boldsymbol{\lambda}'}+\mathbf{u}\cdot\overline{\boldsymbol{\lambda}})\mathrm{d}x-\Big\{\begin{pmatrix} i\sigma & 0\\ 0 & i/\sigma\end{pmatrix}\mathbf{u}\cdot\overline{\boldsymbol{\lambda}}\Big\}_{-1}^{1},$$
$$b_1(\mathbf{u},\boldsymbol{\lambda})=\int_\Omega\mathbf{u}\cdot\big(\frac{\mathsf{N}}{\alpha}-\mathsf{I}\big)\overline{\boldsymbol{\lambda}}\,\mathrm{d}x.$$

The sesquilinear form b_0 is coercive, as for all $\mathbf{u} \in Q$, $\mathrm{Re}\, b_0(\mathbf{u},\mathbf{u}) = \|\mathbf{u}\|^2_{H^1}$. So $B_0 : \mathbf{u} \in Q \mapsto \big(\boldsymbol{\lambda} \mapsto b_0(\mathbf{u},\boldsymbol{\lambda})\big) \in Q'$ is positive and bounded below in the sense of [88]. Denote by B_1 the operator $\mathbf{u} \in Q \mapsto \big(\boldsymbol{\lambda} \mapsto b_1(\mathbf{u},\boldsymbol{\lambda})\big) \in Q'$. All bounded sequences $(\mathbf{u}_n)_{n\in\mathbb{N}} \subset Q$ admit a subsequence strongly converging in $L^2(\Omega)^2$ towards a limit $\mathbf{u} \in Q$. Besides, Cauchy-Schwarz and Hardy's inequalities imply that

$$\big|(B_1\mathbf{u}_n,\boldsymbol{\lambda})_{Q',Q} - (B_1\mathbf{u},\boldsymbol{\lambda})_{Q',Q}\big| = \big|\int_\Omega (\mathbf{u}_n-\mathbf{u})\cdot(\frac{\mathsf{N}}{\alpha}-\mathsf{I})\overline{\boldsymbol{\lambda}}\,\mathrm{d}x\big| \le C\|\mathbf{u}_n-\mathbf{u}\|_{L^2}\|\boldsymbol{\lambda}\|_{H^1}.$$

Hence B_1 is compact. Therefore $B = B_0 + B_1$ is a Fredholm operator of order 0 since it is a compact perturbation of a positive and bounded below operator B_0, see Theorem 2.33 in [88]. The Fredholm's alternative establishes B is onto provided it is injective. This part is verified as follows. Take $\mathbf{u} \in \ker B$. Then

$$\big(B\mathbf{u},\mathbf{u}\big)_{Q',Q} = \int_\Omega \big(|\mathbf{u}'|^2 + \mathbf{u}\cdot\frac{\mathsf{N}}{\alpha}\overline{\mathbf{u}}\big)\mathrm{d}x - \big\{i\sigma|\mathbf{u}_1|^2 + \frac{i}{\sigma}|\mathbf{u}_2|^2\big\}_{-1}^{1} = 0.$$

Once again, taking the imaginary part yields $\mathbf{u}(\pm1) = 0$ on the boundary of the domain.The boundary condition $\mathbf{u}'(\pm1) = \pm\begin{pmatrix} i\sigma & 0 \\ 0 & i/\sigma \end{pmatrix}\mathbf{u}(\pm1)$ yields $\mathbf{u}'(\pm1) = 0$. This is propagated by the equation on Ω, see Proposition 3.4.7, so $\mathbf{u} = 0$. The injectivity of B on $Q\times\{0\}$ is proven and the proof is ended. □

2.3.3 Proof of the third part of the Well-posedness Theorem 2.3.3

The third part of Theorem 2.3.3 states that $\mathbf{u}^+$, the weak H^1 limit of $\mathbf{u}^\nu$ defined in Corollary 2.2.5, is the solution to the variational formulation (2.3.7). In order to establish this result we derive a new variational formulation for $\nu > 0$ which tends to the limit problem as $\nu \to 0^+$. It will also yield additional information about the Lagrange multipliers $(s^+,\boldsymbol{\lambda}^+)$.

For $\nu \in \mathbb{R}$, $(\mathbf{u},s),(\mathbf{v},t) \in V$ and $\boldsymbol{\lambda} \in H^1(\Omega)^2$, define the sesquilinear form a^ν such that

$$\mathrm{Im}\, a^\nu((\mathbf{u},s),(\mathbf{v},t)) = d\mathcal{J}^\nu_{(\mathbf{u},s)}(\mathbf{v},t) \tag{2.3.13}$$

by

$$\begin{aligned} a^\nu\big((\mathbf{u},s),(\mathbf{v},t)\big) \;=\; & \int_\Omega (\overline{\mathbf{v}}\cdot\mathbf{u}' - \mathbf{u}\cdot\overline{\mathbf{v}}')\varphi'\mathrm{d}x \\ & -s\int_\Omega \big((\mathbf{w}_2^\nu\cdot\overline{\mathbf{v}} - \mathbf{w}_1^\nu\cdot\overline{\mathbf{v}}')\varphi' + (\mathbf{z}_2^\nu\cdot\overline{\mathbf{v}}' - \mathbf{z}_1^\nu\cdot\overline{\mathbf{v}})\varphi\big)\mathrm{d}x \\ & +\bar{t}\int_\Omega \big((\overline{\mathbf{w}_2^\nu}\cdot\mathbf{u} - \overline{\mathbf{w}_1^\nu}\cdot\mathbf{u}')\varphi' + (\overline{\mathbf{z}_2^\nu}\cdot\mathbf{u}' - \overline{\mathbf{z}_1^\nu}\cdot\mathbf{u})\varphi\big)\mathrm{d}x \\ & -2is\bar{t}\int_\Omega \mathbf{w}_1^\nu\cdot\mathrm{Im}\,\big(\frac{1}{\alpha+i\nu}\mathsf{N}^\nu\big)\overline{\mathbf{w}_1^\nu}\varphi\,\mathrm{d}x. \end{aligned}$$

We extend trivially the form b^ν defined in (2.2.2) from $H^1(\Omega)^2\times H^1(\Omega)^2$ to $V\times H^1(\Omega)^2$ by

$$b^\nu\big((\mathbf{u},s),\boldsymbol{\lambda}\big) = \int_\Omega \big(\mathbf{u}'\cdot\overline{\boldsymbol{\lambda}'} + \mathbf{u}\cdot\frac{\mathsf{N}^\nu\overline{\boldsymbol{\lambda}}}{\alpha+i\nu}\big)\mathrm{d}x - \Big\{\begin{pmatrix} i\sigma & 0 \\ 0 & i/\sigma \end{pmatrix}\mathbf{u}\cdot\overline{\boldsymbol{\lambda}}\Big\}_{-1}^{1}, \tag{2.3.14}$$

for $(\mathbf{u},s)\in V, \boldsymbol{\lambda}\in H^1(\Omega)^2$. Now that ν regularizes the equations, the form b^ν is defined on all $H^1(\Omega)^2$ without any difficulty.

Proposition 2.3.10. *For any $\nu > 0$, $s \in \mathbb{C}$, $\mathbf{v} \in H^1(\Omega)^2$ and $\boldsymbol{\mu} \in H^1(\Omega)^2$, the solution $\mathbf{u}^\nu$ of (2.2.1) satisfies*

$$b^\nu\big((\mathbf{u}^\nu, s), \boldsymbol{\mu}\big) = \ell^\nu(\boldsymbol{\mu}) \quad \text{and} \quad a^\nu\big((\mathbf{u}^\nu, s), (\mathbf{v}, 0)\big) = \overline{b^{-\nu}\big((\mathbf{v}, 0), -(\mathbf{u}^\nu - s\mathbf{w}_1^\nu)\varphi\big)}. \tag{2.3.15}$$

Moreover $a^\nu\big((\mathbf{u}^\nu, s), (0, t)\big) = 0$ for all $t \in \mathbb{C}$ if and only if

$$\nu \int_\Omega \big(\frac{1}{\alpha^2 + \nu^2}(\mathbf{u}^\nu - s\mathbf{w}_1^\nu)\varphi \cdot \begin{pmatrix} \delta^2 & \delta k_z \\ \delta k_z & k_z^2 \end{pmatrix} \overline{\mathbf{w}_1^\nu} + (\mathbf{u}^\nu - s\mathbf{w}_1^\nu)\varphi \cdot \begin{pmatrix} 1 & 0 \\ 0 & 0 \end{pmatrix} \overline{\mathbf{w}_1^\nu}\big) dx = 0. \tag{2.3.16}$$

Proof. The first relation of (2.3.15) is just a reformulation of (2.2.1), with the extension of b^ν on the whole space V. Now for $s \in \mathbb{C}$ and $\mathbf{v} \in H^1(\Omega)^2$,

$$\begin{aligned} a^\nu\big((\mathbf{u}^\nu, s), (\mathbf{v}, 0)\big) &= \int_\Omega (\overline{\mathbf{v}} \cdot \mathbf{u}^{\nu\prime} - \mathbf{u}^\nu \cdot \overline{\mathbf{v}}')\varphi' \mathrm{d}x \\ &\quad -s \int_\Omega \big((\mathbf{w}_2^\nu \cdot \overline{\mathbf{v}} - \mathbf{w}_1^\nu \cdot \overline{\mathbf{v}}')\varphi' + (\mathbf{z}_2^\nu \cdot \overline{\mathbf{v}}' - \mathbf{z}_1^\nu \cdot \overline{\mathbf{v}})\varphi\big)\mathrm{d}x \\ &= -\int_\Omega \big((\mathbf{u}^\nu - s\mathbf{w}_1^\nu)\varphi\big)' \cdot \overline{\mathbf{v}}' \mathrm{d}x + \int_\Omega (\mathbf{u}^\nu - s\mathbf{w}_1^\nu)' \cdot (\overline{\mathbf{v}}\varphi)' \mathrm{d}x \\ &\quad -s \int_\Omega \big(\mathbf{z}_2^\nu \cdot (\overline{\mathbf{v}}\varphi)' - \mathbf{z}_1^\nu \cdot \overline{\mathbf{v}}\varphi\big)\mathrm{d}x \\ &= -\int_\Omega \big((\mathbf{u}^\nu - s\mathbf{w}_1^\nu)\varphi\big)' \cdot \overline{\mathbf{v}}' \mathrm{d}x - \int_\Omega (\mathbf{u}^\nu - s\mathbf{w}_1^\nu)\varphi \cdot \frac{\mathsf{N}^\nu}{\alpha + i\nu} \overline{\mathbf{v}}\, dx, \end{aligned}$$

which is exactly $\overline{b^{-\nu}\big((\mathbf{v}, 0), -(\mathbf{u}^\nu - s\mathbf{w}_1^\nu)\varphi\big)}$: it yields the second relation of (2.3.15).

Finally if for all $t \in \mathbb{C}$

$$a^\nu\big((\mathbf{u}^\nu, s), (0, t)\big) = -\overline{a^\nu\big((0, t), (\mathbf{u}^\nu, s)\big)} = 0,$$

because of (2.3.13) $\partial_s \mathcal{J}^\nu(\mathbf{u}^\nu, s) = 0$. Then (2.3.16) follows from Proposition 2.2.13 and (2.2.26). □

For $\nu > 0$, define for all $\mathbf{v} \in H^1(\Omega)^2$

$$\Gamma^\nu(\mathbf{v}) = \nu \int_\Omega \big(\frac{1}{\alpha^2 + \nu^2}\mathbf{v} \cdot \begin{pmatrix} \delta^2 & \delta k_z \\ \delta k_z & k_z^2 \end{pmatrix} \overline{\mathbf{w}_1^\nu} + \mathbf{v} \cdot \begin{pmatrix} 1 & 0 \\ 0 & 0 \end{pmatrix} \overline{\mathbf{w}_1^\nu}\big) dx. \tag{2.3.17}$$

As it appears in (2.3.15)-(2.3.16), the candidates for the Lagrange multipliers are

$$s^\nu = \Gamma^\nu(\mathbf{u}^\nu\varphi)/\Gamma^\nu(\mathbf{w}_1^\nu\varphi) \quad \text{and} \quad \boldsymbol{\lambda}^\nu = -(\mathbf{u}^\nu - s^\nu\mathbf{w}_1^\nu)\varphi. \tag{2.3.18}$$

Indeed, by construction, for $Q^\nu = \big\{\mathbf{v} \in H^1(\Omega)^2, \Gamma^\nu(\mathbf{v}) = 0\big\}$, $(\mathbf{u}^\nu, s^\nu) \in V$ and $\lambda^\nu \in Q^\nu$ are a solution to the problem

$$\begin{array}{l} \text{Find } (\mathbf{u}, s) \in V \text{ and } \boldsymbol{\lambda} \in Q^\nu \text{ such that} \\ \left\{ \begin{array}{lcll} a^\nu\big((\mathbf{u}, s), (\mathbf{v}, t)\big) - \overline{b^{-\nu}\big((\mathbf{v}, t), \boldsymbol{\lambda}\big)} & = & 0, & \forall (\mathbf{v}, t) \in V, \\ b^\nu\big((\mathbf{u}, s), \boldsymbol{\mu}\big) & = & \ell^\nu(\boldsymbol{\mu}), & \forall \boldsymbol{\mu} \in Q^\nu. \end{array} \right. \end{array} \tag{2.3.19}$$

And (2.3.19) continuously matches (2.3.7) as $\nu \to 0^+$ in the sense that

$$\mathbf{v} \in Q^\nu \underset{\nu \to 0^+}{\longrightarrow} \mathbf{v} \in Q, \tag{2.3.20}$$

that for all $(\mathbf{u},s),(\mathbf{v},t)\in V$,

$$a^\nu\big((\mathbf{u},s),(\mathbf{v},t)\big)\underset{\nu\to 0^+}{\longrightarrow} a\big((\mathbf{u},s),(\mathbf{v},t)\big), \tag{2.3.21}$$

and that for all $(\mathbf{u},s)\in V$, if $\boldsymbol{\mu}_\nu\in Q^\nu$ is such that $\boldsymbol{\mu}_\nu\underset{\nu\to 0^+}{\to}\boldsymbol{\mu}\in Q$, then

$$b^{\pm\nu}\big((\mathbf{u},s),\boldsymbol{\mu}_\nu\big)\underset{\nu\to 0^+}{\to} b\big((\mathbf{u},s),\boldsymbol{\mu}\big). \tag{2.3.22}$$

Proposition 2.3.11. *The solution to problem* (2.3.7) *is* $(\mathbf{u}^+,s^+)\in V$ *and* $\boldsymbol{\lambda}^+\in Q$ *for* $s^+=-i\big(\delta(0),k_z\big)^t\cdot\mathbf{u}^+(0)$ *and* $\boldsymbol{\lambda}^+=-(\mathbf{u}^+-s^+\mathbf{w}_1^+)\varphi$.

Proof. Let $\mathbf{u}^+$ be such that up to a subsequence, $\mathbf{u}^\nu\overset{H^1}{\rightharpoonup}\mathbf{u}^+$ as $\nu\to 0^+$. For $s^\nu=\Gamma^\nu(\mathbf{u}^\nu\varphi)/\Gamma^\nu(\mathbf{w}_1^\nu\varphi)$, as in (2.2.27),

$$\begin{cases}\Gamma^\nu(\mathbf{u}^\nu\varphi)\to\dfrac{\pi}{|r|}\mathbf{u}^+(0)\cdot\begin{pmatrix}\delta^2(0)&\delta(0)k_z\\ \delta(0)k_z&k_z^2\end{pmatrix}\overline{\mathbf{w}_1^+(0)}\varphi(0)=-i\dfrac{\pi}{|r|}\big(\delta(0),k_z\big)^t\cdot\mathbf{u}^+(0)\varphi(0),\\ \Gamma^\nu(\mathbf{w}_1^\nu\varphi)\to\dfrac{\pi}{|r|}\mathbf{w}_1^+(0)\cdot\begin{pmatrix}\delta^2(0)&\delta(0)k_z\\ \delta(0)k_z&k_z^2\end{pmatrix}\overline{\mathbf{w}_1^+(0)}\varphi(0)=\dfrac{\pi}{|r|}\varphi(0),\end{cases}$$

and $s^\nu\to-i\big(\delta(0),k_z\big)^t\cdot\mathbf{u}^+(0)$ in $\mathbb{C}$. Finally, $\boldsymbol{\lambda}^\nu\overset{H^1}{\rightharpoonup}\boldsymbol{\lambda}^+$ as $\nu\to 0^+$. Now as (2.3.19) is verified by all $(\mathbf{u}^\nu,s^\nu)$ and $\boldsymbol{\lambda}^\nu$ and because of (2.3.20)-(2.3.21)-(2.3.22), $(\mathbf{u}^+,s^+)$ and $\boldsymbol{\lambda}^+$ verify the variational formulation (2.3.7). □

2.4 Numerical illustration

In order to illustrate the qualitative behavior of the solutions and their dependance with respect to ν, we present some numerical results obtained for these variational formulations using Lagrange finite elements of order 1. We refer to [13] for a description of standard discretization methods for such mixed variational problems.

Our numerical solutions are obtained through convenient approximations of (2.3.7) and (2.3.19), which are the new formulations using the manufactured solutions. For the purpose of comparison, we also present the approximation of the more classical formulation of the initial problem (2.2.1). It will show the gain of accuracy of our method in the regime of small ν.

The particular case $k_z=0$ is the normal incidence and the general case $k_z\neq 0$ is the oblique incidence.

In normal incidence, the system of equations is decoupled. Denote $\mathbf{u}^\nu=(e^\nu,b^\nu)$. For b^ν, it is a Helmholtz equation. For e^ν, it writes

$$-e^{\nu\prime\prime}(x)+\big(\frac{\delta^2(x)}{\alpha(x)+i\nu}-(\alpha(x)+i\nu)\big)e^\nu(x)=0\quad\text{in }\Omega, \tag{2.4.1}$$

with boundary conditions

$$e^{\nu\prime}(\pm1)\mp i\sigma e^\nu(\pm1)=f(\pm1). \tag{2.4.2}$$

In the case where Maxwell's equations (2.1.3) are decoupled, equation (2.4.1) concerns $e_y^\nu=e^\nu$, $e_x^\nu=-i\frac{\delta}{\alpha+i\nu}e_y^\nu$ and $b_z^\nu=e_y^{\nu\prime}$. The equations on e_x^ν, e_y^ν and b_z^ν are called the X-mode equations, for

extraordinary mode. The equations that concern e_z^ν, b_x^ν and b_y^ν are called the O-mode equations, for ordinary mode.

We are also able to compute a numerical value of the resonant heating. This quantity is based on the divergence of the Poynting vector $\Pi^\nu = \mathrm{Im}(\mathbf{E}^\nu \times \overline{\mathbf{B}^\nu})$. As computed in [99], $\nabla \cdot \Pi^\nu = \nu \|\mathbf{E}^\nu\|_2^2$, so that

$$\begin{array}{rcl} \displaystyle\int_\Omega \nabla \cdot \Pi^\nu \varphi \,\mathrm{d}x & = & \displaystyle\nu \int_\Omega \big(\frac{1}{\alpha^2+\nu^2}|(\delta, k_z)^t \cdot \mathbf{u}^\nu|^2 + |e^\nu|^2 + |b^{\nu\prime}|^2\big)\varphi \,\mathrm{d}x \\ & \underset{\nu\to 0^+}{\to} & \displaystyle\frac{\pi}{|r|}\varphi(0)\big|\big(\delta(0), k_z\big) \cdot \mathbf{u}^+(0)\big|^2. \end{array} \tag{2.4.3}$$

We will present in Fig. 2.2 a comparison of the values of the resonant heating for three different approximation methods.

2.4.1 The Whittaker test case: a reference solution in normal incidence

In this section, we compare different numerical methods on a test case for which we can compute an exact solution in closed form.

Take the coefficients

$$\alpha = -x \quad \text{and} \quad \delta = \sqrt{1 - x/4 + x^2}. \tag{2.4.4}$$

With these coefficients, the limit of equation (2.4.1) as $\nu \to 0^+$ is the Whittaker equation with unknown e^+

$$-e^{+\prime\prime}(x) + \Big(\frac{1}{4} - \frac{1}{x}\Big)e^+(x) = 0 \quad \text{in } (-1,0) \text{ and } (0,1). \tag{2.4.5}$$

General solutions of the Whittaker equation outside $x = 0$ are linear combinations of the elementary solutions

$$u : x \mapsto x e^{-x/2}, \quad v : x \mapsto -e^{x/2} + \big(\ln|x| + \int_1^x \frac{e^y - 1}{y} dy\big) x e^{-x/2}. \tag{2.4.6}$$

To get a unique solution two additional constraints are missing. This information can be recovered using the fact the solution we are interested in is the H^1 weak limit of (2.4.1) as $\nu \to 0^+$. First, we have the continuity of e^+ in 0. Second, we have the integral relation (2.2.33). As for $k_z = 0$, the second components of $\mathbf{w}_1^+$, $\mathbf{w}_2^+$, $\mathbf{z}_1^+$ and $\mathbf{z}_2^+$ are zero, see (2.2.14)-(2.2.15)-(2.2.17)-(2.2.18), we denote the first components w_1^+, w_2^+, z_1^+ and z_2^+. Relation (2.2.33) then rewrites

$$\int_\Omega (e^+ w_2^+ - e^{+\prime} w_1^+)\varphi' \mathrm{d}x = \int_\Omega (e^+ z_1^+ - e^{+\prime} z_2^+)\varphi \,\mathrm{d}x. \tag{2.4.7}$$

Proposition 2.4.1. *The limit solution e^+ of (2.4.1) as $\nu \to 0^+$ is such that*

$$e^+ = \left| \begin{array}{ll} a_L u + cv, & -1 \le x \le 0 \\ a_R u + cv, & 1 \ge x \ge 0 \end{array} \right. . \tag{2.4.8}$$

for a_L, a_R and $c \in \mathbb{C}$, with the jump condition

$$a_R - a_L = -\frac{i\pi\delta(0)^2}{|r|}\frac{v(0)}{u'(0)}c. \tag{2.4.9}$$

One can check that the limit solution e^- is such that

$$a_R^- - a_L^- = -(a_R - a_L). \tag{2.4.10}$$

Proof. For some a_L, a_R, c_L and $c_R \in \mathbb{C}$, $e^+ = a_L u + c_L v$ in $(-1,0)$ and $e^+ = a_R u + c_R v$ in $(0,1)$. The continuity of e^+ in 0 yields $c_L = c_R$. Denote c that coefficient. As for any $1 > \varepsilon > 0$, (2.4.5) and (2.2.16) yield

$$\begin{aligned}\int_{\varepsilon}^{1}(e^+w_2^+ - e^{+\prime}w_1^+)\varphi'\mathrm{d}x &= \int_{\varepsilon}^{1}(e^+z_1^+ - e^{+\prime}z_2^+)\varphi\,\mathrm{d}x \\ &\quad + \Big(e^{+\prime}(\varepsilon)w_1^+(\varepsilon) - e^+(\varepsilon)w_2^+(\varepsilon)\Big)\varphi(\varepsilon), \\ \int_{-1}^{-\varepsilon}(e^+w_2^+ - e^{+\prime}w_1^+)\varphi'\mathrm{d}x &= \int_{-1}^{-\varepsilon}(e^+z_1^+ - e^{+\prime}z_2^+)\varphi\,\mathrm{d}x \\ &\quad - \Big(e^{+\prime}(-\varepsilon)w_1^+(-\varepsilon) - e^+(-\varepsilon)w_2^+(-\varepsilon)\Big)\varphi(-\varepsilon),\end{aligned}$$

relation (2.4.7) is equivalent to

$$\int_{-\varepsilon}^{\varepsilon}(e^+w_2^+ - e^{+\prime}w_1^+)\varphi'\mathrm{d}x = \int_{-\varepsilon}^{\varepsilon}(e^+z_1^+ - e^{+\prime}z_2^+)\varphi\,\mathrm{d}x - \Big[(e^{+\prime}w_1^+ - e^+w_2^+)\varphi\Big]_{-\varepsilon}^{\varepsilon}. \tag{2.4.11}$$

Both integrals on $(-\varepsilon,\varepsilon)$ vanish as $\varepsilon \to 0$, since $e^+, w_1^+, z_2^+ \in H^1(\Omega)$, $w_2^+, z_1^+ \in L^2(\Omega)$ and $\varphi \in C^1(\Omega)$:

$$\begin{aligned}\left|\int_{-\varepsilon}^{\varepsilon}(e^+w_2^+ - e^{+\prime}w_1^+)\varphi'\mathrm{d}x\right| &\le \Big(\|e^+\|_{L^\infty}\|w_2^+\|_{L^2}\|\varphi'\|_{L^\infty} + \|e^{+\prime}\|_{L^2}\|w_1^+\|_{L^\infty}\|\varphi'\|_{L^\infty}\Big)\sqrt{2\varepsilon}, \\ \left|\int_{-\varepsilon}^{\varepsilon}(e^+z_1^+ - e^{+\prime}z_2^+)\varphi\,\mathrm{d}x\right| &\le \Big(\|e^+\|_{L^\infty}\|z_1^+\|_{L^2}\|\varphi\|_{L^\infty} + \|e^{+\prime}\|_{L^2}\|z_2^+\|_{L^\infty}\|\varphi\|_{L^\infty}\Big)\sqrt{2\varepsilon}.\end{aligned} \tag{2.4.12}$$

The scalar difference converges towards 0 as $\varepsilon \to 0$ because of (2.4.11) and (2.4.12). It also rewrites

$$\begin{aligned}\big[(e^{+\prime}w_1^+ - e^+w_2^+)\varphi\big]_{-\varepsilon}^{\varepsilon} &= w_1^+(\varepsilon)\varphi(\varepsilon)\big(e^{+\prime}(\varepsilon) - e^{+\prime}(-\varepsilon)\big) + e^{+\prime}(-\varepsilon)\int_{-\varepsilon}^{\varepsilon}(w_1^+\varphi)'\mathrm{d}x \\ &\quad - e^+(\varepsilon)\varphi(\varepsilon)\big(w_2^+(\varepsilon) - w_2^+(-\varepsilon)\big) - w_2^+(-\varepsilon)\int_{-\varepsilon}^{\varepsilon}(e^+\varphi)'\mathrm{d}x.\end{aligned}$$

Both integrals can be bounded again by $\sqrt{\varepsilon}$ up to a multiplicative constant. Since $\sqrt{\varepsilon}\ln(\varepsilon) \to 0$ with ε, $\sqrt{\varepsilon}e^{+\prime}(-\varepsilon)$, $\sqrt{\varepsilon}w_2^+(-\varepsilon)$ and $v'(\varepsilon) - v'(-\varepsilon)$ also vanish in 0. So

$$\big[(e^{+\prime}w_1^+ - e^+w_2^+)\varphi\big]_{-\varepsilon}^{\varepsilon} \underset{\varepsilon\to 0}{\to} \frac{i\varphi(0)}{\delta(0)}(a_R - a_L)u'(0) - cv(0)\varphi(0)\frac{\delta(0)\pi}{|r|} = 0$$

and the jump condition is obtained. □

Now that we have (2.4.8)-(2.4.9), the two boundary conditions are sufficient to determine these three coefficients. The numerical results presented here have been obtained for the parameters

$$\sigma = 1,\ f(-1) = 1,\ f(1) = 2,\ \text{and}\ \varphi(x) = e^{\frac{1}{2x-1} - \frac{1}{2x+1}}\mathbf{1}_{(-\frac{1}{2},\frac{1}{2})}. \tag{2.4.13}$$

Note that $\varphi \in \mathcal{C}^1_{0,+}(\Omega)$.

We observe in Fig. 2.1 that for a coarse grid, the discretization of the limit problem is accurate, and that for a small ν, the discretization of our new formulation of (2.1.5)-(2.1.6) using manufactured solutions is more satisfying than the one of the classical formulation (2.2.1).

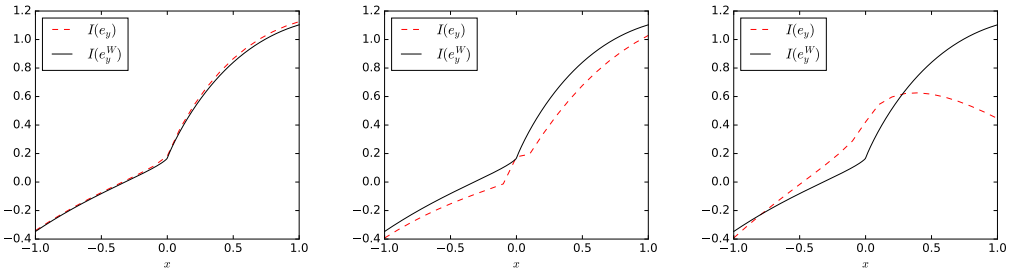

Figure 2.1 – From left to right, imaginary parts of the first component of the numerical solutions on a mesh of 40 cells for the FE discretizations of limit problem with manufactured solutions (2.3.7), for the problem with small $\nu = 10^{-7}$ and manufactured solutions (2.3.19), and for the classical problem with small $\nu = 10^{-7}$ (2.2.1). Analytical solution (2.4.8) in solid line, approximations in dashed lines.

In Fig. 2.2, we also consider the oblique case $k_z = 4$, with boundary conditions

$$\mathbf{f}(-1) = (1, 3)^t, \ \mathbf{f}(1) = (2, 5i)^t.$$

The resonant heating (2.4.3) from the approximate solutions can be computed and it is presented in the right part of Fig. 2.2 for the three different methods in function of the number of cells. The result is very typical of convergence tables with respect to two small parameters which are ν and $h = \frac{1}{N_{\text{cell}}}$ in our case. The classical finite element method for the regularized problem (2.2.1) is very sensitive to small ν since the exact solution and the limit problem become singular or ill-posed at the limit. It explains why a considerable number of cells is necessary to compute the resonant heating. On the contrary the standard finite element discretization of the limit problem (2.3.7) captures the correct resonant heating for a very small number of cells. The intermediate formulation (2.3.19) displays an intermediate behavior, with respect to resonant heating. These results are a direct consequence that a correct numerical value of the resonant heating is, through formula (2.4.3), highly dependent on a correct approximation of the solution at the resonant point $x = 0$. It is already visible in Fig. 2.1 that the new formulation (2.3.7) is much better for the computation of the solution at the resonance point $x = 0$. This result has its own physical interest in the context of fusion plasmas, but it also illustrates the mathematical interest of having a correct formulation of the limit problem. Thus, the findings of Fig. 2.1 and 2.2 are twofold. First, our new formulation of the limit problem without a regularizing parameter is validated on an analytical solution. Second, our mixed formulation of the regularized problem improves significantly the results compared to the classical formulation.

2.4.2 Qualitative behavior: a more physical test case

Let us finally consider a configuration for which a very simplified antenna sends a time-harmonic plane wave into the plasma at $x = -1$. We restore the physical dimension of all coefficients of the tensor (2.1.2) by considering

$$\underline{\underline{\varepsilon}}^{\nu} = \begin{pmatrix} \alpha + i\nu & i\delta & 0 \\ -i\delta & \alpha + i\nu & 0 \\ 0 & 0 & \gamma \end{pmatrix}.$$

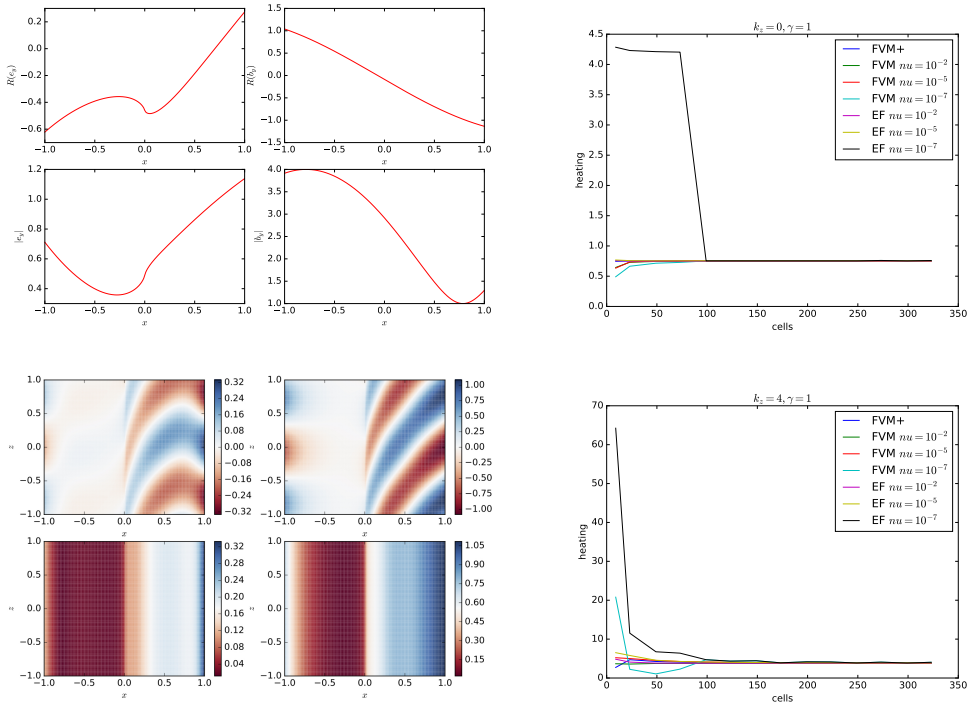

Figure 2.2 – Mesh with 200 cells. Above: solution for $k_z = 0$. Below: solution for $k_z = 4$. On the left, figure above: from left to right, real parts of the approximation of fields e and b by the limit problem (2.3.7) above, modulus of the corresponding fields below. On the left, figure below: same but on the 2D reconstruction of the solution $\mathbf{u}^{2D} = \mathbf{u}e^{ik_z z}$. On the right: discrete heating for the three different methods in function of the number of cells N_{cell}.

We take parameters such that the plasma is propagative on the first sixth part from the left for half a period, and resonant at $x = 0$. The parameters are

$$\alpha(x) = \begin{cases} (6\pi)^2, & x < -\frac{2}{3} \\ -\frac{3x}{2}(6\pi)^2, & -\frac{2}{3} \le x < \frac{1}{3} \\ -\frac{(6\pi)^2}{2}, & x \ge \frac{1}{3} \end{cases}, \ \delta(x) = \begin{cases} 0, & x < -\frac{2}{3} \\ 120x + \frac{240}{3}, & -\frac{2}{3} \le x < \frac{1}{3} \\ 120, & x \ge \frac{1}{3} \end{cases}, \ \gamma = (6\pi)^2. \quad (2.4.14)$$

The boundary conditions are now

$$\begin{pmatrix} 1 & 0 \\ 0 & 1/\gamma \end{pmatrix} \mathbf{u}'(\pm 1) \mp \begin{pmatrix} i\sigma_1 & 0 \\ 0 & i/\sigma_2 \end{pmatrix} \mathbf{u}(\pm 1) = \mathbf{f}(\pm 1).$$

The dispersion relation $k_x^2 + k_z^2 = \alpha(-1)$ characterizes a plane wave propagating on $(-1, -2/3)$, where the coefficients of the equation are constant. We take $k_x = k_z = \left(\frac{\alpha(-1)}{2}\right)^{1/2}$. In the tests

$$\mathbf{f}(-1) = e^{-ik_z}(2ik_z, 20)^t, \ \mathbf{f}(1) = (0, 0)^t,$$

and

$$\sigma_1 = k_z, \ \sigma_2 = \alpha(-1)/k_z.$$

The cut-off function φ is the same as in (2.4.13).

In Fig. 2.3, for normal incidence, approximation of the three fields concerned by the X-mode solution to the limit problem is plotted, as for $\mathbf{u} = (e, b)^t$,

$$e_y^+ = e,\ e_x^+ = \frac{-i\delta}{\alpha} e \ \text{ and } \ b_z^+ = e'.$$

The discontinuity of e_x in $1/x$ appears clearly. In Fig. 2.4, for oblique incidence taking $k_z = \frac{6\pi}{\sqrt{2}}$,

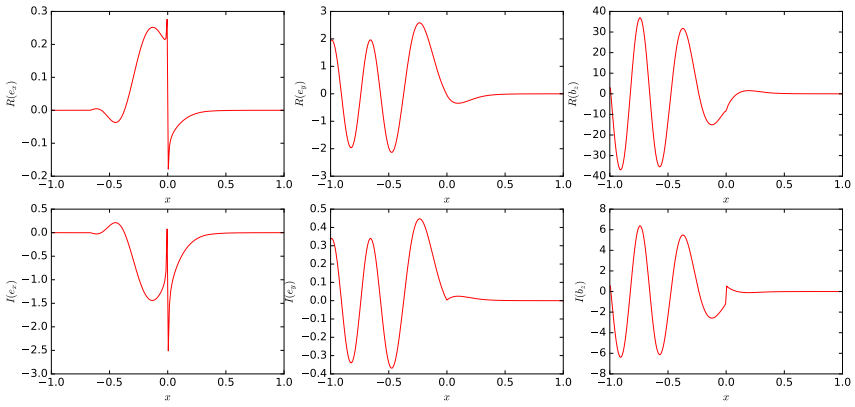

Figure 2.3 – From left to right, approximation of the X-mode fields e_x^+, e_y^+ and b_z^+ using the discretization of the limit formulation (2.3.7). Real parts above, imaginary parts below, for a mesh of 200 cells.

the singular field e_x^+, and the two regular fields e_y^+ and b_y^+ are plotted, as for $\mathbf{u} = (e, b)^t$,

$$e_y^+ = e,\ b_y^+ = b \ \text{ and } \ e_x^+ = -\frac{i\delta}{\alpha} e - \frac{ik_z}{\alpha} b.$$

We observe in figure 2.4 that the second component of the wave is propagated almost until $x = 0$, that its first component behaves as if it was influenced by the singularity in such a way it corresponds to a reflection of the incident plane wave, that the field e_x^+ does present a singularity at $x = 0$, and that all fields are absorbed on the right side of the singularity.

2.5 Appendix

In this Appendix, added to the published article, we precise the modifications of the tools developed previously that need to be made to treat the numerical example from Subsection 2.4.2 as well as the boundary condition's sources for a propagative on one side and absorbing on the other side medium. In this example, for $\nu \geq 0$ the permittivity tensor (2.1.2) is replaced by

$$\underline{\underline{\varepsilon}}^{\nu} = \begin{pmatrix} \alpha + i\nu & i\delta & 0 \\ -i\delta & \alpha + i\nu & 0 \\ 0 & 0 & \gamma \end{pmatrix}, \tag{2.5.1}$$

with coefficients such that for $\nu = 0$, as illustrated in Fig. 2.5, the domain Ω is split into

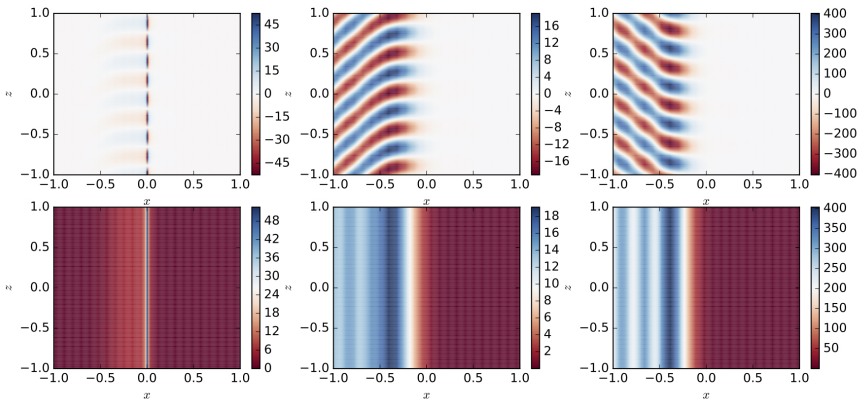

Figure 2.4 – From left to right, 2D reconstruction of the approximation of the fields e_x^+, e_y^+ and b_y^+ using the discretization of the limit formulation (2.3.7), and using again $\mathbf{u}^{2D} = \mathbf{u}e^{ik_z z}$. Real parts above, modulus below, for a mesh of 200 cells.

- a propagative region on one side with $\alpha = \gamma = c > 0$ and $\delta = 0$, and a convenient boundary condition at $x = -1$,
- a transition region between the propagative and resonant regions, where δ increases from 0 to a positive value,
- a resonant region Ω_{res} where α and δ verify the same hypotheses as in Assumption 2.1.1,
- an absorbing region on the other side of the resonance with a convenient boundary condition at $x = 1$.

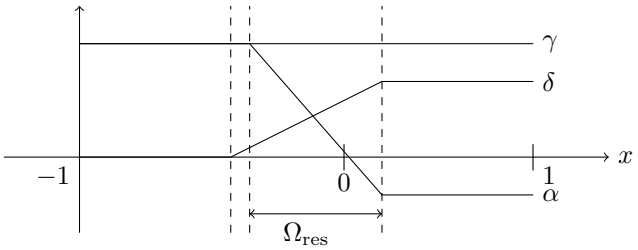

Figure 2.5 – Propagative-resonant-absorbing coefficients.

The system of Maxwell's equations (2.1.1) with tensor (2.5.1) can be recast into a system of two ODEs of second order

$$-\begin{pmatrix} 1 & 0 \\ 0 & 1/\gamma \end{pmatrix} \frac{d^2}{dx^2}\mathbf{u}^\nu(x) + \frac{1}{\alpha(x)+i\nu}\mathsf{N}^\nu(x)\mathbf{u}^\nu(x) = 0 \quad \forall x \in \Omega, \tag{2.5.2}$$

on the unknown $\mathbf{u}^\nu = (E_y^\nu, B_y^\nu)^t$. The boundary conditions considered are

$$\begin{pmatrix} 1 & 0 \\ 0 & 1/\gamma \end{pmatrix} \frac{d}{dx}\mathbf{u}^\nu(\pm 1) \mp \begin{pmatrix} i\sigma_1 & 0 \\ 0 & i/\sigma_2 \end{pmatrix} \mathbf{u}^\nu(\pm 1) = \mathbf{f}(\pm 1), \tag{2.5.3}$$

for $\sigma_1, \sigma_2 > 0$ and $\mathbf{f}$ a $\mathbb{C}^2$ valued function.

In what follows, we detail what is changed when considering (2.5.2)-(2.5.3) instead of (2.1.5)-(2.1.6).

2.5.1 Modification of the tools

Variational formulation for $\nu > 0$

The weak formulation in $H^1(\Omega)^2$ of (2.5.2)-(2.5.3) reads as in Section 2.2

$$\begin{array}{l} \text{Find } \mathbf{u} \in H^1(\Omega)^2 \text{ such that} \\ b^\nu(\mathbf{u}, \mathbf{v}) = \ell^\nu(\mathbf{v}) \quad \text{for all test functions } \mathbf{v} \in H^1(\Omega)^2. \end{array} \tag{2.5.4}$$

The linear form is the same ℓ^ν as (2.2.3), but the sesquilinear form is defined for $(\mathbf{u}, \mathbf{v}) \in H^1(\Omega)^2 \times H^1(\Omega)^2$ by

$$b^\nu(\mathbf{u}, \mathbf{v}) := \int_\Omega \left(\mathbf{u}' \cdot \begin{pmatrix} 1 & 0 \\ 0 & 1/\gamma \end{pmatrix} \overline{\mathbf{v}}' + \mathbf{u} \cdot \frac{\mathsf{N}^\nu}{\alpha + i\nu} \overline{\mathbf{v}} \right) \mathrm{d}x - \left\{ \begin{pmatrix} i\sigma_1 & 0 \\ 0 & i/\sigma_2 \end{pmatrix} \mathbf{u} \cdot \overline{\mathbf{v}} \right\}_{-1}^{1}.$$

On Ω_{res}, the results of Proposition 2.2.3 and Lemma 2.2.4 apply to our new system: it is well posed, and its solution converges as $\nu \to 0^+$ up to a subsequence in $L^2(\Omega)^2$.

Proposition 2.5.1. *For $\nu \in (0, 1]$, $\sigma_1, \sigma_2 > 0$, and $\mathbf{f}$ defined on $\{x_l, x_r\} = \partial\Omega_{\text{res}}$ with values in $\mathbb{C}$, the weak formulation*

$$\int_{\Omega_{\text{res}}} \left(\mathbf{u}' \cdot \begin{pmatrix} 1 & 0 \\ 0 & 1/\gamma \end{pmatrix} \overline{\mathbf{v}}' + \mathbf{u} \cdot \frac{\mathsf{N}^\nu}{\alpha + i\nu} \overline{\mathbf{v}} \right) \mathrm{d}x - \left\{ \begin{pmatrix} i\sigma_1 & 0 \\ 0 & i/\sigma_2 \end{pmatrix} \mathbf{u} \cdot \overline{\mathbf{v}} \right\}_{x_l}^{x_r} = [\mathbf{f} \cdot \overline{\mathbf{v}}]_{x_l}^{x_r} \quad \forall \mathbf{v} \in H^1(\Omega_{\text{res}})^2,$$

of (2.5.2) *on Ω_{res} with Robin boundary conditions*

$$\begin{pmatrix} 1 & 0 \\ 0 & 1/\gamma \end{pmatrix} \frac{d}{dx} \mathbf{u}^\nu(x_r) \mp \begin{pmatrix} i\sigma_1 & 0 \\ 0 & i/\sigma_2 \end{pmatrix} \mathbf{u}^\nu(x_r) = \mathbf{f}(x_r),$$

has a unique solution in $H^1(\Omega_{\text{res}})^2$, that we denote $\mathbf{u}^\nu$. Also, there exists $C > 0$ independent of ν such that $\|\mathbf{u}^\nu\|_{H^1(\Omega_{\text{res}})} \leq C$.

Proof. The proofs of Proposition 2.2.3 and Lemma 2.2.4 still apply. □

Outside of Ω_{res}, in the zone where $\alpha = \gamma = c > 0$ and $\delta \geq 0$ is bounded, and in the zone where α, δ and γ are respectively a negative and two positive constants, the problem is well posed for all $\nu \geq 0$ for mixed boundary conditions of type (2.5.3). It follows from a continuity argument that (2.5.4) is well posed, and that its solution converges as $\nu \to 0^+$ up to a subsequence in $L^2(\Omega)^2$.

Manufactured solutions

In this configuration, manufactured functions $\mathbf{w}_1^\nu, \mathbf{w}_2^\nu$ must be solutions of the non-homogeneous system

$$\left\{ \begin{array}{rcl} -\mathbf{w}_2^{\nu\prime} + \dfrac{1}{\alpha + i\nu} \mathsf{N}^\nu \mathbf{w}_1^\nu & = & \mathbf{z}_1^\nu, \\ \mathbf{w}_2^\nu - \begin{pmatrix} 1 & 0 \\ 0 & 1/\gamma \end{pmatrix} \mathbf{w}_1^{\nu\prime} & = & \mathbf{z}_2^\nu, \end{array} \right. \quad \text{in } \Omega_{\text{res}}. \tag{2.5.5}$$

According to the computations from Subsection 2.2.2, we define the functions

$$\mathbf{w}_1^\nu = \begin{pmatrix} \frac{i}{\delta}\left(1 - \frac{k_z^2}{\alpha+i\nu} + \frac{k_z^2}{rx+i\nu}\right) \\ \\ \frac{ik_z}{\alpha+i\nu} - \frac{ik_z}{rx+i\nu} \end{pmatrix}, \tag{2.5.6}$$

$$\mathbf{w}_2^\nu = \begin{pmatrix} \delta(0) \\ k_z \end{pmatrix} \frac{i}{r}\left(\frac{\log(r^2x^2+\nu^2)}{2} - i\,\mathrm{atan}(\frac{rx}{\nu})\right). \tag{2.5.7}$$

and the right hand sides

$$\mathbf{z}_1^\nu = \begin{pmatrix} \frac{i\delta}{\alpha+i\nu} - \frac{i\delta(0)}{rx+i\nu} + i\frac{k_z^2-(\alpha+i\nu)}{\delta}\left(1 - \frac{k_z^2}{\alpha+i\nu} + \frac{k_z^2}{rx+i\nu}\right) \\ \\ 0 \end{pmatrix}, \tag{2.5.8}$$

$$\mathbf{z}_2^\nu = \begin{pmatrix} \left(\frac{i\delta(0)}{r}\left(\frac{\log(r^2x^2+\nu^2)}{2} - i\,\mathrm{atan}(\frac{rx}{\nu})\right)\right. \\ \quad + \frac{i\delta'}{\delta^2}\left(1 - \frac{k_z^2}{\alpha+i\nu} + \frac{k_z^2}{rx+i\nu}\right) \\ \left. \quad - \frac{ik_z^2}{\delta}\left(\frac{\alpha'}{(\alpha+i\nu)^2} - \frac{r}{(rx+i\nu)^2}\right)\right) \\ \\ \frac{1}{\gamma}\left(\frac{ik_z\alpha'}{(\alpha+i\nu)^2} - \frac{ik_zr}{(rx+i\nu)^2}\right) + \frac{ik_z}{r}\left(\frac{\log(r^2x^2+\nu^2)}{2} - i\,\mathrm{atan}(\frac{rx}{\nu})\right) \end{pmatrix}. \tag{2.5.9}$$

The difference with (2.2.14)-(2.2.15)-(2.2.17)-(2.2.18) is the coefficient $1/\gamma$ that appears in the second component of $\mathbf{z}_2^\nu$, and so Proposition 2.2.7 still holds.

Proposition 2.5.2. *For $1 \geq \nu > 0$, the manufactured solution $(\mathbf{w}_1^\nu, \mathbf{w}_2^\nu)$ and right hand side $(\mathbf{z}_1^\nu, \mathbf{z}_2^\nu)$ are bounded in $L^2(\Omega_{\mathrm{res}})^2$ uniformly with respect to ν. The L^2 limits as $\nu \to 0^+$ of these functions are*

$$\mathbf{w}_1^+ = \begin{pmatrix} \frac{i}{\delta}\left(1 - \frac{k_z^2}{\alpha} + \frac{k_z^2}{rx}\right) \\ \\ \frac{ik_z}{\alpha} - \frac{ik_z}{rx} \end{pmatrix},$$

$$\mathbf{w}_2^+ = \begin{pmatrix} \delta(0) \\ k_z \end{pmatrix} \frac{i}{r}\left(\log|rx| - i\,\mathrm{sign}(rx)\frac{\pi}{2}\right),$$

$$\mathbf{z}_1^+ = \begin{pmatrix} \frac{i\delta}{\alpha} - \frac{i\delta(0)}{rx} + i\frac{k_z^2-\alpha}{\delta}\left(1 - \frac{k_z^2}{\alpha} + \frac{k_z^2}{rx}\right) \\ \\ 0 \end{pmatrix},$$

$$\mathbf{z}_2^+ = \begin{pmatrix} \left(\frac{i\delta(0)}{r}\left(\log|rx| - i\,\mathrm{sign}(rx)\frac{\pi}{2}\right) + \frac{i\delta'}{\delta^2}\left(1 - \frac{k_z^2}{\alpha} + \frac{k_z^2}{rx}\right) - \frac{ik_z^2}{\delta}\left(\frac{\alpha'}{\alpha^2} - \frac{r}{(rx)^2}\right)\right) \\ \\ \frac{1}{\gamma}\left(\frac{ik_z\alpha'}{\alpha^2} - \frac{ik_zr}{(rx)^2}\right) + \frac{ik_z}{r}\left(\log|rx| - i\,\mathrm{sign}(rx)\frac{\pi}{2}\right) \end{pmatrix}.$$

Proof. The proof of Proposition 2.2.7 applies. □

The energy relation

The equivalent to the quadratic form (2.2.25) is

$$\mathcal{J}^\nu(\mathbf{u},s) := -\operatorname{Im}\int_{\Omega_{\rm res}} (\mathbf{u}-s\mathbf{w}_1^\nu)\cdot\overline{\left(\begin{pmatrix}1&0\\0&1/\gamma\end{pmatrix}\mathbf{u}'-s\mathbf{w}_2^\nu\right)}\varphi'\mathrm{d}x$$
$$+\operatorname{Im}\int_{\Omega_{\rm res}}\left(s\mathbf{z}_1^\nu\cdot\overline{(\mathbf{u}-s\mathbf{w}_1^\nu)}-s\begin{pmatrix}1&0\\0&\gamma\end{pmatrix}\mathbf{z}_2^\nu\cdot\overline{\left(\begin{pmatrix}1&0\\0&1/\gamma\end{pmatrix}\mathbf{u}'-s\mathbf{w}_2^\nu\right)}\right)\varphi\,\mathrm{d}x.$$

We prove that Proposition 2.2.13 on the energetic relation still holds, and that the leading coefficient from Lemma 2.2.14 remains unchanged.

Proposition 2.5.3. *Let $\varphi\in\mathcal{C}^1_{0,+}(\Omega_{\rm res})$. For $\nu>0$, $\sigma_1,\sigma_2>0$ and $\mathbf{f}$ defined on $\partial\Omega_{\rm res}$ with values in $\mathbb{C}$, one has*

1. *for $s\in\mathbb{C}$ and $\mathbf{u}^\nu$ the $H^1(\Omega_{\rm res})^2$ weak solution of (2.5.2)-(2.5.3) on $\Omega_{\rm res}$, it holds*

$$\mathcal{J}^\nu(\mathbf{u}^\nu,s)=\nu\int_{\Omega_{\rm res}}\Big(\frac{1}{\alpha^2+\nu^2}\big|(\delta,k_z)^t\cdot(\mathbf{u}^\nu-s\mathbf{w}_1^\nu)\big|^2+\big|(1,0)^t\cdot(\mathbf{u}^\nu-s\mathbf{w}_1^\nu)\big|^2\Big)\varphi\,\mathrm{d}x\geq 0,$$

2. *for $\mathbf{u}\in H^1(\Omega_{\rm res})^2$ and $s\in\mathbb{C}$, the quadratic form $\mathcal{J}^\nu(\mathbf{u},s)$ can be expanded as a second order polynomial with respect to s with leading coefficient*

$$-\int_{\Omega_{\rm res}}\mathbf{w}_1^\nu\cdot\operatorname{Im}\Big(\frac{\mathsf{N}^\nu}{\alpha+i\nu}\Big)\overline{\mathbf{w}_1^\nu}\varphi\,\mathrm{d}x.$$

Proof. Using the definition of $\mathcal{J}^\nu$ and integrating by parts yields

$$\mathcal{J}^\nu(\mathbf{u}^\nu,s)=-\operatorname{Im}\int_{\Omega_{\rm res}}\big((\mathbf{u}^\nu-s\mathbf{w}_1^\nu)\varphi\big)'\cdot\overline{\left(\begin{pmatrix}1&0\\0&1/\gamma\end{pmatrix}\mathbf{u}^{\nu\prime}-s\mathbf{w}_2^\nu\right)}\mathrm{d}x$$
$$+\operatorname{Im}\int_{\Omega_{\rm res}}(\mathbf{u}^\nu-s\mathbf{w}_1^\nu)'\cdot\overline{\left(\begin{pmatrix}1&0\\0&1/\gamma\end{pmatrix}\mathbf{u}^{\nu\prime}-s\mathbf{w}_2^\nu\right)}\varphi\,\mathrm{d}x$$
$$+\operatorname{Im}\int_{\Omega_{\rm res}}\left(s\mathbf{z}_1^\nu\cdot\overline{(\mathbf{u}^\nu-s\mathbf{w}_1^\nu)}-s\begin{pmatrix}1&0\\0&\gamma\end{pmatrix}\mathbf{z}_2^\nu\cdot\overline{\left(\begin{pmatrix}1&0\\0&1/\gamma\end{pmatrix}\mathbf{u}^{\nu\prime}-s\mathbf{w}_2^\nu\right)}\right)\varphi\,\mathrm{d}x.$$

Now using the definition of $\mathbf{u}^\nu$ and relation (2.5.5) verified by the manufactured solution, it gives

$$\mathcal{J}^\nu(\mathbf{u}^\nu,s)=\operatorname{Im}\int_{\Omega_{\rm res}}(\mathbf{u}^\nu-s\mathbf{w}_1^\nu)\varphi\cdot\overline{\frac{\mathsf{N}^\nu}{\alpha+i\nu}(\mathbf{u}^\nu-s\mathbf{w}_1^\nu)}\mathrm{d}x+\operatorname{Im}\int_\Omega\overline{s\mathbf{z}_1^\nu}\cdot(\mathbf{u}^\nu-s\mathbf{w}_1^\nu)\varphi\,\mathrm{d}x$$
$$+\operatorname{Im}\int_{\Omega_{\rm res}}\left((\mathbf{u}^\nu-s\mathbf{w}_1^\nu)'\cdot\begin{pmatrix}1&0\\0&1/\gamma\end{pmatrix}\overline{(\mathbf{u}^\nu-s\mathbf{w}_1^\nu)}'-(\mathbf{u}^\nu-s\mathbf{w}_1^\nu)'\cdot\overline{s\mathbf{z}_2^\nu}\right)\varphi\,\mathrm{d}x$$
$$+\operatorname{Im}\int_{\Omega_{\rm res}}\left(s\mathbf{z}_1^\nu\cdot\overline{(\mathbf{u}^\nu-s\mathbf{w}_1^\nu)}-s\begin{pmatrix}1&0\\0&\gamma\end{pmatrix}\mathbf{z}_2^\nu\cdot\overline{\left(\begin{pmatrix}1&0\\0&1/\gamma\end{pmatrix}\mathbf{u}^{\nu\prime}-s\mathbf{w}_2^\nu\right)}\right)\varphi\,\mathrm{d}x.$$

Because of the imaginary parts, we can rewrite

$$\begin{aligned}\mathcal{J}^\nu(\mathbf{u}^\nu, s) = &- \int_{\Omega_{\rm res}} (\mathbf{u}^\nu - s\mathbf{w}_1^\nu) \cdot \operatorname{Im} \frac{\mathsf{N}^\nu}{\alpha + i\nu} \overline{(\mathbf{u}^\nu - s\mathbf{w}_1^\nu)} \varphi \,\mathrm{d}x \\ &- \operatorname{Im} \int_{\Omega_{\rm res}} (\mathbf{u}^\nu - s\mathbf{w}_1^\nu)' \cdot \overline{s\mathbf{z}_2^\nu} \varphi \,\mathrm{d}x \\ &- \operatorname{Im} \int_{\Omega_{\rm res}} s \begin{pmatrix} 1 & 0 \\ 0 & \gamma \end{pmatrix} \mathbf{z}_2^\nu \cdot \overline{\left(\begin{pmatrix} 1 & 0 \\ 0 & 1/\gamma \end{pmatrix} \mathbf{u}^{\nu\prime} - s\mathbf{w}_2^\nu \right) \varphi} \,\mathrm{d}x,\end{aligned}$$

and ultimately, using the second equation from (2.5.5), one has

$$\mathcal{J}^\nu(\mathbf{u}^\nu, s) = - \int_{\Omega_{\rm res}} (\mathbf{u}^\nu - s\mathbf{w}_1^\nu) \cdot \operatorname{Im} \frac{\mathsf{N}^\nu}{\alpha + i\nu} \overline{(\mathbf{u}^\nu - s\mathbf{w}_1^\nu)} \varphi \,\mathrm{d}x.$$

Using the expression of $\operatorname{Im} \frac{\mathsf{N}^\nu}{\alpha+i\nu}$ from the proof of Proposition 2.1.3, it establishes the first claim.

When expanding $\mathcal{J}^\nu(\mathbf{u}, s)$ in a second order polynomial in s, the lead coefficient is

$$C = - \operatorname{Im} \int_{\Omega_{\rm res}} \left(\mathbf{w}_1^\nu \cdot \overline{\mathbf{w}_2^\nu} \varphi' + \left(\mathbf{z}_1^\nu \cdot \overline{\mathbf{w}_1^\nu} - \begin{pmatrix} 1 & 0 \\ 0 & \gamma \end{pmatrix} \mathbf{z}_2^\nu \cdot \overline{\mathbf{w}_2^\nu} \right) \varphi \right) \mathrm{d}x.$$

Integrating by parts as a first step and then using (2.5.5) as a second step yields

$$\begin{aligned}C &= \operatorname{Im} \int_{\Omega_{\rm res}} \left(-(\mathbf{w}_1^\nu \varphi)' \cdot \overline{\mathbf{w}_2^\nu} + \mathbf{w}_1^{\nu\prime} \cdot \overline{\mathbf{w}_2^\nu} \varphi - \left(\mathbf{z}_1^\nu \cdot \overline{\mathbf{w}_1^\nu} - \begin{pmatrix} 1 & 0 \\ 0 & \gamma \end{pmatrix} \mathbf{z}_2^\nu \cdot \overline{\mathbf{w}_2^\nu} \right) \varphi \right) \mathrm{d}x \\ &= - \int_{\Omega_{\rm res}} \mathbf{w}_1^\nu \cdot \operatorname{Im}\left(\frac{\mathsf{N}^\nu}{\alpha + i\nu} \right) \overline{\mathbf{w}_1^\nu} \varphi \,\mathrm{d}x,\end{aligned}$$

and the second claim is proven. □

These results then lead to the limit $\nu = 0^+$ mixed variational formulation of same strucure as (2.3.7), on the same Hilbert spaces, with the difference that

$$b\left((\mathbf{u}, s), \boldsymbol{\lambda}\right) := \int_\Omega \left(\mathbf{u}' \cdot \begin{pmatrix} 1 & 0 \\ 0 & 1/\gamma \end{pmatrix} \overline{\boldsymbol{\lambda}}' + \mathbf{u} \cdot \frac{\mathsf{N}}{\alpha} \overline{\boldsymbol{\lambda}} \right) \mathrm{d}x - \left\{ \begin{pmatrix} i\sigma_1 & 0 \\ 0 & i/\sigma_2 \end{pmatrix} \mathbf{u} \cdot \overline{\boldsymbol{\lambda}} \right\}_{-1}^{1},$$

and

$$\begin{aligned}a^+\left((\mathbf{u}, s), (\mathbf{v}, t)\right) := &\int_{\Omega_{\rm res}} \left(\overline{\mathbf{v}} \cdot \begin{pmatrix} 1 & 0 \\ 0 & 1/\gamma \end{pmatrix} \mathbf{u}' - \mathbf{u} \cdot \begin{pmatrix} 1 & 0 \\ 0 & 1/\gamma \end{pmatrix} \overline{\mathbf{v}}' \right) \varphi' \mathrm{d}x \\ &- s \int_{\Omega_{\rm res}} \left(\left(\mathbf{w}_2^+ \cdot \overline{v} - \mathbf{w}_1^+ \cdot \begin{pmatrix} 1 & 0 \\ 0 & 1/\gamma \end{pmatrix} \overline{\mathbf{v}}' \right) \varphi' + (\mathbf{z}_2^+ \cdot \overline{\mathbf{v}}' - \mathbf{z}_1^+ \cdot \overline{\mathbf{v}}) \varphi \right) \mathrm{d}x \\ &+ \overline{t} \int_{\Omega_{\rm res}} \left(\left(\overline{\mathbf{w}_2^+} \cdot \mathbf{u} - \overline{\mathbf{w}_1^+} \cdot \begin{pmatrix} 1 & 0 \\ 0 & 1/\gamma \end{pmatrix} \mathbf{u}' \right) \varphi' + (\overline{\mathbf{z}_2^+} \cdot \mathbf{u}' - \overline{\mathbf{z}_1^+} \cdot \mathbf{u}) \varphi \right) \mathrm{d}x \\ &+ 2 \frac{\pi \varphi(0)}{|r|} i s \overline{t}.\end{aligned}$$

This is the modified mixed formulation discretized in Subsection 2.4.2.

2.5.2 Propagative boundary conditions

We start by studying the local dispersion relations for $\nu = 0$ around $x = -1$ to identify the propagative modes $\mathbf{E}(\mathbf{x}) = \hat{\mathbf{E}} \exp(i\mathbf{k} \cdot \mathbf{x})$ with $\mathbf{k} = (k_x, 0, k_z) \in \mathbb{R}^3$, as in Subsection 1.2.2. Then we derive a propagative source $\mathbf{f}(-1)$ related to one of these modes for the boundary conditions (2.5.3) with $\mathbf{f}(1) = 0$ for the absorbing condition.

The permittivity tensor is assumed diagonal with a coefficient $c > 0$ in the propagative region. The dispersion relation is thus $k_x^2 + k_z^2 = c$. Furthermore, as $\nabla \wedge \nabla \wedge \mathbf{E} - c\mathbf{E} = 0$, one has the polarization relation on $\hat{\mathbf{E}}$ $ik_x\hat{E}_x + ik_z\hat{E}_z = 0$. It results from Gauss's law in vacuum that $\hat{\mathbf{E}} \in \mathrm{span}_{\mathbb{C}}\{(0,1,0)^t, (-k_z, 0, k_x)^t\}$. The boundary condition at $x = -1$ must let a given propagative wave go in and out of the domain. Since the second line of (2.5.3) in $x = -1$ is also equal to

$$E_z(-1) + \frac{i}{\sigma_2}(ik_z E_x(-1) - E_z'(-1)),$$

for a given $k_x > 0$, define

$$\mathbf{f}(-1) := \exp(-ik_x) \begin{pmatrix} ik_x\hat{E}_y + i\sigma_1\hat{E}_y \\ \hat{E}_z - \dfrac{1}{\sigma_2}k_z\hat{E}_x + \dfrac{1}{\sigma_2}k_x\hat{E}_z \end{pmatrix} \tag{2.5.10}$$

where σ_1 and σ_2 verify

$$\begin{cases} 0 &= -ik_x\hat{E}_y + i\sigma_1\hat{E}_y, \\ 0 &= \hat{E}_z - \dfrac{1}{\sigma_2}k_z\hat{E}_x - \dfrac{1}{\sigma_2}k_x\hat{E}_z. \end{cases}$$

Using the polarization relation on $\hat{\mathbf{E}}$, this last system is equivalent to $\sigma_1 = k_x$ and $\sigma_2 = c/k_x$. Propagative sources at $x = -1$ are now well defined in association to each propagative mode.

3 From 2D resonances to a degenerate elliptic equation

This work with Martin Campos Pinto, Patrick Ciarlet and Bruno Després is the subject of a submitted article, entitled *A variational formulation for coupled degenerate elliptic equations with different signs.*

We study a coupling of two degenerate elliptic equations in 2D with a smooth sign changing coefficient and compact terms. The degeneracy of the coefficient is critical with respect to the theory of weighted Sobolev spaces. An adapted functional framework is proposed for the description of the solution in the context of the limiting absorption principle. It leads to a new well-posed mixed variational formulation. Numerical experiments illustrate the stability of our formulation.

3.1 Introduction

The model problem for the coupling of degenerate elliptic equations that we consider is written as

$$\left\{ \begin{array}{rcll} -\operatorname{div}(\alpha\nabla u) - u & = & 0 & \text{in } \Omega, \\ \alpha\partial_n u + i\lambda u & = & f & \text{on } \Gamma, \end{array} \right. \tag{3.1.1}$$

where $\lambda > 0$ is a positive scalar and $f \in L^2(\Gamma)$ is complex valued. The degeneracy is due to the fact that $\alpha \in \mathcal{C}^2(\overline{\Omega})$ changes sign inside the domain $\Omega \subset \mathbb{R}^2$, $\Gamma = \partial\Omega$, typically over a closed curve denoted as Σ.

This problem is motivated by the modelling of resonant waves in plasmas, see Section 3.2, but is not covered by the theory so far. We will typically be interested in a coefficient α that behaves as a signed distance to Σ.
However the study of degenerate elliptic equations, as in [49, 38], is usually undertaken for degeneracies that are locally integrable as well as their inverse. But this is the case only for $(\mathrm{dist}_\Sigma)^\beta$ for $-1 < \beta < 1$ in 2D, see [113].
A similar equation arises from the study of the interface between a non-dissipative dielectric, where the permittivity is positive, and a metamaterial, where it is negative. But the permittivity is constant on each side and does not vanish at the interface. It is shown in [37, 34, 33] that the Fredholm well-posedness of the problem depends on the contrast between the two permittivities and on the geometry of the interface. This metamaterial problem was also studied under a limiting absorption principle point of view in combination with Agmon-Douglis-Niremberg elliptic a priori estimates in [91].

As in [99, 93], we thus resort to a limiting absorption principle to select the correct solution u of (3.1.1) via the regularized system

$$\left\{ \begin{array}{rcll} -\operatorname{div}\left((\alpha+i\nu)\nabla u^\nu\right) - u^\nu & = & 0 & \text{in } \Omega, \\ (\alpha+i\nu)\partial_n u^\nu + i\lambda u^\nu & = & f & \text{on } \Gamma. \end{array} \right. \tag{3.1.2}$$

Since (3.1.2) is well-posed according to the Lax-Milgram theorem, the whole point is to find a way to pass to the limit as $\nu \to 0^+$.

In this work, we propose an original variational formulation for the limit problem $\nu = 0^+$. The mathematical idea is to use a domain decomposition approach, decoupling (3.1.1) or (3.1.2) into two similar equations written respectively in subdomains $\Omega_1 = \{\mathbf{x} \in \Omega, \alpha(\mathbf{x}) > 0\}$ and $\Omega_2 = \{\mathbf{x} \in \Omega, \alpha(\mathbf{x}) < 0\}$. The main difficulty consists in finding transmission conditions on $\Sigma = \{\mathbf{x} \in \Omega, \alpha(\mathbf{x}) = 0\}$: indeed, the degeneracy of the equation is such that one can not rely on $H^1(\Omega)$ or $H^2(\Omega)$ elliptic regularity.
Our method is based on a new characterization of the singular behaviour on Σ of the solution, with the design of complex logarithmic quasi-solutions. Before stating the main results of this work, we develop the type of singular solution on a simple explicit solution in dimension one. We will see that although this generic singular solution has no Dirichlet trace at the singular locus Σ, it remains possible to define a Neumann type trace for the flux at Σ. One of the issues of this paper is to incorporate this unidimensional information in a multidimensional formulation of problem (3.1.1) in the frame of the limiting absorption principle.

3.1.1 An explicit singular solution in 1D

In 1D, for $\alpha(x) = x$, problem (3.1.1) writes

$$-(xu'(x))' - u(x) = 0, \quad \forall x \in I, \tag{3.1.3}$$

for an open interval I such that $0 \in I$ and some boundary conditions. We first describe the analytical solutions to (3.1.3), and then introduce convenient weighted functional spaces.
One can check that $v : x \mapsto u(x^2/2)$ verifies the Bessel equation of order 0. Solutions of (3.1.3) are thus spanned on each component $I_1 = I \cap \{x > 0\}$ and $I_2 = I \cap \{x < 0\}$ by $J_0(2\sqrt{.})$ and $Y_0(2\sqrt{.})$, where

$$\left\{ \begin{array}{l} J_0 : z \in \mathbb{C} \mapsto \displaystyle\sum_{k\geq 0} \frac{(-1)^k}{(k!)^2} \left(\frac{z^2}{4}\right)^k, \\ Y_0 : z \in \mathbb{C}^* \mapsto \displaystyle\frac{2}{\pi}\left((\log\frac{z}{2} + \gamma) J_0(z) + \sum_{k\geq 1} \frac{(-1)^{k+1} H_k}{(k!)^2} \left(\frac{z^2}{4}\right)^k \right), \end{array} \right.$$

are the Bessel functions of order 0, with γ the Euler constant and H_k the harmonic sum of order k, see [95] for more details on these special functions. Since Y_0 has a logarithmic singularity, so does a generic solution u. This singularity implies that the continuity relations between the I_1 component and the I_2 component, if they exist, are non trivial: a logarithm has no Dirichlet nor Neumann trace at 0. Nevertheless, a solution u to (3.1.3) is such that $xu'(x)$ is continuous and has a trace at 0.
We next introduce the spaces $H^1_{1/2}(I_j) := \{v \in L^2(I_j), \int_{I_j} |x||v'(x)|^2 \mathrm{d}x < \infty\}$ for $j = 1, 2$, which come naturally when integrating (3.1.3) by parts. A function $u_j \in H^1_{1/2}(I_j)$ that verifies weakly

equation (3.1.3) on I_j is such that $xu_j' \in H^1(I_j)$, therefore

$$xu_j'(x)|_{x=0} = \lim_{\epsilon\to 0}\epsilon^{-1}\int_{I_j\cap\{|x|<\epsilon\}} xu_j'(x)\mathrm{d}x.$$

Since $\sqrt{x}u_j' \in L^2(I_j)$, a Cauchy-Schwarz inequality and the dominated convergence theorem lead to

$$\frac{1}{\epsilon}\int_{I_j\cap\{|x|<\epsilon\}} \left|xu_j'(x)\right|\mathrm{d}x \le \frac{1}{\sqrt{2}}\left(\int_{I_j\cap\{|x|<\epsilon\}} |x|\,|u_j'(x)|^2\mathrm{d}x\right)^{1/2} \underset{\epsilon\to 0}{\to} 0.$$

Hence such a function u_j verifies $xu_j'(x)|_{x=0} = 0$. Of course $J_0|_{I_j} \in H^1_{1/2}(I_j)$, but on the contrary $Y_0 \notin H^1_{1/2}(I_j)$. In fact, in terms of the scale of weighted Sobolev spaces

$$H^1_s(I) := \left\{v \in L^2(I),\ \int_I |x|^{2s}|v'(x)|^2\mathrm{d}x < \infty\right\},$$

with $s > 0$, one can check that $\log|\cdot|$ belongs to $\bigcap_{\epsilon>0} H^1_{1/2+\epsilon}(I)$ but not to $H^1_{1/2}(I)$. This implies among other things that the generic solution u does not belong to these spaces, that is $u|_{I_j} \notin H^1_{1/2}(I_j)$ for $j = 1, 2$. It is therefore natural to introduce the scalar g at $x = 0$ defined by

$$g = xu'(x)|_{x=0}.$$

Lifting g as w_g in $I_1 \cup I_2$, in such a way that w_g is defined on the domain I and verifies $xw_g'(x)|_{x=0} = g$, one is able to decompose the solution u to (3.1.3) on I in regular and singular parts: one writes $u|_{I_j} = u_j + w_g$ on each I_j. The regular part is $u_j \in H^1_{1/2}(I_j)$, and the singular part is w_g which contains a logarithm and is not in $H^1_{1/2}(I_j)$. At the ODE level, one can also remark that for a solution such that $u|_{I_j} = a_jJ_0(2\sqrt{\cdot}) + b_jY_0(2\sqrt{\cdot})$ for $j = 1, 2$, it holds

$$xu'(x)|_{x=0^+} = \frac{b_1}{2}\ell \quad\text{and}\quad xu'(x)|_{x=0^-} = \frac{b_2}{2}\ell, \quad \text{where } \ell = xY_0'(x)|_{x=0}.$$

The solution depends on the four parameters a_1, b_1, a_2 and b_2. The boundary conditions and the continuity of the flux $xu'(x)$ at 0 prescribe three degrees of freedom, and the last one will be characterized by the value of the singular coefficient g. When dealing with related resonant wave propagation problems, we note that this coefficient can be determined by the boundary conditions following a limiting absorption principle as in [99, 93].

In 2D, $\alpha(\gamma, \sigma)$ is proportional to the signed distance σ to Σ. From the above 1D study, we expect a logarithmic growth in the normal direction to the resonant curve. As a consequence, we will consider the ansatz of solutions that are combinations of piecewise $H^1_{1/2}(\Omega_j)$-smooth functions for $j = 1, 2$, and of singularities of the type $\log|\sigma|$, that do not belong to $H^1_{1/2}(\Omega_j)$. We recall that for a given bounded open set with Lipschitz boundary $\omega \subset \mathbb{R}^2$, $H^1_{1/2}(\omega)$ is the weighted Sobolev space of functions $v \in L^2(\omega)$ such that $\sqrt{\mathrm{dist}_{\partial\omega}}\nabla v \in L^2(\omega)^2$.

3.1.2 Outline and main results

We start by introducing some preliminary material in the spirit of Subsection 3.1.1. In Section 3.2 we detail the link between the cold plasma model and the PDE (3.1.1). Our main results rely on

two main ideas. The first one is a specific decomposition of the unknown u into a regular part and a singular part, which is detailed in Section 3.3. The second one is a characterization of the singular part following a limiting absorption principle, described in Section 3.4. The singular part w_g^+ is characterized by the singular coefficient g, which is defined along Σ. The regular part is denoted as $\mathbf{u} = (u_1, u_2)$ and is defined by local problems on the subdomains Ω_1 and Ω_2 that involve the singular coefficient g. We introduce an auxiliary variable h in the same space as g and a Lagrange multiplier $\boldsymbol{\lambda}$ in the same space as $\mathbf{u}$. These functions are such that $(\mathbf{u}, g, h) \in V = Q \times H^2(\Sigma) \times H^2(\Sigma)$ and $\boldsymbol{\lambda} \in Q = H^1_{1/2}(\Omega_1) \times H^1_{1/2}(\Omega_2)$. The validity of the decomposition of the solution relies on a technical lemma.

Lemma 3.1.1. *Let $\omega \subset \mathbb{R}^2$ be a bounded open set with Lipschitz boundary. The weighted Sobolev space $H^1_{1/2}(\omega)$ is compactly embedded into $L^2(\omega)$.*

Using a family of explicit quasi-solutions for the regularized problem (3.1.2), we implement the limiting absorption principle in sections 3.3 and 3.4. This allows us to formulate and prove the following result.

Theorem 3.1.2. *The formal limit $\nu = 0^+$ of problem* (3.1.2) *admits a regularized mixed variational formulation*

$$\begin{array}{l} \text{Find } (\mathbf{u}, g, h) \in V \text{ and } \boldsymbol{\lambda} \in Q \text{ such that} \\ \left\{ \begin{array}{lcll} a_r^+\left((\mathbf{u}, g, h), (\mathbf{v}, k, l)\right) & - & \overline{b^+\left((\mathbf{v}, k, l), \boldsymbol{\lambda}\right)} & = \quad 0, \qquad \forall (\mathbf{v}, k, l) \in V, \\ b^+\left((\mathbf{u}, g, h), \boldsymbol{\mu}\right) & & & = \quad \ell(\boldsymbol{\mu}), \qquad \forall \boldsymbol{\mu} \in Q, \end{array} \right. \end{array} \tag{3.1.4}$$

for b^+ and a_r^+ defined in (3.4.5) *and* (3.4.8) *respectively. Moreover, this formulation is well-posed, in the sense that for all $f \in L^2(\Gamma)$, there exists a unique solution $(\mathbf{u}, g, h) \in V$ and $\boldsymbol{\lambda} \in Q$, which depends continuously on $\|f\|_{L^2(\Gamma)}$.*

In Section 3.5, formulation (3.1.4) is discretized using a classical finite element method. It leads to a new numerical approximation method for (3.1.1). The numerical results illustrate on the one hand the robustness of the discretized formulation, and on the other hand the accuracy of the discrete solution. Of particular importance for the numerical experiments, we verify that the regularization parameter can take abritrary small values, and can even be taken equal to zero.

3.1.3 Geometry and notation

We use a standard parametrization of the geometry, see [39]. The coefficient α is assumed to be smooth with enough derivatives, typically $\mathcal{C}^2$, and non degenerate in the sense that $\nabla\alpha(\mathbf{x}) \neq 0$ in the domain of interest. Under these conditions, we define the curve $\Sigma := \{\mathbf{x} \in \mathbb{R}^2, \alpha(\mathbf{x}) = 0\}$, and to further simplify, we assume that Σ is a closed simple line. We consider the parametrization $\mathbf{f} : [0,1] \to \mathbb{R}^2$ of Σ illustrated in Fig. 3.1, with $\mathbf{f}(0) = \mathbf{f}(1)$ and $\mathbf{f}$ bijective between $[0,1)$ and Σ. We assume γ is a curvilinear abscissa, that is $|\mathbf{f}'(\gamma)| = 1$. The curvature radius of Σ at $\mathbf{f}(\gamma)$ is denoted $R(\gamma)$, and we note the minimal value of the curvature radius $R_* := \min_\gamma R(\gamma) > 0$. This quantity is well-defined for a continuous R. For a given $\gamma \in [0,1]$, the ingoing normal and tangent vectors to Σ at $\mathbf{f}(\gamma)$ are denoted respectively $\mathbf{n}(\gamma)$ and $\mathbf{t}(\gamma)$. For all $\gamma \in [0,1]$ and $\sigma \in \mathbb{R}$, we set $\psi(\gamma, \sigma) := \mathbf{f}(\gamma) + \sigma\mathbf{n}(\gamma)$ which belongs to a neighbourhood of Σ for small values of σ. It is known that ψ is injective on $[0,1) \times (-R_*, R_*)$. We next define the tubular extension of Σ

$$\Sigma_{\text{tub}} := \psi\left([0,1) \times (-\tfrac{1}{2}R_*, \tfrac{1}{2}R_*)\right) \cap \Omega.$$

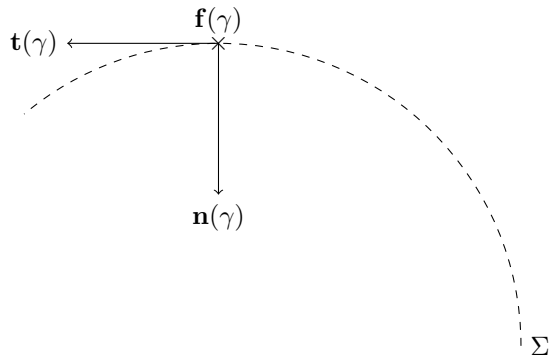

Figure 3.1 – Σ parametrization

It is convenient to consider the change of variable $\mathbf{x} = \psi(\gamma, \sigma)$ for $\mathbf{x} \in \Sigma_{\text{tub}}$. The Jacobian of the transformation

$$p_\Omega(\gamma, \sigma) := \det \nabla \psi = |\mathbf{f}'(\gamma)| - \frac{\sigma}{R(\gamma)} = 1 - \frac{\sigma}{R(\gamma)} \geq \frac{1}{2} \tag{3.1.5}$$

is such that for $O \subset \Sigma_{\text{tub}}$

$$\int_O v(\mathbf{x}) \mathrm{d}\mathbf{x} = \int_{\psi^{-1}(O)} v \circ \psi(\gamma, \sigma) p_\Omega(\gamma, \sigma) \mathrm{d}\sigma \mathrm{d}\gamma.$$

We will always use the notation $\nabla = (\partial_x, \partial_y)^t$, and one has

$$\nabla \gamma(\mathbf{x}) = \frac{\mathbf{t}(\gamma(\mathbf{x}))}{1 - \sigma(\mathbf{x})/R(\gamma(\mathbf{x}))} \quad \text{and} \quad \nabla \sigma(\mathbf{x}) = \mathbf{n}(\gamma(\mathbf{x})). \tag{3.1.6}$$

For any function v we make the abuse of notation $v \circ \psi(\gamma, \sigma) = v(\gamma, \sigma)$. So we define $r(\gamma) = \partial_\sigma \alpha(\gamma, 0) \neq 0$, and we have the local expansion for small σ

$$\alpha(\gamma, \sigma) = r(\gamma)\sigma + O(\sigma^2), \tag{3.1.7}$$

with r of constant sign. We suppose without loss of generality that $r < 0$, therefore on a given $\Sigma^*_{\text{tub}} \subset \Sigma_{\text{tub}}$, one has $0 < c_* \leq -\partial_\sigma \alpha \leq c^*$. In the sequel, we will consider the case $\Omega = \Sigma^*_{\text{tub}}$. In particular,

$$0 < c_* \leq -\frac{\alpha(\gamma, \sigma)}{\sigma} \leq c^*, \quad \forall\, \psi(\gamma, \sigma) \in \Omega. \tag{3.1.8}$$

We also define

$$\Omega_1 := \psi\left([0, 1) \times (-\tfrac{1}{2} R_*, 0)\right) \cap \Omega \quad \text{and} \quad \Omega_2 := \psi\left([0, 1) \times (0, \tfrac{1}{2} R_*)\right) \cap \Omega,$$

such that $\Omega = \Omega_1 \cup \Sigma \cup \Omega_2$, and the exterior boundaries

$$\Gamma_1 := \partial\Omega_1 \cap \Gamma \quad \text{and} \quad \Gamma_2 := \partial\Omega_2 \cap \Gamma,$$

where $\Gamma = \partial\Omega = \Gamma_1 \cup \Gamma_2$. One has $\Omega_1 = \{\alpha > 0\}$ and $\Omega_2 = \{\alpha < 0\}$. Finally, we define the L^2_w weighted norm on Σ such that

$$\|v\|^2_{L^2_w(\Sigma)} := \int_0^1 |v(\gamma, 0)|^2 \frac{1}{|r(\gamma)|} \mathrm{d}\gamma.$$

3.1.4 Functional setting

The unknowns are complex valued, and so are the considered functional spaces. We use the α-weighted Sobolev spaces defined on Ω_j, $j = 1, 2$ as

$$H^1_{1/2}(\Omega_j) := \{u \in L^2(\Omega_j), \int_{\Omega_j} |\alpha(\mathbf{x})||\nabla u(\mathbf{x})|^2 \mathrm{d}\mathbf{x} < \infty\}$$

endowed with the α-weighted norm

$$\|u\|_{H^1_{1/2}(\Omega_j)} := \left(\|u\|^2_{L^2(\Omega_j)} + \|\sqrt{|\alpha|}\nabla u\|^2_{L^2(\Omega_j)}\right)^{1/2}.$$

This norm is equivalent to the standard weighted $H^1_{1/2}$ norm involving the distance to a boundary [70] according to (3.1.8). The dual spaces, in the sense of the spaces of anti-linear maps into $\mathbb{C}$, are noted with a prime.

We recall the definition of T-coercivity as introduced in [37] which is an explicit realization of the inf-sup condition.

Definition 3.1.3. Let H be a Hilbert space. Let $\mathsf{T} : H \to H$ be a continuous linear operator. A bilinear form b defined on $H \times H$ is T-coercive if there exists $C > 0$ such that $|b(u, \mathsf{T}u)| \geq C\|u\|^2_H$.

If T is a bijection, for all continuous linear forms ℓ defined on H, there exists a unique $u \in H$ such that $b(u, v) = \ell(v)$ for all $v \in H$. And as it is the case for coercive forms, up to a compact perturbation, b is associated to a Fredholm operator of index 0. This last property implies that the associated variational formulation admits a unique solution if and only if uniqueness holds. This result will be used further.

For any $x, y \in \mathbb{R}$, we note the complex logarithm $\log(x + iy) := \frac{1}{2}\log(x^2 + y^2) - i\,\mathrm{atan}(x/y)$.

3.2 Modeling of plasma resonances

Our interest for equation (3.1.1) originated in the study of X-mode solutions of the time harmonic resonant Maxwell's equations in 2D. Resonant Maxwell's equations are used to model plasma heating in a tokamak [108, 87]. The X-mode consists of the transverse electric (TE) mode $(E_1, E_2, 0)$. See [32, 99] for the X-mode study in 1D, and [93] for the full (E_1, E_2, E_3) case in 1D. For $\mathbf{E} = (E_1, E_2)$, the system of PDEs is

$$\left\{ \begin{array}{rcl} \mathbf{curl}\, B - \underline{\underline{\varepsilon}}\mathbf{E} & = & 0, \\ B - \mathrm{curl}\, \mathbf{E} & = & 0. \end{array} \right. \tag{3.2.1}$$

The permittivity tensor for the resonant Maxwell equations writes

$$\underline{\underline{\varepsilon}} = \begin{pmatrix} \alpha & i\delta \\ -i\delta & \alpha \end{pmatrix}$$

where the coefficients depend on $\mathbf{x}$ through plasma parameters, and on the constant frequency $\omega > 0$ of the wave sent in the plasma. Precisely,

$$\alpha(\mathbf{x}) = \left(\frac{\omega}{c}\right)^2 \left(1 - \frac{\omega_p^2(\mathbf{x})}{\omega^2 - \omega_c^2}\right) \in \mathbb{R}, \quad \delta(\mathbf{x}) = \left(\frac{\omega}{c}\right)^2 \left(\frac{\omega_c \omega_p^2(\mathbf{x})}{\omega(\omega^2 - \omega_c^2)}\right) \in \mathbb{R}.$$

Here ω_p is the plasma frequency. It varies in space and corresponds to the frequency of oscillations of slightly perturbed electrons as they return to equilibrium. And ω_c is the cyclotron frequency, the frequency to which electrons gyrate around the magnetic field. We are interested in the lower hybrid resonance, localized at $\Sigma = \{\mathbf{x} \in \mathbb{R}^2, \omega^2 = \omega_p^2(\mathbf{x}) + \omega_c^2\} = \{\mathbf{x} \in \mathbb{R}^2, \alpha(\mathbf{x}) = 0\}$. We concentrate on a connected component of Σ, which we assume to be a closed curve that separates the domain Ω in two. On Σ, the off-diagonal coefficient is $\delta = \frac{\omega\omega_c}{c^2} > 0$. We thus consider δ to be positive and bounded below by a non-zero constant.
The solution of problem (3.2.1) is expected to have a singularity of order $1/\alpha$ on Σ: this singularity does not belong to $L^2(\Omega)$, nor to $L^1(\Omega)$. Conclusions drawn from the 1D case [99, 93] led us to consider the auxiliary fields $\tilde{\mathbf{E}} := \mathbf{E} - \nabla\frac{B}{i\delta}$ and $u := \frac{B}{i\delta}$. The field $\tilde{\mathbf{E}}$ is the so-called regular part of the electric field [2, Chap. 6]. From now on, we take δ equal to a constant non zero value for simplicity. Developing the algebra, it yields $i\delta\,\mathbf{curl}\,u + i\delta\underline{\underline{\varepsilon}}\nabla u = \alpha\nabla u$. Therefore the fields $\tilde{\mathbf{E}}$ and u verify

$$\left\{ \begin{array}{rcl} \alpha\nabla u - \underline{\underline{\varepsilon}}\tilde{\mathbf{E}} & = & 0, \\ i\delta u - \operatorname{curl}\tilde{\mathbf{E}} & = & 0. \end{array} \right.$$

Reformulated on the unknown u, it gives $\operatorname{curl}\left(\alpha\underline{\underline{\varepsilon}}^{-1}\nabla u\right) - i\delta u = 0$, where

$$\underline{\underline{\varepsilon}}^{-1} = \frac{1}{\alpha^2 - \delta^2}\begin{pmatrix} \alpha & -i\delta \\ i\delta & \alpha \end{pmatrix} = -\sum_{n\geq 0}\frac{\alpha^{2n+1}}{\delta^{2n+2}}\begin{pmatrix} 1 & 0 \\ 0 & 1 \end{pmatrix} + \sum_{n\geq 0}\frac{\alpha^{2n}}{\delta^{2n+1}}\begin{pmatrix} 0 & i \\ -i & 0 \end{pmatrix}.$$

It yields the expansion

$$-\frac{1}{\delta^2}\operatorname{div}(\alpha\nabla u) - \sum_{n\geq 0}\operatorname{div}\left(\frac{\alpha^{2n+2}}{\delta^{2n+3}}\begin{pmatrix} \alpha/\delta & i \\ -i & \alpha/\delta \end{pmatrix}\nabla u\right) - u = 0.$$

We study these equations in the geometry introduced in section 3.1.3. Given that α vanishes on Σ, the terms under the summation sign can be neglected as they are factor of α^{2n+2} with $n \geq 0$. Adding mixed boundary conditions, it comes down to solving

$$\left\{ \begin{array}{rcll} -\frac{1}{\delta^2}\operatorname{div}(\alpha\nabla u) - u & = & 0 & \text{in } \Omega, \\ \alpha\partial_n u + i\lambda u & = & f & \text{on } \Gamma, \end{array} \right.$$

which for $\delta = 1$ is our model problem (3.1.1).

3.3 Limit viscosity $\nu \to 0^+$ solution

3.3.1 Variational formulations

Because the sign of α changes on Σ, it is natural to separate the problem on each side of Σ, where it has a fixed sign. For these subproblems, we show a well-posedness result in the Hilbert space

$$\begin{array}{l} Q := H^1_{1/2}(\Omega_1) \times H^1_{1/2}(\Omega_2), \text{ equipped with the norm} \\ \|\mathbf{u}\|_Q := \|u_1\|_{H^1_{1/2}(\Omega_1)} + \|u_2\|_{H^1_{1/2}(\Omega_2)} \text{ for } \mathbf{u} = (u_1, u_2). \end{array} \tag{3.3.1}$$

Define the following problem

$$\begin{array}{l} \text{Find } \mathbf{u} \in Q \text{ such that for all } \mathbf{v} \in Q, \\ b(\mathbf{u}, \mathbf{v}) = \ell(\mathbf{v}), \end{array} \tag{3.3.2}$$

where for $\mathbf{u} = (u_1, u_2)$ and $\mathbf{v} = (v_1, v_2) \in Q$,

$$\begin{aligned} b((u_1,u_2),(v_1,v_2)) &:= \sum_{j=1,2} \left(\int_{\Omega_j} \left(\alpha \nabla u_j \cdot \overline{\nabla v_j} - u_j \overline{v_j} \right) \mathrm{d}\mathbf{x} + \int_{\Gamma_j} i\lambda u_j \overline{v_j} \mathrm{d}s \right) \\ \ell(v_1,v_2) &:= \int_{\Gamma_1} f \overline{v_1} \mathrm{d}s + \int_{\Gamma_2} f \overline{v_2} \mathrm{d}s. \end{aligned} \tag{3.3.3}$$

Proposition 3.3.1. *Let $\lambda > 0$ and $f \in L^2(\Gamma)$. Problem (3.3.2) has a unique solution in Q.*

Before proving Proposition 3.3.1, we prove Lemma 3.1.1 for $\omega = \Omega_1$.

Lemma 3.3.2. *The weighted Sobolev space $H^1_{1/2}(\Omega_1)$ is compactly embedded into $L^2(\Omega_1)$.*

Proof. Let $(u_n)_{n\in\mathbb{N}} \subset H^1_{1/2}(\Omega_1)$ be a bounded sequence. Up to a subsequence, u_n weakly converges towards a limit in $H^1_{1/2}(\Omega_1)$, and substracting this limit to the sequence, one can consider $u_n \rightharpoonup 0$. For all $\epsilon > 0$, define $\Omega_1^\epsilon := \{(\gamma,\sigma) \in \Omega_1, |\sigma| < \epsilon\}$. The H^1 and $H^1_{1/2}$ norms are equivalent on any set $\Omega_1 \backslash \Omega_1^\epsilon$ since the weight α is positively bounded below on this domain: so $\|u_n\|_{L^2(\Omega_1\backslash\Omega_1^\epsilon)} \to 0$. To prove our claim, we show that as ϵ goes to 0,

$$\int_{\Omega_1^\epsilon} |u_n|^2 \mathrm{d}\mathbf{x} \to 0 \quad \text{uniformly in } n.$$

Introducing the value of u_n on Γ_1, see subsection 3.1.3, it yields

$$\begin{aligned} \int_{\Omega_1^\epsilon} |u_n|^2 \mathrm{d}\mathbf{x} &= \int_\gamma \int_{-\epsilon}^0 |u_n(\gamma,\sigma)|^2 p_\Omega(\gamma,\sigma) \mathrm{d}\sigma \mathrm{d}\gamma \\ &\leq 2 \int_\gamma \int_{-\epsilon}^0 |u_n(\gamma,\sigma) - u_n(\gamma, -\frac{R^*}{2})|^2 p_\Omega(\gamma,\sigma) \mathrm{d}\sigma \mathrm{d}\gamma \\ &\quad + 2 \int_\gamma \int_{-\epsilon}^0 |u_n(\gamma, -\frac{R^*}{2})|^2 p_\Omega(\gamma,\sigma) \mathrm{d}\sigma \mathrm{d}\gamma. \end{aligned}$$

The second term is uniformly controlled by ϵ as

$$\int_\gamma \int_{-\epsilon}^0 |u_n(\gamma, -\frac{R^*}{2})|^2 p_\Omega(\gamma,\sigma) \mathrm{d}\sigma \mathrm{d}\gamma \leq C\epsilon \|u_n\|^2_{L^2(\Gamma_1)} \leq \tilde{C}\epsilon.$$

For the first term, a Cauchy-Schwarz argument applied twice gives

$$\begin{aligned} &\int_\gamma \int_{-\epsilon}^0 |u_n(\gamma,\sigma) - u_n(\gamma, -\frac{R^*}{2})|^2 p_\Omega(\gamma,\sigma) \mathrm{d}\sigma \mathrm{d}\gamma \\ &= \int_\gamma \int_{-\epsilon}^0 \left| \int_{-\frac{R^*}{2}}^\sigma \partial_\sigma u_n(\gamma,s) \mathrm{d}s \right|^2 p_\Omega(\gamma,\sigma) \mathrm{d}\sigma \mathrm{d}\gamma \\ &\leq \int_\gamma \int_{-\epsilon}^0 \left(\int_{-\frac{R^*}{2}}^\sigma |s| \left|\partial_\sigma u_n(\gamma,s)\right|^2 \mathrm{d}s \right) \log\left|\frac{R^2}{2\sigma}\right| p_\Omega(\gamma,\sigma) \mathrm{d}\sigma \mathrm{d}\gamma \\ &\leq \int_\gamma \left(\int_{-\frac{R^*}{2}}^0 |s| \left|\partial_\sigma u_n(\gamma,s)\right|^2 \mathrm{d}s \right) \left(\int_{-\epsilon}^0 \log\left|\frac{R^*}{2\sigma}\right| p_\Omega(\gamma,\sigma) \mathrm{d}\sigma \right) \mathrm{d}\gamma \\ &\leq \sup_\gamma \left(\int_{-\epsilon}^0 \log\left|\frac{R^*}{2\sigma}\right| p_\Omega(\gamma,\sigma) \mathrm{d}\sigma \right) \left(\int_\gamma \int_{-\frac{R^*}{2}}^0 |s| \left|\partial_\sigma u_n(\gamma,s)\right|^2 \mathrm{d}s \mathrm{d}\gamma \right). \end{aligned}$$

The first term is such that

$$\sup_{\gamma} \int_{-\epsilon}^{0} \log \left| \frac{R^*}{2\sigma} \right| p_\Omega(\gamma, \sigma) \mathrm{d}\sigma \leq C\epsilon(1 + |\log \epsilon|) \underset{\epsilon \to 0}{\to} 0,$$

and the second one verifies

$$\int_\gamma \int_{-\frac{R^*}{2}}^{0} |s| \left| \partial_\sigma u_n(\gamma, s) \right|^2 \mathrm{d}s \mathrm{d}\gamma \leq C \|\alpha^{1/2} \nabla u_n\|^2_{L^2(\Omega_1)} \leq M,$$

with $M > 0$ a constant independent of n. The result is established. □

Proof. [Proposition 3.3.1] Let $\lambda > 0$ and $f \in L^2(\Gamma)$. First, ℓ is a continuous antilinear form on Q. In fact, for a given constant $C > 0$,

$$\begin{array}{rcl} \|\ell(\mathbf{v})\| & \leq & \|f\|_{L^2(\Gamma)} \left(\|v_1\|_{L^2(\Gamma_1)} + \|v_2\|_{L^2(\Gamma_2)} \right) \\ & \leq & C \|f\|_{L^2(\Gamma)} \|\mathbf{v}\|_Q, \end{array}$$

since the L^2 norm on Γ is controlled by the H^1 norm in a neighbourhood of Γ in Ω, and that H^1 and $H^1_{1/2}$ norms are equivalent away from Σ.
Second, the sesquilinear form b is continuous on $Q \times Q$ since there exists a constant $C > 0$ such that for all $\mathbf{u}, \mathbf{v} \in Q$,

$$|b(\mathbf{u}, \mathbf{v})| \leq (2 + \lambda C) \|\mathbf{u}\|_Q \|\mathbf{v}\|_Q.$$

Third, b is the sum of coercive and compact forms. Denote b_0 and b_1 the forms such that for $\mathbf{u}, \mathbf{v} \in Q$,

$$\left\{ \begin{array}{l} b_0(\mathbf{u}, \mathbf{v}) := -2 \displaystyle\int_{\Omega_1} u_1 \overline{v_1} \mathrm{d}\mathbf{x} \\ b_1(\mathbf{u}, \mathbf{v}) := (u_1, v_1)_{H^1_{1/2}(\Omega_1)} - (u_2, v_2)_{H^1_{1/2}(\Omega_2)} + \displaystyle\sum_{j=1,2} \int_{\Gamma_j} i\lambda u_j \overline{v_j} \mathrm{d}s. \end{array} \right.$$

One can check that $b_0(\mathbf{u}, \mathbf{v}) + b_1(\mathbf{u}, \mathbf{v}) = b(\mathbf{u}, \mathbf{v})$. This artificial decomposition is obtained by adding and removing the L^2 scalar product of u_1 and v_1, to obtain sign-definite problems on Ω_1 and Ω_2.
For all $\mathbf{v} \in Q$,

$$\mathrm{Re}\, b_1(\mathbf{v}, \mathsf{T}\mathbf{v}) = \|\mathbf{v}\|^2_Q \quad \text{for} \quad \mathsf{T} = \begin{pmatrix} 1 & 0 \\ 0 & -1 \end{pmatrix},$$

hence b_1 is T-coercive for the bijective operator T defined above.
The form b_0, equivalent to the L^2 scalar product on Ω_1, is a compact perturbation of b_1 on Q according to Lemma 3.3.2: for a bounded sequence $(\mathbf{v}^n)_{n \in \mathbb{N}} \subset Q$, and up to a subsequence, its first component v_1^n converges in $L^2(\Omega_1)$.
Thus b is associated to a Fredholm operator of zero index. The Fredholm alternative indicates it suffices to prove injectivity, in the sense that if $b(\mathbf{v}, .) = 0$ for a given $\mathbf{v} \in Q$, then $\mathbf{v} = 0$, to have bijectivity.
Testing against $(0, v_2)$ and taking the real part, we obtain $\|v_2\|_{H^1_{1/2}(\Omega_1)} = 0$. Testing against $(v_1, 0)$ we obtain first $\|v_1\|_{L^2(\Gamma_1)} = 0$. For all $\epsilon > 0$, the function v_1 also verifies the Helmholtz equation on $\Omega_1 \backslash \Omega_1^\epsilon = \{\mathbf{x} \in \Omega_1, \mathrm{dist}_\Sigma(\mathbf{x}) \geq \epsilon\}$

$$-\operatorname{div}(\alpha \nabla v) - v = 0.$$

Going back to the variational formulation one finds that $\partial_n v_1|_{\Gamma_1} = 0$. The unique continuation principle from partial Cauchy data implies that in $\Omega_1 \backslash \Omega_1^\epsilon$ one has $v_1 = 0$. Letting ϵ go to 0, the claim follows. □

Since the weak formulation (3.3.2) of (3.1.1) is restricted to $H^1_{1/2}$ solutions, it excludes $\log|\sigma|$ singularities as seen in Subsection 3.1.1. Thus, it will only allow us to describe the regular part. For the singular part, we will follow a limiting absorption principle which relies on a regularized problem. The classical way is to introduce a complex shift $\alpha + i\nu$ [93, 33], and then pass to the limit $\nu \to 0^+$. We will prove that for $\nu = 0^+$ the limit solution decomposes into a regular part in the weighted space Q plus a complementary singular part.

The remaining part of this section is devoted to show that the problem for $\nu > 0$ is well-posed in $H^1(\Omega)$, which poses no real difficulties. For any $\nu > 0$, problem (3.1.2) can be formulated in a variational way as

$$\begin{array}{l} \text{Find } u \in H^1(\Omega) \text{ such that for all } v \in H^1(\Omega), \\ b^\nu(u,v) = \ell(v). \end{array} \tag{3.3.4}$$

The sesquilinear form is

$$b^\nu(u,v) = \int_\Omega \left((\alpha + i\nu)\nabla u \cdot \overline{\nabla v} - u\overline{v}\right) \mathrm{d}\mathbf{x} + \int_\Gamma i\lambda u\overline{v}\mathrm{d}s,$$

and for purpose of simplicity we redefine another function ℓ that coincides with (3.3.3) on $H^1(\Omega)$

$$\ell(v) := \int_\Gamma f\overline{v}\mathrm{d}s.$$

Proposition 3.3.3. *Let $\nu > 0$, $\lambda > 0$ and $f \in L^2(\Gamma)$. The weak formulation* (3.3.4) *of problem* (3.1.2) *has a unique solution u^ν in $H^1(\Omega)$.*

Proof. The continuity of forms b^ν and ℓ is straightforward, α being bounded and the L^2 norm on Γ being controlled by the H^1 norm on Ω. Let us show b^ν is coercive. For all $u \in H^1(\Omega)$,

$$\mathrm{Im}\, b^\nu(u,u) \geq \nu\|\nabla u\|^2_{L^2(\Omega)^2} \quad \text{and} \quad \mathrm{Re}\, b^\nu(u,u) \leq \|\alpha\|_{L^\infty(\Omega)} \int_\Omega |\nabla u|^2 \mathrm{d}\mathbf{x} - \|u\|^2_{L^2(\Omega)},$$

so that for all $C > \|\alpha\|_{L^\infty(\Omega)}/\nu$, $\mathrm{Re}\left(-(1+iC)b^\nu(u,u)\right) \geq \min(1, C\nu - \|\alpha\|_{L^\infty(\Omega)})\|u\|^2_{H^1(\Omega)}$ and b^ν is coercive. The Lax-Milgram Theorem can be applied to (3.3.4), which thus has a unique solution u^ν in $H^1(\Omega)$. □

3.3.2 A family of quasisolutions

For any $\nu > 0$, we define a family of quasisolutions to problem (3.1.2). It is composed of functions w^ν_g approximating the expected logarithmic singular behaviour as $\nu \to 0$ with data $g \in H^2(\Sigma)$:

$$w^\nu_g(\gamma,\sigma) := \frac{g(\gamma)}{r(\gamma)} \left(\frac{\log\left(r(\gamma)^2\sigma^2 + \nu^2\right)}{2} - i\,\mathrm{atan}\left(\frac{r(\gamma)\sigma}{\nu}\right)\right). \tag{3.3.5}$$

When applying the differential operators $(-\nabla\cdot((\alpha+i\nu)\nabla) - \mathrm{id})$ in Ω and $((\alpha+i\nu)\partial_n + i\lambda\mathrm{id})$ on Γ to the family, we define the resulting quantities

$$\left\{ \begin{array}{rcll} q^\nu_g & := & -\nabla\cdot((\alpha+i\nu)\nabla w^\nu_g) - w^\nu_g & \text{in } \Omega, \\ z^\nu_g & := & (\alpha+i\nu)\partial_n w^\nu_g + i\lambda w^\nu_g & \text{on } \Gamma. \end{array} \right. \tag{3.3.6}$$

Developing the equation in Ω from (3.3.6) and using (3.1.6), one has

$$\begin{aligned} q_g^\nu(\gamma,\sigma) &= -\partial_\gamma\left((\alpha+i\nu)\partial_\gamma w_g^\nu\right)|\nabla\gamma|^2 + (\alpha+i\nu)\partial_\gamma w_g^\nu(\partial_\gamma\nabla\gamma)\cdot\nabla\gamma \\ &\quad +(\alpha+i\nu)\partial_\sigma w_g^\nu(\partial_\gamma\nabla\sigma)\cdot\nabla\gamma - \partial_\sigma\left((\alpha+i\nu)\partial_\sigma w_g^\nu\right)|\nabla\sigma|^2 - w_g^\nu \\ &= \left[\frac{-\partial_\gamma}{(1-\sigma/R(\gamma))^2} + \frac{\sigma R'(\gamma)R(\gamma)}{(R(\gamma)-\sigma)^3}\right] \\ &\quad \left((\alpha+i\nu)\left(\left(g'(\gamma) - \frac{g(\gamma)r'(\gamma)}{r(\gamma)}\right)w_1^\nu + \frac{g(\gamma)}{r(\gamma)}\frac{r'(\gamma)\sigma}{r(\gamma)\sigma+i\nu}\right)\right) \\ &\quad + \left[-\partial_\sigma + \frac{1}{R(\gamma)-\sigma}\right]\left(g(\gamma)\frac{\alpha+i\nu}{r(\gamma)\sigma+i\nu}\right) - w_g^\nu(\gamma,\sigma), \end{aligned} \tag{3.3.7}$$

where $w_1^\nu(\gamma,\sigma) = r(\gamma)^{-1}\left(\frac{1}{2}\log\left(r(\gamma)^2\sigma^2+\nu^2\right) - i\,\mathrm{atan}(\frac{r(\gamma)\sigma}{\nu})\right)$.

Proposition 3.3.4. *Let $\nu \in (0,1)$ and $g \in H^2(\Sigma)$. The manufactured solution w_g^ν, the right hand side q_g^ν belong to $L^2(\Omega)$ and the boundary term z_g^ν belongs to $L^2(\Gamma)$. Moreover, the bounds are uniform with respect to ν.*

Proof. Let $\nu \in (0,1)$ and $g \in H^2(\Sigma)$. The manufactured solution is defined in (3.3.5) as a product of g which is an H^2 function with respect to γ, of $1/r$ which is a bounded coefficient, and of the sum of a logarithm and of a bounded term. As a consequence, w_g^ν belongs to $L^2(\Omega)$, and the bound is uniform with respect to ν.
Assumption (3.1.7) ensures that the fractions

$$\frac{\alpha+i\nu}{r(\gamma)\sigma+i\nu}, \quad \frac{\sigma}{r(\gamma)\sigma+i\nu}, \quad \frac{\sigma(\alpha+i\nu)}{(r(\gamma)\sigma+i\nu)^2},$$

are bounded, i.e. $O(1)$, for small σ with a constant independent of ν. For the term

$$\partial_\sigma\left[\frac{\alpha+i\nu}{r(\gamma)\sigma+i\nu}\right] = \frac{\partial_\sigma\alpha}{r(\gamma)\sigma+i\nu} - \frac{r(\gamma)(\alpha+i\nu)}{(r(\gamma)\sigma+i\nu)^2},$$

one finds once again that

$$\left|\frac{\partial_\sigma\alpha}{r(\gamma)\sigma+i\nu} - \frac{r(\gamma)(\alpha+i\nu)}{(r(\gamma)\sigma+i\nu)^2}\right| \le \frac{|r(\gamma)\sigma\partial_\sigma\alpha - r(\gamma)\alpha|}{(r(\gamma)\sigma)^2} + \frac{\nu|\partial_\sigma\alpha - r(\gamma)|}{2\nu|r(\gamma)\sigma|} = O(1) \quad \text{for small } \sigma.$$

Refering to (3.3.7), q_g^ν thus amounts to a sum of square integrable terms independently of the value of ν.
Finally, for z_g^ν, since it involves the function w_g^ν and its derivatives away from the curve Σ, it is indeed in $L^2(\Gamma)$ with a bound that is uniform with respect to ν. □

Lemma 3.3.5. *Let $g \in H^2(\Sigma)$. As $\nu \to 0^+$, the L^2 limit of the manufactured functions defined above are*

$$\begin{cases} w_g^+(\gamma,\sigma) &= \dfrac{g(\gamma)}{r(\gamma)}\left(\log|r(\gamma)\sigma| - \dfrac{i\pi}{2}\,\mathrm{sign}(r(\gamma)\sigma)\right) \quad \textit{in } L^2(\Omega), \\ q_g^+(\gamma,\sigma) &= \left[\dfrac{-\partial_\gamma}{(1-\sigma/R(\gamma))^2} + \dfrac{\sigma R'(\gamma)R(\gamma)}{(R(\gamma)-\sigma)^3}\right] \\ &\quad \left(\left(g'(\gamma) - \dfrac{g(\gamma)r'(\gamma)}{r(\gamma)}\right)\alpha(\gamma,\sigma)w_1^+(\gamma,\sigma) + \dfrac{g(\gamma)}{r(\gamma)}\dfrac{\alpha(\gamma,\sigma)r'(\gamma)\sigma}{r(\gamma)\sigma}\right) \\ &\quad + \left[-\partial_\sigma + \dfrac{1}{R(\gamma)-\sigma}\right]\left(g(\gamma)\dfrac{\alpha(\gamma,\sigma)}{r(\gamma)\sigma}\right) - w_g^+(\gamma,\sigma) \quad \textit{in } L^2(\Omega), \\ z_g^+(\gamma,\sigma) &= \alpha\partial_n w_g^+ + i\lambda w_g^+ \quad \textit{in } L^2(\Gamma). \end{cases} \tag{3.3.8}$$

Proposition 3.3.6. *For $g \in H^2(\Sigma)$, the associated manufactured solutions depend in the following way on g*

$$\|w_g^+\|_{L^2(\Omega)} \leq C\|g\|_{L^2(\Sigma)}, \quad \|\alpha\nabla w_g^+\|_{L^2(\Omega)^2} \leq C\|g\|_{H^1(\Sigma)},$$
$$\|q_g^+\|_{L^2(\Omega)} \leq C\|g\|_{H^2(\Sigma)}, \quad \textit{and} \quad \|z_g^+\|_{L^2(\Gamma)} \leq C\|g\|_{H^1(\Sigma)},$$

for four positive constants C independent of g.

Remark 3.3.7. For any non trivial $g \in H^2(\Sigma)$, function w_g^+ does not belong to $H^1_{1/2}(\Omega)$. On the other hand, for any smooth function ϕ that vanishes on Σ, the term $\left(|\alpha|^{1/2}\nabla w_g^+\right)\phi$ is square integrable. In fact, the most singular term in $\int_\Omega |\alpha||\nabla w_g^+|^2\phi^2$ is

$$\int_0^1 \int_{-R}^R |\alpha| \frac{|g(\gamma)|^2}{r^2(\gamma)\sigma^2}\phi^2(\gamma,\sigma)p_\Omega(\gamma,\sigma)\mathrm{d}\sigma\mathrm{d}\gamma,$$

which is indeed integrable since $\alpha(\gamma,\sigma) = r(\gamma)\sigma + O(\sigma^2)$. Therefore $w_g^+ \in \bigcap_{\epsilon>0} H^1_{1/2+\epsilon}(\Omega)$.

Proposition 3.3.8. *Let $g \in H^2(\Sigma)$. The α-weighted flux of w_g^+ on Σ is equal to g, in the sense that for all $h \in L^2(\Sigma)$,*

$$\int_\gamma \alpha(\gamma,0)\nabla w_g^+(\gamma,0)\cdot\mathbf{n}(\gamma)\overline{h(\gamma)}\mathrm{d}\gamma = \int_\gamma g(\gamma)\overline{h(\gamma)}\mathrm{d}\gamma.$$

Proof. Let $\nu > 0$. For all $g \in H^2(\Sigma)$, and $\gamma \in [0,1]$,

$$(\alpha(\gamma,0)+i\nu)\nabla w_g^\nu(\gamma,0)\cdot\mathbf{n}(\gamma) = \frac{\alpha(\gamma,0)+i\nu}{r(\gamma)\times 0 + i\nu}g(\gamma)|\mathbf{n}(\gamma)|^2 = g(\gamma).$$

According to Proposition 3.3.6, $(\alpha+i\nu)\nabla w_g^\nu$ converges weakly in $L^2(\Sigma)$ towards $\alpha\nabla w_g^+$, so the result is proven. □

Remark 3.3.9. This last proposition is essential for the decomposition in regular and singular parts. We will introduce a singular coefficient g supported on Σ representing the α-weighted flux over the curve Σ of the whole solution of (3.1.1). Going back to the 1D case, it corresponds to the fact xY_0' has a trace at $x = 0$ and in this case the unknown g is reduced to the coefficient b, see Subsection 3.1.1.

3.3.3 Decomposition of the solution in regular and singular parts

According to the Ansatz introduced in Subsection 3.1.1, we decompose u as

$$u = \left| \begin{array}{ll} u_1 - w_g^+, & \text{in } \Omega_1, \\ u_2 - w_g^+, & \text{in } \Omega_2, \end{array} \right. \tag{3.3.9}$$

with the singular coefficient $g \in H^2(\Sigma)$ yet to be characterized, and for $j = 1, 2$, the regular part $u_j \in H^1_{1/2}(\Omega_j)$ such that

$$\left\{ \begin{array}{rcll} -\nabla\cdot(\alpha\nabla u_j) - u_j &=& q_g^+, & \text{in } \Omega_j \\ \alpha\partial_n u_j + i\lambda u_j &=& f + z_g^+, & \text{on } \Gamma_j \\ \alpha\partial_n u_j &=& 0, & \text{on } \Sigma. \end{array} \right. \tag{3.3.10}$$

For a fixed g, these equations rewrite in a classical variational way

$$\begin{array}{l} \text{Find } \mathbf{u} \in Q \text{ such that for all } \mathbf{v} \in Q, \\ b(\mathbf{u}, \mathbf{v}) = \ell_g(\mathbf{v}), \end{array} \tag{3.3.11}$$

where this time the antilinear form ℓ_g is defined by

$$\ell_g(v_1, v_2) := \sum_{j=1,2} \int_{\Omega_j} q_g^+ \overline{v_j} \mathrm{d}\mathbf{x} + \int_{\Gamma_j} (f + z_g^+) \overline{v_j} \mathrm{d}s.$$

For $f = 0$ and $g \in H^2(\Sigma)$, we denote the solution $\mathbf{u}(g) = (u_1(g), u_2(g))$.

Proposition 3.3.10. *Let $\lambda > 0$, $f \in L^2(\Gamma)$ and $g \in H^2(\Sigma)$. There exists a unique solution $(u_1, u_2) \in Q$ solution of the weak formulation (3.3.11) of (3.3.10). The solution is such that*

$$\begin{array}{c} \|u_1\|_{H^1_{1/2}(\Omega_1)} \leq C \left(\|g\|_{H^2(\Sigma)} + \|f\|_{L^2(\Gamma)} \right) \\ \text{and} \quad \|u_2\|_{H^1_{1/2}(\Omega_2)} \leq C \left(\|g\|_{H^2(\Sigma)} + \|f\|_{L^2(\Gamma)} \right), \end{array} \tag{3.3.12}$$

for constants $C > 0$ that are independent of f and g.

Proof. Under the assumption that ℓ_g is continuous, the proof of Prop. 3.3.1 shows that the problem is well-posed for any $\lambda > 0$, $f \in L^2(\Gamma)$ and $g \in H^2(\Sigma)$. And the continuity of ℓ_g is immediate considering Prop. 3.3.6.
Testing against $(u_1, 0)$ and $(0, u_2)$ respectively, we obtain the bounds

$$\|u_1\|_{H^1_{1/2}(\Omega_1)} - \|u_1\|_{L^2(\Omega_1)} \leq C(\|g\|_{H^2(\Sigma)} + \|f\|_{L^2(\Gamma)}), \tag{3.3.13}$$

and

$$\|u_2\|_{H^1_{1/2}(\Omega_2)} \leq C(\|g\|_{H^2(\Sigma)} + \|f\|_{L^2(\Gamma)}).$$

Let us now precise the bound (3.3.13). We show that there exists a constant $C > 0$ that is independent of f and g such that

$$\|u_1\|_{L^2(\Omega_1)} \leq C(\|f\|_{L^2(\Gamma_1)} + \|g\|_{H^2(\Sigma)}).$$

We proceed by contradiction as in *e.g.* [48]. Consider there exists sequences $(f_k)_{k\in\mathbb{N}} \subset L^2(\Gamma)$, $(g_k)_{k\in\mathbb{N}} \subset H^2(\Sigma)$ and $(u_{1,k})_{k\in\mathbb{N}} \subset H^1_{1/2}(\Omega_1)$ that verify for all $k \in \mathbb{N}$,

$$\left\{ \begin{array}{rcll} -\nabla \cdot (\alpha \nabla u_{1,k}) - u_{1,k} & = & q_{g_k}^+, & \text{in } \Omega_1 \\ \alpha \partial_n u_{1,k} + i\lambda u_{1,k} & = & f_k + z_{g_k}^+, & \text{on } \Gamma_1 \\ \alpha \partial_n u_{1,k} & = & 0, & \text{on } \Sigma \end{array} \right.$$

and such that $\|u_{1,k}\|_{L^2(\Omega_1)} = 1$ for all k and $\|f_k\|_{L^2(\Gamma)} + \|g_k\|_{H^2(\Sigma)} \to 0$. Using relation (3.3.13), we get that $(u_{1,k})_{k\in\mathbb{N}}$ is bounded in $H^1_{1/2}(\Omega_1)$ norm. Therefore there exists $u_1^* \in H^1_{1/2}(\Omega_1)$ towards which, up to a subsequence, $u_{1,k}$ converges weakly in $H^1_{1/2}(\Omega_1)$ and strongly in $L^2(\Omega_1)$ according to Lemma 3.3.2. Thus u_1^* is the weak solution of

$$\left\{ \begin{array}{rcll} -\nabla \cdot (\alpha \nabla u_1) - u_1 & = & 0, & \text{in } \Omega_1 \\ \alpha \partial_n u_1 + i\lambda u_1 & = & 0, & \text{on } \Gamma_1 \\ \alpha \partial_n u_1 & = & 0, & \text{on } \Sigma \end{array} \right.$$

which means $u_1^* = 0$. But this contradicts the fact that $\|u_1^*\|_{L^2(\Omega_1)} = 1$.
So the bound (3.3.13) can be expressed exclusively in terms of the $H^1_{1/2}(\Omega_1)$ norm of u_1 as

$$\|u_1\|_{H^1_{1/2}(\Omega_1)} \leq C(\|g\|_{H^2(\Sigma)} + \|f\|_{L^2(\Gamma)})$$

and the proof is finished. □

It is now necessary to find how to characterize the transmission condition on Σ, quantified by the unknown g, to close the system.

3.4 A mixed variational formulation of the limit problem

3.4.1 Energy estimates

Let u^ν denote the solution of (3.1.2). We introduce the set of compactly supported, smooth and positive cutoff around Σ functions depending only on σ, and not on γ

$$\mathcal{C}^1_{0,+}(\Omega) = \left\{\varphi \in \mathcal{C}^1_0(\Omega), \partial_\gamma \varphi = 0,\, \varphi \geq 0,\, \varphi|_\Sigma = 1\right\}. \tag{3.4.1}$$

Let $\varphi \in \mathcal{C}^1_{0,+}(\Omega)$. We introduce a new unknown $h \in H^2(\Sigma)$, which corresponds to a dual variable associated to the unknown g. For a given h, testing the equation verified by $u^\nu + w_h^\nu$ against $\overline{(u^\nu + w_h^\nu)}\varphi$ gives

$$\int_\Omega \left(-\nabla \cdot ((\alpha + i\nu)\nabla(u^\nu + w_h^\nu))\, \overline{(u^\nu + w_h^\nu)}\varphi - |u^\nu + w_h^\nu|^2 \varphi\right) \mathrm{d}\mathbf{x} = \int_\Omega q_h^\nu \overline{(u^\nu + w_h^\nu)}\varphi \mathrm{d}\mathbf{x}.$$

Integrating by parts, it yields

$$\begin{aligned}\int_\Omega \Big((\alpha + i\nu)\,|\nabla(u^\nu + w_h^\nu)|^2 \varphi + (\alpha + i\nu)\overline{(u^\nu + w_h^\nu)}\nabla(u^\nu + w_h^\nu)\cdot\nabla\varphi - |u^\nu + w_h^\nu|^2 \varphi\Big)\mathrm{d}\mathbf{x} \\ = \int_\Omega q_h^\nu \overline{(u^\nu + w_h^\nu)}\varphi \mathrm{d}\mathbf{x},\end{aligned}$$

wich implies

$$\begin{aligned}\mathrm{Im}\int_\Omega \left((\alpha + i\nu)(u^\nu + w_h^\nu)\nabla\overline{(u^\nu + w_h^\nu)}\cdot\nabla\varphi + q_h^\nu\overline{(u^\nu + w_h^\nu)}\varphi\right)\mathrm{d}\mathbf{x} \\ = \int_\Omega \nu\,|\nabla(u^\nu + w_h^\nu)|^2\,\mathrm{d}\mathbf{x} \geq 0.\end{aligned} \tag{3.4.2}$$

Definition 3.4.1. Let $\nu > 0$, $\varphi \in \mathcal{C}^1_{0,+}(\Omega)$. For all $u \in H^1(\Omega)$ and $h \in H^2(\Sigma)$, define the quadratic form

$$\mathcal{J}^\nu(u,h) = \mathrm{Im}\int_\Omega \left((\alpha + i\nu)(u + w_h^\nu)\nabla\overline{(u + w_h^\nu)}\cdot\nabla\varphi + q_h^\nu\overline{(u + w_h^\nu)}\varphi\right)\mathrm{d}\mathbf{x}.$$

We also define the Hilbert space

$$\begin{aligned}V := Q \times H^2(\Sigma) \times H^2(\Sigma), \text{equipped with the norm} \\ \|(\mathbf{u}, g, h)\|_V := \|\mathbf{u}\|_Q + \|g\|_{H^2(\Sigma)} + \|h\|_{H^2(\Sigma)}.\end{aligned} \tag{3.4.3}$$

and the limit quadratic form such that for all $(\mathbf{u}, g, h) \in V$ with $\mathbf{u} = (u_1, u_2)$

$$\mathcal{J}^+(\mathbf{u}, g, h) = \sum_{j=1,2} \mathrm{Im}\int_{\Omega_j} \left(\alpha(u_j - w^+_{g-h})\nabla\overline{(u_j - w^+_{g-h})}\cdot\nabla\varphi + q_h^+\overline{(u_j - w^+_{g-h})}\varphi\right)\mathrm{d}\mathbf{x}.$$

For a given $(\mathbf{u}, g, h)$, the quantity $\mathcal{J}^+(\mathbf{u}, g, h)$ is the formal pointwise limit of $\mathcal{J}^\nu(u, h)$ where $u|_{\Omega_j}$ is a regularization of $u_j - w_g^+$ for $j = 1, 2$. Since relation (3.4.2) holds, the idea is now to minimize $\mathcal{J}^+$ under the constraint that $(\mathbf{u}, g)$ verifies equation (3.3.11). We define for this purpose the following Lagrangian on $V \times Q$, such that for all $(\mathbf{u}, g, h) \in V$ and $\mathbf{v} \in Q$

$$\mathcal{L}^+(\mathbf{u}, g, h, \mathbf{v}) = \mathcal{J}^+(\mathbf{u}, g, h) + \mathrm{Im}\left(b(\mathbf{u}, \mathbf{v}) - \ell_g(\mathbf{v})\right). \tag{3.4.4}$$

3.4.2 Mixed variational formulation

To begin with, define b^+ the sesquilinear form on $V \times Q$ such that for all $(\mathbf{u}, g, h) \in V$ and $\mathbf{v} \in Q$,

$$b^+\left((\mathbf{u}, g, h), \mathbf{v}\right) = \sum_{j=1,2} \left(\int_{\Omega_j} \left(\alpha \nabla u_j \cdot \nabla \overline{v_j} - (u_j + q_g^+)\overline{v_j}\right) \mathrm{d}\mathbf{x} + \int_{\Gamma_j} (i\lambda u_j - z_g^+)\overline{v_j} \mathrm{d}s \right). \tag{3.4.5}$$

Remark 3.4.2. On $V \times Q$, it holds that $b^+((\mathbf{u}, g, h), \mathbf{v}) = b^+((\mathbf{u}, g, 0), \mathbf{v}) = b(\mathbf{u}, \mathbf{v}) - \ell_g(\mathbf{v}) + \ell(\mathbf{v})$.

Define a^+ a sesquilinear form on $V \times V$ that verifies $\mathrm{Im}\, a^+ = d\mathcal{J}^+$. We choose the form defined for all $(\mathbf{u}, g, h), (\mathbf{v}, k, l) \in V$ by

$$\begin{aligned} &a^+\left((\mathbf{u}, g, h), (\mathbf{v}, k, l)\right) \\ &\quad = \sum_{j=1,2} \int_{\Omega_j} \left(\alpha(u_j - w_{g-h}^+)\nabla\overline{(v_j - w_{k-l}^+)} \cdot \nabla\varphi + q_h^+\overline{(v_j - w_{k-l}^+)}\varphi\right) \mathrm{d}\mathbf{x} \\ &\qquad - \int_{\Omega_j} \left(\alpha\overline{(v_j - w_{k-l}^+)}\nabla(u_j - w_{g-h}^+) \cdot \nabla\varphi + \overline{q_l^+}(u_j - w_{g-h}^+)\varphi\right) \mathrm{d}\mathbf{x}. \end{aligned} \tag{3.4.6}$$

Note that a^+ is anti-hermitian.

The Euler-Lagrange equations associated to the minimization of (3.4.4) have the following structure

$$\begin{array}{l} \text{Find } (\mathbf{u}, g, h) \in V \text{ and } \boldsymbol{\lambda} \in Q \text{ such that} \\ \left\{ \begin{array}{lcllll} a^+\left((\mathbf{u}, g, h), (\mathbf{v}, k, l)\right) & - & \overline{b^+\left((\mathbf{v}, k, l), \boldsymbol{\lambda}\right)} & = & 0, & \forall (\mathbf{v}, k, l) \in V, \\ b^+\left((\mathbf{u}, g, h), \boldsymbol{\mu}\right) & & & = & \ell(\boldsymbol{\mu}), & \forall \boldsymbol{\mu} \in Q. \end{array} \right. \end{array} \tag{3.4.7}$$

We will see that with an arbitrary small regularization in g and h for the form a^+, this form is T-coercive on V, which allows us to apply the classical results of [13] and lead to the conclusion that the regularized problem is well-posed.
For $\rho, \mu \in \mathbb{R}^+$, we introduce the regularized form on $V \times V$

$$a_r^+\left((\mathbf{u}, g, h), (\mathbf{v}, k, l)\right) = a^+\left((\mathbf{u}, g, h), (\mathbf{v}, k, l)\right) + i\left(-\rho\left(g, k\right)_{H^2(\Sigma)} + \mu\left(h'', l''\right)_{L^2(\Sigma)}\right). \tag{3.4.8}$$

Theorem 3.4.3. *Let $\lambda > 0$, $f \in L^2(\Gamma)$, and ρ, $\mu > 0$. The regularized formulation of* (3.4.7)

$$\begin{array}{l} \textit{Find } (\mathbf{u}, g, h) \in V \textit{ and } \boldsymbol{\lambda} \in Q \textit{ such that} \\ \left\{ \begin{array}{lcllll} a_r^+\left((\mathbf{u}, g, h), (\mathbf{v}, k, l)\right) & - & \overline{b^+\left((\mathbf{v}, k, l), \boldsymbol{\lambda}\right)} & = & 0, & \forall (\mathbf{v}, k, l) \in V, \\ b^+\left((\mathbf{u}, g, h), \boldsymbol{\mu}\right) & & & = & \ell(\boldsymbol{\mu}), & \forall \boldsymbol{\mu} \in Q, \end{array} \right. \end{array} \tag{3.4.9}$$

admits a unique solution.

Remark 3.4.4. Theorem 3.4.3 means that the regularization in ν across the curve Σ has been replaced by a regularization in ρ and μ along Σ.

3.4.3 Proof of the well-posedness

Denote $B^+ : V \to Q'$ the linear continuous operator such that for all $(\mathbf{v}, k, l) \in V$ and $\boldsymbol{\mu} \in Q$,

$$\left(B^+(\mathbf{v}, k, l), \boldsymbol{\mu}\right)_{Q',Q} = b^+\left((\mathbf{v}, k, l), \boldsymbol{\mu}\right),$$

and let $K := \ker B^+$. Denote $A^+_{KK'} : K \to K'$ the linear continuous operator such that for all $(\mathbf{u}, g, h), (\mathbf{v}, k, l) \in K$,

$$\left(A^+_{KK'}(\mathbf{u}, g, h), (\mathbf{v}, k, l)\right)_{K',K} = a^+_r\left((\mathbf{u}, g, h), (\mathbf{v}, k, l)\right), \tag{3.4.10}$$

The proof of Theorem 3.4.3 will consist in applying the following classical result.

Theorem 3.4.5 (Theorem 4.2.2 of Boffi-Brezzi-Fortin [13] in $\mathbb{C}$)**.** *For any $\kappa \in V'$ and $\varkappa \in Q'$, the mixed system*

$$\begin{array}{l} \textit{Find } (\mathbf{u}, g, h) \in V \textit{ and } \boldsymbol{\lambda} \in Q \textit{ such that} \\ \left\{ \begin{array}{lcll} a^+_r\left((\mathbf{u}, g, h), (\mathbf{v}, k, l)\right) & - & \overline{b^+\left((\mathbf{v}, k, l), \boldsymbol{\lambda}\right)} & = \quad (\kappa, (\mathbf{v}, k, l))_{V',V}, \quad \forall (\mathbf{v}, k, l) \in V, \\ b^+\left((\mathbf{u}, g, h), \boldsymbol{\mu}\right) & & & = \quad (\varkappa, \boldsymbol{\mu})_{Q',Q}, \qquad\qquad \forall \boldsymbol{\mu} \in Q. \end{array} \right. \end{array} \tag{3.4.11}$$

has a unique solution if and only if $A^+_{KK'}$ is an isomorphism from K to K' and if $\operatorname{Im} B^+ = Q'$.

Proposition 3.4.6. *Operator B^+ is onto Q'.*

Proof. This is a consequence of Prop. 3.3.10. Indeed, according to (3.4.5), B^+ is such that

$$\left(B^+(\mathbf{u}, g, h), \boldsymbol{\mu}\right)_{Q',Q} = b\left(\mathbf{u}, \boldsymbol{\mu}\right) - \sum_{j=1,2} \left(\int_{\Omega_j} q^+_g \overline{\mu_j} \mathrm{d}\mathbf{x} + \int_{\Gamma_j} z^+_g \overline{\mu_j} \mathrm{d}s \right).$$

For any $\varkappa \in Q'$, it has been proven that for all $g \in H^2(\Sigma)$, there exists $\mathbf{u} \in Q$ such that

$$b\left(\mathbf{u}, \boldsymbol{\mu}\right) = \sum_{j=1,2} \left(\int_{\Omega_j} q^+_g \overline{\mu_j} \mathrm{d}\mathbf{x} + \int_{\Gamma_j} z^+_g \overline{\mu_j} \mathrm{d}s \right) + (\varkappa, \boldsymbol{\mu})_{Q',Q} \quad \forall \boldsymbol{\mu} \in Q.$$

As a result, operator B^+ is onto Q'. □

Proposition 3.4.7. *The kernel K of operator B^+ can be described as*

$$K = \left\{ (\mathbf{u}, g, h) \in V, \quad \mathbf{u}(g) = (u_1(g), u_2(g)) \right\}.$$

Proof. As the last component in $H^2(\Sigma)$ is a silent variable for B^+, it is not constrained. Necessarily $(\mathbf{u}, g)$ is such that $b(\mathbf{u}, \boldsymbol{\mu}) = \ell_g(\boldsymbol{\mu})$ for all $\boldsymbol{\mu} \in Q$, where the boundary term $f \in L^2(\Gamma)$ is taken equal to 0. Refering to Prop. 3.3.10, this is verified for all $g \in H^2(\Sigma)$ by $\mathbf{u}(g) = (u_1(g), u_2(g))$. □

Let us now address the properties verified by a^+.

Proposition 3.4.8. *For all* $(\mathbf{u},g,h)$, $(\mathbf{v},k,l)\in K$,

$$\begin{aligned} a^+\left((\mathbf{u},g,h),(\mathbf{v},k,l)\right) &= \sum_{j=1,2}\int_{\Omega_j} q_h^+\overline{(v_j-w_{k-l}^+)}-\overline{q_l^+}(u_j-w_{g-h}^+)\mathrm{d}\mathbf{x} \\ &\quad+\int_{\Gamma_j}\Big(z_h^+\overline{(v_j-w_{k-l}^+)}-\overline{z_l^+}(u_j-w_{g-h}^+) \\ &\qquad -2i\lambda(u_j-w_{g-h}^+)\overline{(v_j-w_{k-l}^+)}\Big)\,\mathrm{d}s \end{aligned} \tag{3.4.12}$$

and a^+ *is independent of the cutoff* φ*, as long as* $\varphi\in\mathcal{C}^1_{0,+}(\Omega)$*, see* (3.4.1).

Proof. Let $(\mathbf{u},g,h)$, $(\mathbf{v},k,l)\in K$, with $\mathbf{u}=(u_1,u_2)=(u_1(g),u_2(g))$ and $\mathbf{v}=(v_1,v_2)=(u_1(k),u_2(k))$ according to Prop. 3.4.7. Remark that

$$\begin{aligned} &a^+\left((\mathbf{u},g,h),(\mathbf{v},k,l)\right)\\ &\quad=\sum_{j=1,2}\int_{\Omega_j}\Big(\alpha(u_j-w_{g-h}^+)\nabla\overline{(v_j-w_{k-l}^+)}\cdot\nabla(\varphi-1)+q_h^+\overline{(v_j-w_{k-l}^+)}(\varphi-1)\Big)\,\mathrm{d}\mathbf{x}\\ &\qquad-\int_{\Omega_j}\Big(\alpha\overline{(v_j-w_{k-l}^+)}\nabla(u_j-w_{g-h}^+)\cdot\nabla(\varphi-1)+\overline{q_l^+}(u_j-w_{g-h}^+)(\varphi-1)\Big)\,\mathrm{d}\mathbf{x}\\ &\qquad+\int_{\Omega_j}\Big(q_h^+\overline{(v_j-w_{k-l}^+)}-\overline{q_l^+}(u_j-w_{g-h}^+)\Big)\,\mathrm{d}\mathbf{x}. \end{aligned}$$

Since $\varphi|_\Sigma=1$ and $\alpha\left|\nabla w_\cdot^+\right|^2=\frac{c_0(\gamma,\sigma)}{\sigma}+c_1(\gamma,\sigma)$ with $c_0,c_1\in L^2(\Omega)$, the terms in $\alpha\left|\nabla w_\cdot^+\right|^2(\varphi-1)$ are integrable thanks to Hardy's inequality, which ensures that $\frac{\varphi-1}{\sigma}$ is square integrable on Ω. Therefore the quantity

$$\sum_{j=1,2}\int_{\Omega_j}\alpha\nabla\overline{(v_j-w_{k-l}^+)}\cdot\nabla(u_j-w_{g-h}^+)\,(\varphi-1)\mathrm{d}\mathbf{x}$$

is well defined. The first two lines above thus rewrite

$$\begin{aligned} A &:= \sum_{j=1,2}\int_{\Omega_j}\Big(\alpha(u_j-w_{g-h}^+)\nabla\overline{(v_j-w_{k-l}^+)}\cdot\nabla(\varphi-1)+q_h^+\overline{(v_j-w_{k-l}^+)}(\varphi-1)\Big)\,\mathrm{d}\mathbf{x}\\ &\quad-\int_{\Omega_j}\Big(\alpha\overline{(v_j-w_{k-l}^+)}\nabla(u_j-w_{g-h}^+)\cdot\nabla(\varphi-1)+\overline{q_l^+}(u_j-w_{g-h}^+)(\varphi-1)\Big)\,\mathrm{d}\mathbf{x}\\ &= \sum_{j=1,2}\int_{\Omega_j}\Big(\alpha\nabla\overline{(v_j-w_{k-l}^+)}\cdot\nabla\Big((u_j-w_{g-h}^+)(\varphi-1)\Big)+q_h^+\overline{(v_j-w_{k-l}^+)}(\varphi-1)\Big)\,\mathrm{d}\mathbf{x}\\ &\quad-\int_{\Omega_j}\Big(\alpha\nabla(u_j-w_{g-h}^+)\cdot\nabla\Big(\overline{(v_j-w_{k-l}^+)}(\varphi-1)\Big)+\overline{q_l^+}(u_j-w_{g-h}^+)(\varphi-1)\Big)\,\mathrm{d}\mathbf{x}\\ &= \sum_{j=1,2}\int_{\Omega_j}\Big(\alpha\nabla\overline{(v_j-w_{k-l}^+)}\cdot\nabla\Big((u_j-w_{g-h}^+)(\varphi-1)\Big)\\ &\qquad+(u_j-w_{g-h}^++q_h^+)\overline{(v_j-w_{k-l}^+)}(\varphi-1)\Big)\,\mathrm{d}\mathbf{x}\\ &\quad-\int_{\Omega_j}\Big(\alpha\nabla(u_j-w_{g-h}^+)\cdot\nabla\Big(\overline{(v_j-w_{k-l}^+)}(\varphi-1)\Big)\\ &\qquad+\overline{(v_j-w_{k-l}^++q_l^+)}(u_j-w_{g-h}^+)(\varphi-1)\Big)\,\mathrm{d}\mathbf{x}. \end{aligned}$$

Since on each Ω_j $u_j - w^+_{g-h}$ verifies weakly $-\nabla\cdot(\alpha\nabla(u_j - w^+_{g-h})) - (u_j - w^+_{g-h}) = q^+_h$ with boundary conditions on Γ_j $\alpha\partial_n(u_j - w^+_{g-h}) + i\lambda(u_j - w^+_{g-h}) = f + z^+_h$, and since $v_j - w^+_{k-l}$ verifies the corresponding relations for $g = k$, $h = l$ and $u_j = v_j = u_j(k)$, integrating by parts and using that $(\varphi - 1)|_\Sigma = 0$ it yields

$$\begin{aligned} A &= \sum_{j=1,2}\int_{\Gamma_j}\Big(\overline{(v_j - w^+_{k-l})}\alpha\partial_n(u_j - w^+_{g-h}) - (u_j - w^+_{g-h})\alpha\partial_n\overline{(v_j - w^+_{k-l})}\Big)\,\mathrm{d}s \\ &= \sum_{j=1,2}\int_{\Gamma_j}\Big(\overline{(v_j - w^+_{k-l})}(-i\lambda(u_j - w^+_{g-h}) + z^+_h) \\ &\qquad - (u_j - w^+_{g-h})\overline{(-i\lambda(v_j - w^+_{k-l}) + z^+_l)}\Big)\,\mathrm{d}s \end{aligned}$$

and the result is proven. □

Lemma 3.4.9. *For all $g \in H^2(\Sigma)$,*

$$\mathrm{Im}\int_\Omega q^+_g\overline{w^+_g}\mathrm{d}\mathbf{x} = \pi\|g\|^2_{L^2_w(\Sigma)} - \mathrm{Im}\int_\Gamma(z^+_g - i\lambda w^+_g)\overline{w^+_g}\mathrm{d}s.$$

Proof. For all $\epsilon > 0$, define ψ_ϵ a cutoff of Σ, a real valued piecewise affine function of σ such that $\psi_\epsilon(\gamma,\sigma) = 0$ if $|\sigma| < \epsilon/2$ and $\psi_\epsilon(\gamma,\sigma) = 1$ if $|\sigma| > \epsilon$. For all $g \in H^2(\Sigma)$, using ψ_ϵ and integrating by parts,

$$\begin{aligned} \mathrm{Im}\int_\Omega q^+_g\overline{w^+_g}\mathrm{d}\mathbf{x} &= \lim_{\epsilon\to0}\mathrm{Im}\int_\Omega q^+_g\overline{w^+_g}\psi_\epsilon\mathrm{d}\mathbf{x} \\ &= \lim_{\epsilon\to0}\mathrm{Im}\Bigg(\int_\Omega\Big(\alpha|\nabla w^+_g|^2\psi_\epsilon + \alpha\overline{w^+_g}\nabla w^+_g\cdot\nabla\psi_\epsilon - |w^+_g|^2\psi_\epsilon\Big)\mathrm{d}\mathbf{x} \\ &\qquad - \int_\Gamma\alpha\partial_n w^+_g\overline{w^+_g}\mathrm{d}s\Bigg) \\ &= \lim_{\epsilon\to0}\mathrm{Im}\left(\int_\Omega\alpha\overline{w^+_g}\nabla w^+_g\cdot\nabla\psi_\epsilon\mathrm{d}\mathbf{x} - \int_\Gamma(z^+_g - i\lambda w^+_g)\overline{w^+_g}\mathrm{d}s\right). \end{aligned}$$

Let us now compute this first integral on Ω for a given $\epsilon > 0$. Expressing the functions in terms of (γ,σ),

$$\begin{aligned} &\mathrm{Im}\int_\Omega\alpha\overline{w^+_g}\nabla w^+_g\cdot\nabla\psi_\epsilon\mathrm{d}\mathbf{x} \\ &= \mathrm{Im}\int_\gamma\int_{-\epsilon}^{-\epsilon/2}\frac{-2|g(\gamma)|^2}{\epsilon r(\gamma)}\frac{\alpha}{r(\gamma)\sigma}\left(\log|r(\gamma)\sigma| - i\frac{\pi}{2}\,\mathrm{sign}(r(\gamma))\right)p_\Omega(\gamma,\sigma)\mathrm{d}\sigma\mathrm{d}\gamma \\ &\quad + \mathrm{Im}\int_\gamma\int_{\epsilon/2}^{\epsilon}\frac{2|g(\gamma)|^2}{\epsilon r(\gamma)}\frac{\alpha}{r(\gamma)\sigma}\left(\log|r(\gamma)\sigma| + i\frac{\pi}{2}\,\mathrm{sign}(r(\gamma))\right)p_\Omega(\gamma,\sigma)\mathrm{d}\sigma\mathrm{d}\gamma \\ &= \mathrm{Im}\int_\gamma\int_{\epsilon/2}^{\epsilon}\Big[\frac{-2|g(\gamma)|^2}{\epsilon r(\gamma)}\frac{\alpha}{r(\gamma)\sigma}\left(\log|r(\gamma)\sigma| - i\frac{\pi}{2}\,\mathrm{sign}(r(\gamma))\right)p_\Omega(\gamma,-\sigma) \\ &\qquad + \frac{2|g(\gamma)|^2}{\epsilon r(\gamma)}\frac{\alpha}{r(\gamma)\sigma}\left(\log|r(\gamma)\sigma| + i\frac{\pi}{2}\,\mathrm{sign}(r(\gamma))\right)p_\Omega(\gamma,\sigma)\Big]\mathrm{d}\sigma\mathrm{d}\gamma \end{aligned}$$

for the weight $p_\Omega(\gamma,\sigma) = 1 - \sigma/R(\gamma)$ defined in (3.1.5). Identifying the imaginary part, it follows

$$\begin{aligned} \mathrm{Im}\int_\Omega\alpha\overline{w^+_g}\nabla w^+_g\cdot\nabla\psi_\epsilon\mathrm{d}\mathbf{x} &= \int_\gamma\int_{\epsilon/2}^{\epsilon}\frac{2|g(\gamma)|^2}{\epsilon|r(\gamma)|}\frac{\alpha}{r(\gamma)\sigma}\pi\mathrm{d}\sigma\mathrm{d}\gamma \\ &\underset{\epsilon\to0}{\to} \int_\gamma\frac{|g(\gamma)|^2}{|r(\gamma)|}\pi\mathrm{d}\gamma, \end{aligned}$$

which is equal to $\pi\|g\|_{L^2_w(\Sigma)}$ The proof is ended. □

With this technical lemma we can now state the following.

Proposition 3.4.10. *For all* $(\mathbf{u}(g), g, h) \in K$*, one has*

$$\begin{cases} a^+\left((0,0,h),(0,0,h)\right) = 2i\pi\|h\|^2_{L^2_w(\Sigma)}, \\ a^+\left((\mathbf{u}(g),g,0),(\mathbf{u}(g),g,0)\right) = -2i\lambda\sum_{j=1,2}\int_{\Gamma_j}|u_j(g)-w_g^+|^2\mathrm{d}s. \end{cases}$$

Proof. Let $h \in H^2(\Sigma)$. According to (3.4.12),

$$\begin{aligned} a^+\left((0,0,h),(0,0,h)\right) &= \int_\Omega (q_h^+\overline{w_h^+} - \overline{q_h^+}w_h^+)\mathrm{d}\mathbf{x} + \int_\Gamma (z_h^+\overline{w_h^+} - \overline{z_h^+}w_h^+ - 2i\lambda|w_h^+|^2)\mathrm{d}s \\ &= 2i\,\mathrm{Im}\left(\int_\Omega q_h^+\overline{w_h^+}\mathrm{d}\mathbf{x} + \int_\Gamma (z_h^+\overline{w_h^+} - i\lambda|w_h^+|^2)\mathrm{d}s\right). \end{aligned}$$

By Lemma 3.4.9, it is thus equal to $2i\pi\|h\|^2_{L^2_w(\Sigma)}$. Now let $g \in H^2(\Sigma)$ and $\mathbf{u} = \mathbf{u}(g) \in Q$. Relying again on (3.4.12), it follows

$$a^+\left((\mathbf{u}(g),g,0),(\mathbf{u}(g),g,0)\right) = \sum_{j=1,2}\int_{\Gamma_j} -2i\lambda|u_j - w_g^+|^2\mathrm{d}s.$$

□

Proposition 3.4.11. *Let* ρ, $\mu > 0$*. The sesquilinear form* a_r^+ *defined in* (3.4.8) *is* T*-coercive on* K *in the sense that there exists a positive constant* C *such that for all* $(\mathbf{u}(g), g, h) \in K$*,*

$$\mathrm{Im}\, a_r^+\left((\mathbf{u}(g),g,h),\mathsf{T}(\mathbf{u}(g),g,h)\right) \geq C\|(\mathbf{u}(g),g,h)\|_V,$$

for $\mathsf{T} : (\mathbf{u}, g, h) \in V \mapsto (-\mathbf{u}, -g, h) \in V$*. In particular, the operator* $A^+_{KK'}$ *defined in* (3.4.10) *is an isomorphism.*

Proof. Let ρ, $\mu > 0$, and $(\mathbf{u}(g), g, h) \in K$. Using the definition of form a_r^+ and the fact that a^+ is anti-hermitian, it follows from Proposition 3.4.10 that

$$\begin{aligned} \mathrm{Im}\, a_r^+\left((\mathbf{u}(g),g,h),(-\mathbf{u}(g),-g,h)\right) &= 2\pi\|h\|^2_{L^2_w(\Sigma)} + 2\lambda\sum_{j=1,2}\|u_j(g)-w_g^+\|^2_{L^2(\Gamma_j)} \\ &\quad +\rho\|g\|^2_{H^2(\Sigma)} + \mu|h|^2_{H^2(\Sigma)} \\ &\geq C(\|g\|^2_{H^2(\Sigma)} + \|h\|^2_{H^2(\Sigma)}) \end{aligned}$$

for a $C > 0$. Using Proposition 3.3.10 on the control of $\|\mathbf{u}(g)\|_Q$ by $\|g\|_{H^2(\Sigma)}$, we are able to conclude. □

Proof. [Theorem 3.4.3] The hypotheses of Theorem 3.4.5 have been verified in Propositions 3.4.6 and 3.4.11. □

Remark 3.4.12. An equivalence between $g \mapsto \lambda\|u_j(g) - w_g^+\|_{L^2(\Gamma)}$ and the $L^2(\Sigma)$ norm can be obtained on the kernel of a^+, see Appendix 4.3.

3.5 Numerical illustration

The general objectives of this section are to confirm the theoretical analysis by showing numerical results for the approximation of singular solutions of system (3.4.9) and to show that the mixed variational method developed in this work is compatible with standard finite element solvers, such as Freefem++ [62] in our case. To do so, we construct simple reference analytical solutions with and without a logarithmic singularity and use them for numerical error measurements.

3.5.1 Construction of analytical solutions

We construct an analytical solution on a simplified model. Dropping out the 0 order term, which is a compact perturbation, in (3.1.1), one has

$$\left\{ \begin{array}{rcll} -\operatorname{div}(\alpha\nabla u) & = & 0 & \text{in } \Omega, \\ \alpha\partial_n u + i\lambda u & = & f & \text{on } \Gamma. \end{array} \right. \tag{3.5.1}$$

Let Ω be $(-1,1)\times(-1,1)$ with periodic boundary conditions at $y=\pm 1$, with $\Sigma=\{x=0\}$ and $\alpha = x$. A Fourier decomposition in the y-direction $u(\mathbf{x}) = \sum_{k\in\mathbb{Z}} u_k(x)\exp(ik\pi y)$ yields for all modes

$$xu_k'' + u_k' - x(k\pi)^2 u_k = 0 \quad \text{in } (-1,1).$$

The general solution is

$$u_k(x) = \left| \begin{array}{ll} a_k I_0(k\pi x) + b_k K_0(k\pi x) & \forall k \neq 0, \\ a_0 + b_0\left(\log|x| - \dfrac{i\pi}{2}\operatorname{sign}(x)\right) & k = 0, \end{array} \right.$$

where the modified Bessel functions are given by

$$\left\{ \begin{array}{rcl} I_0(x) & = & J_0(ix), \\ K_0(x) & = & -\dfrac{\pi}{2}\left(iJ_0(ix) + Y_0(-ix)\right), \end{array} \right.$$

see Subsection 3.1.1 for the Bessel functions. We consider four test cases which respective solutions are

$$\begin{array}{c} u^1(\mathbf{x}) = 1, \quad u^2(\mathbf{x}) = \log|x| - \dfrac{i\pi}{2}\operatorname{sign}(x), \\ u^3(\mathbf{x}) = e^{i\pi y} I_0(\pi x) \quad \text{and} \quad u^4(\mathbf{x}) = e^{i\pi y} K_0(\pi x). \end{array} \tag{3.5.2}$$

The functions u^1 and u^2 are solutions for the $k=0$ mode. For these two functions, one computes easily the associated $(\mathbf{u}, g, h) \in V$ and $\boldsymbol{\lambda} \in Q$ solution of the variational formulation (3.4.9). According to the decomposition (3.3.9), one has

$$\left\{ \begin{array}{ll} u_j^1 = 1 \quad \text{and} & g^1 = 0, \\ u_j^2 = 0 \quad \text{and} & g^2 = -1, \end{array} \right. \tag{3.5.3}$$

and in both cases, $h = g$ and $\lambda_j = u_j\varphi$, where φ is the cut-off function that localizes near Σ. In the illustration below, the cut-off function is $\varphi(x) = \exp\left(4x^2/(4x^2-1)\right)\mathbf{1}_{(-1/2,1/2)}(x)$.
On the other hand, the functions u^3 and u^4 are solutions for the $k=1$ mode. One can compute the corresponding $(\mathbf{u}, g, h) \in V$ and $\boldsymbol{\lambda} \in Q$ as well.
The functions u^1 and u^3 are regular, while the functions u^2 and u^4 exhibit the logarithmic singularity

which is the object of this study.
With $\lambda = 1$, the boundary condition source term f in (3.5.1) is determined accordingly and

$$f^1(\mathbf{x}) = i,\ f^2(\mathbf{x}) = (1 + \frac{\pi}{2})\,\mathrm{sign}(x),$$
$$f^3(\mathbf{x}) = e^{i\pi y}\left(\pi I_0'(\pi x) + iI_0(\pi x)\right),\ f^4(\mathbf{x}) = e^{i\pi y}\left(\pi K_0'(\pi x) + iK_0(\pi x)\right).$$

3.5.2 Principle of the discretization

The tests were implemented using the Freefem++ [62] code. Freefem++ offers a large choice of bidimensional finite elements, but does not allow so far to discretize a generic bilinear form like $\mathsf{a_h}(\mathsf{u_h}, \mathsf{v_h})$ where $\mathsf{u_h}$ belongs to a 1D FE space and $\mathsf{v_h}$ to a 2D FE space. Since we need this feature, we have decided to focus on simple geometry and to use a penalization method to constrain a 2D FE space to unidimensionality. For this reason, the $H^2(\Sigma)$ space is discretized using 2D P3 Hsieh-Clough-Tocher (HCT) elements [28] penalized in the x-direction on a 2D triangular mesh denoted Σ^M. The upper script M stands for the number of triangles that lie on Σ. The more standard $H^1(\Omega_j)$ 2D spaces are discretized using P1 elements on uniform triangular meshes of Ω_j denoted Ω_j^N, where the upper script N stands for the number of edges on each Γ_j. In the presented test cases, the parameters are $M = 4$ for the P3 elements and $N = 40$ for the P1 elements.

The discretization of (3.4.9) leads to the linear system

$$\mathsf{AU} = \mathsf{L} \tag{3.5.4}$$

with $\mathsf{U} = (\underline{u}_1, \underline{u}_2, \underline{g}, \underline{h}, \underline{\lambda}_1, \underline{\lambda}_2)$ the coefficients of the solution in the appropriate FE bases, and where A and L have block matricial structures

$$\mathsf{A} = \begin{pmatrix} A_1 & 0 & A_{g1} & A_{h1} & B_1 & 0 \\ * & A_2 & A_{g2} & A_{h2} & 0 & B_2 \\ * & * & A_g & A_{hk} & B_{1k} & B_{2k} \\ * & * & * & A_h & 0 & 0 \\ * & * & * & * & 0 & 0 \\ * & * & * & * & * & 0 \end{pmatrix}, \quad \mathsf{L} = \begin{pmatrix} 0 \\ 0 \\ 0 \\ 0 \\ \underline{\ell}_1 \\ \underline{\ell}_2 \end{pmatrix}. \tag{3.5.5}$$

As a consequence of the structure (3.4.9) and because the sesquilinear form a^+ (3.4.6) is anti-hermitian, the matrix A is anti-hermitian $\mathsf{A} = -\overline{\mathsf{A}}^t$. Note that the penalization used to achieve unidimensionality is performed in a similar way to (3.4.8), so that the anti-hermitian nature of the matrix is preserved.

3.5.3 Numerical results

The numerical solution is obtained by solving the linear system (3.5.4)-(3.5.5). With the numerical implementation described above, we observe that the matrices are non-singular and the computations run smoothly.

Numerical errors

In Table 3.1 we present the relative errors in $L^2(\Omega)$ norms for the four test cases on the total solution u of (3.5.1). We observe a relative error of order 10^{-2} for all problems even for this coarse

mesh. We also observe that the error magnitude is slightly smaller for the case 1 in mode 0 and case 3 in mode 1. Our interpretation is that it is due to the regularity of u^1 and u^3, whereas u^2 and u^4 have logarithmic singularities.

	case 1	case 2	case 3	case 4
$\frac{\|u_{ex}-u_{num}\|_{L^2}}{\|u_{ex}\|_{L^2}}$	0.017	0.047	0.008	0.024

Table 3.1 – For the four test cases of (3.5.2), relative $L^2(\Omega)$ error between the exact solution u_{ex} and its approximation $u_{num} = u_j - w_g^+$.

In Table 3.2, we present the block residual errors of $\mathsf{AU} - \mathsf{L}$. The block residuals are defined from (3.5.5) as the residuals for each of the 6 unknowns. It allows a more accurate description of the residual error. We perform the test for the test cases 1 and 2, which means that U takes the two exact values

$$\mathsf{U}^1 = \begin{pmatrix} 1_N^{\Omega_1} \\ 1_N^{\Omega_2} \\ 0 \\ 0 \\ \varphi_N^{\Omega_1} \\ \varphi_N^{\Omega_2} \end{pmatrix} \quad \text{and} \quad \mathsf{U}^2 = \begin{pmatrix} 0 \\ 0 \\ -1_M^{\Sigma} \\ -1_M^{\Sigma} \\ 0 \\ 0 \end{pmatrix}. \tag{3.5.6}$$

In this expression cf. (3.5.3), $1_N^{\Omega_j}$ and $\varphi_N^{\Omega_j}$ are the coefficients of the P1 interpolations of the functions 1 and φ in $H^1(\Omega_j)$, and 1_M^{Σ} are the coefficients of 1 in the HCT space.
A priori, a residual error is the result of three main contributions which are an interpolation error, a penalization error, and errors due to the approximation of the bilinear forms.
We observe in Table 3.2 that all block residual errors are close to machine precision, except for the first four blocks in test case 1. After inspection of the structure of A and the nature of the exact solutions (3.5.6), our interpretation is that when machine precision is reached, the only significant error comes from interpolation errors.

	norm	case 1	case 2
u_1 block	$L^2(\Omega)$	0.0419775	7.76013e-16
u_2 block	$L^2(\Omega)$	0.0491617	7.14962e-16
g block	$L^2(\Sigma)$	0.0360422	3.86971e-12
h block	$L^2(\Sigma)$	0.0361913	4.37914e-12
λ_1 block	$L^2(\Omega)$	7.04875e-15	7.68808e-16
λ_2 block	$L^2(\Omega)$	7.29193e-15	2.70813e-15

Table 3.2 – Residual errors in L^2 norms for the two first test cases.

Plot of the numerical solutions in cases 3 and 4

The imaginary part of the numerical approximation of the solutions u^3 and u^4 is shown on the right part of figures 3.2 and 3.3. The exact solutions, which are Bessel functions modulated in the direction y, are shown on the left part of the figures. The trace of the 2D FE mesh is also visible, together with the vertical line Σ. In Fig. 3.2, we observe that the numerical solution on the right is qualitatively and quantitatively very similar to the exact one on the left. The Fig. 3.3 is of greater interest since the exact solution presents the logarithmic singular behaviour. Qualitatively,

the results are very similar and the logarithmic singularity seems to be correctly captured by the numerical solution. Quantitatively, the L^2 norm of the relative error is small, as reported in Table 3.1, even if a small discrepancy is visible, partly due to a different scaling between both representations.

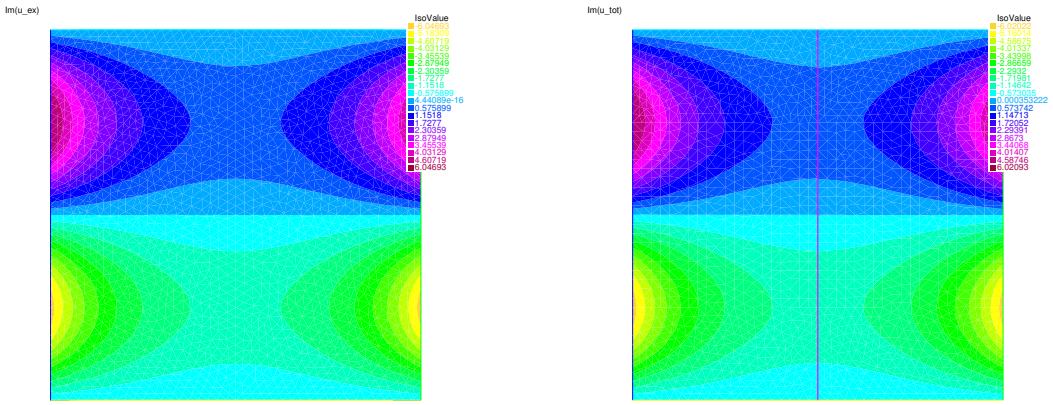

Figure 3.2 – Imaginary parts of the exact solution $u^3(\mathbf{x}) = e^{i\pi y} I_0(\pi x)$ (left) and its approximation (right).

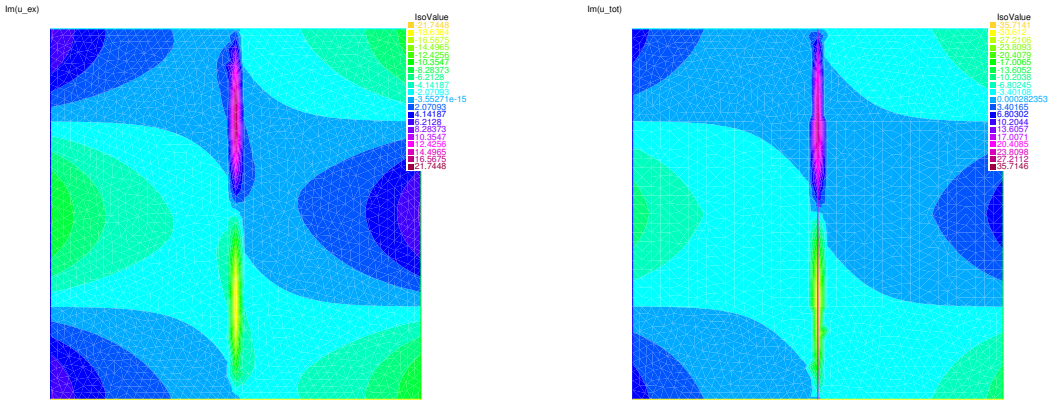

Figure 3.3 – Imaginary parts of the exact solution $u^4(\mathbf{x}) = e^{i\pi y} K_0(\pi x)$ (left) and its approximation (right).

Plot of the numerical solution of the full problem

We now consider the initial equation $-\nabla \cdot (\alpha \nabla u) - u = 0$ from (3.1.1). For this problem, we do not know any analytical solution. In the matrix A (3.5.5), only the blocks A_1 and A_2 are modified by adding block diagonal terms corresponding to the discretization of $\int_{\Omega_j} u_j^N \overline{v_j^N}$. The results are displayed in Fig. 3.4 and can be compared to the results of figures 3.2 and 3.3. We observe that the logarithmic singularity seems to be present in both illustrations in Fig. 3.4.

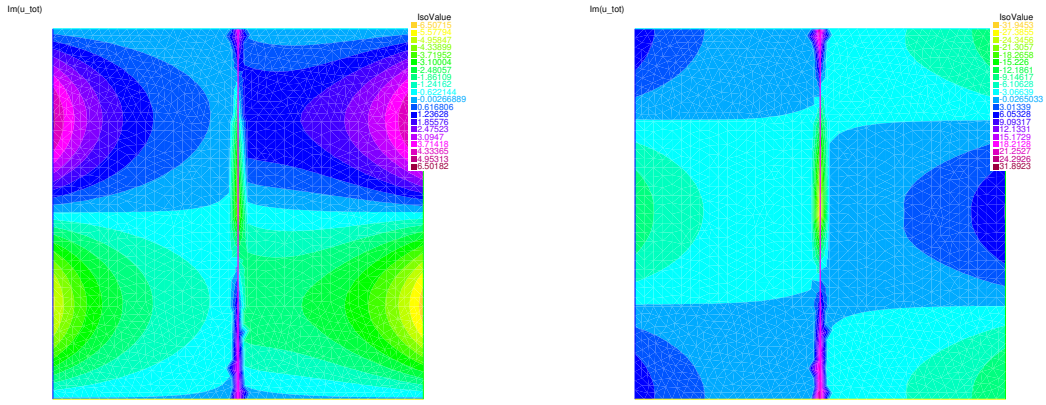

Figure 3.4 – Imaginary parts of the numerical solutions to the complete variational formulation (3.4.9) with BC f^3 (left) and f^4 (right).

Comments on the value of the penalization parameters

The numerical illutrations presented above have been obtained with small non-zero values for the penalization parameters (3.4.8). Non-zero values of the penalization parameters are compatible with the theory presented in this work. Arbitrarily, we used the values $\rho = 10^{-2}$ and $\mu = 10^{-4}$. However, other simulations taking these parameters equal to 0 lead to results with similar accuracy.

4 More numerical results

In this Chapter are gathered two classical results about error estimates from the book of Boffi, Brezzi and Fortin [13] applied to the discretization of complex mixed variational formulations of type

$$\begin{array}{l}\text{Find } \big(U,\boldsymbol{\lambda}\big)\in\mathcal{V}\times\mathcal{Q} \text{ such that}\\ \left\{\begin{array}{lcll} a\big(U,W\big)-\overline{b\big(W,\boldsymbol{\lambda}\big)} &=& k(V), & \forall W\in\mathcal{V},\\ b\big(U,\boldsymbol{\mu}\big) &=& \ell(\boldsymbol{\mu}), & \forall\boldsymbol{\mu}\in\mathcal{Q},\end{array}\right.\end{array} \tag{4.0.1}$$

along with illustrations by the 1D mode coupling case or by the 2D X-mode case. A Python code was fully developed for the 1D simulations, and the FreeFem software was used in 2D.

In what follows, we assume that $\mathcal{V}$ and $\mathcal{Q}$ are two Hilbert spaces, that a and b are two sesquilinear forms defined on $\mathcal{V}\times\mathcal{V}$ and $\mathcal{V}\times\mathcal{Q}$ respectively, and we set

$$\mathcal{K}:=\{W\in\mathcal{V},\, b(W,\boldsymbol{\mu})=0\,\forall\boldsymbol{\mu}\in\mathcal{Q}\}.$$

4.1 Discretization of mixed variational formulations

The structure of (4.0.1) encompasses the two mixed formulations derived for $\nu=0^+$, (2.3.7) in 1D and (3.4.7) in 2D. In these cases, the Hilbert spaces are:

- in 1D: $\mathcal{V}=H^1(\Omega)\times H^1(\Omega)\times\mathbb{C}$ and $\mathcal{Q}=\{\boldsymbol{\mu}\in H^1(\Omega)\times H^1(\Omega),\,\mathsf{N}(0)\boldsymbol{\mu}(0)=0\}$,
- in 2D: $\mathcal{V}=H^1_{1/2}(\Omega_1)\times H^1_{1/2}(\Omega_2)\times H^2(\Sigma)\times H^2(\Sigma)$ and $\mathcal{Q}=H^1_{1/2}(\Omega_1)\times H^1_{1/2}(\Omega_2)$.

The following theorem gives error bounds between the exact solution and its approximation by a solution in the finite dimensional subspace $\mathcal{V}_\mathsf{h}\times\mathcal{Q}_\mathsf{h}\subset\mathcal{V}\times\mathcal{Q}$ under the condition that both the problem in $\mathcal{V}\times\mathcal{Q}$ and the problem in $\mathcal{V}_\mathsf{h}\times\mathcal{Q}_\mathsf{h}$ are well-posed. Before stating the result, we define the operator $B_\mathsf{h}:\mathcal{V}_\mathsf{h}\to\mathcal{Q}'_\mathsf{h}$ such that for all $(V_\mathsf{h},\boldsymbol{\mu}_\mathsf{h})\in\mathcal{V}_\mathsf{h}\times\mathcal{Q}_\mathsf{h}$, one has $(B_\mathsf{h}W_\mathsf{h},\boldsymbol{\mu}_\mathsf{h})_{\mathcal{Q}'_\mathsf{h},\mathcal{Q}_\mathsf{h}}=b(W_\mathsf{h},\boldsymbol{\mu}_\mathsf{h})$.

Theorem 4.1.1 (From Theorem 5.2.5 in Boffi-Brezzi-Fortin [13]). *Let $\big(U,\boldsymbol{\lambda}\big)\in\mathcal{V}\times\mathcal{Q}$ and $\big(U_\mathsf{h},\boldsymbol{\lambda}_\mathsf{h}\big)\in\mathcal{V}_\mathsf{h}\times\mathcal{Q}_\mathsf{h}$ be respectively solutions of problems* (4.0.1) *and*

$$\begin{array}{l}\textit{Find } \big(U_\mathsf{h},\boldsymbol{\lambda}_\mathsf{h}\big)\in\mathcal{V}_\mathsf{h}\times\mathcal{Q}_\mathsf{h} \textit{ such that}\\ \left\{\begin{array}{lcll} a\big(U_\mathsf{h},W_\mathsf{h}\big)-\overline{b\big(W_\mathsf{h},\boldsymbol{\lambda}_\mathsf{h}\big)} &=& k(W_\mathsf{h}), & \forall W_\mathsf{h}\in\mathcal{V}_\mathsf{h},\\ b\big(U_\mathsf{h},\boldsymbol{\mu}_\mathsf{h}\big) &=& \ell(\boldsymbol{\mu}_\mathsf{h}), & \forall\boldsymbol{\mu}_\mathsf{h}\in\mathcal{Q}_\mathsf{h}.\end{array}\right.\end{array} \tag{4.1.1}$$

Assume that the $\inf - \sup$ *condition*

$$\inf_{\boldsymbol{\mu}_\mathsf{h} \in \mathcal{Q}_\mathsf{h}} \sup_{W_\mathsf{h} \in \mathcal{V}_\mathsf{h}} \frac{|b\left(W_\mathsf{h}, \boldsymbol{\mu}_\mathsf{h}\right)|}{\|W_\mathsf{h}\|_\mathcal{V} \|\boldsymbol{\mu}_\mathsf{h}\|_\mathcal{Q}} = \beta > 0$$

is satisfied and let $a(.,.)$ *be uniformly coercive on* $\mathcal{K}_\mathsf{h} := \ker B_\mathsf{h}$*, that is, there exists* $\alpha_0 > 0$ *such that*

$$\mathrm{Re}\left(a\left(W_{0,\mathsf{h}}, W_{0,\mathsf{h}}\right)\right) \geq \alpha_0 \|W_{0,\mathsf{h}}\|^2_{\mathcal{V}_\mathsf{h}} \quad \forall W_{0,\mathsf{h}} \in \mathcal{K}_\mathsf{h}.$$

Then, one has the following estimate, with a constant C *depending on* a *and* b *but independent of* h*:*

$$\|U - U_\mathsf{h}\|_\mathcal{V} + \|\boldsymbol{\lambda} - \boldsymbol{\lambda}_\mathsf{h}\|_\mathcal{Q} \leq C \left(\inf_{W_\mathsf{h} \in \mathcal{V}_\mathsf{h}} \|U - W_\mathsf{h}\|_\mathcal{V} + \sup_{\boldsymbol{\mu}_\mathsf{h} \in \mathcal{Q}_\mathsf{h}} \|\boldsymbol{\lambda} - \boldsymbol{\mu}_\mathsf{h}\|_\mathcal{Q} \right).$$

Moreover, when we have the inclusion of kernels $\mathcal{K}_\mathsf{h} \subset \mathcal{K}$*, we have the better estimate*

$$\|U - U_\mathsf{h}\|_\mathcal{V} \leq C \inf_{W_\mathsf{h} \in \mathcal{V}_\mathsf{h}} \|U - W_\mathsf{h}\|_\mathcal{V}.$$

In the three following subsections, we present the discretizations performed for the numerical simulations of the mixed formulations (2.3.7) and (3.4.7) as well as the numerical simulations of the mixed formulation in 1D for $\nu > 0$ (2.3.19), that does not exactly fit the frame presented above.

4.1.1 Discrete problem in 1D for $\nu = 0^+$

For the 1D problem of Chapter 2, the finite dimensional Hilbert spaces considered are

$$\begin{aligned}
\mathcal{V}_\mathsf{h} &= \mathbb{P}_1(\Omega^\mathsf{h}) \times \mathbb{P}_1(\Omega^\mathsf{h}) \times \mathbb{C}, \\
\mathcal{Q}_\mathsf{h} &= \left\{ \boldsymbol{\mu} \in \mathbb{P}_1(\Omega^\mathsf{h}) \times \mathbb{P}_1(\Omega^\mathsf{h}),\, \boldsymbol{\mu}(0) \in \mathrm{span}_\mathbb{C} \begin{pmatrix} k_z \\ -\delta(0) \end{pmatrix} \right\}.
\end{aligned}$$

Here $\mathbb{P}_1(\Omega^\mathsf{h})$ is the 1^{st} order Lagrange finite element space on the 1D mesh

$$\Omega^\mathsf{h} = \bigcup_{i=0}^{N-1} \left(x_{-\frac{N}{2}+i}, x_{-\frac{N}{2}+i+1} \right), \tag{4.1.2}$$

where $x_i = i\mathsf{h}$, $\mathsf{h}N = 2$ and N is even so that $x_0 = 0$ is a node.

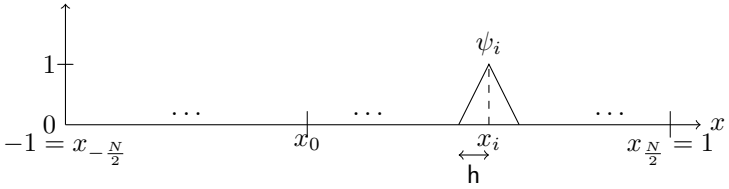

Figure 4.1 – Sketch of the mesh Ω^h and of a Lagrange $\mathbb{P}_1$ basis function ψ_i.

The space $\mathcal{Q}_\mathsf{h}$ is thus spanned by the basis composed of

$$\begin{cases} (0, \psi_i)^t & \forall i \neq 0, \\ (\psi_i, 0)^t & \forall i \neq 0, \\ (k_z, -\delta(0))^t \psi_0, & \end{cases} \tag{4.1.3}$$

where the ψ_i are the Lagrange $\mathbb{P}_1$ basis functions centered at x_i, as sketched in Fig. 4.1.

4.1.2 Discrete problem in 2D for $\nu = 0^+$

For the 2D problem of Chapter 3, we used

$$\mathcal{V}_\mathsf{h} = \mathbb{P}_1(\Omega_1^\mathsf{h}) \times \mathbb{P}_1(\Omega_2^\mathsf{h}) \times \mathrm{HCT}(\Sigma_{\mathrm{virt}}^\mathsf{h}) \times \mathrm{HCT}(\Sigma_{\mathrm{virt}}^\mathsf{h}),$$
$$\mathcal{Q}_\mathsf{h} = \mathbb{P}_1(\Omega_1^\mathsf{h}) \times \mathbb{P}_1(\Omega_2^\mathsf{h}),$$

with Lagrange $\mathbb{P}_1$ finite elements on 2D triangular meshes Ω_j^h of Ω_j, $j = 1, 2$, and with Hsiegh-Clough-Tocher (HCT) finite elements on a virtual 2D mesh for Σ, as explained in Subsection 3.5.2. The HCT elements are globally $\mathcal{C}^1$, and $\mathbb{P}_3$ by parts [27, 10].

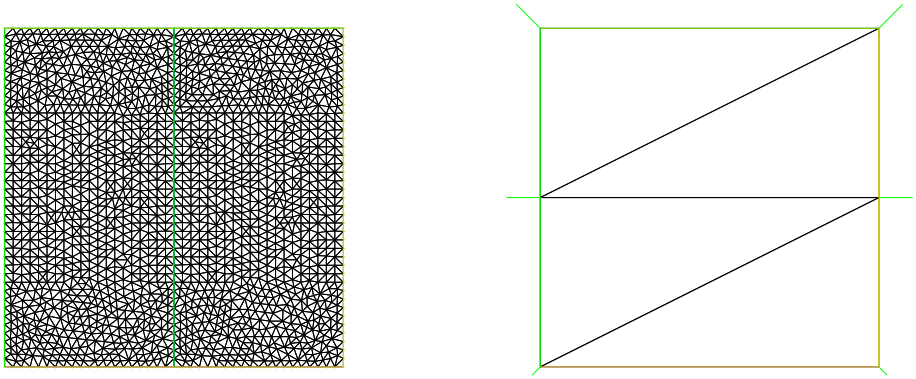

Figure 4.2 – Meshes of Ω_1^h and Ω_2^h (left) and of $\Sigma_{\mathrm{virt}}^\mathsf{h}$ (right) for $\mathsf{h} =$.

This non standard discretization choice was prescribed by the avaiblable features of the FreeFem software. 1D elements are not available, so that we chose to extend the line Σ in a virtual Σ_{virt}, and to penalize the unknowns in the transverse direction to Σ. Furthermore, because of the terms in a^+ consisting in integrals on Ω_j mixing unknowns on Σ and on Ω_j, it was necessary to take $\Sigma_{\mathrm{virt}} = \Omega$. See Figure 4.2 for the meshes of both Ω_j and of Σ_{virt} for a given h. Finally, since these unknowns must be $\mathcal{C}^1$, the only finite element space on hand with such regularity was the HCT. We discretized a toy geometry with exact solution, to have numerical evidence that the new formulation at $\nu = 0^+$ could catch the singular solution.

4.1.3 Discrete problem in 1D for $\nu > 0$

The $\nu > 0$ mixed formulation in 1D (2.3.19) is slightly different since its structure is

$$\left\{ \begin{array}{lcll} a\big(U, W\big) - \overline{b^{-\nu}\big(W, \boldsymbol{\lambda}\big)} & = & k(W), & \forall W \in \mathcal{V}, \\ b^\nu\big(U, \boldsymbol{\mu}\big) & = & \ell(\boldsymbol{\mu}), & \forall \boldsymbol{\mu} \in \mathcal{Q}. \end{array} \right.$$

By definition of b^ν with respect to ν, see (2.3.14), this problem is not equivalent to (4.0.1). Yet it is still a variational formulation and we carry on a straightforward finite element discretization. The Hilbert spaces are here $\mathcal{V} = H^1(\Omega) \times H^1(\Omega) \times \mathbb{C}$, as in the 1D $\nu = 0^+$ case, and $\mathcal{Q} = \{\boldsymbol{\mu} \in H^1(\Omega) \times H^1(\Omega),\ \Gamma^\nu(\boldsymbol{\mu}) = 0\}$. Once again, we used Ω^h as defined in (4.1.2). The finite dimensional spaces are

$$\mathcal{V}_\mathsf{h} = \mathbb{P}_1(\Omega^\mathsf{h}) \times \mathbb{P}_1(\Omega^\mathsf{h}) \times \mathbb{C},$$
$$\mathcal{Q}_\mathsf{h} = \left\{\boldsymbol{\mu} \in \mathbb{P}_1(\Omega^\mathsf{h}) \times \mathbb{P}_1(\Omega^\mathsf{h}),\ \Gamma^\nu(\boldsymbol{\mu}) = 0\right\}.$$

We restate the definition (2.3.17) of Γ^ν

$$\Gamma^\nu(\boldsymbol{\mu}) = \nu \int_\Omega \big(\frac{1}{\alpha^2+\nu^2}\boldsymbol{\mu}\cdot\begin{pmatrix}\delta^2 & \delta k_z\\ \delta k_z & k_z^2\end{pmatrix}\overline{\mathbf{w}_1^\nu} + \boldsymbol{\mu}\cdot\begin{pmatrix}1 & 0\\ 0 & 0\end{pmatrix}\overline{\mathbf{w}_1^\nu}\big)dx.$$

It yields that $\Gamma^\nu(\boldsymbol{\mu}) = 0$ is a non-local relation. This non-locality is treated by taking as basis functions for the space $\mathcal{Q}_\mathsf{h}$ linear combinations of ψ_i and ψ_0. The basis for $\mathcal{Q}_\mathsf{h}$ is composed of

$$\begin{cases} (0, \Lambda_0\psi_i - \Lambda_i\psi_0)^t & \forall i \neq 0,\\ (\Delta_0\psi_i - \Delta_i\psi_0, 0)^t & \forall i \neq 0,\\ (-k_z\Lambda_0, \Delta_0)^t\psi_0, & \end{cases} \tag{4.1.4}$$

for the coefficients defined for $0 \leq |i| \leq N/2$ by

$$\Lambda_i := \int_\Omega \frac{\nu}{\alpha^2(x)+\nu^2}\psi_i(x)\overline{\big(k_z C_z^\nu(x) + \delta F_y^\nu(x)\big)}\mathrm{d}x,$$
$$\Delta_i := \int_\Omega \left(\frac{\nu\delta(x)}{\alpha^2(x)+\nu^2}\psi_i(x)\overline{\big(k_z C_z^\nu(x) + \delta(x) F_y^\nu(x)\big)} + \nu\psi_i(x)\overline{F_y^\nu(x)}\right)\mathrm{d}x.$$

Remark 4.1.2. As $\nu \to 0^+$, both Λ_i and Δ_i go to zero for $i \neq 0$, and

$$\Lambda_0 \to -\frac{\pi}{|r|},$$
$$\Delta_0 \to -\frac{\pi\delta(0)}{|r|}.$$

Therefore, the basis (4.1.4) converges towards (4.1.3).

4.2 Numerical experiments in 1D

In this section we present a convergence table for the three formulations considered in Chapter 2: the classical formulation of the regularized equation (2.2.1) and the two new mixed formulations, (2.3.19) for $\nu > 0$ and (2.3.7) for $\nu = 0^+$. We recall and renumber these equations:

$$\begin{array}{l}\text{Find } \mathbf{u} \in H^1(\Omega)^2 \text{ such that}\\ b^\nu\big(\mathbf{u}, \mathbf{v}\big) = \ell^\nu(\mathbf{v}) \quad \forall \mathbf{v} \in H^1(\Omega)^2,\end{array} \tag{1}$$

$$\begin{array}{l}\text{Find } (\mathbf{u}, s) \in V \text{ and } \boldsymbol{\lambda} \in Q^\nu \text{ such that}\\ \left\{\begin{array}{lcll} a^\nu\big((\mathbf{u},s),(\mathbf{v},t)\big) - \overline{b^{-\nu}\big((\mathbf{v},t),\boldsymbol{\lambda}\big)} & = & 0, & \forall (\mathbf{v},t) \in V,\\ b^\nu\big((\mathbf{u},s),\boldsymbol{\mu}\big) & = & \ell^\nu(\boldsymbol{\mu}), & \forall \boldsymbol{\mu} \in Q^\nu,\end{array}\right.\end{array} \tag{2}$$

$$\begin{array}{l}\text{Find } \big((\mathbf{u}, s), \boldsymbol{\lambda}\big) \in V \times Q^+ \text{ such that}\\ \left\{\begin{array}{lcll} a^+\big((\mathbf{u},s),(\mathbf{v},t)\big) - \overline{b\big((\mathbf{v},t),\boldsymbol{\lambda}\big)} & = & 0, & \forall (\mathbf{v},t) \in V,\\ b\big((\mathbf{u},s),\boldsymbol{\mu}\big) & = & \ell(\boldsymbol{\mu}), & \forall \boldsymbol{\mu} \in Q^+.\end{array}\right.\end{array} \tag{3}$$

The convergence table corresponds to the Whittaker test case detailed in Subsection 2.4.1. In this configuration, the solution to the limit $\nu = 0^+$ resonant Maxwell's equations is known and we denote E_y^W the exact solution for the component E_y. Table 4.1 corresponds to the relative errors on the component E_y

$$\frac{\|E_y^\mathsf{h} - E_y^\mathrm{W}\|_{L^2(\Omega)}}{\|E_y^\mathrm{W}\|_{L^2(\Omega)}},$$

ν	Eq.	N=8	16	32	64	128	256	512	1024	2048	4096
10^{-1}	(1)	1.52e-01	1.19e-01	1.10e-01	1.07e-01	1.06e-01	1.06e-01	1.06e-01	1.06e-01	1.06e-01	1.06e-01
	(2)	2.15e-01	1.37e-01	1.14e-01	1.08e-01	1.07e-01	1.06e-01	1.06e-01	1.06e-01	1.06e-01	1.06e-01
10^{-3}	(1)	1.21e-01	6.18e-02	3.04e-02	1.46e-02	7.1e-03	3.5e-03	2.0e-03	1.4e-03	1.3e-03	1.2e-03
	(2)	3.98e-01	1.22e-01	3.77e-02	1.53e-02	7.2e-03	3.6e-03	2.0e-03	1.5e-03	1.3e-03	1.2e-03
10^{-5}	(1)	1.23e-01	6.39e-02	3.22e-02	1.61e-02	8.1e-03	4.0e-03	2.0e-03	1.0e-03	4.9e-04	2.3e-04
	(2)	4.06e-01	1.24e-01	3.83e-02	1.60e-02	7.9e-03	3.9e-03	2.0e-03	9.9e-04	4.9e-04	2.3e-04
10^{-7}	(1)	2.23e-01	1.03	1.02	1.02	1.02	4.0e-03	2.1e-03	1.0e-03	5.1e-04	2.5e-04
	(2)	2.23e-01	1.03	1.02	1.02	1.02	4.0e-03	2.1e-03	1.0e-03	5.1e-04	2.5e-04
10^{-9}	(1)	1.03	1.03	1.02	1.02	1.02	1.60e-02	2.10e-03	1.02	1.02	1.02
	(2)	5.22e-01	1.63	3.11	4.23	4.74	4.73	5.24	5.18	5.20	5.21
0^+	(3)	1.26e-01	6.25e-02	3.17e-02	1.60e-02	8.1e-03	4.0e-03	2.0e-03	1.0e-03	5.1e-04	2.5e-04

Table 4.1 – L^2 relative errors $\|E_y^{\mathsf{h}} - E_y^{\mathrm{W}}\|_{L^2(\Omega)}/\|E_y^{\mathrm{W}}\|_{L^2(\Omega)}$ between the computed solution E_y^{h} and the Whittaker solution for $\nu = 0^+$ E_y^{W}, $\mathsf{h}N = 2$.

where E_y^{h} is the solution of the finite element discretizations of the three systems above, see Subsections 4.1.1 and 4.1.3, for different values of N the number of cells ($\mathsf{h}N = 2$). For each N, the errors for systems (1) and (2) are given for different values of ν.

The Table 4.1 is a double entry table of convergence with respect to the mesh parameter in abscissa and to the viscosity parameter in ordinate for the discretizations of formulations (1) and (2). The last line corresponds to a viscosity $\nu = 0^+$, and to the convergence with respect to the mesh of the discretization of formulation (3). We observe that:

- down to $\nu = 10^{-7}$, both errors of the discretizations of (1) and (2) are the same,
- for $\nu = 10^{-5}$, the error of the discretizations of (1) and (2) converge at order 1,
- for $\nu = 10^{-7}$, the errors of the discretizations of (1) and (2) are unacceptable for the meshes ranging from 16 to 128 nodes,
- for $\nu = 10^{-9}$, the errors of the discretizations of (1) and (2) are unacceptable,
- for $\nu = 0^+$, the error of the discretization of the limit formulation (3) converges at order 1.

These tests justify the utility of the limit formulation (3) in the regime of small viscosity.

4.3 Relaxation of the regularization in 2D

In this Section, we present some results that suggest that the regularization of the mixed formulation (3.4.7) in Chapter 3 is unnecessary. Recall the mixed formulation in 2D

$$\begin{array}{l}\text{Find } (\mathbf{u},g,h)\in V \text{ and } \boldsymbol{\lambda}\in Q \text{ such that}\\ \left\{\begin{array}{lcrcll} a^+\left((\mathbf{u},g,h),(\mathbf{v},k,l)\right) & - & \overline{b^+\left((\mathbf{v},k,l),\boldsymbol{\lambda}\right)} & = & 0, & \forall(\mathbf{v},k,l)\in V,\\ b^+\left((\mathbf{u},g,h),\boldsymbol{\mu}\right) & & & = & \ell(\boldsymbol{\mu}), & \forall\boldsymbol{\mu}\in Q. \end{array}\right. \end{array} \tag{4.3.1}$$

The form a^+ is continuous in norm $\|.\|_V$ (3.4.3), and it is T-coercive, see Definition 3.1.3, in a weaker norm with respect to the unknowns $g, h \in H^2(\Sigma)$, see Proposition 3.4.10. The addition of terms proportional to the H^2 scalar product of g and k via a parameter $\rho > 0$ and to the H^2 scalar product of h and l via a parameter $\mu > 0$ regularizes the problem in the sense it yields well-posedness. The regularized form a_r^+ reads

$$a_r^+\left((\mathbf{u},g,h),(\mathbf{v},k,l)\right) = a^+\left((\mathbf{u},g,h),(\mathbf{v},k,l)\right) + i\left(-\rho\,(g,k)_{H^2(\Sigma)} + \mu\,(h'',l'')_{L^2(\Sigma)}\right), \tag{4.3.2}$$

and the formulation is proved to be well posed in Theorem 3.4.3 for any $\lambda > 0$, $f \in L^2(\Gamma)$, and $\rho, \mu > 0$, is

$$\begin{array}{l}\text{Find } (\mathbf{u}, g, h) \in V \text{ and } \boldsymbol{\lambda} \in Q \text{ such that} \\ \left\{ \begin{array}{lcll} a_r^+\left((\mathbf{u}, g, h), (\mathbf{v}, k, l)\right) & - & \overline{b^+\left((\mathbf{v}, k, l), \boldsymbol{\lambda}\right)} & = 0, \qquad \forall (\mathbf{v}, k, l) \in V, \\ b^+\left((\mathbf{u}, g, h), \boldsymbol{\mu}\right) & & & = \ell(\boldsymbol{\mu}), \qquad \forall \boldsymbol{\mu} \in Q. \end{array} \right. \end{array} \tag{4.3.3}$$

Yet the parameters ρ, μ of the regularization can be taken infinitely small for the theory, and we observe that with small or without regularization the numerical results are the same.

In the litterature, there exists error bounds for problems that are elliptic in a weaker norm than the continuity norm. Let $\|.\|_{\mathcal{V}^*}$ be a norm on $\mathcal{V}$ such that $\|W\|_{\mathcal{V}^*} \leq \|W\|_{\mathcal{V}}$ for all W in $\mathcal{V}$. The weak ellipticity assumption on a form a consists in the two following hypotheses

$$\exists c_1 > 0 \text{ s.t. } \mathrm{Re}\left((a(W, W)\right) \geq c_1 \|W\|_{\mathcal{V}^*}^2 \qquad \forall W \in \mathcal{K}_\mathsf{h}, \tag{4.3.4}$$

$$\exists c_2 \text{ s.t. } |a(U, W)| \leq c_2 \|U\|_{\mathcal{V}^*} \|W\|_{\mathcal{V}^*} \qquad \forall U, W \in \mathcal{V}. \tag{4.3.5}$$

The typical example for a weak norm is the L^2 norm on H^1.

Theorem 4.3.1 (From Propositions 5.1.1 and 5.1.3 and Theorem 5.2.6 in Boffi-Brezzi-Fortin [13])**.** *Assume that the* $\inf - \sup$ *condition*

$$\inf_{\boldsymbol{\mu}_\mathsf{h} \in \mathcal{Q}_\mathsf{h}} \sup_{W_\mathsf{h} \in \mathcal{V}_\mathsf{h}} \frac{|b\left(W_\mathsf{h}, \boldsymbol{\mu}_\mathsf{h}\right)|}{\|W_\mathsf{h}\|_{\mathcal{V}^*} \|\boldsymbol{\mu}_\mathsf{h}\|_{\mathcal{Q}}} \geq \beta > 0$$

is satisfied, and that the bilinear form a satisfies (4.3.4) *and* (4.3.5)*. Let $k \in \mathcal{V}'$ and $\ell \in \mathcal{Q}'$. Assume that the continuous problem* (4.0.1) *has a solution $(U, \boldsymbol{\lambda})$ and let $(U_\mathsf{h}, \boldsymbol{\lambda}_\mathsf{h})$ be the solution of the discretized problem* (4.1.1)*. Assume that there exists a linear operator $\Pi_\mathsf{h} : \mathcal{V} \to \mathcal{V}_\mathsf{h}$ such that $b(U - \Pi_\mathsf{h} W, \boldsymbol{\mu}_\mathsf{h}) = 0$ for all $W \in \mathcal{V}$ and $\boldsymbol{\mu}_\mathsf{h} \in \mathcal{Q}_\mathsf{h}$. Then, we have the estimates*

$$\|U - U_\mathsf{h}\|_{\mathcal{V}^*} + \|\boldsymbol{\lambda} - \boldsymbol{\lambda}_\mathsf{h}\|_{\mathcal{Q}} \leq C\Big(\inf_{W_\mathsf{h} \in \mathcal{V}_\mathsf{h}} \|U - W_\mathsf{h}\|_{\mathcal{V}^*} + \inf_{\boldsymbol{\mu}_\mathsf{h} \in \mathcal{Q}_\mathsf{h}} \|\boldsymbol{\lambda} - \boldsymbol{\mu}_\mathsf{h}\|_{\mathcal{Q}}\Big).$$

If, moreover, $\mathcal{K}_\mathsf{h} \subset \mathcal{K}$, then we also have

$$\|U - U_\mathsf{h}\|_{\mathcal{V}^*} \leq C \inf_{W_\mathsf{h} \in \mathcal{V}_\mathsf{h}} \|U - W_\mathsf{h}\|_{\mathcal{V}^*}.$$

In (4.3.1), a^+ is T-coercive in norm $\|.\|_* : g \mapsto (\sum_j \|u_j(g) - w_g^+\|_{L^2(\Gamma)}^2)^{1/2}$ with respect to g and in L^2 norm with respect to h, see Proposition 3.4.10. We now present a computation that gives the equivalence of this norm $\|.\|_*$ with the L^2 norm under the constraint that $(\mathbf{u}(g), g, 0)$ is in the kernel of the operator $A_{KK'}^+$ (3.4.10).

Proposition 4.3.2. *For all $g \in H^2(\Sigma)$, if $(\mathbf{u}(g), g, 0) \in \ker A_{KK'}^+$, then*

$$\lambda \|u_j(g) - w_g^+\|_{L^2(\Gamma)}^2 = \pi \|g\|_{L_w^2(\Sigma)}^2.$$

Proof. Let $g \in H^2(\Sigma)$. For $\epsilon > 0$, let ψ_ϵ be the cutoff function defined in the proof of Lemma 3.4.9 that removes a neighbourhood of size ϵ around Σ. One has $(\mathbf{u}(g), g, 0) \in K$, so that noting $\mathbf{u}(g) = (u_1, u_2)$,

$$\sum_{j=1,2} \left(\int_{\Omega_j} \left(\alpha \nabla(u_j - w_g^+) \cdot \nabla\overline{\left(\psi_\epsilon (u_j - w_g^+)\right)} - |u_j - w_g^+|^2 \psi_\epsilon \right) \mathrm{d}\mathbf{x} + \int_{\Gamma_j} i\lambda |u_j - w_g^+|^2 \mathrm{d}s \right) = 0,$$

and

$$\mathrm{Im}\sum_{j=1,2}\int_{\Omega_j}\alpha\nabla\overline{(u_j-w_g^+)}\cdot\nabla\left(\psi_\epsilon(u_j-w_g^+)\right)\mathrm{d}\mathbf{x}=\lambda\sum_{j=1,2}\|u_j-w_g^+\|^2_{L^2(\Gamma_j)}.$$

The left hand term can be expanded as

$$\begin{aligned}&\mathrm{Im}\sum_{j=1,2}\int_{\Omega_j}\alpha\nabla\overline{(u_j-w_g^+)}\cdot\nabla\left(\psi_\epsilon(u_j-w_g^+)\right)\mathrm{d}\mathbf{x}\\=&\,\mathrm{Im}\sum_{j=1,2}\int_{\Omega_j}\Big(\alpha\nabla\overline{u_j}\cdot\nabla\psi_\epsilon u_j-\alpha\nabla\overline{u_j}\cdot\nabla(\psi_\epsilon w_g^+)-\alpha\nabla\overline{w_g^+}\cdot\nabla(\psi_\epsilon u_j)+\alpha\nabla\overline{w_g^+}\cdot\nabla\psi_\epsilon w_g^+\Big)\mathrm{d}\mathbf{x}.\end{aligned}$$

We compute in a first instance the limit as ϵ goes to 0 of $\int\alpha\nabla\overline{u_j}\cdot\nabla\psi_\epsilon u_j$. Noticing that $1-\psi_\epsilon=\varphi_\epsilon\in\mathcal{C}^1_{0,+}(\Omega)$, it yields

$$\begin{aligned}\mathrm{Im}\sum_{j=1,2}\int_{\Omega_j}\alpha\nabla\overline{u_j}\cdot\nabla\psi_\epsilon u_j\mathrm{d}\mathbf{x}&=-\mathrm{Im}\sum_{j=1,2}\int_{\Omega_j}\alpha\nabla\overline{u_j}\cdot\nabla\varphi_\epsilon u_j\mathrm{d}\mathbf{x}\\&=-\mathrm{Im}\sum_{j=1,2}\int_{\Omega_j}\alpha\nabla\overline{u_j}\cdot\nabla(\varphi_\epsilon u_j)\mathrm{d}\mathbf{x}\\&=-\mathrm{Im}\sum_{j=1,2}\int_{\Omega_j}\overline{(u_j-q_g^+)}\varphi_\epsilon u_j\mathrm{d}\mathbf{x}\underset{\epsilon\to0}{\to}0.\end{aligned}$$

Secondly, the integral $\int\alpha\nabla\overline{w_g^+}\cdot\nabla\psi_\epsilon w_g^+$ has already been studied in the proof of Lemma 3.4.9 and

$$\mathrm{Im}\sum_{j=1,2}\int_{\Omega_j}\alpha\nabla\overline{w_g^+}\cdot\nabla\psi_\epsilon w_g^+\mathrm{d}\mathbf{x}\underset{\epsilon\to0}{\to}-\pi\|g\|^2_{L^2_w(\Sigma)}.$$

Lastly, the remaining terms are gathered in

$$A_\epsilon:=\mathrm{Im}\sum_{j=1,2}\int_{\Omega_j}\Big(\alpha\nabla\overline{u_j}\cdot\nabla(\psi_\epsilon w_g^+)+\alpha\nabla\overline{w_g^+}\cdot\nabla(\psi_\epsilon u_j)\Big)\mathrm{d}\mathbf{x},$$

and it follows

$$\lambda\sum_{j=1,2}\|u_j-w_g^+\|^2_{L^2(\Gamma_j)}+\pi\|g\|^2_{L^2_w(\Sigma)}+\lim_{\epsilon\to0}A_\epsilon=0.\tag{4.3.6}$$

It remains to compute the limit value of A_ϵ. Under the hypothesis that $(\mathbf{u}(g),g,0)\in\ker A^+_{KK'}$, taking as a test function $(\mathbf{v},k,l)=(0,0,g)$ and keeping in mind that a^+ is independent of the cutoff function as proved in Proposition 3.4.8, one has

$$\begin{aligned}0=&\,\mathrm{Im}\,a^+\left((\mathbf{u}(g),g,0),(0,0,g)\right)\\=&\,\mathrm{Im}\sum_{j=1,2}\int_{\Omega_j}\Big(\alpha(u_j-w_g^+)\nabla\overline{w_g^+}\cdot\nabla\varphi_\epsilon-\alpha\overline{w_g^+}\nabla(u_j-w_g^+)\cdot\nabla\varphi_\epsilon\\&\qquad-\overline{q_g^+}(u_j-w_g^+)\varphi_\epsilon\Big)\mathrm{d}\mathbf{x}\end{aligned}$$

Since q_g^+ and $u_j - w_g^+$ are in $L^2(\Omega_j)$ and that $\varphi_\epsilon \to 0$ with ϵ in $L^2(\Omega)$, it implies

$$\begin{aligned}
0 &= \lim_{\epsilon\to 0} \operatorname{Im} \sum_{j=1,2} \int_{\Omega_j} \left(\alpha(u_j - w_g^+)\nabla\overline{w_g^+} \cdot \nabla\varphi_\epsilon - \alpha\overline{w_g^+}\nabla(u_j - w_g^+) \cdot \nabla\varphi_\epsilon \right) \mathrm{d}\mathbf{x} \\
&= -\lim_{\epsilon\to 0} \operatorname{Im} \sum_{j=1,2} \int_{\Omega_j} \left(\alpha(u_j - w_g^+)\nabla\overline{w_g^+} \cdot \nabla\psi_\epsilon - \alpha\overline{w_g^+}\nabla(u_j - w_g^+) \cdot \nabla\psi_\epsilon \right) \mathrm{d}\mathbf{x} \\
&= -\lim_{\epsilon\to 0} \operatorname{Im} \sum_{j=1,2} \int_{\Omega_j} \Big(\Big(\alpha u_j \nabla\overline{w_g^+} \cdot \nabla\psi_\epsilon - \alpha\overline{w_g^+}\nabla u_j \cdot \nabla\psi_\epsilon \Big) \\
&\qquad\qquad + \Big(\alpha w_g^+ \nabla\overline{w_g^+} \cdot \nabla\psi_\epsilon - \alpha\overline{w_g^+}\nabla w_g^+ \cdot \nabla\psi_\epsilon \Big) \Big) \mathrm{d}\mathbf{x} \\
&= -\lim_{\epsilon\to 0} \left(A_\epsilon + 2\operatorname{Im} \sum_{j=1,2} \int_{\Omega_j} \alpha w_g^+ \nabla\overline{w_g^+} \cdot \nabla\psi_\epsilon \mathrm{d}\mathbf{x} \right) \\
&= -\lim_{\epsilon\to 0} A_\epsilon + 2\pi \|g\|^2_{L^2_w(\Sigma)}.
\end{aligned}$$

Substituting $\lim A_\epsilon$ by its value, using (4.3.6), the result is proven. □

These preliminary results seem to point the well-posedness of the discretized problem without regularization. However, the analysis of the problem must be completed to obtain a convenient well-posedness proof. In addition, using other tools and studying the limit as $\rho, \mu \to 0$ of problem (4.3.3) might also lead to a proof of well-posedness for the continuous problem (4.3.1).

5 An advanced model

In this chapter, we adapt the construction method of manufactured solutions to a plasma model with thermal effects [110, 41]. In this model, the viscosity is not a linear contribution as for the cold plasma model: thermal effects add a differential term of order 2.

5.1 The warm plasma model

A simple way to add thermal corrections to the cold plasma model is to add an isotropic pressure, and consider the tensor $\underline{\underline{p}} = pI$ in (1.2.3). The Euler equations with Lorentz force, friction and pressure we consider are

$$\left\{ \begin{array}{rcl} m_e N_e(-i\omega \mathbf{u}_e + \mathbf{u}_e \cdot \nabla \mathbf{u}_e) & = & -q_e N_e(\mathbf{E} + \mathbf{u}_e \wedge \mathbf{B}) - m_e N_e \nu \mathbf{u}_e - \nabla p, \\ -i\omega N_e + \nabla \cdot (N_e \mathbf{u}_e) & = & 0. \end{array} \right. \tag{5.1.1}$$

We assume that p obeys to the isothermal equation of state

$$p(\mathbf{x}) = N_e(\mathbf{x}) k_B T_{\text{ref}}. \tag{5.1.2}$$

We define the thermal speed of electrons $v_{\text{th}} = \sqrt{\frac{k_B T_{\text{ref}}}{m_e}}$, and suppose that these thermal effects are small. Following the scheme of Fig. 1.3, as for the cold plasma model, this equation on the dynamics of electrons is then coupled to the Maxwell's equations on the electromagnetic field via a linear current

$$\left\{ \begin{array}{rcl} \nabla \wedge \mathbf{B} - \left(\frac{\omega}{c}\right)^2 \mathbf{E} & = & -i\omega \mu_0 q_e N_e \mathbf{u}_e, \\ \mathbf{B} - \nabla \wedge \mathbf{E} & = & 0. \end{array} \right. \tag{5.1.3}$$

Similarily to Section 1.2, we then study oscillations around a steady state. The steady state now consists of $\left(\widetilde{\mathbf{E}}, \widetilde{\mathbf{B}}, \widetilde{\mathbf{u}_e}, \widetilde{N_e}\right) = (0, \mathbf{B}_0, 0, N_{e,0})$, and the pressure reads at first order

$$p = p_0 + p_1 = N_{e,0} k_B T_{\text{ref}} + N_{e,1} k_B T_{\text{ref}}.$$

For simplicity of notation, we further design by $\mathbf{B}$, p and N_e the first order terms $\mathbf{B}_1$, p_1 and $N_{e,1}$. The electrons' dynamics (5.1.1) write at first order

$$\left\{ \begin{array}{rcl} -i\omega m_e N_{e,0} \mathbf{u}_e & = & -q_e N_{e,0}(\mathbf{E} + \mathbf{u}_e \wedge \mathbf{B}_0) - m_e N_{e,0} \nu \mathbf{u}_e - \nabla p, \\ -i\omega N_e + N_{e,0} \nabla \cdot \mathbf{u}_e & = & 0. \end{array} \right. \tag{5.1.4}$$

By definition of the isothermal pressure (5.1.2) and Gauss' law which states

$$\nabla \cdot \mathbf{E} = \frac{\rho}{\varepsilon_0} = \frac{-q_e N_e}{\varepsilon_0}, \tag{5.1.5}$$

system (5.1.4) allows to express $\mathbf{u}_e$ in function of the electric field $\mathbf{E}$ as

$$-i\omega m_e N_{e,0}\mathbf{u}_e = -q_e N_{e,0}(\mathbf{E} + \mathbf{u}_e \wedge \mathbf{B}^0) - m_e N_{e,0}\nu\mathbf{u}_e + \frac{\varepsilon_0 m_e}{q_e} v_{\text{th}}^2 \nabla \otimes \nabla \mathbf{E}. \tag{5.1.6}$$

Equation (5.1.6) only differs from the corresponding cold plasma approximation equation (1.2.5) by the last term, proportional to $\nabla \otimes \nabla \mathbf{E}$. Therefore, refering to the computations of Section 1.2, it leads to the dependency

$$\mathbf{u}_e = \begin{pmatrix} \frac{\tilde{\omega}}{\tilde{\omega}^2-\omega_c^2} & \frac{-i\omega_c}{\tilde{\omega}^2-\omega_c^2} & 0 \\ \frac{i\omega_c}{\tilde{\omega}^2-\omega_c^2} & \frac{\tilde{\omega}}{\tilde{\omega}^2-\omega_c^2} & 0 \\ 0 & 0 & \frac{1}{\tilde{\omega}} \end{pmatrix} \left(-i\frac{q_e}{m_e} + i\frac{\varepsilon_0}{q_e N_{e,0}} v_{\text{th}}^2 \nabla \otimes \nabla \right) \mathbf{E},$$

for $\tilde{\omega} = \omega + i\nu$. Introducing this quantity in (5.1.3), one has

$$\left\{ \begin{array}{rcl} \nabla \wedge \mathbf{B} - \left(\frac{\omega}{c}\right)^2 \begin{pmatrix} \frac{\tilde{\omega}\omega_p^2}{\tilde{\omega}(\tilde{\omega}^2-\omega_c^2)} & \frac{-i\omega_c\omega_p^2}{\tilde{\omega}(\tilde{\omega}^2-\omega_c^2)} & 0 \\ \frac{i\omega_c\omega_p^2}{\tilde{\omega}(\tilde{\omega}^2-\omega_c^2)} & \frac{\tilde{\omega}\omega_p^2}{\tilde{\omega}(\tilde{\omega}^2-\omega_c^2)} & 0 \\ 0 & 0 & \frac{\omega_p^2}{\tilde{\omega}^2} \end{pmatrix} \left(I - \frac{v_{\text{th}}^2}{\omega_p^2} \nabla \otimes \nabla \right) \mathbf{E} & = & 0, \\ \mathbf{B} - \nabla \wedge \mathbf{E} & = & 0. \end{array} \right.$$

After simplification, we focus on

$$\left\{ \begin{array}{rcl} \nabla \wedge \mathbf{B} - \left(\underline{\underline{\varepsilon}}^{\nu} + \nu^3 \tau \nabla \otimes \nabla \right) \mathbf{E} & = & 0, \\ \mathbf{B} - \nabla \wedge \mathbf{E} & = & 0, \end{array} \right. \tag{5.1.7}$$

where $\underline{\underline{\varepsilon}}^{\nu}$ is the tensor already defined in (1.3.10), and $\tau > 0$ is a constant related to the thermal effects.

The divergence of the Poynting vector is now

$$\begin{array}{rcl} \nabla \cdot \Pi(\mathbf{E}^{\nu}, \mathbf{B}^{\nu}) & = & \text{Im}\, \nabla \cdot \left(\mathbf{E}^{\nu} \wedge \overline{\mathbf{B}^{\nu}} \right) \\ & = & \text{Im}\left(\nabla \wedge \mathbf{E}^{\nu} \cdot \overline{\mathbf{B}^{\nu}} - \mathbf{E}^{\nu} \cdot \nabla \wedge \overline{\mathbf{B}^{\nu}} \right) \\ & = & \text{Im}\left(|\mathbf{B}^{\nu}|^2 - \mathbf{E}^{\nu} \cdot \overline{\left(\underline{\underline{\varepsilon}}^{\nu} + \nu^3 \tau \nabla \otimes \nabla \right) \mathbf{E}^{\nu}} \right) \\ & = & \nu |\mathbf{E}|^2 - \nu^3 \tau\, \text{Im}\left(\mathbf{E}^{\nu} \cdot \nabla \otimes \nabla \overline{\mathbf{E}^{\nu}} \right), \end{array} \tag{5.1.8}$$

and the heating for $\varphi \in \mathcal{C}^1_{0,+}(\Omega)$ is

$$\text{Im} \int_{\Omega} \left(\left(\mathbf{E}^{\nu} \wedge \overline{\mathbf{B}^{\nu}} \right) \cdot \nabla \varphi + \nu^3 \tau \left(\mathbf{E}^{\nu} \cdot \nabla \otimes \nabla \overline{\mathbf{E}^{\nu}} \right) \varphi \right) \mathrm{d}\mathbf{x} \geq 0.$$

In 1D X-mode, the regularized system writes

$$\left\{ \begin{array}{rcll} \left(-(\alpha + i\nu) + \nu^3 \tau \partial_x^2 \right) E_x^{\nu} - i\delta E_y^{\nu} & = & 0, & \text{in } \Omega = (-1, 1), \\ -\partial_x B_z + i\delta E_x^{\nu} - (\alpha + i\nu) E_y^{\nu} & = & 0, & \text{in } \Omega, \\ B_z^{\nu} - \partial_x E_y & = & 0, & \text{in } \Omega. \end{array} \right. \tag{5.1.9}$$

The new term which enriches the mathematical model (1.3.9) is the viscosity related term $\nu^2\tau\partial_x^2 E_x^\nu$. The heating is now

$$\mathrm{Im}\int_\Omega \left(E_y^\nu\overline{B_z^\nu} - \nu^3\tau E_x^\nu\overline{E_x^\nu}'\right)\varphi'\mathrm{d}x \geq 0.$$

At $\nu = 0$, the resulting system of equations is the same as for the cold plasma model.

5.2 Construction of manufactured solutions

The goal here is to show it is possible to construct a manufactured solution $\mathbf{F}^\nu = (F_x^\nu, F_y^\nu, 0)$, $\mathbf{C}^\nu = (0, 0, C_z^\nu)$ and $\mathbf{g}^\nu = (g_x^\nu, g_y^\nu, 0)$, $\mathbf{q}^\nu = (0, 0, q_z^\nu)$ for the system (5.1.9). This manufactured solution must verify the relations

$$\left\{\begin{array}{rcl} \big(-(\alpha+i\nu)+\nu^3\tau\partial_x^2\big)F_x^\nu - i\delta F_y^\nu &=& g_x^\nu, \\ -\partial_x C_z^\nu + i\delta F_x^\nu - (\alpha+i\nu)F_y^\nu &=& g_y^\nu, \\ C_z^\nu - \partial_x F_z^\nu &=& q_z^\nu, \end{array}\right. \tag{5.2.1}$$

and hypotheses (H1)-(H2) from Section 1.3. Formally, similar computations to (5.1.8) lead to

$$\begin{aligned} &\nabla\cdot\Pi(\mathbf{E}^\nu - \mathbf{F}^\nu, \mathbf{B}^\nu - \mathbf{C}^\nu) \\ &= \mathrm{Im}\Big(|\mathbf{B}^\nu - \mathbf{C}^\nu|^2 + \mathbf{q}^\nu\cdot\overline{(\mathbf{B}^\nu - \mathbf{C}^\nu)} \\ &\quad -(\mathbf{E}^\nu - \mathbf{F}^\nu)\cdot\overline{(\underline{\underline{\varepsilon}}^\nu + \nu^2\tau\nabla\otimes\nabla)(\mathbf{E}^\nu - \mathbf{F}^\nu)} + (\mathbf{E}^\nu - \mathbf{F}^\nu)\cdot\overline{\mathbf{g}^\nu}\Big) \\ &= \nu|\mathbf{E}^\nu - \mathbf{F}^\nu|^2 + \mathrm{Im}\Big(q^\nu\cdot\overline{(\mathbf{B}^\nu - \mathbf{C}^\nu)} + (\mathbf{E}^\nu - \mathbf{F}^\nu)\cdot\overline{\mathbf{g}^\nu}\Big) \\ &\quad - \nu^3\tau\,\mathrm{Im}\Big((\mathbf{E}^\nu - \mathbf{F}^\nu)\cdot\overline{\nabla\otimes\nabla(\mathbf{E}^\nu - \mathbf{F}^\nu)}\Big) \end{aligned}$$

and the dissipation associated to the Poynting vector for $\varphi \in \mathcal{C}^1_{0,+}(\Omega)$ is

$$\begin{aligned} \mathrm{Im}\int_\Omega &\Big((E_y^\nu - F_y^\nu)\overline{(B_z^\nu - C_z^\nu)} - \nu^3\tau(E_x^\nu - F_x^\nu)\overline{(E_x^\nu - F_x^\nu)}'\Big)\varphi' \\ &+ \Big(g_x^\nu\overline{(E_x^\nu - F_x^\nu)} + g_y^\nu\overline{(E_y^\nu - F_y^\nu)} - q_z^\nu\overline{(B_z^\nu - C_z^\nu)}\Big)\varphi\,dx \geq 0. \end{aligned}$$

The system at $\nu = 0$ is the same as the cold plasma model with no viscosity: the same kind of singularity is expected. Therefore, we combine the two $\nu \lesseqgtr 0$ solutions and define for $\nu > 0$

$$F_x^\nu := \frac{\mu_1}{\alpha+i\nu} + \frac{\mu_2}{\alpha-i\nu} \quad \text{for} \quad \mu_1, \mu_2 \in \mathbb{C}.$$

Set

$$F_y^\nu := \frac{-1}{i\delta}.$$

It follows from the first equation of (5.2.1) that

$$g_x^\nu = 1 - (\alpha+i\nu)\Big(\frac{\mu_1}{\alpha+i\nu} + \frac{\mu_2}{\alpha-i\nu}\Big) + \nu^3\tau\Big(\frac{-\mu_1\alpha''}{(\alpha+i\nu)^2} + \frac{2\mu_1(\alpha')^2}{(\alpha+i\nu)^3} + \frac{-\mu_2\alpha''}{(\alpha-i\nu)^2} + \frac{2\mu_2(\alpha')^2}{(\alpha-i\nu)^3}\Big). \tag{5.2.2}$$

For the product $F_x^\nu g_x^\nu$ to converge in $L^1(\Omega)$ towards the product of the limits $F_x^+ g_x^+$, and as F_x^+ is proportional to $1/x$, necessarily the limit of g_x^ν must vanish at 0. To begin with,

$$g_x^\nu(0) = 1 - (1 - 2i\tau r^2)(\mu_1 - \mu_2) + \nu\tau\alpha''(0)\big(\mu_1 + \mu_2\big),$$

so that if $\mu_1 - \mu_2 = (1 - 2i\tau r^2)^{-1}$, $g_x^\nu(0) \to 0$ as ν goes to 0. Recasting g_x^ν with respect to μ_2 and to the value of $\mu_1 - \mu_2$ yields

$$\begin{aligned} g_x^\nu(x) =& 1 - \frac{1 - 2(\alpha')^2\tau\frac{\nu^3}{(\alpha+i\nu)^3} + \alpha''\tau\frac{\nu^3}{(\alpha+i\nu)^2}}{1 - 2r^2\tau i} \\ & - \mu_2\left(2\frac{\alpha}{\alpha - i\nu} + 2(\alpha')^2\tau\frac{6\alpha\nu^5 - 2\alpha^3\nu^3}{(\alpha^2+\nu^2)^2} + 2\alpha''\tau\frac{\alpha^2\nu^3 - \nu^5}{(\alpha^2+\nu^2)^2}\right). \end{aligned}$$

As $\nu \to 0^+$ one has

$$g_x^+(x) = \begin{cases} 0 & x = 0, \\ 1 - \mu_1 - \mu_2 & x \neq 0. \end{cases}$$

We now present a computation of the integral of $F_x^\nu g_x^\nu \varphi$ over $(-1, 1)$.

Proposition 5.2.1. *For $\varphi \in \mathcal{C}^1_{0,+}(\Omega)$, one has*

$$\int_{-1}^{1} F_x^\nu(x) g_x^\nu(x)\varphi(x) \underset{\nu\to 0}{\to} \text{p.v.} \int_{-1}^{1} F_x^+(x) g_x^+(x)\varphi(x).$$

Proof. For simplicity, we prove the result under the assumption $\alpha(x) = rx$ instead of $rx + O(x^2)$. Let $\nu > 0$. The function $x \mapsto xF_x^\nu(x)$ is in $L^\infty(\Omega)$ uniformly in ν. Therefore, we consider the function

$$h(\nu, x) := \frac{g_x^\nu(x)}{x}.$$

According to the definition of g_x^ν (5.2.2), h is homogeneous of degree -1 as a function of two variables. Rewriting all the terms of function h with the same denominator, it gives

$$h(\nu, x) = \frac{P(\nu, x)}{(r^2x^2 + \nu^2)^3} \tag{5.2.3}$$

for a 5^{th} order polynomial $P(\nu, x) = a_5x^5 + a_4x^4\nu + a_3x^3\nu^2 + a_2x^2\nu^3 + a_1x\nu^4 + a_0\nu^5$. By homogenity, one has

$$\int_{-1}^{1} h(\nu, x)\, dx = \int_{-1}^{1} \frac{h(1, x/\nu)}{\nu}\, dx = \int_{-1/\nu}^{1/\nu} h(1, y)\, dy.$$

Using (5.2.3), one can eliminate the odd degree terms on x since

$$\begin{aligned} \int_{-1/\nu}^{1/\nu} h(1, x)\, dx &= \int_{-1/\nu}^{1/\nu} \frac{P(1, x)}{(r^2x^2 + 1)^3}\, dx \\ &= \int_{0}^{1/\nu} \frac{P(1, x) + P(1, -x)}{(r^2x^2 + 1)^3}\, dx. \end{aligned}$$

Consequently, $P(1, x) + P(1, -x)$ is at most of degree 4 on x, and as $\nu \to 0^+$ one has

$$\int_{-\infty}^{\infty} h(1, x)\, dx = 2\int_{0}^{\infty} \frac{a_4x^4 + a_2x^2 + a_0}{(r^2x^2 + 1)^3}\, dx = \int_{-\infty}^{\infty} \frac{a_4x^4 + a_2x^2 + a_0}{(r^2x^2 + 1)^3}\, dx.$$

Define the function such that for all $x \in \mathbb{C}$,

$$\ell(x) = \frac{a_4 x^4 + a_2 x^2 + a_0}{(r^2 x^2 + 1)^3}.$$

The residue theorem [101] ensures

$$\int_{-\infty}^{\infty} \frac{a_4 x^4 + a_2 x^2 + a_0}{(r^2 x^2 + 1)^3}\, dx = 2i\pi\, \mathsf{Res}\Big(\ell, \frac{i}{|r|}\Big).$$

Since $i/|r|$ is a triple pole, the following formula gives the residue of ℓ at this point

$$\begin{aligned}
\mathsf{Res}\Big(\ell, \frac{i}{|r|}\Big) &= \frac{1}{2} \lim_{z \to \frac{i}{|r|}} \frac{\partial^2}{\partial z^2} \Big(\big(z - \frac{i}{|r|}\big)^3 \ell(z) \Big) \\
&= \frac{1}{2} \lim_{z \to \frac{i}{|r|}} \frac{\partial^2}{\partial z^2} \Big(\frac{a_4 x^4 + a_2 x^2 + a_0}{r^6 \big(z + \frac{i}{|r|}\big)^3} \Big) \\
&= \frac{3a_0 + a_2 r^2 + 3a_4 r^4}{16 i r^6} |r|.
\end{aligned}$$

At last,

$$\lim_{\nu \to 0} \int_{-1}^{1} h(\nu, x) \mathrm{d}x = \frac{3a_0 + a_2 r^2 + 3a_4 r^4}{8 r^6} |r| \pi.$$

Since

$$\text{p.v.} \int_{-1}^{1} \frac{g_x^+(x)}{x} \mathrm{d}x = \lim_{\nu \to 0} \int_{-1}^{1} h(\nu, x) \mathrm{d}x,$$

the claim follows. □

II Domain decomposition methods for wave propagation

6 Introduction to domain decomposition methods for wave propagation

In the study of resonant Maxwell's equations from Part I, the equations were separated on two subdomains and a non-local transmission condition over their interface was derived. In this Part, we focus on domain decomposition methods for wave propagation, which are numerical methods for which an iteration consists in solving the problem independently in several subdomains and then exchanging information between the local solutions. The model problem is the propagation of time harmonic acoustic waves in the free space governed by the Helmholtz equation coupled to the Sommerfeld radiation condition

$$\left\{ \begin{array}{rcll} -\Delta u - \omega^2 u & = & f & \text{in } \mathbb{R}^2, \\ \nabla u(\mathbf{x}) \cdot \frac{\mathbf{x}}{\|\mathbf{x}\|} - \mathbf{i}\omega u(\mathbf{x}) & = & \underset{\|\mathbf{x}\|\to\infty}{o}\left(\|\mathbf{x}\|^{-1/2}\right), & \end{array} \right. \tag{6.0.1}$$

where $0 \neq \omega \in \mathbb{R}$ and f is of compact support. A computational domain Ω is defined as a bounded domain containing the support of the source f, and the free space behaviour is simulated by defining boundary conditions that approximate the radiation condition on $\Gamma = \partial\Omega$. Before presenting the new results in Chapter 7, we briefly recall the historical background of these methods and introduce the main tools used in the sequel.

6.1 Idea of the method

The original idea of domain decomposition was given by Schwarz in 1870 [104]. The figure illustrating the article is represented in Figure 6.1. The issue was to prove the existence of harmonic solutions

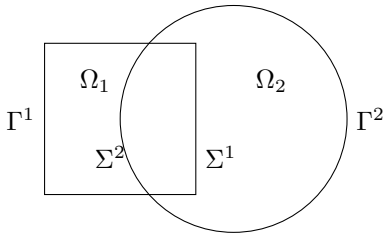

Figure 6.1 – Hybrid domain $\Omega = \Omega_1 \cup \Omega_2$ consisting in the union of a square and of an overlapping disc.

to the Laplace equation in Ω with Dirichlet boundary conditions on $\Gamma = \partial\Omega$

$$\left\{ \begin{array}{rcll} \Delta u & = & 0 & \text{in } \Omega, \\ u & = & g & \text{on } \Gamma. \end{array} \right. \tag{6.1.1}$$

Since on each subdomain Ω_i, with Dirichlet conditions on $\partial\Omega_i$, the solution was known, the suggestion was to solve alternatively the problem in Ω_1 and in Ω_2. Let $\Gamma^i = \partial\Omega_i \cap \Gamma$ be the exterior boundary and $\Sigma^i = \partial\Omega_i \backslash \Gamma$ be the interior boundary of Ω_i, for $i = 1, 2$. After initializing u^0 solution to

$$\left\{ \begin{array}{rcll} \Delta u^0 & = & 0 & \text{in } \Omega_2, \\ u^0 & = & g & \text{on } \Gamma^2, \\ u^0 & = & \inf\limits_{\Gamma} g & \text{on } \Sigma^2, \end{array} \right.$$

define the further iterations for $p = 0, 1, \ldots$ by

$$\left\{ \begin{array}{rcll} \Delta u^{2p+1} & = & 0 & \text{in } \Omega_1, \\ u^{2p+1} & = & g & \text{on } \Gamma^1, \\ u^{2p+1} & = & u^{2p} & \text{on } \Sigma^1, \end{array} \right. \quad \text{and then} \quad \left\{ \begin{array}{rcll} \Delta u^{2p+2} & = & 0 & \text{in } \Omega_2, \\ u^{2p+2} & = & g & \text{on } \Gamma^2, \\ u^{2p+2} & = & u^{2p+1} & \text{on } \Sigma^2. \end{array} \right.$$

This is called the alternating Schwarz algorithm. As explained in [53, 52], Schwarz proved using the maximum principle that the positive series

$$v := u^1 + \sum_{p \geq 1} (u^{2p+1} - u^{2p-1}),$$
$$w := u^2 + \sum_{p \geq 1} (u^{2p+2} - u^{2p}),$$

are dominated by convergent geometric series and hence well defined, and that they coincide on $\Omega_1 \cap \Omega_2$. The function such that $u := v$ in Ω_1 and $u := w$ in Ω_2 is in turn well defined, and is a harmonic solution to (6.1.1).

A second keystone was the study of the method brought up to date by Lions, published in a serie of three papers *On the Schwarz alternating method* from 1988 to 1990 [80, 81, 82]. We emphasize three improvements:

- the parallelization of Schwarz' algorithm,
- the adaptation of the algorithm to more than two subdomains,
- new transmission conditions for nonoverlapping subdomains

$$(\partial_{n_1} + \lambda_1) u_1^{p+1} = (-\partial_{n_2} + \lambda_1) u_2^{p+1} \quad \text{and} \quad (\partial_{n_2} + \lambda_2) u_2^{p+1} = (-\partial_{n_1} + \lambda_2) u_1^{p+1}$$

  with $0 \neq \lambda_i \in \mathbb{R}$ and a proof of convergence of the algorithm using energy estimates.

After initializing u_i^0 in Ω_i for $i = 1, 2$, the parallel Schwarz method on the example of the Laplace equation (6.1.1) is given for $p = 0, 1, \ldots$ by

$$\left\{ \begin{array}{rcll} \Delta u_1^{p+1} & = & 0 & \text{in } \Omega_1, \\ u_1^{p+1} & = & g & \text{on } \Gamma^1, \\ u_1^{p+1} & = & u_2^p & \text{on } \Sigma^1, \end{array} \right. \quad \text{and} \quad \left\{ \begin{array}{rcll} \Delta u_2^{p+1} & = & 0 & \text{in } \Omega_2, \\ u_2^{p+1} & = & g & \text{on } \Gamma^2, \\ u_2^{p+1} & = & u_1^p & \text{on } \Sigma^2. \end{array} \right.$$

Remark 6.1.1. The illustration is given here on a two subdomains decomposition for simplicity, but the interest of this parallel method lies in its use for more than two subdomains. Indeed, since $u_2^{p+1} = u_1^p$, the computed u_1^{p+2} in Ω_1 coincides with an alternating Schwarz iteration based on u_1^p in Ω_1.

In the case of solving numerically (6.0.1) in a domain Ω, a boundary condition on Γ that lets the wave propagate outside of the domain and introducing the least artificial reflection must first be derived. But the Helmholtz equation is not a coercive problem, and is not endowed to a maximum principle: the convergence of the algorithm is not guaranteed. In the next Subsection we present how to adapt the Schwarz algorithm for this problem.

6.2 Three tools for Helmholtz numerical resolution using domain decomposition

6.2.1 Absorbing boundary conditions

The first step towards the numerical resolution of (6.0.1) is the truncation of the space and the definition of a boundary condition to close the problem

$$-\Delta u - \omega^2 u = f \quad \text{in } \Omega. \tag{6.2.1}$$

There are several possibilities to model the free space behaviour. We focus in this work on the definition of absorbing boundaries [42, 43, 45, 5, 74]. Another possibility is to define an artificial layer near the boundary of the domain that behaves as an absorbing material, these are called perfectly matched layers and were introduced by Berenger in 1994 [9].

Let $\mathbf{n}$ be the outgoing normal vector defined on Γ, and $\mathbf{t}$ be the associated counter clockwise tangent vector. The absorbing boundary condition

$$\partial_{\mathbf{n}} u - \mathbf{i}\omega u = 0, \tag{6.2.2}$$

yields a well-posed problem in $H^1(\Omega)$. However, the accuracy of this condition is of first order, and it is known that second order ABC yield better results.

A classical second order condition is

$$\partial_{\mathbf{n}} u - \mathbf{i}\omega \left(1 + \frac{1}{2\omega^2}\partial_{\mathbf{tt}}\right) u = 0. \tag{6.2.3}$$

Another one, that has the property of being elliptic, is

$$\left(1 - \frac{1}{2\omega^2}\partial_{\mathbf{tt}}\right) \partial_{\mathbf{n}} u - \mathbf{i}\omega u = 0. \tag{6.2.4}$$

However, for a domain Ω that has corners on its boundary, these second order conditions are not sufficient, and additional conditions on the corners must be prescribed [74, 89].

6.2.2 Transmission conditions

We now focus on a domain decomposition $\Omega = \overset{N_{\rm dom}-1}{\underset{i=0}{\cup}} \Omega_i$, for $N_{\rm dom} \geq 2$. The transmission conditions account for the continuity of the solution and of its normal derivative on the interfaces. Prescribing both of these conditions comes down to computing the Dirichlet to Neumann operator, and is not feasible. A first order condition is

$$\partial_{\mathbf{n}^i} u_i + \mathbf{i}\omega u_i = -\partial_{\mathbf{n}^j} u_j + \mathbf{i}\omega u_j. \tag{6.2.5}$$

After initializing u_i^0 in Ω_i for $0 \leq i \leq N_{\rm dom} - 1$, the associated domain decomposition algorithm using ABC (6.2.2) is given for $p = 0, 1, \ldots$ by

$$\left\{ \begin{array}{rcll} -\Delta u_i^{p+1} - \omega^2 u_i^{p+1} & = & f & \text{in } \Omega_i, \\ \partial_{\mathbf{n}^i} u_i^{p+1} + \mathbf{i}\omega u_i^{p+1} & = & 0 & \text{on } \partial\Omega_i \cap \Gamma, \\ \partial_{\mathbf{n}^i} u_i^{p+1} + \mathbf{i}\omega u_i^{p+1} & = & -\partial_{\mathbf{n}^j} u_j^p + \mathbf{i}\omega u_j^p & \text{on } \partial\Omega_i \cap \partial\Omega_j. \end{array} \right. \tag{6.2.6}$$

At a discretized level, the issue is that the convergence of this first order transmission condition is not satisfactory, and that second order conditions require additional conditions as soon as $\partial\Omega_i$ presents corners, or even more critically when there are cross points, intersections of more than three subdomain frontiers. A possibility is thus to use a layered decomposition of the domain [8, 16, 25], as illustrated in Figure 6.2.

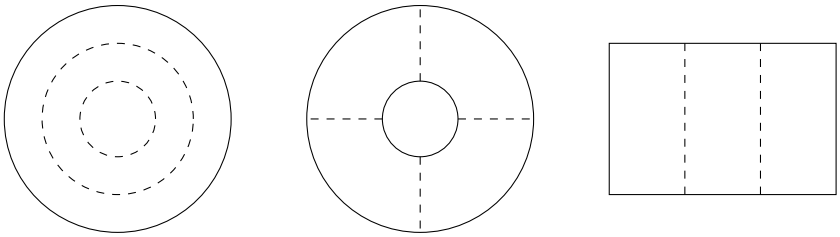

Figure 6.2 – Domain decomposition geometries without interior corners or cross points.

6.2.3 Decaying energy

In this Subsection, we show how to use an energy related to the domain decomposition to prove convergence of the method on the example of algorithm (6.2.6). See [8] for the original presentation on a similar DDM. For $0 \leq i \leq N_{\rm dom} - 1$, let u_i^{p+1} be the solution to (6.2.6) with $f = 0$, for a given initialization $(u_i^0)_{i=0}^{N_{\rm dom}}$. Define the so-called energy for $p \geq 0$

$$E^p := \sum_{\substack{i,j=0 \\ i \neq j}}^{N_{\rm dom}-1} \int\limits_{\partial\Omega_i \cap \partial\Omega_j} \left(|\partial_{\mathbf{n}^i} u_i^p|^2 + \omega^2 |u_i^p|^2 \right) \mathrm{d}\gamma. \tag{6.2.7}$$

Proposition 6.2.1. *The energy defined by* (6.2.7) *is decaying and verifies for all* $p \geq 0$

$$E^{p+1} = E^p - 2\omega^2 \sum_{i=0}^{N_{dom}-1} \int\limits_{\partial\Omega_i \cap \Gamma} \left(|u_i^{p+1}|^2 + |u_i^p|^2 \right) \mathrm{d}\gamma.$$

Proof. Let $p \geq 0$. The definition of the energy gives

$$\begin{aligned} E^{p+1} &= \sum_{\substack{i,j=0\\ i\neq j}}^{N_{\mathrm{dom}}-1} \int_{\partial\Omega_i\cap\partial\Omega_j} \left(\left|\partial_{\mathbf{n}^i} u_i^{p+1}\right|^2 + \omega^2 \left|u_i^{p+1}\right|^2 \right) \mathrm{d}\gamma \\ &= \sum_{\substack{i,j=0\\ i\neq j}}^{N_{\mathrm{dom}}-1} \int_{\partial\Omega_i\cap\partial\Omega_j} \left|\partial_{\mathbf{n}^i} u_i^{p+1} + \mathbf{i}\omega u_i^{p+1}\right|^2 \mathrm{d}\gamma - 2\,\mathrm{Re} \sum_{\substack{i,j=0\\ i\neq j}}^{N_{\mathrm{dom}}-1} \int_{\partial\Omega_i\cap\partial\Omega_j} \mathbf{i}\omega u_i^{p+1} \overline{\partial_{\mathbf{n}^i} u_i^{p+1}} \mathrm{d}\gamma. \end{aligned}$$

It then follows from the transmission conditions that

$$\begin{aligned} E^{p+1} &= \sum_{\substack{i,j=0\\ i\neq j}}^{N_{\mathrm{dom}}-1} \int_{\partial\Omega_i\cap\partial\Omega_j} \left|\partial_{\mathbf{n}^j} u_j^{p} - \mathbf{i}\omega u_j^{p}\right|^2 \mathrm{d}\gamma - 2\,\mathrm{Re} \sum_{\substack{i,j=0\\ i\neq j}}^{N_{\mathrm{dom}}-1} \int_{\partial\Omega_i\cap\partial\Omega_j} \mathbf{i}\omega u_i^{p+1} \overline{\partial_{\mathbf{n}^i} u_i^{p+1}} \mathrm{d}\gamma \\ &= E^p - 2\,\mathrm{Re} \sum_{\substack{i,j=0\\ i\neq j}}^{N_{\mathrm{dom}}-1} \int_{\partial\Omega_i\cap\partial\Omega_j} \mathbf{i}\omega u_j^{p} \overline{\partial_{\mathbf{n}^j} u_j^{p}} \mathrm{d}\gamma - 2\,\mathrm{Re} \sum_{\substack{i,j=0\\ i\neq j}}^{N_{\mathrm{dom}}-1} \int_{\partial\Omega_i\cap\partial\Omega_j} \mathbf{i}\omega u_i^{p+1} \overline{\partial_{\mathbf{n}^i} u_i^{p+1}} \mathrm{d}\gamma. \end{aligned}$$

The second term rewrites

$$\begin{aligned} &- 2\,\mathrm{Re} \sum_{\substack{i,j=0\\ i\neq j}}^{N_{\mathrm{dom}}-1} \int_{\partial\Omega_i\cap\partial\Omega_j} \mathbf{i}\omega u_j^{p} \overline{\partial_{\mathbf{n}^j} u_j^{p}} \mathrm{d}\gamma \\ &= -2\,\mathrm{Re} \sum_{j=0}^{N_{\mathrm{dom}}-1} \int_{\partial\Omega_j} \mathbf{i}\omega u_j^{p} \overline{\partial_{\mathbf{n}^j} u_j^{p}} \mathrm{d}\gamma + 2\,\mathrm{Re} \sum_{j=0}^{N_{\mathrm{dom}}-1} \int_{\partial\Omega_j\cap\Gamma} \mathbf{i}\omega u_j^{p} \overline{\partial_{\mathbf{n}^j} u_j^{p}} \mathrm{d}\gamma. \end{aligned}$$

First, the ABC yields $\partial_{\mathbf{n}^j} u_j^p = -\mathbf{i}\omega u_j^p$ on $\partial\Omega_j \cap \Gamma$. Second, on each subdomain one has

$$\int_{\Omega_j} \left(|\nabla u_j^p|^2 - \omega |u_j^p|^2 \right) \mathrm{d}\mathbf{x} - \int_{\partial\Omega_j} u_j^p \overline{\partial_{\mathbf{n}^j} u_j^p} \mathrm{d}\gamma = 0,$$

and therefore

$$-2\,\mathrm{Re} \sum_{\substack{i,j=0\\ i\neq j}}^{N_{\mathrm{dom}}-1} \int_{\partial\Omega_i\cap\partial\Omega_j} \mathbf{i}\omega u_j^{p} \overline{\partial_{\mathbf{n}^j} u_j^{p}} \mathrm{d}\gamma = -2\omega^2 \sum_{j=0}^{N_{\mathrm{dom}}-1} \int_{\partial\Omega_j\cap\Gamma} |u_j^p|^2 \mathrm{d}\gamma.$$

The same relation holds at iteration $p+1$, and it completes the proof. □

It follows from Proposition 6.2.1 that E^p converges towards a finite limit. Hence u_i^p converges to zero on $\partial\Omega_i \cap \Gamma$ in L^2 since for $P > 0$,

$$E^0 - E^P \geq 2\omega^2 \sum_{p=0}^{P} \sum_{i=0}^{N_{\mathrm{dom}}-1} \int_{\partial\Omega_i\cap\Gamma} |u_i^p|^2 \mathrm{d}\gamma.$$

Because of the boundary condition, $\partial_{\mathbf{n}^i} u_i^p$ also converges to zero in L^2 on the exterior boundary, and a unique continuation principle leads to the convergence towards zero of u_i^p in $H^1(\Omega_i)$ for all the exterior layer subdomains Ω_i, such that $\partial\Omega_i \cap \Gamma \neq 0$. Applying the same arguments layer by layer leads to $u_i^p = 0$ in $H^1(\Omega)$, and proves the convergence of the algorithm towards the global solution $u = 0$.

7 Corner conditions for domain decomposition

This work is the first part of an ongoing project with Bruno Després and Bertrand Thierry.

7.1 Introduction

In this chapter, we define and study a family of second order absorbing boundary conditions for the Helmholtz equation on a polygonal domain. The originality is that the algebraic properties of these new absorbing boundary conditions yield convergent iterative domain decomposition methods, even with corners on the exterior boundary. With respect to the litterature, it seems to be the most original feature of this approach.

The reference problem for this work is the propagation of a time-harmonic wave u in $\mathbb{R}^2$ generated by a compactly supported source f. It is modeled by the Helmholtz equation coupled to the Sommerfeld radiation condition

$$\left\{ \begin{array}{rcl} (-\Delta - \omega^2)u & = & f \quad \text{in } \mathbb{R}^2, \\ \nabla u(\mathbf{x}) \cdot \dfrac{\mathbf{x}}{\|\mathbf{x}\|} - \mathbf{i}\omega u(\mathbf{x}) & = & \underset{\|\mathbf{x}\|\to\infty}{o}\left(\|\mathbf{x}\|^{-1/2}\right). \end{array} \right. \tag{7.1.1}$$

The radiation condition ensures that there is no sink of energy and hence that the problem is well-posed.

To solve (7.1.1) using a finite element method, the propagation domain must first be truncated. To introduce as little artefacts and reflection as possible one can use for example a perfectly matched layer or an ABC, see Subsection 6.2.1. Define a bounded domain Ω containing the support of f, and its boundary $\Gamma := \partial\Omega$. Assume the computational domain is meshed with triangles, making it a polygonal domain. These considerations lead to the Helmholtz equation in a polygonal domain

$$(-\Delta - \omega^2)u = f \quad \text{in } \Omega, \tag{7.1.2}$$

to which boundary conditions on Γ must be added. Let $\mathbf{n}$ and $\mathbf{t}$ be the unit outgoing normal and tangential vectors to Γ such that the local system $(\mathbf{n}, \mathbf{t})$ is direct. The system made of (7.1.2) and of the first order ABC $\partial_{\mathbf{n}} u - \mathbf{i}\omega u = 0$ is a well-posed problem in $H^1(\Omega)$, but it is known that second

order ABCs yield better results. In this work, we use the coercive second order ABC

$$\left\{\begin{array}{rcll} (-\Delta-\omega^2)u & = & f & \text{in } \Omega, \\ \left(1-\dfrac{1}{2\omega^2}\partial_{\mathbf{tt}}\right)\partial_{\mathbf{n}}u-\mathbf{i}\omega u & = & 0 & \text{on } \Gamma. \end{array}\right. \tag{7.1.3}$$

The boundary Γ considered in this work is a closed broken line. Because of the differentiation of $\partial_{\mathbf{n}}u$ along Γ in the absorbing condition (7.1.3), additional relations have to be prescribed at the corners of Γ, where $\mathbf{n}$ is not defined. The purpose of this work is to elaborate such relations.

A central idea for the development of corner relations that complement (7.1.3) is that the algebraic properties of convergent DDMs for the Helmhotz equation must be preserved by the new conditions.

Conventions. The indices k and ℓ are reserved for the edges of the exterior boundary. The indices i and j are reserved for subdomains of Ω. With these notations, a point denoted $\mathbf{A}_{kl}^{ij}$ belongs to the intersection of the k^{th} and of the ℓ^{th} edges, and to the border of the i^{th} and of the j^{th} subdomains. A subtle distinction will be made by using either the subscripted $\mathbf{n}_k$ for the exterior normal to Ω on the k^{th} edge of Γ or the superscripted $\mathbf{n}^i$ for the exterior normal to Ω_i on its boundary $\partial\Omega_i$. The same distinction will be made between the tangent unit vectors $\mathbf{t}_k$ and $\mathbf{t}^i$. The index p is reserved for algorithm iterations. The purely imaginary number is written in bold $\mathbf{i}^2=-1$. Norm $\|.\|$ stands for the Euclidian norm in $\mathbb{R}^2$.

7.2 Construction of corner conditions

7.2.1 Geometry and notation

We need notations which correspond to the edge and corner geometries illustrated in Figures 7.1 and 7.2. On an oriented edge $\Gamma_k=(\mathbf{a}_k,\mathbf{b}_k)$ of Γ, the unit tangential vector is $\mathbf{t}_k=\frac{\mathbf{b}_k-\mathbf{a}_k}{\|\mathbf{b}_k-\mathbf{a}_k\|}$ and the unit normal vector is $\mathbf{n}_k=-\mathbf{t}_k^{\perp}$. At the boundary points $\mathbf{a}_k$ and $\mathbf{b}_k$ of Γ_k, which are corner points, a unit vector $\boldsymbol{\tau}_k$ colinear to $\mathbf{t}_k$ and pointing outside Γ_k is introduced. With these notations, for two

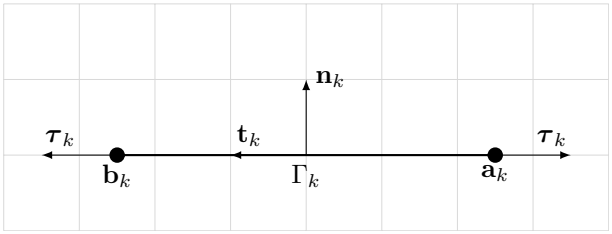

Figure 7.1 – Tangent and normal vectors $\mathbf{t}_k$ and $\mathbf{n}_k$, and outgoing corner vectors $\boldsymbol{\tau}_k$ on a segment $\Gamma_k=(\mathbf{a}_k,\mathbf{b}_k)$.

segments $\Gamma_k=(\mathbf{a}_k,\mathbf{b}_k)$ and $\Gamma_\ell=(\mathbf{a}_\ell,\mathbf{b}_\ell)$ with a common vertex $\mathbf{b}_k=\mathbf{a}_\ell$, we denote this vertex

$$\mathbf{A}_{k\ell}=\mathbf{A}_{\ell k}=\mathbf{b}_k=\mathbf{a}_\ell.$$

The chosen convention is to characterize the angle between two such segments by a negative value $\theta_{k\ell}\in(-2\pi,0)$, see Figure 7.2. The geometrically degenerate case $\theta_{k\ell}=-\pi$ will appear to be a mathematical singularity of some of the formulations in this work. Another singularity will show up for right angles $\theta_{k\ell}=-\frac{\pi}{2},-\frac{3\pi}{2}$ in other formulations.

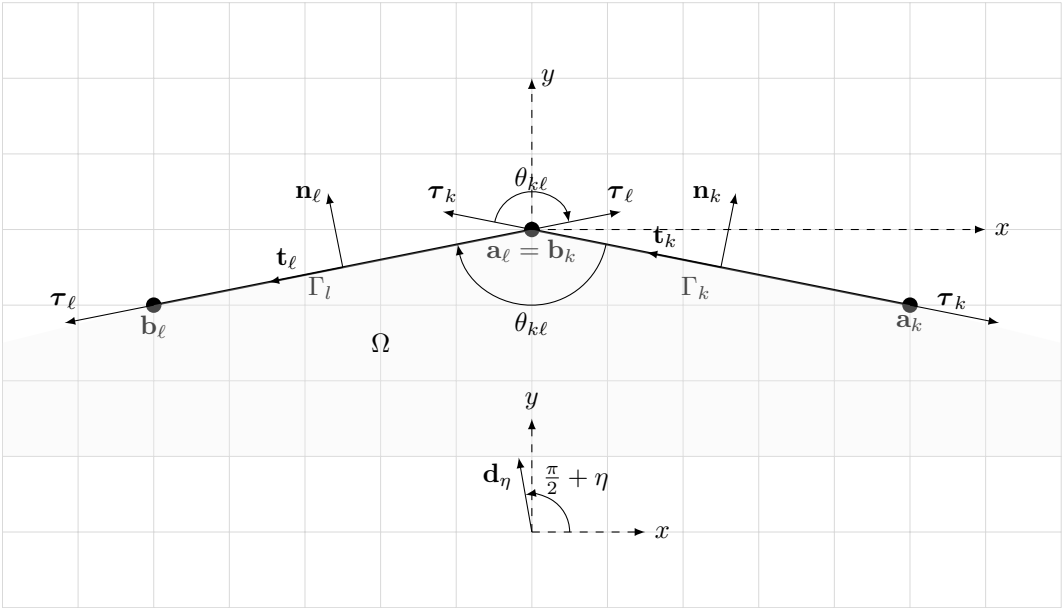

Figure 7.2 – Local geometry at the intersection of two segments Γ_k and Γ_ℓ with $\mathbf{b}_k = \mathbf{a}_\ell$.

Segment Γ_k			Segment Γ_ℓ		
$\mathbf{n}_k$	=	$\left(\cos\left(\frac{\theta_{k\ell}}{2}\right), -\sin\left(\frac{\theta_{k\ell}}{2}\right)\right)$	$\mathbf{n}_\ell$	=	$\left(-\cos\left(\frac{\theta_{k\ell}}{2}\right), -\sin\left(\frac{\theta_{k\ell}}{2}\right)\right)$
$\boldsymbol{\tau}_k$	=	$\left(\sin\left(\frac{\theta_{k\ell}}{2}\right), \cos\left(\frac{\theta_{k\ell}}{2}\right)\right)$	$\boldsymbol{\tau}_\ell$	=	$\left(-\sin\left(\frac{\theta_{k\ell}}{2}\right), \cos\left(\frac{\theta_{k\ell}}{2}\right)\right)$

Table 7.1 – Expression of Γ_k and Γ_ℓ tangent and normal vectors with respect to the angle $\theta_{k\ell}$ for two intersecting segments at $\mathbf{b}_k = \mathbf{a}_\ell$.

7.2.2 Quasicontinuity relations

The first goal here is to obtain two quasicontinuity relations at a corner point $\mathbf{A}_{k\ell}$ between two segments for a plane wave u_η as in Figure 7.2 with an incident angle $\frac{\pi}{2} + \eta$

$$u_\eta(\mathbf{x}) = e^{\mathbf{i}\omega(\mathbf{d}_\eta, \mathbf{x})}, \quad \text{with} \quad \mathbf{d}_\eta = \left(\cos\left(\frac{\pi}{2} + \eta\right), \sin\left(\frac{\pi}{2} + \eta\right)\right) = (-\sin(\eta), \cos(\eta)) \in \mathbb{R}^2.$$

At a corner point $\mathbf{A}_{k\ell}$, one has the following expressions of the derivatives of u_η

$$\left\{\begin{array}{rcl} \partial_{\mathbf{n}_k} u_\eta(\mathbf{A}_{k\ell}) &=& \mathbf{i}\omega(\mathbf{n}_k, \mathbf{d}_\eta) u_\eta(\mathbf{A}_{k\ell}), \\ \partial_{\mathbf{n}_\ell} u_\eta(\mathbf{A}_{k\ell}) &=& \mathbf{i}\omega(\mathbf{n}_\ell, \mathbf{d}_\eta) u_\eta(\mathbf{A}_{k\ell}), \\ \partial_{\boldsymbol{\tau}_k}\partial_{\mathbf{n}_k} u_\eta(\mathbf{A}_{k\ell}) &=& -\omega^2(\boldsymbol{\tau}_k, \mathbf{d}_\eta)(\mathbf{n}_k, \mathbf{d}_\eta) u_\eta(\mathbf{A}_{k\ell}), \\ \partial_{\boldsymbol{\tau}_\ell}\partial_{\mathbf{n}_\ell} u_\eta(\mathbf{A}_{k\ell}) &=& -\omega^2(\boldsymbol{\tau}_\ell, \mathbf{d}_\eta)(\mathbf{n}_\ell, \mathbf{d}_\eta) u_\eta(\mathbf{A}_{k\ell}). \end{array}\right. \tag{7.2.1}$$

Referring to Table 7.1, the scalar products between the wave vector $\mathbf{d}_\eta$ and the normal and tangent vectors of Γ_k are

$$\left\{\begin{array}{rcl} (\mathbf{n}_k, \mathbf{d}_\eta) &=& -\cos\left(\dfrac{\theta_{k\ell}}{2}\right)\sin(\eta) - \sin\left(\dfrac{\theta_{k\ell}}{2}\right)\cos(\eta) \\ (\boldsymbol{\tau}_k, \mathbf{d}_\eta) &=& -\sin\left(\dfrac{\theta_{k\ell}}{2}\right)\sin(\eta) + \cos\left(\dfrac{\theta_{k\ell}}{2}\right)\cos(\eta) \end{array}\right. = \left\{\begin{array}{r} -\sin\left(\dfrac{\theta_{k\ell}}{2}+\eta\right), \\ \cos\left(\dfrac{\theta_{k\ell}}{2}+\eta\right), \end{array}\right.$$

while the scalar products between the direction $\mathbf{d}_\eta$ of the wave and the normal and tangent vectors of Γ_ℓ are

$$\left\{\begin{array}{rcl} (\mathbf{n}_\ell, \mathbf{d}_\eta) &=& \cos\left(\dfrac{\theta_{k\ell}}{2}\right)\sin(\eta) - \sin\left(\dfrac{\theta_{k\ell}}{2}\right)\cos(\eta) \\ (\boldsymbol{\tau}_\ell, \mathbf{d}_\eta) &=& \sin\left(\dfrac{\theta_{k\ell}}{2}\right)\sin(\eta) + \cos\left(\dfrac{\theta_{k\ell}}{2}\right)\cos(\eta) \end{array}\right. = \left\{\begin{array}{r} -\sin\left(\dfrac{\theta_{k\ell}}{2}-\eta\right), \\ \cos\left(\dfrac{\theta_{k\ell}}{2}-\eta\right). \end{array}\right.$$

We outline two linear combinations of u_η derivatives (7.2.1) that are small for small η. We will use these linear combinations to define quasicontinuity relations.

Lemma 7.2.1. *Consider a corner point $\mathbf{A}_{k\ell}$. For η close to zero, the following relation holds*

$$\mathbf{i}\omega\cos(\theta_{k\ell})\left(\partial_{\mathbf{n}_k}u_\eta - \partial_{\mathbf{n}_\ell}u_\eta\right)(\mathbf{A}_{k\ell}) - \cos\left(\frac{\theta_{k\ell}}{2}\right)\left(\partial_{\boldsymbol{\tau}_k}\partial_{\mathbf{n}_k}u_\eta - \partial_{\boldsymbol{\tau}_\ell}\partial_{\mathbf{n}_\ell}u_\eta\right)(\mathbf{A}_{k\ell}) = O\left(\eta^3\right). \quad (7.2.2)$$

Proof. On the one hand, the difference of the first order derivatives from (7.2.1) is

$$\begin{aligned}(\partial_{\mathbf{n}_k}u_\eta - \partial_{\mathbf{n}_\ell}u_\eta)(\mathbf{A}_{k\ell}) &= \mathbf{i}\omega\left(-\sin\left(\frac{\theta_{k\ell}}{2}+\eta\right) + \sin\left(\frac{\theta_{k\ell}}{2}-\eta\right)\right)u_\eta(\mathbf{A}_{k\ell}) \\ &= -2\mathbf{i}\omega\eta\cos\left(\frac{\theta_{k\ell}}{2}\right)u_\eta(\mathbf{A}_{k\ell}) + O\left(\eta^3\right).\end{aligned}$$

On the other hand, the difference of the second order derivatives from (7.2.1) is

$$\begin{aligned}&(\partial_{\boldsymbol{\tau}_k}\partial_{\mathbf{n}_k}u_\eta - \partial_{\boldsymbol{\tau}_\ell}\partial_{\mathbf{n}_\ell}u_\eta)(\mathbf{A}_{k\ell}) \\ &= -\omega^2\left(-\cos\left(\frac{\theta_{k\ell}}{2}+\eta\right)\sin\left(\frac{\theta_{k\ell}}{2}+\eta\right) + \cos\left(\frac{\theta_{k\ell}}{2}-\eta\right)\sin\left(\frac{\theta_{k\ell}}{2}-\eta\right)\right)u_\eta(\mathbf{A}_{k\ell}) \\ &= -\omega^2\left(-\frac{1}{2}\sin\left(\theta_{k\ell}+2\eta\right) + \frac{1}{2}\sin\left(\theta_{k\ell}-2\eta\right)\right)u_\eta(\mathbf{A}_{k\ell}) \\ &= -\omega^2\left(-2\cos\left(\theta_{k\ell}\right) + O\left(\eta^3\right)\right)u_\eta(\mathbf{A}_{k\ell}) \\ &= 2\omega^2\eta\cos\left(\theta_{k\ell}\right)u_\eta + O\left(\eta^3\right).\end{aligned}$$

Combining these two relations yields the claim. □

Lemma 7.2.2. *Consider a corner point $\mathbf{A}_{k\ell}$. For η close to zero, the following relation holds*

$$-\mathbf{i}\omega\cos\left(\frac{\theta_{k\ell}}{2}\right)\left(\partial_{\mathbf{n}_k}u_\eta + \partial_{\mathbf{n}_\ell}u_\eta\right)(\mathbf{A}_{k\ell}) + \left(\partial_{\boldsymbol{\tau}_k}\partial_{\mathbf{n}_k}u_\eta + \partial_{\boldsymbol{\tau}_\ell}\partial_{\mathbf{n}_\ell}u_\eta\right)(\mathbf{A}_{k\ell}) = O\left(\eta^2\right). \quad (7.2.3)$$

Proof. First, adding the two first order derivatives from (7.2.1) gives

$$\begin{aligned}(\partial_{\mathbf{n}_k} u_\eta + \partial_{\mathbf{n}_\ell} u_\eta)(\mathbf{A}_{k\ell}) &= -\mathbf{i}\omega \left(\sin\left(\frac{\theta_{k\ell}}{2} + \eta\right) + \sin(\frac{\theta_{k\ell}}{2} - \eta) \right) u_\eta(\mathbf{A}_{k\ell}) \\ &= -2\mathbf{i}\omega \sin\left(\frac{\theta_{k\ell}}{2}\right) \cos(\eta) u_\eta(\mathbf{A}_{k\ell}) \\ &= -2\mathbf{i}\omega \sin\left(\frac{\theta_{k\ell}}{2}\right) u_\eta(\mathbf{A}_{k\ell}) + O\left(\eta^2\right).\end{aligned}$$

Second, adding the two second order derivatives from (7.2.1) gives

$$\begin{aligned}&(\partial_{\boldsymbol{\tau}_k} \partial_{\mathbf{n}_k} u_\eta + \partial_{\boldsymbol{\tau}_\ell} \partial_{\mathbf{n}_\ell} u_\eta)(\mathbf{A}_{k\ell}) \\ &= \omega^2 \left(\sin\left(\frac{\theta_{k\ell}}{2} + \eta\right) \cos\left(\frac{\theta_{k\ell}}{2} + \eta\right) + \sin\left(\frac{\theta_{k\ell}}{2} - \eta\right) \cos\left(\frac{\theta_{k\ell}}{2} - \eta\right) \right) u_\eta(\mathbf{A}_{k\ell}) \\ &= \omega^2 \left(\frac{1}{2}\sin\left(\theta_{k\ell} + 2\eta\right) + \frac{1}{2}\sin\left(\theta_{k\ell} - 2\eta\right) \right) u_\eta(\mathbf{A}_{k\ell}) \\ &= \omega^2 \sin\left(\theta_{k\ell}\right) u_\eta(\mathbf{A}_{k\ell}) + O\left(\eta^2\right) \\ &= 2\omega^2 \sin\left(\frac{\theta_{k\ell}}{2}\right) \cos\left(\frac{\theta_{k\ell}}{2}\right) u_\eta(\mathbf{A}_{k\ell}) + O\left(\eta^2\right).\end{aligned}$$

Combining these two relations yields the claim. □

We now introduce the following quantity on each segment Γ_k

$$\varphi_k := \frac{1}{\mathbf{i}\omega} \partial_{\mathbf{n}_k} u_\eta.$$

Rewriting (7.2.2) and (7.2.3) using these new variables and dropping the $O(\eta^2)$ and $O(\eta^3)$ terms, one gets the quasicontinuity relations

$$\left\{ \begin{array}{rcl} \mathbf{i}\omega \cos(\theta_{k\ell}) \left(\varphi_k - \varphi_\ell\right)(\mathbf{A}_{k\ell}) - \cos\left(\frac{\theta_{k\ell}}{2}\right) \left(\partial_{\boldsymbol{\tau}_k}\varphi_k - \partial_{\boldsymbol{\tau}_\ell}\varphi_\ell\right)(\mathbf{A}_{k\ell}) &=& 0, \\ -\mathbf{i}\omega \cos\left(\frac{\theta_{k\ell}}{2}\right) \left(\varphi_k + \varphi_\ell\right)(\mathbf{A}_{k\ell}) + \left(\partial_{\boldsymbol{\tau}_k}\varphi_k + \partial_{\boldsymbol{\tau}_\ell}\varphi_\ell\right)(\mathbf{A}_{k\ell}) &=& 0. \end{array} \right. \tag{7.2.4}$$

For a flat angle $\theta_{k\ell} = -\pi$, the system corresponds exactly to the continuity relations

$$\left\{ \begin{array}{rcl} \varphi_k(\mathbf{A}_{k\ell}) - \varphi_\ell(\mathbf{A}_{k\ell}) &=& 0, \\ \partial_{\boldsymbol{\tau}_k}\varphi_k(\mathbf{A}_{k\ell}) + \partial_{\boldsymbol{\tau}_\ell}\varphi_\ell(\mathbf{A}_{k\ell}) &=& 0. \end{array} \right. \tag{7.2.5}$$

We now recast these equations to have symmetric relations with respect to k and ℓ. A first symmetric system of quasicontinuity relations is derived for corners such that $\theta_{k\ell} \neq -\pi$, so for non flat corners (such that $\theta_{k\ell} \neq -\pi$).

Lemma 7.2.3. *Consider a corner point $\mathbf{A}_{k\ell}$ such that $\theta_{k\ell} \neq -\pi$. If relations* (7.2.4) *are satisfied,*

then the following second order quasicontinuity relations are also satisfied

$$\left\{\begin{array}{l} \partial_{\boldsymbol{\tau}_k}\varphi_k(\mathbf{A}_{k\ell}) - \mathbf{i}\dfrac{\omega}{2}\left(\dfrac{\cos\left(\theta_{k\ell}\right)}{\cos\left(\frac{\theta_{k\ell}}{2}\right)} + \cos\left(\dfrac{\theta_{k\ell}}{2}\right)\right)\varphi_k(\mathbf{A}_{k\ell}) \\ \qquad = \mathbf{i}\dfrac{\omega}{2}\left(-\dfrac{\cos\left(\theta_{k\ell}\right)}{\cos\left(\frac{\theta_{k\ell}}{2}\right)} + \cos\left(\dfrac{\theta_{k\ell}}{2}\right)\right)\varphi_\ell(\mathbf{A}_{k\ell}), \\ \partial_{\boldsymbol{\tau}_\ell}\varphi_\ell(\mathbf{A}_{k\ell}) - \mathbf{i}\dfrac{\omega}{2}\left(\dfrac{\cos\left(\theta_{\ell k}\right)}{\cos\left(\frac{\theta_{\ell k}}{2}\right)} + \cos\left(\dfrac{\theta_{\ell k}}{2}\right)\right)\varphi_\ell(\mathbf{A}_{k\ell}) \\ \qquad = \mathbf{i}\dfrac{\omega}{2}\left(-\dfrac{\cos\left(\theta_{\ell k}\right)}{\cos\left(\frac{\theta_{\ell k}}{2}\right)} + \cos\left(\dfrac{\theta_{\ell k}}{2}\right)\right)\varphi_k(\mathbf{A}_{k\ell}). \end{array}\right. \tag{7.2.6}$$

Proof. For $\theta_{k\ell} \neq -\pi$, system (7.2.4) is equivalent to

$$\left\{\begin{array}{rcl} -\mathbf{i}\omega\dfrac{\cos(\theta_{k\ell})}{\cos\left(\frac{\theta_{k\ell}}{2}\right)}\left(\varphi_k - \varphi_\ell\right)(\mathbf{A}_{k\ell}) + \left(\partial_{\boldsymbol{\tau}_k}\varphi_k - \partial_{\boldsymbol{\tau}_\ell}\varphi_\ell\right)(\mathbf{A}_{k\ell}) & = & 0, \\ -\mathbf{i}\omega\cos\left(\dfrac{\theta_{k\ell}}{2}\right)\left(\varphi_k + \varphi_\ell\right)(\mathbf{A}_{k\ell}) + \left(\partial_{\boldsymbol{\tau}_k}\varphi_k + \partial_{\boldsymbol{\tau}_\ell}\varphi_\ell\right)(\mathbf{A}_{k\ell}) & = & 0. \end{array}\right. \tag{7.2.7}$$

The first relation of (7.2.6) is obtained by adding these two lines and dividing by 2, and the second one is obtained by susbtracting the first line to the second and dividing by 2. □

A family of mixed symmetric systems of quasicontinuity relations parametrized by a coefficient $\beta \neq 0$ can be constructed, a priori for corners such that $\theta_{k\ell} \neq -\frac{\pi}{2}, -\frac{3\pi}{2}$, wich comes down to non right angles.

Lemma 7.2.4. *Consider a corner point $\mathbf{A}_{k\ell}$ such that $\theta_{k\ell} \neq -\frac{\pi}{2}, -\frac{3\pi}{2}$. Let $\beta \neq 0$. If relations* (7.2.4) *are satisfied, then the following second order quasicontinuity relations are also satisfied*

$$\left\{\begin{array}{l} \left(1 + \beta\dfrac{\mathbf{i}\cos\left(\frac{\theta_{k\ell}}{2}\right)}{\omega\cos(\theta_{k\ell})}\right)\partial_{\boldsymbol{\tau}_k}\varphi_k(\mathbf{A}_{k\ell}) + \left(\beta - \mathbf{i}\omega\cos\left(\dfrac{\theta_{k\ell}}{2}\right)\right)\varphi_k(\mathbf{A}_{k\ell}) \\ \qquad = \left(-1 + \beta\dfrac{\mathbf{i}\cos\left(\frac{\theta_{k\ell}}{2}\right)}{\omega\cos(\theta_{k\ell})}\right)\partial_{\boldsymbol{\tau}_\ell}\varphi_\ell(\mathbf{A}_{k\ell}) + \left(\beta + \mathbf{i}\omega\cos\left(\dfrac{\theta_{k\ell}}{2}\right)\right)\varphi_\ell(\mathbf{A}_{k\ell}), \\ \left(1 + \beta\dfrac{\mathbf{i}\cos\left(\frac{\theta_{\ell k}}{2}\right)}{\omega\cos(\theta_{\ell k})}\right)\partial_{\boldsymbol{\tau}_\ell}\varphi_\ell(\mathbf{A}_{k\ell}) + \left(\beta - \mathbf{i}\omega\cos\left(\dfrac{\theta_{\ell k}}{2}\right)\right)\varphi_\ell(\mathbf{A}_{k\ell}) \\ \qquad = \left(-1 + \beta\dfrac{\mathbf{i}\cos\left(\frac{\theta_{\ell k}}{2}\right)}{\omega\cos(\theta_{\ell k})}\right)\partial_{\boldsymbol{\tau}_k}\varphi_k(\mathbf{A}_{k\ell}) + \left(\beta + \mathbf{i}\omega\cos\left(\dfrac{\theta_{\ell k}}{2}\right)\right)\varphi_k(\mathbf{A}_{k\ell}). \end{array}\right. \tag{7.2.8}$$

Proof. Multiplying the first line of (7.2.4) by $\frac{\beta}{\mathbf{i}\omega\cos(\theta_{k\ell})}$, and adding it to the second line leads to the first relation of (7.2.8). Multiplying by $\frac{-\beta}{\mathbf{i}\omega\cos(\theta_{k\ell})}$ instead gives the second relation. This algebra is non singular for $\beta \neq 0$. □

Desingularization near $\cos\theta_{k\ell} = 0$ and homogeneity considerations lead to take β proportional to $\omega\cos(\theta_{k\ell})$. For energy reasons explained in the sequel, see 7.4.3, the sign of β is also prescribed.

Therefore, we set

$$\beta = -|\omega| \cos \theta_{k\ell}. \tag{7.2.9}$$

We now consider relations (7.2.8) for any angle $\theta_{k\ell}$: for $\theta_{k\ell} = -\pi/2$ or $-3\pi/2$, the relations are desingularized beforehand using the definition of β. We note here that there exists works [74, 89] treating this specific case of right angles, for which $\mathbf{n}_k$ and $\mathbf{t}_\ell$ are colinear as well as $\mathbf{t}_k$ and $\mathbf{n}_\ell$.

Remark 7.2.5. When adapting these relations for transmission conditions, considering a corner on the interface of two subdomains Ω_i and Ω_j, one will have to dissociate the angles $\theta^i_{k\ell}$ where Ω_i is the interior domain from $\theta^j_{k\ell}$ where Ω_j is the interior domain. Indeed, as $\theta^i_{k\ell} + \theta^j_{k\ell} = -2\pi$, see Figure 7.2, notice the change of sign

$$\cos\left(\frac{\theta^i_{k\ell}}{2}\right) = -\cos\left(\frac{\theta^j_{k\ell}}{2}\right).$$

Considering Ω_i instead of Ω_j as the interior domain comes down to taking the conjugate of each coefficient from (7.2.6) or (7.2.8).

7.3 Definition of a 2nd order ABC with corner conditions

We now come back to problem (7.1.3). Assume the boundary $\Gamma := \overline{\bigcup_{k=0}^{K-1} \Gamma_k}$ is polygonal and decomposes in $K \geq 3$ segments, as illustrated in Figure 7.3. We set $\Gamma_K := \Gamma_0$ and $\Gamma_{-1} := \Gamma_{K-1}$. The segments are numbered consecutively and we use the notations previously defined: on a segment Γ_k, the normal vector $\mathbf{n}_k$ is pointing outside the computational domain Ω; the tangential vector $\mathbf{t}_k$ varies counter-clockwise; and at the two corners, $\mathbf{A}_{k\ell}$ for $\ell = k \pm 1$, the vectors $\boldsymbol{\tau}_k(\mathbf{A}_{k\ell})$ are tangent to Γ_k and pointing outside.

For $u \in L^2(\Gamma)$, we define $\varphi \in \oplus_k H^1(\Gamma_k)$ such that, for $k = 0, \ldots, K-1$, the quantity $\varphi_k = \varphi|_{\Gamma_k}$ is the variational solution of

$$\begin{cases} \left(1 - \dfrac{1}{2\omega^2}\dfrac{\partial^2}{\partial \mathbf{t}_k^2}\right)\varphi_k = u, & \text{in } \Gamma_k, \\ \partial_{\boldsymbol{\tau}_k}\varphi_k(\mathbf{A}_{k\ell}) - \mathbf{i}\dfrac{\omega}{2}\left(\dfrac{\cos(\theta_{k\ell})}{\cos\left(\frac{\theta_{k\ell}}{2}\right)} + \cos\left(\dfrac{\theta_{k\ell}}{2}\right)\right)\varphi_k(\mathbf{A}_{k\ell}) & \\ \qquad = \mathbf{i}\dfrac{\omega}{2}\left(-\dfrac{\cos(\theta_{k\ell})}{\cos\left(\frac{\theta_{k\ell}}{2}\right)} + \cos\left(\dfrac{\theta_{k\ell}}{2}\right)\right)\varphi_\ell(\mathbf{A}_{k\ell}), \quad \ell = k \pm 1. \end{cases} \tag{7.3.1}$$

The variational formulation of (7.3.1) is constructed as follows. Let $\varphi \in \oplus_k H^1(\Gamma_k)$ verify (7.3.1). Integrating by parts the equation on each Γ_k against the conjugate of $\psi \in \oplus_k H^1(\Gamma_k)$ gives

$$\sum_{k=0}^{K-1}\left(\int_{\Gamma_k}\left(\varphi_k\overline{\psi_k} + \frac{1}{2\omega^2}\frac{\partial\varphi_k}{\partial\mathbf{t}_k}\overline{\frac{\partial\psi_k}{\partial\mathbf{t}_k}}\right)\mathrm{d}\gamma - \frac{1}{2\omega^2}\sum_{\ell=k\pm1}\left(\frac{\partial\varphi_k}{\partial\boldsymbol{\tau}_k}\overline{\psi_k}\right)(\mathbf{A}_{k\ell})\right) = \sum_{k=0}^{K-1}\int_{\Gamma_k} u\overline{\psi_k}\,\mathrm{d}\gamma. \tag{7.3.2}$$

The boundary Γ is closed, and the corner terms can be regrouped, yielding

$$\sum_{k=0}^{K-1}\sum_{\ell=k\pm1}\left(\frac{\partial\varphi_k}{\partial\boldsymbol{\tau}_k}\overline{\psi_k}\right)(\mathbf{A}_{k\ell}) = \sum_{\substack{k=0\\ \ell=k+1}}^{K-1}\left(\frac{\partial\varphi_k}{\partial\boldsymbol{\tau}_k}\overline{\psi_k} + \frac{\partial\varphi_\ell}{\partial\boldsymbol{\tau}_\ell}\overline{\psi_\ell}\right)(\mathbf{A}_{k\ell}).$$

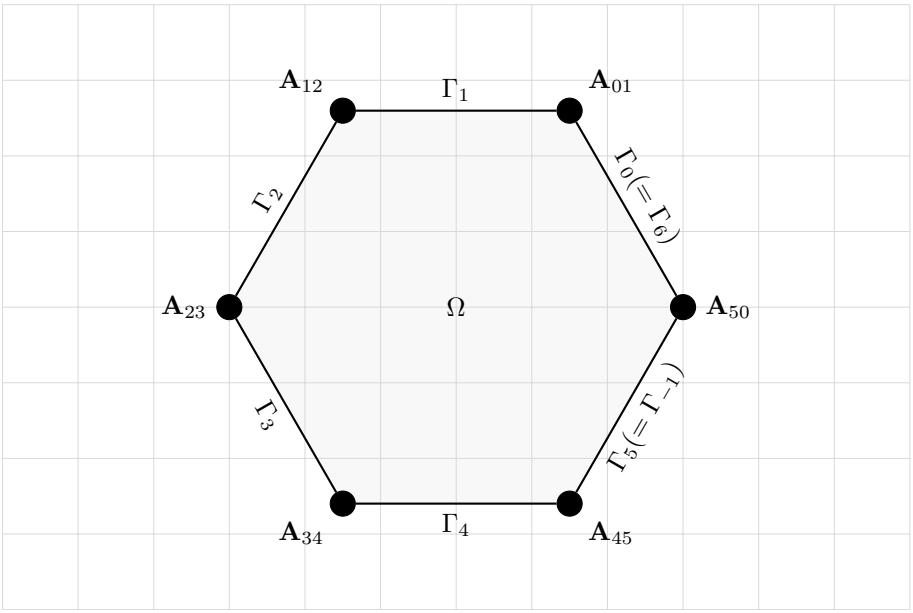

Figure 7.3 – Example of a polygonal domain Ω with boundary $\Gamma = \cup_{k=0}^{5} \Gamma_k$.

The continuity relations (7.2.6) ensure that at $\mathbf{A}_{k\ell}$ one has

$$\begin{aligned}\frac{\partial \varphi_k}{\partial \boldsymbol{\tau}_k}\overline{\psi_k} + \frac{\partial \varphi_\ell}{\partial \boldsymbol{\tau}_\ell}\overline{\psi_\ell} &= \frac{1}{2}\left(\frac{\partial \varphi_k}{\partial \boldsymbol{\tau}_k} + \frac{\partial \varphi_\ell}{\partial \boldsymbol{\tau}_\ell}\right)\left(\overline{\psi_k} + \overline{\psi_\ell}\right) + \frac{1}{2}\left(\frac{\partial \varphi_k}{\partial \boldsymbol{\tau}_k} - \frac{\partial \varphi_\ell}{\partial \boldsymbol{\tau}_\ell}\right)\left(\overline{\psi_k} - \overline{\psi_\ell}\right) \\ &= \frac{\mathbf{i}\omega}{2}\left(\cos\left(\frac{\theta_{k\ell}}{2}\right)(\varphi_k + \varphi_\ell)(\overline{\psi_k} + \overline{\psi_\ell}) + \frac{\cos(\theta_{k\ell})}{\cos\left(\frac{\theta_{k\ell}}{2}\right)}(\varphi_k - \varphi_\ell)(\overline{\psi_k} - \overline{\psi_\ell})\right).\end{aligned}$$

After substitution in (7.3.2), the variational formulation reads

Find $\varphi \in \oplus_k H^1(\Gamma_k)$ such that for every test function $\psi \in \oplus_k H^1(\Gamma_k)$,

$$\begin{aligned}&\sum_{k=0}^{K-1} \int_{\Gamma_k} \left(\varphi_k \overline{\psi_k} + \frac{1}{2\omega^2}\frac{\partial \varphi_k}{\partial \mathbf{t}_k}\overline{\frac{\partial \psi_k}{\partial \mathbf{t}_k}}\right) \mathrm{d}\gamma \\ &-\frac{\mathbf{i}}{4\omega} \sum_{\substack{k=0 \\ \ell=k+1}}^{K-1} \left(\cos\left(\frac{\theta_{k\ell}}{2}\right)(\varphi_k + \varphi_\ell)(\overline{\psi_k} + \overline{\psi_\ell}) + \frac{\cos(\theta_{k\ell})}{\cos\left(\frac{\theta_{k\ell}}{2}\right)}(\varphi_k - \varphi_\ell)(\overline{\psi_k} - \overline{\psi_\ell})\right)(\mathbf{A}_{k\ell}) \\ &= \sum_{k=0}^{K-1} \int_{\Gamma_k} u\overline{\psi_k}\, \mathrm{d}\gamma.\end{aligned} \tag{7.3.3}$$

Theorem 7.3.1. *Let $u \in L^2(\Gamma)$. There exists a unique solution $\varphi \in \oplus_k H^1(\Gamma_k)$ of the variational formulation* (7.3.3).

Proof. The well-posedness of the problem (7.3.3) amounts to show that a certain system of linear ordinary differential equations admits a unique solution. Since it is ODE based, it can be reduced to a system in finite dimension, so it is sufficient to show the uniqueness of the solution to obtain the

well-posedness. One can also invoke the Lax-Milgram Theorem since the bilinear form is continuous and coercive as shown by the algebra below.

In the variational formulation (7.3.3), take $\psi_k = \varphi_k$ for all k: the real part

$$\sum_{k=0}^{K-1} \int_{\Gamma_k} \left(|\varphi_k|^2 + \frac{1}{2\omega^2} \left| \frac{\partial \varphi_k}{\partial \mathbf{t}_k} \right|^2 \right) \mathrm{d}\gamma = \mathrm{Re} \left(\sum_{k=0}^{K-1} \int_{\Gamma_k} u \overline{\varphi_k} \, \mathrm{d}\gamma \right), \tag{7.3.4}$$

implies that

$$\|\varphi\|^2_{L^2(\Gamma)} + \frac{1}{2\omega^2} \sum_{k=0}^{K-1} \left\| \frac{\partial \varphi_k}{\partial \mathbf{t}_k} \right\|^2_{L^2(\Gamma_k)} \leq \|\varphi\|_{L^2(\Gamma)} \|u\|_{L^2(\Gamma)} .$$

Taking $u = 0$ leads to $\varphi = 0$ which proves the uniqueness of the variational solution for $u \in L^2(\Gamma)$, and therefore its existence. □

Proposition 7.3.2. *Define the operator $T : u \in L^2(\Gamma) \mapsto \varphi \in L^2(\Gamma)$, where φ is the unique solution to* (7.3.3) *for a given $u \in L^2(\Gamma)$. One has $\|T\|_{\mathcal{L}(L^2(\Gamma))} \leq 1$.*

Proof. Let $u \in L^2(\Gamma)$. For $T(u) = \varphi \in \oplus_k H^1(\Gamma_k) \subset L^2(\Gamma)$, one has

$$(T(u), T(u))_{L^2(\Gamma)} = \sum_{k=0}^{K-1} \int_{\Gamma_k} \left(\frac{-1}{2\omega^2} \left| \frac{\partial \varphi_k}{\partial \mathbf{t}_k} \right|^2 + \mathrm{Re}(u \overline{\varphi_k}) \right) \mathrm{d}\gamma \leq \mathrm{Re} \, (u, T(u))_{L^2(\Gamma)} . \tag{7.3.5}$$

Consequently, it holds $\|T\|_{\mathcal{L}(L^2(\Gamma))} = \inf\limits_{\substack{u \in L^2(\Gamma) \\ u \neq 0}} \dfrac{\|T(u)\|_{L^2(\Gamma)}}{\|u\|_{L^2(\Gamma)}} \leq 1.$ □

The second order ABC deriving from operator T is introduced in the Helmholtz equation to obtain

$$\left\{ \begin{array}{rcll} (-\Delta - \omega^2) u & = & f & \text{in } \Omega, \\ \partial_{\mathbf{n}} u - \mathbf{i}\omega T(u) & = & 0 & \text{on } \Gamma. \end{array} \right. \tag{7.3.6}$$

The associated weak formulation writes

$$\left\{ \begin{array}{l} \text{Find } u \in H^1(\Omega) \text{ such that } \forall v \in H^1(\Omega), \\ \displaystyle\int_\Omega \left(\nabla u \cdot \nabla \overline{v} - \omega^2 u \overline{v} \right) \mathrm{d}\mathbf{x} - \mathbf{i}\omega \int_\Gamma T(u) \overline{v} \, \mathrm{d}\gamma = \int_\Omega f \overline{v} \, \mathrm{d}\mathbf{x}. \end{array} \right. \tag{7.3.7}$$

Classical methods based on a coercive plus compact decomposition, Fredholm's alternative and a unique continuation principle yield the existence and uniqueness of the variational solution $u \in H^1(\Omega)$. The key step is the uniqueness of the solution. Assume the source term is $f = 0$. One has $(T(u), u)_{L^2(\Gamma)} = 0$ according to (7.3.7), and therefore $T(u) = 0$ as a consequence of (7.3.5). Referring to (7.3.6), the normal derivative $\partial_{\mathbf{n}} u$ vanishes on Γ. Now since problem (7.3.3) is well posed, see Theorem 7.3.1, u necessarily vanishes on Γ. Since $\partial_{\mathbf{n}} u = u = 0$ on Γ, a unique continuation principle yields $u = 0$ in Ω.

7.4 Three domain decomposition algorithms using the 2^{nd} order ABC

7.4.1 DDM-1

Consider as in Figure 7.4 a decomposition of Ω into subdomains Ω_i, for $0 \leq i \leq N_{\text{dom}} - 1$ with $N_{\text{dom}} \geq 2$ the total number of subdomains. The exterior normal to a subdomain Ω_i is denoted as $\mathbf{n}^i$.

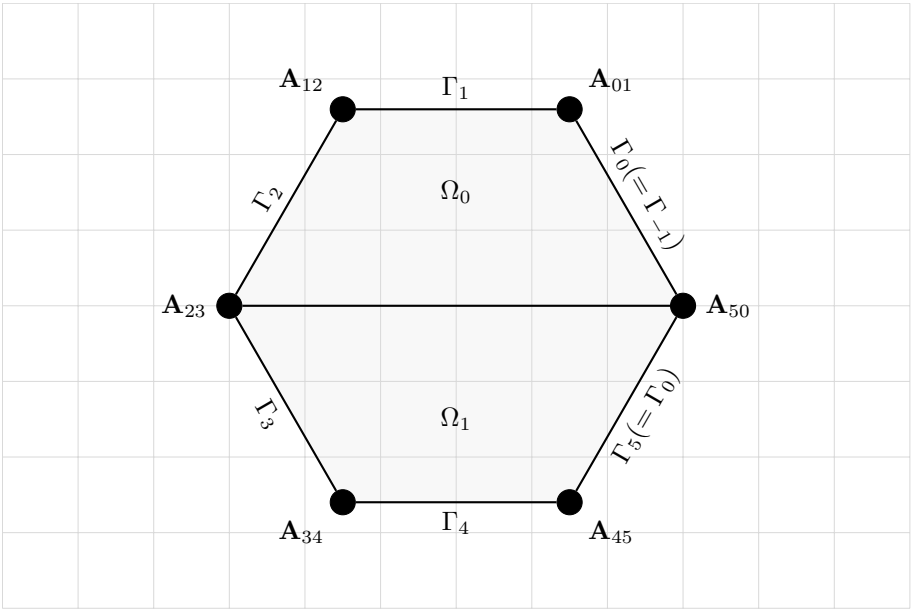

Figure 7.4 – Example of a decomposition of an hexagonal domain.

A natural DDM writes: for all subdomain, initialize $u_i^0 \in H^1(\Omega_i)$ with square integrable normal derivatives and iterate for $p = 0, 1, \ldots$

$$\left\{ \begin{array}{rcll} (-\Delta - \omega^2) u_i^{p+1} & = & f & \text{in } \Omega_i, \\ \left(\dfrac{\partial}{\partial \mathbf{n}^i} - \mathbf{i}\omega \right) u_i^{p+1} & = & -\left(\dfrac{\partial}{\partial \mathbf{n}^j} + \mathbf{i}\omega \right) u_j^p & \text{on } \partial\Omega_i \cap \partial\Omega_j, \forall j \neq i, \\ \dfrac{\partial}{\partial \mathbf{n}} u_i^{p+1} & = & \mathbf{i}\omega T(u^{p+1}) & \text{on } \partial\Omega_i \cap \Gamma. \end{array} \right. \tag{DDM-1}$$

We show that the algorithm is convergent. To do so, we define the following energy

$$E^p := \sum_{i=0}^{N_{\text{dom}}-1} \int_{\partial\Omega_i \setminus \Gamma} \left| \left(\frac{\partial}{\partial \mathbf{n}^i} - \mathbf{i}\omega \right) u_i^p \right|^2 \mathrm{d}\gamma.$$

This quantity is well defined since iterating on p gives that the normal derivatives of u_i^p are square integrable. To prove the convergence of (DDM-1), we prove it is endowed to a decreasing energy, see Subsection 6.2.3.

Lemma 7.4.1. *The algorithm* (DDM-1) *with zero source $f = 0$ has decreasing energy*

$$E^{p+1} \leq E^p - 4 \left\| \frac{\partial u^p}{\partial \mathbf{n}} \right\|^2_{L^2(\Gamma)}. \tag{7.4.1}$$

Proof. One has by definition

$$E^{p+1} = \sum_{i=0}^{N_{\text{dom}}-1} \int_{\partial\Omega_i \setminus \Gamma} \left| \left(\frac{\partial}{\partial \mathbf{n}^i} - \mathbf{i}\omega \right) u_i^{p+1} \right|^2 d\gamma = \sum_{j=0}^{N_{\text{dom}}-1} \int_{\partial\Omega_j \setminus \Gamma} \left| \left(\frac{\partial}{\partial \mathbf{n}^j} + \mathbf{i}\omega \right) u_j^{p} \right|^2 d\gamma.$$

Algebraic manipulations and an integration by parts on the closed border $\partial\Omega_i$ give

$$\begin{aligned}
E^{p+1} &= \sum_{j=0}^{N_{\text{dom}}-1} \int_{\partial\Omega_j \setminus \Gamma} \left| \left(\frac{\partial}{\partial \mathbf{n}^j} - \mathbf{i}\omega \right) u_j^{p} \right|^2 d\gamma + 4 \operatorname{Re} \sum_{j=0}^{N_{\text{dom}}-1} \int_{\partial\Omega_j - \Gamma} \frac{\partial u_j^p}{\partial \mathbf{n}^j} \overline{\mathbf{i}\omega u_j^p} d\gamma \\
&= \sum_{j=0}^{N_{\text{dom}}-1} \int_{\partial\Omega_j \setminus \Gamma} \left| \left(\frac{\partial}{\partial \mathbf{n}^j} - \mathbf{i}\omega \right) u_j^{p} \right|^2 d\gamma \\
&\quad - 4 \operatorname{Re} \sum_{j=0}^{N_{\text{dom}}-1} \left(\int_{\partial\Omega_j} \mathbf{i}\omega \partial_{\mathbf{n}^j} \frac{|u_j^p|^2}{2} d\gamma + \int_{\partial\Omega_j \cap \Gamma} \frac{\partial u_j^p}{\partial \mathbf{n}^j} \overline{\mathbf{i}\omega u_j^p} d\gamma \right) \\
&= \sum_{j=0}^{N_{\text{dom}}-1} \int_{\partial\Omega_j \setminus \Gamma} \left| \left(\frac{\partial}{\partial \mathbf{n}^j} - \mathbf{i}\omega \right) u_j^{p} \right|^2 d\gamma - 4 \operatorname{Re} \sum_{j=0}^{N_{\text{dom}}-1} \int_{\partial\Omega_j \cap \Gamma} \frac{\partial u_j^p}{\partial \mathbf{n}^j} \overline{\mathbf{i}\omega u_j^p} d\gamma.
\end{aligned}$$

It follows from (7.3.5) and the condition on $\partial\Omega_i \cap \Gamma$ that

$$\begin{aligned}
E^{p+1} &= E^p - 4\omega^2 \operatorname{Re} \left(T(u^p), u^p \right)_{L^2(\Gamma)} \\
&\leq E^p - 4\omega^2 \left\| T(u^p) \right\|^2_{L^2(\Gamma)} \\
&= E^p - 4 \left\| \frac{\partial u^p}{\partial \mathbf{n}} \right\|^2_{L^2(\Gamma)},
\end{aligned}$$

and the claim is proven. □

This method lacks one original asset of DDMs, which is the full decoupling between local problems. Indeed, since the operator T is non-local, see (7.3.3), all subdomains Ω_i such that $\partial\Omega_i \cap \Gamma \neq 0$ are coupled through the ABC.

7.4.2 DDM-2: subdomains decoupled

This second method, denoted DDM-2, restores the full-decoupling between subdomains. The starting point is that the coupling between the subdomains on the boundary is due to the corner conditions (7.3.1) which define the operator T. This operator is constructed through the solution of a differential operator on the boundary, and it is possible to decouple this problem with another level of DDM for the boundary problem.

Each corner must be indexed by k and ℓ to know at the intersection of which edges of Γ it corresponds, as before, and by i and j to know at the intersection of which subdomains it lies. The

intersection of a subdomain's border $\partial\Omega_i$ and of an exterior edge Γ_k is noted $\Gamma_k^i := \partial\Omega_i \cap \Gamma_k$. It can either be empty or be a segment, as illustrated in Figure 7.5. It is convenient to introduce the two sets of points $\mathcal{C}_k^i$ and $\mathcal{F}_k^i$ such that $\partial\Gamma_k^i = \mathcal{C}_k^i \cup \mathcal{F}_k^i$ and $\mathcal{C}_k^i \cap \mathcal{F}_k^i = \emptyset$. The first set contains the endpoints of Γ_k^i that are corners of Γ and writes

$$\mathcal{C}_k^i := \{\mathbf{A}_{k\ell}^{ij} = \Gamma_k^i \cap \Gamma_\ell^j, \forall j, \forall \ell \neq k\}. \tag{7.4.2}$$

The second set contains the endpoints of Γ_k^i that are interior points of Γ_k and writes

$$\mathcal{F}_k^i := \{\mathbf{B}_k^{ij} = \Gamma_k^i \cap \Gamma_k^j, \forall j\}. \tag{7.4.3}$$

In the case where $\Gamma_k^i = \emptyset$, which is frequent, we set by convention $\mathcal{C}_k^i = \emptyset$ and $\mathcal{F}_k^i = \emptyset$.

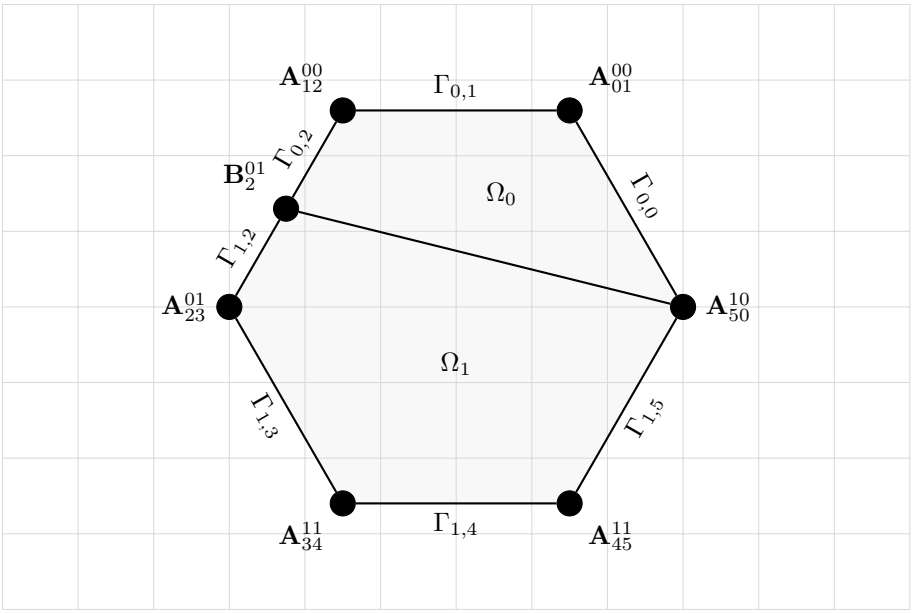

Figure 7.5 – Example of a hexagonal domain split in two subdomains.

An auxiliary unknown $\varphi_{i,k}$ is introduced on each segment Γ_k^i, which stands for the local value of the global quantity $T(u)$. Algorithm (DDM-1) is adapted as follows. As before, for all subdomains, initialize $u_i^0 \in H^1(\Omega_i)$ with square integrable normal derivatives. Then, for $p = 0, 1, \ldots$, solve for

each subdomain

$$\left\{\begin{array}{rcll}(-\Delta-\omega^2)u_i^{p+1} &=& f & \text{in } \Omega_i,\\ \left(\dfrac{\partial}{\partial \mathbf{n}^i}-\mathbf{i}\omega\right)u_i^{p+1} &=& -\left(\dfrac{\partial}{\partial \mathbf{n}^j}+\mathbf{i}\omega\right)u_j^{p} & \text{on } \partial\Omega_i\cap\partial\Omega_j, \forall j\neq i,\\ \dfrac{\partial}{\partial \mathbf{n}^i}u_i^{p+1} &=& \mathbf{i}\omega\varphi_{i,k}^{p+1} & \text{on } \Gamma_k^i, \forall k.\end{array}\right. \tag{DDM-2a}$$

$$\left\{\begin{array}{l}\left(1-\dfrac{1}{2\omega^2}\dfrac{\partial^2}{\partial \mathbf{t}_k^2}\right)\varphi_{i,k}^{p+1}(\mathbf{x}) = u_i^{p+1}(\mathbf{x}), \qquad \mathbf{x}\in\Gamma_k^i,\\ \\ \left(\left(1+\dfrac{\mathbf{i}\beta}{\omega}\dfrac{\cos\left(\frac{\theta_{k\ell}}{2}\right)}{\cos\theta_{k\ell}}\right)\dfrac{\partial\varphi_{i,k}^{p+1}}{\partial\boldsymbol{\tau}_k}+\left(\beta-\mathbf{i}\omega\cos\left(\dfrac{\theta_{k\ell}}{2}\right)\right)\varphi_{i,k}^{p+1}\right)(\mathbf{A}_{k\ell}^{ij})\\ =\left(\left(-1+\dfrac{\mathbf{i}\beta}{\omega}\dfrac{\cos\left(\frac{\theta_{k\ell}}{2}\right)}{\cos\theta_{k\ell}}\right)\dfrac{\partial\varphi_{j,\ell}^{p}}{\partial\boldsymbol{\tau}_\ell}+\left(\beta+\mathbf{i}\omega\cos\left(\dfrac{\theta_{k\ell}}{2}\right)\right)\varphi_{j,\ell}^{p}\right)(\mathbf{A}_{k\ell}^{ij}), \quad \mathbf{A}_{k\ell}^{ij}\in\mathcal{C}_k^i,\\ \\ \left(\partial_{\boldsymbol{\tau}_k}\varphi_{i,k}^{p+1}+\mathbf{i}\beta\varphi_{i,k}^{p+1}\right)(\mathbf{B}_k^{ij}) = \left(-\partial_{\boldsymbol{\tau}_k}\varphi_{j,k}^{p}+\mathbf{i}\beta\varphi_{j,k}^{p}\right)(\mathbf{B}_k^{ij}), \qquad \mathbf{B}_k^{ij}\in\mathcal{F}_k^i.\end{array}\right. \tag{DDM-2b}$$

Remark 7.4.2. Once again, the singularity $\frac{\beta}{\cos\theta_{k\ell}}$ for $\theta_{k\ell}=-\pi/2,-3\pi/2$ is artificial. It is systematically removed by taking $\beta=-|\omega|\cos(\theta_{k\ell})$, see (7.2.9).

The resolution of (DDM-2a)-(DDM-2b) can be done in parallel for all subdomain by solving local problems in $\Omega_i\times\left(\oplus_k\Gamma_k^i\right)$ with unknowns $(u_i^{p+1},(\varphi_{i,k}^{p+1})_k)$. To show the algorithm is convergent, we use the decreasing energy method. Define

$$\begin{aligned}F^p := \sum_{i=0}^{N_{\rm dom}-1}\Bigg(&\int_{\partial\Omega_i\setminus\Gamma}\left|\left(\frac{\partial}{\partial\mathbf{n}^i}-\mathbf{i}\omega\right)u_i^p\right|^2 d\gamma\\ &+\sum_{\substack{k=0\\ \mathbf{A}_{k\ell}^{ij}\in\mathcal{C}_k^i}}^{K-1}\frac{1}{2\beta\left(1-\frac{\cos^2\left(\frac{\theta_{k\ell}}{2}\right)}{\cos\theta_{k\ell}}\right)}\left|\left(1+\frac{\mathbf{i}\beta}{\omega}\frac{\cos\left(\frac{\theta_{k\ell}}{2}\right)}{\cos\theta_{k\ell}}\right)\frac{\partial\varphi_{i,k}^p}{\partial\boldsymbol{\tau}_k}+\left(\beta-\mathbf{i}\omega\cos\left(\frac{\theta_{k\ell}}{2}\right)\right)\varphi_{i,k}^p\right|^2(\mathbf{A}_{k\ell}^{ij})\\ &+\sum_{\substack{k=0\\ \mathbf{B}_k^{ij}\in\mathcal{F}_k^i}}^{K-1}\frac{1}{2\omega}\left|\partial_{\boldsymbol{\tau}_k}\varphi_{i,k}^p+\omega\varphi_{i,k}^p\right|^2(\mathbf{B}_k^{ij})\Bigg).\end{aligned}$$

Remark 7.4.3. For $\beta=b\omega\cos(\theta_{k\ell})$, the denominator on the second line rewrites

$$2\beta\left(1-\frac{\cos^2\left(\frac{\theta_{k\ell}}{2}\right)}{\cos\theta_{k\ell}}\right)=3b\omega\left(\cos^2\left(\frac{\theta_{k\ell}}{2}\right)-1\right)=-2b\omega\sin^2\left(\frac{\theta_{k\ell}}{2}\right),$$

and is positive for $b\,\mathrm{sign}\,\omega<0$. Therefore, in the sequel, we take $b:=-\,\mathrm{sign}\,\omega$. It justifies the choice $\beta=-|\omega|\cos(\theta_{k\ell})$, so that F^p is non negative.

It follows that $\beta=-|\omega|\cos\theta_{k\ell}$, and that F^p is indeed positive.

Lemma 7.4.4. *The algorithm* (DDM-2a)-(DDM-2b) *with zero source $f=0$ has decreasing energy*

$$F^{p+1}\leq F^p-2\sum_{j=0}^{N_{dom}-1}\sum_{\ell=0}^{K-1}\int_{\Gamma_\ell^j}\left(2\omega^2|\varphi_{j,\ell}^p|^2+|\partial_{\mathbf{t}_\ell}\varphi_{j,\ell}^p|^2\right)\mathrm{d}\gamma. \tag{7.4.4}$$

Proof. Using the definition of the energy F^{p+1} and of the quantities u_i^{p+1} and $\varphi_{i,k}^{p+1}$, it gives

$$
\begin{aligned}
&F^{p+1}\\
&= \sum_{i=0}^{N_{\mathrm{dom}}-1} \Bigg(\int_{\partial\Omega_i\setminus\Gamma} \left| \left(\frac{\partial}{\partial \mathbf{n}^i} - \mathbf{i}\omega \right) u_i^{p+1} \right|^2 d\gamma \\
&\quad + \sum_{\substack{k=0 \\ \mathbf{A}_{k\ell}^{ij}\in\mathcal{C}_k^i}}^{K-1} \frac{1}{2|\omega|\sin^2\left(\frac{\theta_{k\ell}}{2}\right)} \left| \left(1 + \frac{\mathbf{i}\beta}{\omega} \frac{\cos\left(\frac{\theta_{k\ell}}{2}\right)}{\cos\theta_{k\ell}} \right) \frac{\partial \varphi_{i,k}^{p+1}}{\partial \boldsymbol{\tau}_k} + \left(\beta - \mathbf{i}\omega\cos\left(\frac{\theta_{k\ell}}{2}\right) \right) \varphi_{i,k}^{p+1} \right|^2 (\mathbf{A}_{k\ell}^{ij}) \\
&\quad + \sum_{\substack{k=0 \\ \mathbf{B}_k^{ij}\in\mathcal{F}_k^i}}^{K-1} \frac{1}{2\omega} \left| \omega\varphi_{i,k}^{p+1} + \partial_{\boldsymbol{\tau}_k}\varphi_{i,k}^{p+1} \right|^2 (\mathbf{B}_k^{ij}) \Bigg) \\
&= \sum_{j=0}^{N_{\mathrm{dom}}-1} \Bigg(\int_{\partial\Omega_j\setminus\Gamma} \left| \left(\frac{\partial}{\partial \mathbf{n}^j} + \mathbf{i}\omega \right) u_j^{p} \right|^2 d\gamma \\
&\quad + \sum_{\substack{\ell=0 \\ \mathbf{A}_{k\ell}^{ij}\in\mathcal{C}_\ell^j}}^{K-1} \frac{1}{2|\omega|\sin^2\left(\frac{\theta_{k\ell}}{2}\right)} \left| \left(-1 + \frac{\mathbf{i}\beta}{\omega} \frac{\cos\left(\frac{\theta_{k\ell}}{2}\right)}{\cos\theta_{k\ell}} \right) \frac{\partial \varphi_{j,\ell}^{p}}{\partial \boldsymbol{\tau}_\ell} + \left(\beta + \mathbf{i}\omega\cos\left(\frac{\theta_{k\ell}}{2}\right) \right) \varphi_{j,\ell}^{p} \right|^2 (\mathbf{A}_{k\ell}^{ij}) \\
&\quad + \sum_{\substack{\ell=0 \\ \mathbf{B}_\ell^{ij}\in\mathcal{F}_\ell^j}}^{K-1} \frac{1}{2\omega} \left| \omega\varphi_{j,\ell}^{p} - \partial_{\boldsymbol{\tau}_\ell}\varphi_{j,\ell}^{p} \right|^2 (\mathbf{B}_\ell^{ij}) \Bigg).
\end{aligned}
$$

The integrals on the boundary are treated as in the proof of Lemma 7.4.1. One has

$$
\begin{aligned}
&\sum_{j=0}^{N_{\mathrm{dom}}-1} \int_{\partial\Omega_j\setminus\Gamma} \left| \left(\frac{\partial}{\partial \mathbf{n}^j} + \mathbf{i}\omega \right) u_j^{p} \right|^2 d\gamma \\
&= \sum_{j=0}^{N_{\mathrm{dom}}-1} \int_{\partial\Omega_j\setminus\Gamma} \left| \left(\frac{\partial}{\partial \mathbf{n}^j} - \mathbf{i}\omega \right) u_j^{p} \right|^2 d\gamma - 4 \sum_{j=0}^{N_{\mathrm{dom}}-1} \mathrm{Re} \int_{\partial\Omega_j\cap\Gamma} \frac{\partial u_j^p}{\partial \mathbf{n}^j} \overline{\mathbf{i}\omega u_j^p}.
\end{aligned}
$$

For the terms concerning the non flat corners $\mathbf{A}_{k\ell}^{ij}$, similar algebraic relations yield

$$\begin{aligned}
&\sum_{\substack{\ell=0\\ \mathbf{A}_{k\ell}^{ij}\in\mathcal{C}_\ell^j}}^{K-1} \frac{1}{2|\omega|\sin^2\left(\frac{\theta_{k\ell}}{2}\right)} \left|\left(-1+\frac{\mathbf{i}\beta}{\omega}\frac{\cos\left(\frac{\theta_{k\ell}}{2}\right)}{\cos\theta_{k\ell}}\right)\frac{\partial\varphi_{j,\ell}^p}{\partial\boldsymbol{\tau}_\ell}+\left(\beta+\mathbf{i}\omega\cos\left(\frac{\theta_{k\ell}}{2}\right)\right)\varphi_{j,\ell}^p\right|^2(\mathbf{A}_{k\ell}^{ij})\\
&=\sum_{\substack{\ell=0\\ \mathbf{A}_{k\ell}^{ij}\in\mathcal{C}_\ell^j}}^{K-1} \frac{1}{2|\omega|\sin^2\left(\frac{\theta_{k\ell}}{2}\right)} \left|\left(1+\frac{\mathbf{i}\beta}{\omega}\frac{\cos\left(\frac{\theta_{k\ell}}{2}\right)}{\cos\theta_{k\ell}}\right)\frac{\partial\varphi_{j,\ell}^p}{\partial\boldsymbol{\tau}_\ell}+\left(\beta-\mathbf{i}\omega\cos\left(\frac{\theta_{k\ell}}{2}\right)\right)\varphi_{j,\ell}^p\right|^2(\mathbf{A}_{k\ell}^{ij})\\
&\quad-4\,\mathrm{Re}\sum_{\substack{\ell=0\\ \mathbf{A}_{k\ell}^{ij}\in\mathcal{C}_\ell^j}}^{K-1} \frac{1}{2|\omega|\sin^2\left(\frac{\theta_{k\ell}}{2}\right)} \left(\frac{\mathbf{i}\beta}{\omega}\frac{\cos\left(\frac{\theta_{k\ell}}{2}\right)}{\cos\theta_{k\ell}}\frac{\partial\varphi_{j,\ell}^p}{\partial\boldsymbol{\tau}_\ell}+\beta\varphi_{j,\ell}^p\right)\overline{\left(\frac{\partial\varphi_{j,\ell}^p}{\partial\boldsymbol{\tau}_\ell}-\mathbf{i}\omega\cos\left(\frac{\theta_{k\ell}}{2}\right)\varphi_{j,\ell}^p\right)}(\mathbf{A}_{k\ell}^{ij})\\
&=\sum_{\substack{\ell=0\\ \mathbf{A}_{k\ell}^{ij}\in\mathcal{C}_\ell^j}}^{K-1} \frac{1}{2|\omega|\sin^2\left(\frac{\theta_{k\ell}}{2}\right)} \left|\left(1+\frac{\mathbf{i}\beta}{\omega}\frac{\cos\left(\frac{\theta_{k\ell}}{2}\right)}{\cos\theta_{k\ell}}\right)\frac{\partial\varphi_{j,\ell}^p}{\partial\boldsymbol{\tau}_\ell}+\left(\beta-\mathbf{i}\omega\cos\left(\frac{\theta_{k\ell}}{2}\right)\right)\varphi_{j,\ell}^p\right|^2(\mathbf{A}_{k\ell}^{ij})\\
&\quad-4\,\mathrm{Re}\sum_{\substack{\ell=0\\ \mathbf{A}_{k\ell}^{ij}\in\mathcal{C}_\ell^j}}^{K-1} \frac{1}{2|\omega|\sin^2\left(\frac{\theta_{k\ell}}{2}\right)} \left(\mathbf{i}b\cos\left(\frac{\theta_{k\ell}}{2}\right)\frac{\partial\varphi_{j,\ell}^p}{\partial\boldsymbol{\tau}_\ell}+b\omega\cos\theta_{k\ell}\varphi_{j,\ell}^p\right)\overline{\left(\frac{\partial\varphi_{j,\ell}^p}{\partial\boldsymbol{\tau}_\ell}-\mathbf{i}\omega\cos\left(\frac{\theta_{k\ell}}{2}\right)\varphi_{j,\ell}^p\right)}(\mathbf{A}_{k\ell}^{ij})\\
&=\sum_{\substack{\ell=0\\ \mathbf{A}_{k\ell}^{ij}\in\mathcal{C}_\ell^j}}^{K-1} \frac{1}{2|\omega|\sin^2\left(\frac{\theta_{k\ell}}{2}\right)} \left|\left(1+\frac{\mathbf{i}\beta}{\omega}\frac{\cos\left(\frac{\theta_{k\ell}}{2}\right)}{\cos\theta_{k\ell}}\right)\frac{\partial\varphi_{j,\ell}^p}{\partial\boldsymbol{\tau}_\ell}+\left(\beta-\mathbf{i}\omega\cos\left(\frac{\theta_{k\ell}}{2}\right)\right)\varphi_{j,\ell}^p\right|^2(\mathbf{A}_{k\ell}^{ij})\\
&\quad-2\,\mathrm{Re}\sum_{\substack{\ell=0\\ \mathbf{A}_{k\ell}^{ij}\in\mathcal{C}_\ell^j}}^{K-1} \frac{\partial\varphi_{j,\ell}^p}{\partial\boldsymbol{\tau}_\ell}(\mathbf{A}_{k\ell}^{ij})\overline{\varphi_{j,\ell}^p}(\mathbf{A}_{k\ell}^{ij}).
\end{aligned}$$

Similarily, for the flat corners $\mathbf{B}_\ell^{ij}$, it gives

$$\begin{aligned}
&\sum_{\substack{\ell=0\\ \mathbf{B}_\ell^{ij}\in\mathcal{F}_\ell^j}}^{K-1} \frac{1}{2\omega}\left|\omega\varphi_{j,\ell}^p-\partial_{\boldsymbol{\tau}_\ell}\varphi_{j,\ell}^p\right|^2(\mathbf{B}_\ell^{ij})\\
&\quad=\sum_{\substack{\ell=0\\ \mathbf{B}_\ell^{ij}\in\mathcal{F}_\ell^j}}^{K-1} \frac{1}{2\omega}\left|\omega\varphi_{j,\ell}^p+\partial_{\boldsymbol{\tau}_\ell}\varphi_{j,\ell}^p\right|^2(\mathbf{B}_\ell^{ij})-2\,\mathrm{Re}\sum_{\substack{\ell=0\\ \mathbf{B}_\ell^{ij}\in\mathcal{F}_\ell^j}}^{K-1}\frac{\partial\varphi_{j,\ell}^p}{\partial\boldsymbol{\tau}_\ell}(\mathbf{B}_\ell^{ij})\overline{\varphi_{j,\ell}^p}(\mathbf{B}_\ell^{ij}).
\end{aligned}$$

Therefore, it holds that

$$F^{p+1}=F^p-4\,\mathrm{Re}\sum_{j=0}^{N_{\mathrm{dom}}-1}\int_{\partial\Omega_j\cap\Gamma}\frac{\partial u_j^p}{\partial\mathbf{n}^j}\overline{\mathbf{i}\omega u_j^p}\,\mathrm{d}\gamma-2\,\mathrm{Re}\sum_{j=0}^{N_{\mathrm{dom}}-1}\sum_{\substack{\ell\\ \mathbf{A}\in\mathcal{C}_\ell^j\cup\mathcal{F}_\ell^j}}\frac{\partial\varphi_{j,\ell}^p}{\partial\boldsymbol{\tau}_\ell}(\mathbf{A})\overline{\varphi_{j,\ell}^p}(\mathbf{A}).$$

It remains to compute the two last terms. It follows from (DDM-2a) that for all j

$$\int_{\partial\Omega_j\cap\Gamma}\frac{\partial u_j^p}{\partial\mathbf{n}^j}\overline{\mathbf{i}\omega u_j^p}\,\mathrm{d}\gamma=\sum_{\ell=0}^{K-1}\int_{\Gamma_\ell^j}\frac{\partial u_j^p}{\partial\mathbf{n}^j}\overline{\mathbf{i}\omega u_j^p}\,\mathrm{d}\gamma=\sum_{\ell=0}^{K-1}\int_{\Gamma_\ell^j}\omega^2\varphi_{j,\ell}^p\overline{u_j^p}\,\mathrm{d}\gamma.$$

Integrating by parts the equation from (DDM-2b) at iteration p on Γ_ℓ^j against $\varphi_{j,\ell}^p$ and suming over all subdomain and edge indices j and ℓ yields

$$\sum_{j=0}^{N_{\rm dom}-1}\sum_{\ell=0}^{K-1}\left(\int_{\Gamma_\ell^j}\left(|\varphi_{j,\ell}^p|^2+\frac{1}{2\omega^2}\left|\frac{\partial\varphi_{j,\ell}^p}{\partial\mathbf{t}_\ell}\right|^2\right)\mathrm{d}\gamma-\frac{1}{2\omega^2}\sum_{\mathbf{A}\in\mathcal{C}_\ell^j\cup\mathcal{F}_\ell^j}\frac{\partial\varphi_{j,\ell}^p}{\partial\boldsymbol{\tau}_\ell}(\mathbf{A})\overline{\varphi_{j,\ell}^p}(\mathbf{A})\right)$$
$$=\sum_{j=0}^{N_{\rm dom}-1}\sum_{\ell=0}^{K-1}\int_{\Gamma_\ell^j}u_j^p\overline{\varphi_{j,\ell}^p}\,\mathrm{d}\gamma.$$

Therefore $F^{p+1}=F^p-4\sum_{j=0}^{N_{\rm dom}-1}\sum_{\ell=0}^{K-1}\int_{\Gamma_\ell^j}\left(\omega^2|\varphi_{j,\ell}^p|^2+\frac{1}{2}\left|\frac{\partial\varphi_{j,\ell}^p}{\partial\mathbf{t}_\ell}\right|^2\right)\mathrm{d}\gamma$ and the proof is ended. □

Algorithm (DDM-2a)-(DDM-2b) restored the full-decoupling with respect to the subdomains. However, a coupling remains between u_i^{p+1} and $(\varphi_{i,k}^{p+1})_k$ since in the DDM defining u_i^{p+1}, it is imposed that $\partial_{\mathbf{n}^i}u_i^{p+1}=\mathbf{i}\omega\varphi_{i,k}^{p+1}$ on each Γ_k^i, and that at the same time, in the DDM defining $\varphi_{i,k}^{p+1}$, it is imposed that $\varphi_{i,k}^{p+1}-\partial_{\mathbf{t}_k^2}\varphi_{i,k}^{p+1}/(2\omega^2)=u_i^{p+1}$ on Γ_k^i. Decoupling the systems (DDM-2a) and (DDM-2b) of the DDM will allow to solve the equation on u_i^{p+1} as a classical Helmholtz boundary value problem.

7.4.3 DDM-3: subdomains and unknowns decoupled

In this section, we modify the algorithm DDM-2 by decoupling (DDM-2a) from (DDM-2b) at the price of introducing a new auxiliary unknown on each edge Γ_k^i. This unknown, denoted $\psi_{i,k}$, represents the Dirichlet trace of u_i on Γ_k^i.

Initialize $u_i^0\in H^1(\Omega_i)$ with square integrable normal derivatives on each subdomain, and $(\varphi_{i,k}^0)_k\in\oplus_k H^1(\Gamma_k^i)$, $(\psi_{i,k}^0)_k\in\oplus_k L^2(\Gamma_k^i)$ on the exterior boundary of each subdomain. For $p=0,1,\ldots$, solve for each subdomain

$$\left\{\begin{array}{rcll}(-\Delta-\omega^2)u_i^{p+1}&=&f&\text{in }\Omega_i,\\ \left(\dfrac{\partial}{\partial\mathbf{n}^i}-\mathbf{i}\omega\right)u_i^{p+1}&=&-\left(\dfrac{\partial}{\partial\mathbf{n}^j}+\mathbf{i}\omega\right)u_j^p&\text{on }\partial\Omega_i\cap\partial\Omega_j,\forall j\neq i,\\ \left(\dfrac{\partial}{\partial\mathbf{n}^i}-\mathbf{i}\omega\right)u_i^{p+1}&=&\mathbf{i}\omega\left(\varphi_{i,k}^p-\psi_{i,k}^p\right)&\text{on }\Gamma_k^i,\forall k,\end{array}\right.\qquad\text{(DDM-3a)}$$

and for each edge

$$\begin{cases} \left(1-\dfrac{1}{2\omega^2}\dfrac{\partial^2}{\partial \mathbf{t}_k^2}\right)\varphi_{i,k}^{p+1}(\mathbf{x}) = \psi_{i,k}^{p+1}(\mathbf{x}), & \mathbf{x}\in\Gamma_k^i,\\ \varphi_{i,k}^{p+1}(\mathbf{x}) + \psi_{i,k}^{p+1}(\mathbf{x}) = \dfrac{1}{\mathbf{i}\omega}\dfrac{\partial u_i^p}{\partial \mathbf{n}^i}(\mathbf{x}) + u_i^p(\mathbf{x}), & \mathbf{x}\in\Gamma_k^i,\\ \left(\left(1+\dfrac{\mathbf{i}\beta}{\omega}\dfrac{\cos\left(\frac{\theta_{k\ell}}{2}\right)}{\cos\theta_{k\ell}}\right)\dfrac{\partial\varphi_{i,k}^{p+1}}{\partial\boldsymbol{\tau}_k} + \left(\beta-\mathbf{i}\omega\cos\left(\dfrac{\theta_{k\ell}}{2}\right)\right)\varphi_{i,k}^{p+1}\right)(\mathbf{A}_{k\ell}^{ij}) & \\ \quad = \left(\left(-1+\dfrac{\mathbf{i}\beta}{\omega}\dfrac{\cos\left(\frac{\theta_{k\ell}}{2}\right)}{\cos\theta_{k\ell}}\right)\dfrac{\partial\varphi_{j,\ell}^{p}}{\partial\boldsymbol{\tau}_\ell} + \left(\beta+\mathbf{i}\omega\cos\left(\dfrac{\theta_{k\ell}}{2}\right)\right)\varphi_{j,\ell}^{p}\right)(\mathbf{A}_{k\ell}^{ij}), & \mathbf{A}_{k\ell}^{ij}\in\mathcal{C}_k^i,\\ \left(\mathbf{i}\omega\varphi_{i,k}^{p+1} + \partial_{\boldsymbol{\tau}_k}\varphi_{i,k}^{p+1}\right)(\mathbf{B}_k^{ij}) = \left(\mathbf{i}\omega\varphi_{j,k}^{p} - \partial_{\boldsymbol{\tau}_k}\varphi_{j,k}^{p}\right)(\mathbf{B}_k^{ij}), & \mathbf{B}_k^{ij}\in\mathcal{F}_k^i. \end{cases} \tag{DDM-3b}$$

To show convergence of (DDM-3a)-(DDM-3b), as for (DDM-1) and (DDM-2a)-(DDM-2b), we show the algorithm is endowed to a decreasing energy. Define

$$\begin{aligned} G^p := &\sum_{i=0}^{N_{\mathrm{dom}}-1}\left(\int_{\partial\Omega_i\setminus\Gamma}\left|\left(\frac{\partial}{\partial\mathbf{n}^i}-\mathbf{i}\omega\right)u_i^p\right|^2 d\gamma + \sum_{k=0}^{K-1}\int_{\Gamma_k^i}\omega^2\left|\varphi_{i,k}^p+\psi_{i,k}^p\right|^2\mathrm{d}\gamma\right.\\ &+\sum_{\substack{k=0\\ \mathbf{A}_{k\ell}^{ij}\in\mathcal{C}_k^i}}^{K-1}\frac{1}{2|\omega|\sin^2\left(\frac{\theta_{k\ell}}{2}\right)}\left|\left(1+\frac{\mathbf{i}\beta}{\omega}\frac{\cos\left(\frac{\theta_{k\ell}}{2}\right)}{\cos\theta_{k\ell}}\right)\frac{\partial\varphi_{i,k}^p}{\partial\boldsymbol{\tau}_k}+\left(\beta-\mathbf{i}\omega\cos\left(\frac{\theta_{k\ell}}{2}\right)\right)\varphi_{i,k}^p\right|^2(\mathbf{A}_{k\ell}^{ij})\\ &\left.+\sum_{\substack{k=0\\ \mathbf{B}_k^{ij}\in\mathcal{F}_k^i}}^{K-1}\frac{1}{2\omega}\left|\omega\varphi_{i,k}^p+\partial_{\boldsymbol{\tau}_k}\varphi_{i,k}^p\right|^2(\mathbf{B}_k^{ij})\right)\\ =&F^p+\sum_{i=0}^{N_{\mathrm{dom}}-1}\sum_{k=0}^{K-1}\int_{\Gamma_k^i}\omega^2\left|\varphi_{i,k}^p+\psi_{i,k}^p\right|^2\mathrm{d}\gamma. \end{aligned}$$

Lemma 7.4.5. *The algorithm* (DDM-3a)-(DDM-3b) *with zero source $f=0$ has decreasing energy*

$$G^{p+1}\le G^p - 2\sum_{j=0}^{N_{dom}-1}\sum_{\ell=0}^{K-1}\int_{\Gamma_\ell^j}\left(2\omega^2|\varphi_{j,\ell}^p|^2+|\partial_{\mathbf{t}_\ell}\varphi_{j,\ell}^p|^2\right)\mathrm{d}\gamma.$$

Proof. Similar computations to the ones of the proof of Lemma 7.4.4 give

$$G^{p+1} = G^p - 4\,\mathrm{Re}\sum_{j=0}^{N_{\mathrm{dom}}-1}\sum_{\ell=0}^{K-1}\int_{\Gamma_\ell^j}\omega^2\varphi_{j,\ell}^p\overline{\psi_{j,\ell}^p}\,\mathrm{d}\gamma - 2\,\mathrm{Re}\sum_{j=0}^{N_{\mathrm{dom}}-1}\sum_{\substack{\ell=0\\ \mathbf{A}\in\mathcal{C}_\ell^j\cup\mathcal{F}_\ell^j}}^{K-1}\frac{\partial\varphi_{j,\ell}^p}{\partial\boldsymbol{\tau}_\ell}(\mathbf{A})\overline{\varphi_{j,\ell}^p}(\mathbf{A}).$$

Integrating the first equation of system (DDM-3b) at iteration p on Γ_ℓ^j against $\varphi_{j,\ell}^p$ and summing

over all subdomain and edge indices j and ℓ gives

$$\sum_{j=0}^{N_{\text{dom}}-1}\sum_{\ell=0}^{K-1}\int_{\Gamma_\ell^j}\left(|\varphi_{j,\ell}^p|^2+\frac{1}{2\omega^2}\left|\frac{\partial\varphi_{j,\ell}^p}{\partial\mathbf{t}_\ell}\right|^2\right)\mathrm{d}\gamma-\frac{1}{2\omega^2}\sum_{j=0}^{N_{\text{dom}}-1}\sum_{\substack{\ell=0\\ \mathbf{A}\in\mathcal{C}_\ell^j\cup\mathcal{F}_\ell^j}}^{K-1}\frac{\partial\varphi_{j,\ell}^p}{\partial\boldsymbol{\tau}_\ell}(\mathbf{A})\overline{\varphi_{j,\ell}^p}(\mathbf{A})$$
$$=\sum_{j=0}^{N_{\text{dom}}-1}\sum_{\ell=0}^{K-1}\int_{\Gamma_\ell^j}\psi_{j,\ell}^p\overline{\varphi_{j,\ell}^p}\,\mathrm{d}\gamma,$$

and so the result is proven. □

7.5 Numerical tests

In this Section, we present a few results obtained on the discretizations of the global problem (7.3.7) and (DDM-1). These are preliminary results, and so far their analysis is qualitative. The simulations were performed using Gmsh and GetGP [57, 40].

The problem is slightly different to the model (7.1.3), instead of a compact source we study the problem of a plane wave scattered by a disc

$$\begin{cases}(-\Delta-\omega^2)u &= 0 \quad \text{in } \Omega,\\ (1-\frac{1}{2\omega^2}\partial_{\mathbf{tt}})\partial_{\mathbf{n}}u-\mathbf{i}\omega u &= g \quad \text{on } \Gamma,\end{cases}$$

with $g=0$ on Γ_{int} the boundary of the obstacle and $g=g^{\text{inc}}$ and corresponds to an incident plane wave that comes from the right on Γ_{ext} the exterior boundary. The real part of the exact solution is plotted in Figure 7.6.

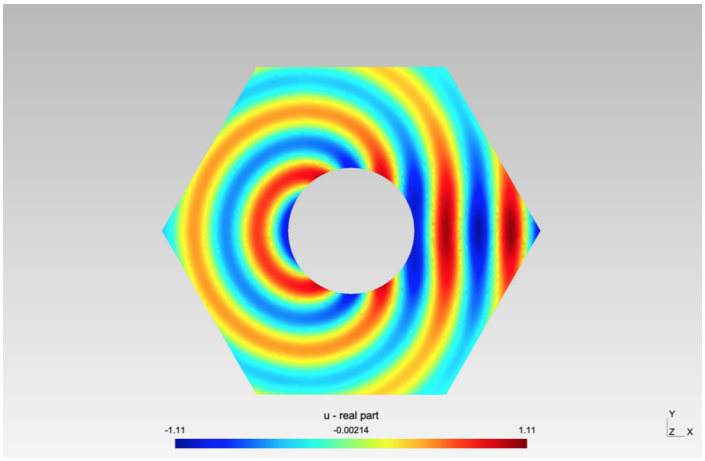

Figure 7.6 – Real part of the solution.

To visualize the differences between the various discretized methods, Figures 7.7, 7.9 and 7.10 represent the modulus of the computed solution and the error with respect to the exact solution.

Figure 7.7 corresponds to the discretization of the global problem with ABC

$$\partial_{\mathbf{n}} u - \mathbf{i}\omega T(u) = 0. \tag{7.5.1}$$

On the left is represented the solution for the non local operator T as defined in Proposition 7.3.2, corresponding to the discretization of system (7.3.7) with second order ABC. On the right is represented the solution for a different operator T that imposes $\partial_{\boldsymbol{\tau}} \partial_{\mathbf{n}} u(\mathbf{A}_{k\ell}) = 0$ and neglects the corner terms of the variational formulation (7.3.3). Comparing the 2^{nd} order method to the one without corner treatment, we observe that the absolute value of the wave is less oscillating. The error is concentrated at the right corner for both methods, but with a stronger amplitude without corner treatment.

Figures 7.9 and 7.10 correspond to the discretization of the DDM associated to (7.5.1) by defining at iteration p and for each subdomain index i

$$\partial_{\mathbf{n}} u_i^p = \mathbf{i}\omega T(u_i^p). \tag{7.5.2}$$

On the left is the solution to (DDM-1) and on the right to the same domain decomposition but without second order corner treatment. In Figure 7.9 the domain is decomposed into 3 subdomains, and in Figure 7.10 into 6 subdomains. The corresponding meshes are given in Figure 7.8.

The interpretation of the observations in these cases is not straightforward. Also, the functional spaces used with GetDP are $\mathbb{P}_1$ elements

$$u_i^h \in \mathbb{P}_1(\Omega_i^h) \quad \text{and} \quad T(u)^h|_{\Gamma \cap \partial\Omega_i} = (\varphi_{i,k}^h)_k \in \mathbb{P}_1({\Gamma_k^i}^h).$$

Consequently, $\partial_{\mathbf{n}} u_i^h$ is in $\mathbb{P}_0$ on each ${\Gamma_k^i}^h$, and not in $\mathbb{P}_1$ as the auxiliary unknowns $\varphi_{i,k}^h$, whereas at the continuous level $\varphi_{i,k}$ stands for $(\mathbf{i}\omega)^{-1}\partial_{\mathbf{n}} u_i$ and they lie in the same space.

Lastly, the errors obtained with the first order ABC (6.2.2) for the global problem and the DDM are represented in Figure 7.11: for each method, the new second order ABC improves the error.

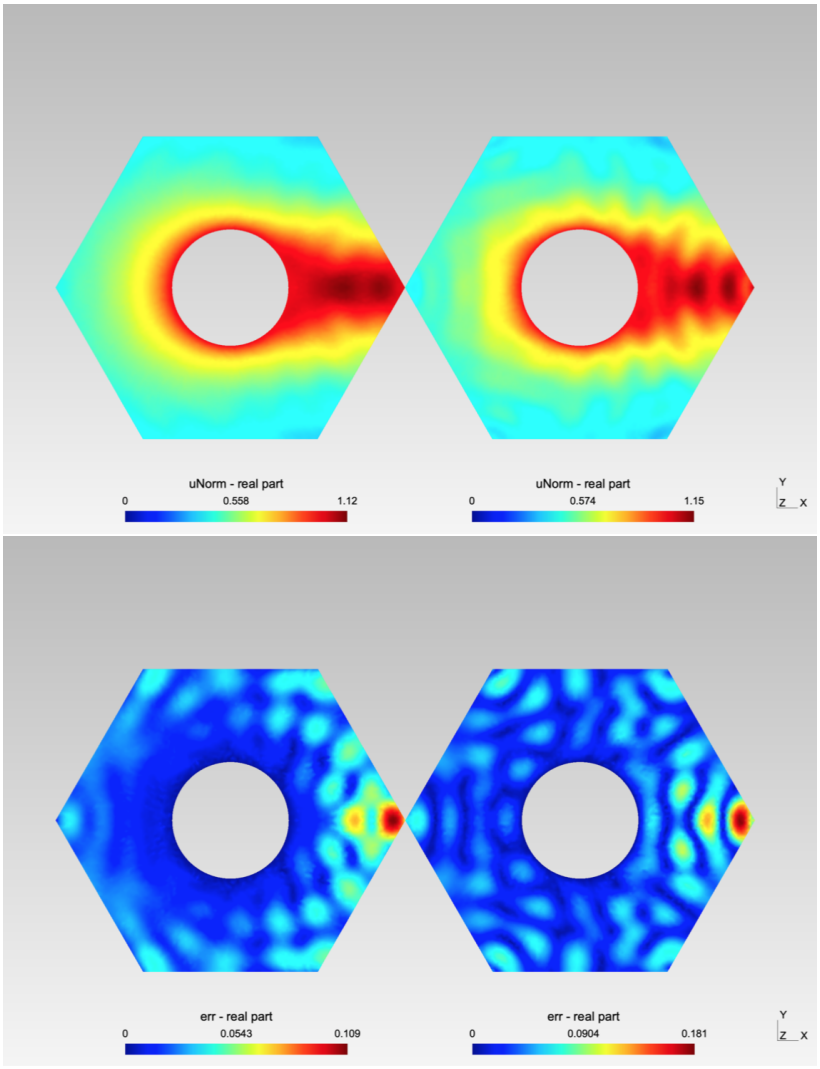

Figure 7.7 – Modulus (above) and error on the real part with respect to the exact solution (below) for the discretization of the global problem with 2^{nd} order ABC and with corner treatment (7.3.7) (left) and without corner treatment (right).

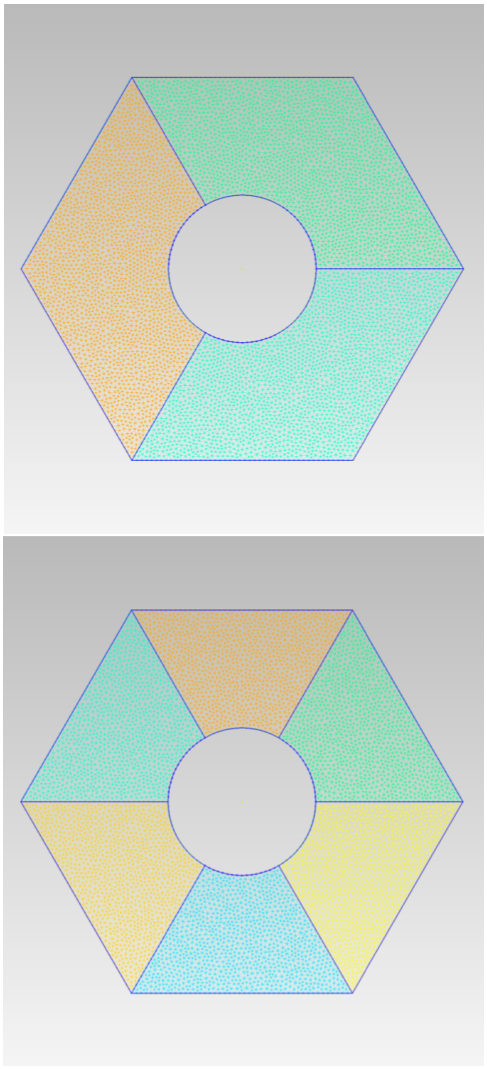

Figure 7.8 – Meshes of the 3 subdomains decomposition (above), and of the 6 subdomains decomposition (below).

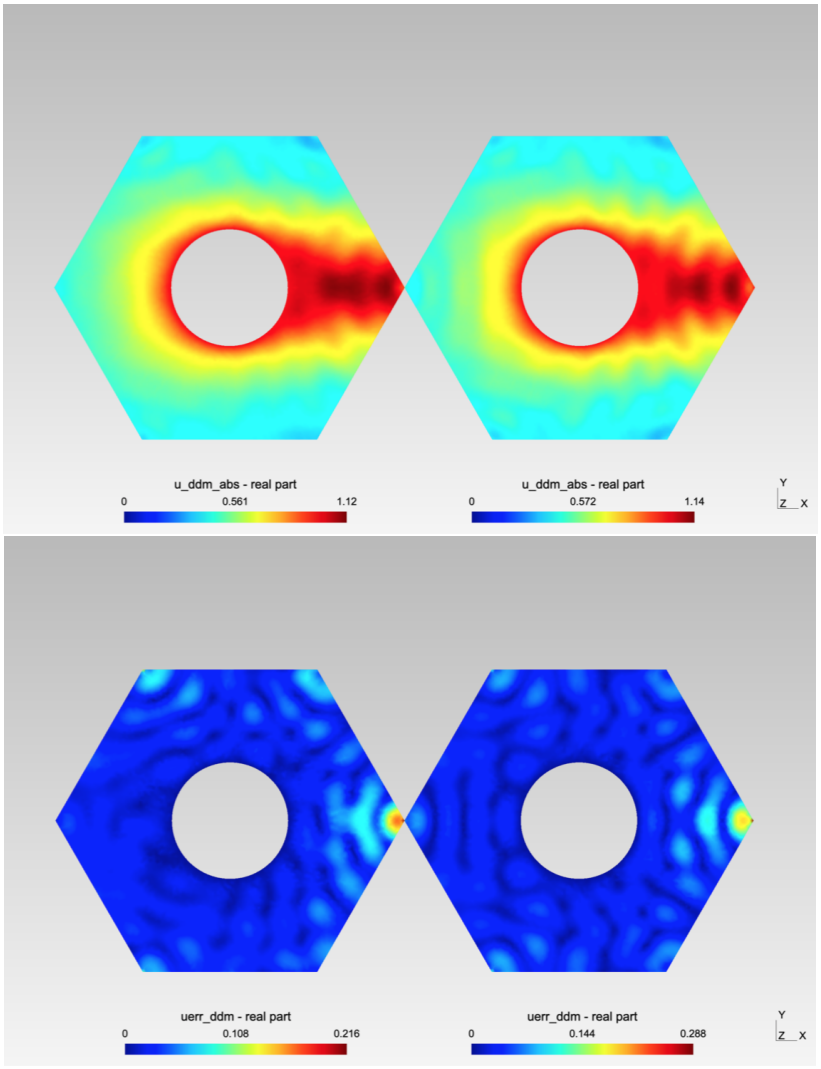

Figure 7.9 – Modulus (above) and error on the real part with respect to the exact solution (below) for the discretization of the DDM on 3 subdomains with 2^{nd} order ABC and with corner treatment (DDM-1) (left) and without corner treatment (right).

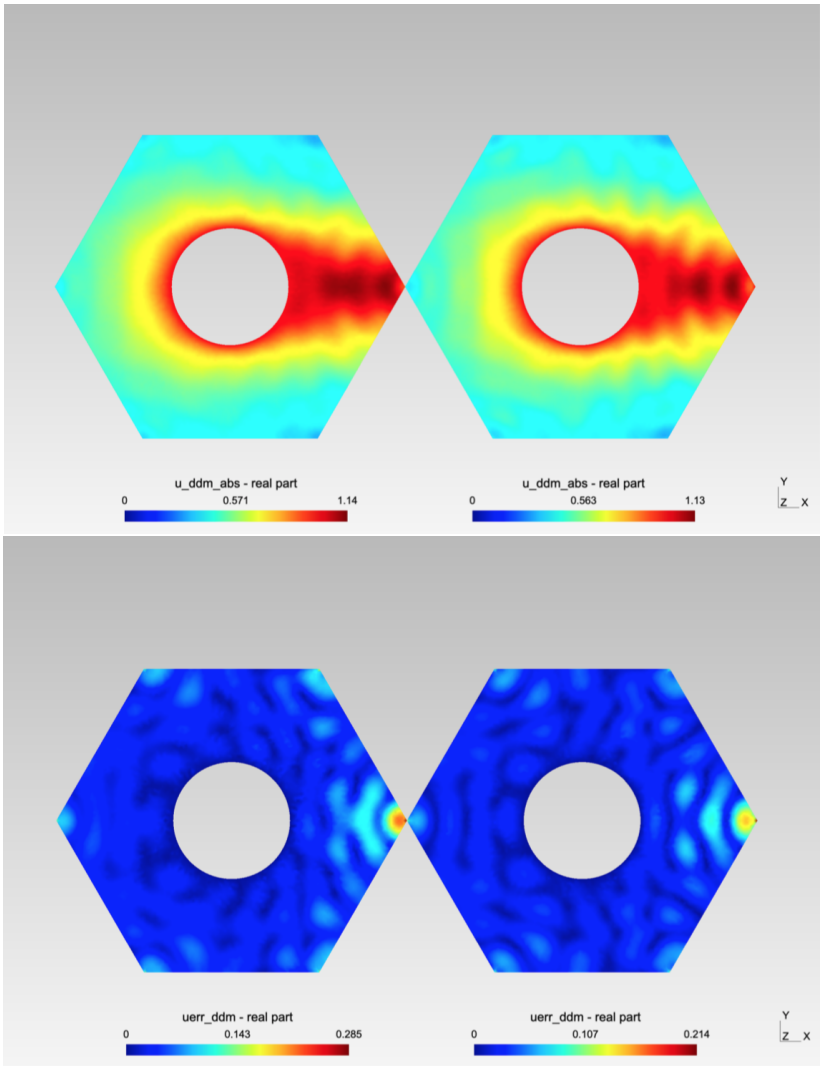

Figure 7.10 – Modulus (above) and error on the real part with respect to the exact solution (below) for the discretization of the DDM on 6 subdomains with 2^{nd} order ABC and with corner treatment (DDM-1) (left) and without corner treatment (right).

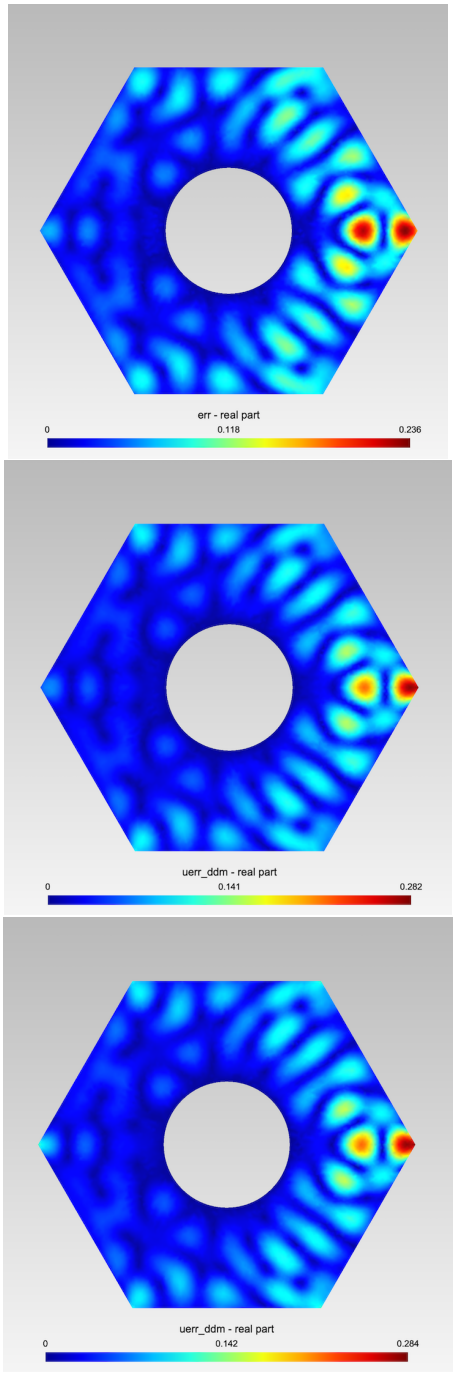

Figure 7.11 – Errors between the computed solutions and the exact solution with the ABC of order 1 (6.2.2) for the global problem (above) the DDM with 3 subdomains (middle) and the DDM with 6 subdomains (below).

Bibliography

[1] H. Ammari, G. Ciraolo, H. Kang, H. Lee, and G. W. Milton. Spectral theory of a Neumann-Poincaré-type operator and analysis of cloaking due to anomalous localized resonance. *Arch. Rational Mech. Anal.*, 218:667–692, 2013.

[2] F. Assous, P. Ciarlet Jr., and S. Labrunie. *Mathematical foundations of computational electromagnetism*. Springer-Verlag, 2018.

[3] A. Back, T. Hattori, S. Labrunie, J.-R. Roche, and P. Bertrand. Electromagnetic wave propagation and absorption in magnetized plasmas: variational formulations and domain decomposition. *ESAIM: Mathematical Modeling and Numerical Analysis*, 49(5):1239–1260, 2015.

[4] M. Badsi, M. Campos Pinto, and B. Després. A minimization formulation of a bi-kinetic sheath. *Kinetic and Related Models*, 9(4):621–656, 2016.

[5] A. Bamberger, P. Joly, and J. E. Roberts. Second-order absorbing boundary conditions for the wave equation: a solution for the corner problem. *SIAM J. Numer. Anal.*, 27(2):323–352, 1990.

[6] R. Bank, M. Holst, O. Widlund, and J. Xu, editors. *On the applicability of Lions' energy estimates in the analysis of discrete optimized Scwharz methods with cross points*. Springer Verlag, 2013.

[7] M. S. Baouendi and C. Goulaouic. Régularité et théorie spectrale pour une classe d'opérateurs elliptiques dégénérés. *Arch. Rational Mech. Anal.*, 34:361–379, 1969.

[8] J.-D. Benamou and B. Després. A domain decomposition method for the Helmholtz equation and related optimal control problems. *Journal of Computational Physics*, 136:68–82, 1997.

[9] J.-P. Berenger. A perfectly matched layer for the absorption of electromagnetic waves. *Journal of Computational Physics*, 114:185–200, 1994.

[10] M. Bernadou, J.-M. Boisserie, and K. Hassan. Sur l'implémentation des éléments finis de Hsieh-Clough-Tocher complet et réduit. Technical report, INRIA, 1980.

[11] I. B. Bernstein and S. K. Trehan. Plasma oscillations (I). *Nuclear Fusion*, 1(1):3–41, 1960.

[12] V. Bobkov and et al. Impact of ICRF on the scrape-off layer and on plasma wall interactions: from present experiments to fusion reactor. *Nuclear Materials and Energy*, 18:131–140, 2019.

[13] D. Boffi, F. Brezzi, and M. Fortin. *Mixed finite element methods and applications*. Springer-Verlag, 2013.

[14] A. Bonito and J.-L. Guermond. Approximation of the eingenvalue problem for the time harmonic Maxwell system by continuous Lagrange finite elements. *Mathematics of Computation*, 80(276):1887–1910, 2011.

[15] A. Bonito, J.-L. Guermond, and F. Luddens. Regularity of the Maxwell equations in heterogeneous media and Lipschitz domains. *Journal of Mathematical Analysis and Applications*, 408(2):498–512, 2013.

[16] Y. Boubendir, X. Antoine, and C. Geuzaine. A quasi-optimal non-overlapping domain decomposition algorithm for the Helmholtz equation. *Journal of Computational Physics*, 231(2):262–280, 2012.

[17] M. Brambilla. *Kinetic Theory of Plasma Waves*. Oxford University Press, 2008.

[18] C. Bressan, M. Kraus, P. J. Morrison, and O. Maj. Relaxation to magnetohydrodynamics equilibria via collision brackets. *Journal of Physics: Conference Series*, 1125, 2018.

[19] H. Brezis. *Functional Analysis, Sobolev Spaces and Partial Differential Equations*. Springer, 2011.

[20] K. G. Budden. *Radio Waves in the Ionosphere*. Cambridge University Press, 1961.

[21] J. W. Burby, A. J. Brizard, P. J. Morrison, and H. Qin. Hamiltonian gyrokinetic Vlasov-Maxwell system. *Physics Letters A*, 379:2073–2077, 2015.

[22] L. Caffarelli and L. Silvestre. An extension problem related to the fractional Laplacian. *Communications in Partial Differential Equations*, 32(8):1245–1260, 2007.

[23] C. Caldini-Queiros, B. Després, L.-M. Imbert-Gérard, and M. Kachanovska. A numerical study of the solution of X-mode equations around the hybrid resonance. *ESAIM: Proceedings and Surveys*, 53:1–21, 2016.

[24] A. C. Cavalheiro. The Neumann problem for some degenerate elliptic equations. *Applications of Mathematics*, 51(6):619–628, 2006.

[25] Z. Chen and X. Xiang. A source transfer domain decomposition method for Helmholtz equations in unbounded domain. *SIAM J. Numer. Anal.*, 51:2331–2356, 2013.

[26] C. Cheverry. Can one hear whistler waves? *Comm. Math. Phys.*, 338(2):641–703, 2015.

[27] P. G. Ciarlet. Sur l'élément de Clough et Tocher. *Revue française d'automatique, informatique, recherche opérationnelle. Analyse Numérique*, 8(2):19–27, 1974.

[28] P. G. Ciarlet. Interpolation error estimates for the reduced Hsieh-Clough-Tocher triangle. *Math. of Comp.*, 32(142):335–344, 1978.

[29] F. Collino, S. Ghanemi, and P. Joly. Domain decomposition method for harmonic wave propagation: a general presentation. *Comput. Methods Appl. Mech. Engrg*, 184:171–211, 2000.

[30] D. Colton and R. Kress. *Integral Equation Methods in Scattering Theory*. SIAM, 2013.

[31] B. Després, L.-M. Imbert-Gérard, and O. Lafitte. Singular solutions for the plasma at the resonance. *Journal de l'Ecole Polytechnique*, 4:177–222, 2017.

[32] B. Després, L.-M. Imbert-Gérard, and R. Weder. Hybrid resonance of Maxwell's equations in slab geometry. *J. Math. Pures Appl.*, 101(5):623–653, 2014.

[33] A.-S. Bonnet-Ben Dhia, L. Chesnel, and X. Claeys. Radiation condition for a non-smooth interface between a dielectric and a metamaterial. *Math. Models Methods Appl. Sci.*, 23(9):1629–1662, 2013.

[34] A.-S. Bonnet-Ben Dhia, L. Chesnel, and P. Ciarlet Jr. T-coercivity for scalar interface problems between dielectrics and metamaterials. *ESAIM: Mathematical Modeling and Numerical Analysis*, 46(6):1363–1387, 2012.

[35] A.-S. Bonnet-Ben Dhia, L. Chesnel, and P. Ciarlet Jr. T-coercivity for the Maxwell problem with sign-changing coefficients. *Communications in Partial Differential Equations*, 39(9):1007–1031, 2014.

[36] A.-S. Bonnet-Ben Dhia, L. Chesnel, and P. Ciarlet Jr. Two-dimensional Maxwell's equations with sign-changing coefficients. *Applied Numerical Mathematics*, 79:29–41, 2014.

[37] A.-S. Bonnet-Ben Dhia, P. Ciarlet Jr., and C.M. Zwölf. Time harmonic wave diffraction problems in materials with sign-shifting coefficients. *Journal of Computational and Applied Mathematics*, 234:1912–1919 (Corrigendum 2616), 2010.

[38] G. Di Fazio, M.S. Fanciullo, and P. Zamboni. Harnack inequality and smoothness for quasilinear degenerate elliptic equations. *Journal of Differential Equations*, 245(10):2939–2957, 2008.

[39] M. P. do Carmo. *Differential Geometry of Curves and Surfaces*. Prentice-Hall, 1976.

[40] P. Dular and C. Geuzaine. GetDP reference manual: the documentation for GetDP, a general environment for the treatment of discrete problems.

[41] R. Dumont. *Waves in Plasmas*. CEA, IRFM, 2013.

[42] B. Engquist and A. Majda. Absorbing boundary conditions for the numerical simulation of waves. *Mathematics of Computation*, 31(139):629–651, 1977.

[43] B. Engquist and A. Majda. Radiation boundary conditions for acoustic and elastic wave calculations. *Communications on Pure and Applied Mathematics*, 32:313–357, 1979.

[44] A. Ern and J.-L. Guermond. *Theory and Practice of Finite Elements*. Springer, 2004.

[45] O. Ernst and G. H. Golub. A domain decomposition approach to solving the Helmholtz equation with a radiation boundary condition. In *Domain Decomposition in Science and Engineering*, pages 177–192. American Mathematical Society, 1992.

[46] O. G. Ernst and M. J. Gander. Why is it difficult to solve Helmholtz problems with classical iterative methods. In I. Graham, T. Hou, and O. Lakkis, editors, *Numerical Analysis of Multiscale Problems*, volume 83 of *Lecture Notes in Computational Science and Engineering*, pages 325–363. Springer, 2012.

[47] EuroFusion. http://figures.euro-fusion.org/images/.

[48] L. C. Evans. *Partial Differential Equations*. American Mathematical Society, 2010.

[49] E. B. Fabes, C. E. Kenig, and R. P. Serapioni. The local regularity of solutions of degenerate elliptic equations. *Communications in Partial Differential Equations*, 7(1):77–116, 1982.

[50] A. Fontaine. *Relations de dispersion dans les plasmas magnétisés*. PhD thesis, Université de Rennes 1, 2017.

[51] M. J. Gander. Optimized Schwarz methods. *SIAM J. Numer. Anal.*, 44(2):699–731, 2006.

[52] M. J. Gander. Schwarz methods over the course of time. *ETNA*, 31:228–255, 2008.

[53] M. J. Gander and L. Halpern. Méthodes de décomposition de domaines - Notions de base. *Techniques de l'ingénieur Mathématiques*, 2012.

[54] M. J. Gander, F. Magoulès, and F. Nataf. Optimized Schwarz methods without overlap for the Helmholtz equation. *SIAM J. Sci. Comput.*, 24(1):38–60, 2002.

[55] M. J. Gander and K. Santugini. Cross-points in domain decomposition methods with a finite element discretization. *ETNA*, 45:219–240, 2016.

[56] M. J. Gander and H. Zhang. A class of iterative solvers for the Helmholtz equation: factorizations, sweeping preconditioners, source transfer, single layer potentials, polarized traces, and optimized Schwarz methods. *SIAM review*, 61(1):3–76, 2019.

[57] C. Geuzaine and J.-F. Remacle. Gmsh: a three-dimensional finite element mesh generator with built-in pre- and post-processing facilities. *Int. J. Numer. Meth. Engng*, 79(11):1309–1331, 2009.

[58] E. Gravier, M. Lesur, X. Garbet, Y. Sarazin, J. Médina, K. Lim, and M. Idouakass. Diffusive impurity transport driven by trapped particle turbulence in tokamak plasmas. *Physics of Plasmas*, 26(8), 2019.

[59] L. Halpern and O. Lafitte. Dirichlet to Neumann map for domains with corners and approximate boundary conditions. *Journal of Computational and Applied Mathematics*, 204(2):505–514, 2007.

[60] L. Halpern and J. Rauch. Error analysis for absorbing boundary conditions. *Numerische Mathematik*, 51:459–467, 1987.

[61] T. Hattori. *Décomposition de domaine pour la simulation Full-Wave dans un plasma froid.* PhD thesis, Université de Lorraine, 2014.

[62] F. Hecht. New development in FreeFem++. *J. Numer. Math.*, 20(3-4):251–265, 2012.

[63] J. Hillairet, R. Ragona, L. Colas, W. Helou, and F. Bocquet. Lower hybrid range cold magnetized plasma modelling in ANSYS HFSS. *Fusion Engineering and Design*, 2019.

[64] R. Hiptmair. Finite elements in computational electromagnetism. *Acta Numerica*, pages 237–339, 2002.

[65] R. Hiptmair, I. Perugia, and A. Moiola. Stability results for the time-harmonic Maxwell equations with impedance boundary conditions. *Math. Models Methods Appl. Sci.*, 21(11):2263–2287, 2011.

[66] J. D. Huba. NRL Plasma Formulary, 2018.

[67] L.-M. Imbert-Gérard. *Analyse mathématique et numérique de problèmes d'ondes apparaissant dans les plasmas magnétiques.* PhD thesis, Université Pierre et Marie Curie, 2013.

[68] L.-M. Imbert-Gérard. *Discussions around the cold plasma model*, 2017.

[69] IRFM. http://irfm.cea.fr/fusion/grands-principes/introduction.

[70] S. A. Iskhokov, M. G. Gadoev, and T. P. Konstantinova. Variational Dirichlet problem for degenerate elliptic operators generated by noncoervice forms. *Doklady Mathematics*, 91(3):255–258, 2015.

[71] ITER. https://www.iter.org.

[72] J. Jacquot. *Description non-linéaire auto-cohérente de la propagation d'ondes radiofréquences et de la périphérie d'un plasma magnétisé*. PhD thesis, Université de Lorraine, 2013.

[73] S. Jin. Efficient asymptotic-preserving (ap) schemes for some multiscale kinetic equations. *SIAM J. Sci. Comput.*, 21(2):441–454, 1999.

[74] P. Joly, S. Lohrengel, and O. Vacus. Un résultat d'existence et d'unicité pour l'équation de Helmholtz aux conditions aux limites absorbantes d'ordre 2. *C. R. Acad. Sci. Paris Sér. 1 Math.*, 329(3):193–198, 1999.

[75] J. J. Kohn and L. Nirenberg. Degenerate elliptic-parabolic equations of second order. *Communications on Pure and Applied Mathematics*, 20:797–872, 1967.

[76] A. Kufner. *Weighted Sobolev Spaces*. John Wiley and Sons, 1985.

[77] A. G. Kutlin, E. D. Gospodchikov, and A. G. Shalashov. Linear coupling of the fast extraordinary wave to electrostatic plasma oscillations: a revised theory. *Physics of Plasmas*, 24, 2017.

[78] O. Lafitte. Hybrid singularity for the oblique incidence response of a cold plasma. 2018.

[79] M. Lecouvez, B. Stupfel, P. Joly, and F. Collino. Quasi-local transmission conditions for non-overlapping domain decomposition methods for the helmholtz equation. *C. R. Physique*, 15(5):403–414, 2014.

[80] P.-L. Lions. On the Schwarz alternating method I. In *Domain decomposition methods for partial differential equations, Proc. 1st Int. Symp.*, pages 1–42, 1988.

[81] P.-L. Lions. On the Schwarz alternating method II: Stochastic interpretation and order properties. In *Domain decomposition methods for partial differential equations, Proc. 2nd Int. Symp.*, pages 47–70, 1989.

[82] P.-L. Lions. On the Schwarz alternating method III: A variant for nonoverlapping subdomains. In *Domain decomposition methods for partial differential equations, Proc. 3rd Int. Symp.*, pages 202–223, 1990.

[83] X. Litaudon and et al. Overview of the JET results in support to ITER. *Nuclear Fusion*, 57(10), 2017.

[84] S. Loisel. Condition number estimates for the nonoverlapping optimized schwarz method and the 2-lagrange multiplier method for general domains and cross points. *SIAM J. Numer. Anal.*, 51(6):3062–3083, 2013.

[85] L. Lu, L. Colas, J. Jacquot, B. Després, S. Heuraux, E. Faudot, D. Van Eester, K. Crombé, A. Krivska, and J.-M. Noterdaeme. Modelling of radio frequency sheath and fast wave coupling on the realistic ion cyclotron resonant antenna surroundings and the outer wall. *Plasma Phys. Control. Fusion*, 60(3), 2018.

[86] L. Lu, K. Crombé, D. Van Eester, L. Colas, and J. Jacquot. Wave coupling in the magnetized plasma edge: impact of a finite, inhomogeneous density inside the antenna box. In *AIP Conference Proceedings*, volume 1689, 2015.

[87] L. Lu, K. Crombé, D. Van Eester, L. Colas, J. Jacquot, and S. Heuraux. Ion cyclotron wave coupling in the magnetized plasma edge of tokamaks: impact of a finite, inhomogeneous density inside the antenna box. *Plasma Phys. Control. Fusion*, 58, 2016.

[88] W. McLean. *Strongly Elliptic Systems and Boundary Integral Equations*. Cambridge University Press, 2000.

[89] A. Modave, C. Geuzaine, and X. Antoine. Corner tratments for high-order absorbing boundary conditions in high-frequency acoustic scattering problems. HAL preprint [hal-01925160], 2019.

[90] P. Monk. *Finite element methods for Maxwell's equations. Numerical Mathematics and Scientific Computation*. Oxford University Press, 2003.

[91] H.-M. Nguyen. Limiting absorption principle and well-posedness for the Helmholtz equation with sign changing coefficients. *Journal de Mathématiques Pures et Appliquées*, 106(2):342–374, 2016.

[92] H.-M. Nguyen and Q.-H. Nguyen. Discreteness of interior transmission eigenvalues revisited. *Calculus of Variations and Partial Differential Equations*, 56(51), 2017.

[93] A. Nicolopoulos, M. Campos Pinto, and B. Després. A stable formulation of resonant Maxwell's equations in cold plasma. *Journal of Computational and Applied Mathematics*, 362:185–204, 2019.

[94] A. Nicolopoulos, M. Campos Pinto, P. Ciarlet Jr., and B. Després. A variational formulation for coupled degenerate elliptic equations with different signs. 2019.

[95] F. W. J. Olver, D. W. Lozier, R. F. Boisvert, and C. W. Clark. *NIST Handbook of Mathematical Functions*. Cambridge University Press, 2010.

[96] J. Peetre. Another approach to elliptic boundary problems. *Communications on Pure and Applied Mathematics*, 14:711–731, 1961.

[97] A. D. Piliya and E. N. Tregubova. Linear conversion of electromagnetic waves into electron Bernstein waves in an arbitrary inhomogeneous plasma slab. *Plasma Phys. Control. Fusion*, 47:143–154, 2005.

[98] M. Campos Pinto. Analysis and design of numerical methods for problems arising in plasma physics, 2017.

[99] M. Campos Pinto and B. Després. Constructive formulations of resonant Maxwell's equations. *SIAM J. Math. Anal.*, 49(5):3647–3670, 2017.

[100] J.-M. Rax. *Physique des plasmas*. Dunod, 2005.

[101] W. Rudin. *Real and Complex Analysis*. McGraw-Hill, 1987.

[102] A. Samain. *Introduction to tokamak physics*. CEA, 1984.

[103] H. A. Schwarz. Über einige Abbildungsaufgaben. *J. Reine Angew. Math.*, 70:105–120, 1869.

[104] H. A. Schwarz. Über einen Grenzübergang durch alternirendes Verfahren. *Naturforschende Gesellschaft in Zürich*, 15:272–286, 1870.

[105] M. Slemrod. A limiting "viscosity" approach to the Riemann problem for materials exhibiting a change of phase. *Arch. Rational Mech. Anal.*, 105(4):327–365, 1989.

[106] T. H. Stix. *The Theory of Plasma Waves*. McGraw-Hill, 1962.

[107] T. H. Stix. Radiation and absorption via mode conversion in an inhomoheneous collision-free plasma. *Physical Review Letters*, 15(23):878–882, 1965.

[108] T. H. Stix. Fast-wave heating of a two-component plasma. Technical report, Plasma Physics Laboratory, Princeton University, 1975.

[109] A. Strugarek. *Turbulence, transport et confinement: des tokamaks au magnétisme des étoiles*. PhD thesis, Université Paris-Diderot, 2012.

[110] D. G. Swanson. *Plasma Waves*. Institute of Physics Pub., 2003.

[111] L. Tartar. Sur un lemme d'équivalence utilisé en analyse numérique. *Calcolo*, 24(2):129–140, 1987.

[112] F. Triki and M. Vauthrin. Mathematical modeling of the photoacoustic effect generated by the heating of metallic nanoparticles. *Quarterly of Applied Mathematics*, 76(4):673–698, 2018.

[113] B. O. Turesson. *Nonlinear Potential Theory and Weighted Sobolev Spaces*. Springer-Verlag, 2000.

[114] R. B. White and F. F. Chen. Amplification and absorption of electromagnetic waves in overdense plasmas. *Plasma Physics*, 16:565–587, 1974.

[115] L. Zepeda-Nuñez and L. Demanet. The method of polarized traces for the 2D Helmholtz equation. *Journal of Computational Physics*, 308:347–388, 2016.

[116] W. Zhang and et al. Plasma edge modelling with ICRF coupling. *EPJ Web of Conferences*, 157, 2017.

Résumé
Dans une première partie, des formulations variationnelles associées aux équations mal posées de Maxwell résonantes sont construites. Le caractère mal posé est lié à une dégénérescence des équations à l'intérieur du domaine, entraînant la non-unicité et la singularité des solutions. L'ajout de viscosité dans les équations permet de les désingulariser, et c'est par un procédé d'absorption limite qu'on identifie la solution physique, lorsque ce paramètre de viscosité tend vers zéro. Il reste que la dégénérescence à l'intérieur du domaine sépare le problème à la limite en deux équations sur des domaines différents couplés par leur interface le long de laquelle les solutions explosent. Ce travail caractérise pour la première fois la solution limite de manière explicite comme solution d'une formulation bien posée. Pour cela, une décomposition ad hoc en parties régulière et singulière est proposée. Cette formulation à la limite permet de calculer une approximation numérique de la solution physique des équations de Maxwell résonantes sans passer par une désingularisation, qui induit des contraintes de maillage. C'est une étude motivée par la modélisation des résonances hybrides dans un plasma de fusion, dans un régime où les ions sont supposés figés, et la viscosité infiniment petite. La singularité de la solution n'est pas un artefact du modèle mathématique et correspond à un transfert d'énergie d'une onde envoyée dans le plasma aux particules.
Ce problème de couplage d'équations sur différents domaines à travers leur interface nous amène à la seconde partie, qui concerne les méthodes numériques de décomposition de domaine. En présence de coins et de points de croisement, lorsqu'on utilise un mailleur automatique pour décomposer le domaine par exemple, il est nécessaire de traiter ces points pour obtenir des conditions d'absorption ou de transmission d'ordre supérieur à 1. Nous définissons des conditions absorbantes d'ordre 2 pour l'équation de Helmholtz sur un domaine à coins, avec en vue des conditions de transmission traitant les points de croisement. Un point original de ce travail est que chaque algorithme de décomposition de domaine associé à ces conditions absorbantes que l'on propose est lié à une énergie décroissante, et converge.

Abstract
In a first part, we derive variational formulations associated to the a priori ill-posed resonant Maxwell's equations. The ill-posedness is related to the degeneracy of the equations inside the domain, resulting in the non-uniqueness of solutions, and in their singular behavior. Adding a viscosity term desingularizes the equations, and it is by a limit absorption principle that we identify the physical solution, when this non-negative viscosity parameter goes to zero. It remains that the degeneracy inside the domain separates the problem at the limit into two equations on different domains coupled through their interface, on which the solutions blow up. This work gives a new explicit characterization of the limit solution as a solution of a well-posed formulation. To do so, an ad hoc decomposition in regular and singular parts is performed. This formulation of the limit problem allows to compute an approximation of the physical solution to the resonant Maxwell's equations without relying on its desingularized form, which induces mesh constraints. This study is motivated by the modelization of hybrid resonances in fusion plasma, in a regime where ions are supposed to be static, hence the infinitely small viscosity. The singularity of the solution is not an artefact of the mathematical model, and corresponds to a transfer of energy from an incoming wave to the particles.
This coupling of equations set on different domains via their interface leads us to the second part, which concerns domain decomposition methods. When there are corners or cross points, e.g. if an automatic mesher was used to decompose the domain, it is necessary to define conditions at these points in order to have absorbing or transmission conditions of order greater than 1. We define absorbing boundary conditions of order two for Helmholtz equation on a domain with corners, with the further intention of deriving transmission conditions at cross points of the mesh. An original feature of this work is that each domain decomposition algorithm associated to these absorbing conditions is endowed with a decreasing energy and converges.

Keywords: *Maxwell, Helmholtz, plasma heating, upper hybrid resonance, degenerate elliptic, singularities, weighted Sobolev, manufactured solutions, mixed variational formulations, FE, DDM, ABC, corners*